SYSTEMATICS AND EVOLUTION OF THE LEAF-BEETLE TRIBE DORYNOTINI (COLEOPTERA: CHRYSOMELIDAE: CASSIDINAE)

By

© 2017

Marianna V. P. Simões
M.Sc., Universidade Federal do Rio de Janeiro, 2012

Submitted to the graduate degree program in Ecology and Evolutionary Biology and the Graduate Faculty of the University of Kansas in partial fulfillment of the requirements for the degree of Doctor of Philosophy.

_____

Chairperson Andrew Short

_____

Chairperson A. Townsend Peterson

_____

Jorge Soberón

_____

Bruce S. Lieberman

_____

J. Christopher Brown

Date Defended: 1 December, 2017

The dissertation committee for Marianna V.P. Simões certifies that
this is the approved version of the following dissertation:

SYSTEMATICS AND EVOLUTION OF THE LEAF-BEETLE TRIBE DORYNOTINI
(COLEOPTERA: CHRYSOMELIDAE: CASSIDINAE)

_____

Co-Chair: Andrew Short

_____

Co-Chair: A. Townsend Peterson

Date approved: 20 December, 2017

Abstract

The impact of environmental gradients on morphology has been an important topic in ecology and evolutionary biology, as geographic variation in environmental conditions may be a major factor involved in diversification. As such, phenotypic gradients (clines) associated with environmental gradients are worth investigating and understanding in greater detail. The Neotropical tribe Dorynotini Monrós and Viana, 1949 is a monophyletic group of tortoise beetles distributed from central Mexico to northern Argentina. Members are morphologically characterized by possessing an elytral suture that is distinctly adorned with a tubercle or a narrow vertical spiniform post-scutrellar projection. This spine exhibits a latitudinal gradient of continuous increase in height and decrease in width towards south of the tribe's range. This cline provides initial evidence for geographic radiation, and grounds to investigate the interaction of climatic factors associated with the geographic complexity within the clade's distribution, which may be the potential drivers to the group's morphological and ecological diversity. Here, I reconstruct the evolutionary history of Dorynotini and seek the mechanisms driving the morphological heterogeneity contemplated by the group. The steps towards this goal included (Chapter 1, 2, 3 and 4) complete a species-level taxonomic revision of the tribe, to allow derive decisions about species delimitation; patterns of species distribution, morphology and ecology; (Chapter 5) test the monophyly of the tribe and its genera by combining morphological and molecular data, to elucidate biogeographical patterns, and investigate the homology and evolution of the elytral post-scutellar projection and other key characters using ancestral character state reconstruction; and finally (Chapter 6), I explore the evidence behind the apparent cline by testing associations between climate and morphology across

the clade's distribution using an approach based on ecological niche modeling and morphological and environmental hypervolumes.

Acknowledgements

I wish to express my deepest gratitude to both of my mentors, Andrew Short and A. Townsend Peterson, to whom I am immensely indebted for accepting me into their labs, helping me throughout this long learning experience, and for providing great assistance and guidance. I would also like to thank my co-advisor Andrew Short, who has provided immense support throughout this journey and given me the freedom to pursue and explore a wide variety of research interests and approaches, even if they were only partially (or completely!) unrelated to my dissertation topic. Thank you for accepting this terrestrial leaf-beetle student into your lab, integrating me so that I never felt like a "fish out of water"…better, beetle out of water! Secondly, but just as important, I thank my co-advisor Town Peterson. His insight and guidance have been invaluable to my education and progress here at the University of Kansas. I appreciate his willingness to support and guide my exploration of the Ecological Niche Modeling field. I am very glad to have had the opportunity to work on this and other projects with him. Thank you for those "5 minutes" that you would always take to exchange ideas, share comments or ansewer doubts. Thank you for teaching me to see problems through different perspectives, and for teaching me that a low *p*-value is not the end of the world. I cannot thank you enough for all your patience and support.

Thanks are also due to my committee members Bruce Lieberman, Jorge Soberón, and Chris Brown for dedicating their time to serving on my committee and all the scientific knowledge gained through working with them. Their support throughout my work on this dissertation as well as other academic activities at KU was invaluable. Special thanks to Bruce Lieberman for the immense and indispensable support, guidance, friendship and those 10 minutes of talk that would

last for hours. Extended thanks goes to the wider community of faculty and students at KU that provided an amazing environment in which to pursue a dissertation, with a diverse array of amazing scientists providing help, advice, support, and companionship. I thank also Aagje Ashe, Jaime Keeler, Lori Schlenker and Dorothy Johanning, the EEB administrative team, who provided so much assistance with paper-work, as well as general doubts and making sure details were all in order.

I feel privileged to count myself among the collaborative team that developed from the Macroevolution discussion and work group. This group has been one of the most significant components of my academic exercises at KU. From this group I thank my fellow graduate students Becky Dorward, Jacob Cooper, Jennifer Girón, Julien Kimming, Kaylee Herzog, Laura Breitkreuz, Liam Heins, Luke Stroltz, Mabel Alvarado, Matthew Girard, Stephen Baca. Thank you for all the discussions and fun we had working together. And once again, I thank Bruce L., for unquestionably accepting to be our guide and mentor through the amazing and broad field of Macroevolution. I sincerely hope the group continues on with the quest for the final frontier, *boldly going where no one has gone before*!

I have also had the privilege of participating the KU-ENM working group. Thank you for so many stimulating discussions and projects that helped to push my boundaries in the field of Ecology. From this group I thank: Abbadalah Samy, Lindsay Campbell, Andres Lira, Erin Saupe, Kate Ingloff, Narayani and Vijay Barve, Daniel Jiménez, Abdu Elkeesh, Daniel Romero, Chris Henz, Kate ingenloff, Ali Khalighifar (aka, “Prince”), Fernando Stredel, Tashitso, Daniel Romero, Sumudu and Thilina de Silva. And of course, the great external visitors from my

homeland: Guto Hashimoto and Vivian Ribeiro. Thank you for being such an energetic and fun group to work with. That made science and waking up at 7:30AM, easier!

I am extremely grateful to the institutions and individuals who provided specimens and tissues for this study. Thank goes to Dr. Ed Riley (TAMU), Dr. Michael Geiser (BNHM), Dr. Max Barclay (BNHM), Dr. Phillip Perkins (MCZ), Dra. Cibele Ribeiro-Costa (DZUP), Dra. Sonia Casari (MZSP), Dr. Dmitri Lugonov (MM), Dr. Lech Borowiec (DBET), Dr. Lee Herman (AMNH), Dr. Antoine Mantilleri (MNHN), Dr. Ricardo Mermudes (DZRJ), Dr. Miguel Monné (MNRJ), Dr. Johannes Bergsten (SMNH), Dr. Shawn Clark (BYU) and Dr. Olof Biström (MZH).

Special thanks goes to the tortoise-beetle researchers: Dr. Lech Borowiec, Dra. Jolanta Świętojańska, Dr. Lukas Sekerka, Dr. Fernando Frieiro, Michele Leocádio, Paula Akeho, Dr. Choru Shin and Sara Li. Without your insightful comments and help, this crazy and unique group would not have received the appropriate treatment.

For their contributions to the fieldwork research, I thank the team of friends that assisted with fieldwork in Brazil and the Dominican Republic: Antonio Tosto; Carlos De Soto Molinari; Claydson de Assis; Juan P. Botero; Mario Cupello; and Rob van Brussel. Without you, my dissertation wouldn't be possible! Especially to Claydson de Assis, who besides helping me on fieldwork, also provided unconditional guidance and support throughout my dissertation (Brigada Clay!).

Many thanks to members of the Entomology Division, especially to Zack Falin, Jennifer Thomas and Michael Engel for your patience and always providing assistance whenever needed. I extend thanks as well to the friends and colleagues made throughout the years, for their assistance and guidance: Steve Davis, Laura Breitkreuz, Mabel Alvarado, Sofia Munoz, Baruch Arroyo,

Victor Gonzales, Stephen Baca, Grey Gustafson, Emmanuel Toussaint, Jennifer Girón and Crystal Maier. I am a better scientist for having known and worked with these amazingly bright individuals. Special shout-out to Stephen Baca, who I could count for assistance, guidance, support, friendship.

I extend my special thanks to my amazing roommates, who transformed our house into a home far from home, at the "Vermont Haus". For that I thank Stephanie Crowford, Laura Breitkreuz and Mika. Thank you for all the "family dinners", conversations, discussions, movie nights, support, days and nights of friendship and most importantly, patience during difficult and stressful times. I thank Stephanie Crowford (#littleSister) for her friendship, momments of silliness, real talks, and for being such an amazing climbing partner; to Laura Breitkreuz (#bigSister), who I am immensely and deeply grateful for being such an amazing partner. Thank you for bringing Mika (#LindadaCasa) into our lives, who has been such a great source of joy and happiness. Thank you for always being there in moments of laughter or tears, health or sickness; for all the silly and serious discussions; for all internal jokes, roadtrips, endless Star Trek nights … In summary, thank you for being my partner in crime throughout this journey. Very few have the priviledge to find their best friend in a place so far from home. Thank you for making me one of those lucky bastards.

I've been very fortunate to make so many truly amazing friends outside the EEB, which helped me to keep my mental sanity throughout this journey. For that, thanks goes to "The Internationals". Special thanks to: Shannon O'Shea, Claire Jelly, Carlos Zambrana, Maulik Nariya and Gloria Funcheon for giving me support, friendship, especially during the last semester. I also

thank my friends back in Brazil for always being there for me. Special thanks to Gigi, my best friend back home.

Thanks also goes to my climbing friends: Mellissa Meyer, Cythia Siew, Andy Rhoades and Mel Ginther, with whom I've learned so much, shared laughters and pushed physical boundries. Thank you for the climbing trips, and having so much patience on sharing your immense experience with me. And thank you to reminiding me that I should not be afraid of failing, but not trying. You girls, inspire me!

Lastly, I would like to thank my family for their unconditional love and immense support. Thank you for all the visits, roadtrips, long and late Skype talks. Despite the distance, my parents, Elizabeth and William, have never measured efforts to be present throughout this long journey. Thank you for understanding and supporting the passion I have for my"other family" (that's how they refer to the Leaf-beetles back at home). Thank you for being such great role-models; and for giving me the tools to explore and define the world as I want. By handing me a shapeless and boundaryless world, you certainly shaped mine.

This work was supported by several sources of funding, including the Scholarship support from Conselho Nacional de Ciencia e Tecnologia (CNPq), Brazil (201275/2012-0) which covered my living expenses and the first four years of studies at KU. Collecting trips and museum collection visits were possible thanks to University of Kansas Entomology Endowment, University of Kansas Biodiversity Institute Panorama small grant award (Bunker Fund), and the Ernst Mayr Travel Grant in Animal Systematics, Harvard University. Molecular work was only possible due to financial support provided by the University of Kansas Entomology Endowment and Graduate Student Research Enhancement Award from the Coleopterist Society. Living expenses were also

provided by Summer Research grant from 2013-2017 from the KU Department of Ecology and Evolutionary Biology. Participation in conferences was possible thanks to financial support from the KU Department of Ecology and Evolutionary Biology, the KU Office of Graduate Studies, the KU Biodiversity Institute,

Almost six years of Ph.D. far from home was a difficult journey. However, it would have been a lot more difficult without the help, support and friendship of all those cited above. For that, I am eternally grateful.

Table of Contents

List of Tables

List of Figures

Disclaimer

All taxonomic actions in this work are hereby disclaimed for nomenclatural purposes, as recommended in Article 8 of the International Code of Zoological Nomenclature.

Introduction

Cassidinae *sensu lato* is the second largest subfamily of leaf-beetles with worldwide distribution and ca. 6300 split among 36 tribes (Bouchard *et al.*, 2011; Borowiec & Świetojańska, 2017). They present a large morphological diversity and plasticity in all life stages, with often specialized trophic interactions with flowering plants. The members of Cassidinae are generally divided into two groups, the tortoise beetles and the leaf-mining beetles, with the later accepted as a basal grade to the more derived cassidoid beetles (Borowiec, 1995; Hsiao & Windsor, 1999; Chaboo, 2007; Staines, 2014; Borowiec & Świętojańska, 2017). The subfamily monophyly is supported by three main synapomorphies. They are: 1) mouth positioned ventrally on the head; 2) antennal insertions are proximal and positioned anteroventrally on the head; and loss of tarsomere IV (Chapuis, 1874; 1875; Crowson, 1953; Chen *et al.*, 1986, Schmitt, 1989, Riley *et al.*, 2002; Chaboo, 2007).

The tortoise-beetle tribe Dorynotini Monrós and Viana, 1949 is an exclusively Neotropical monophyletic group of tortoise beetles (Borowiec 1995; Chaboo 2007) distributed from central Mexico to northern Argentina (Borowiec & Świetojańska, 2017). The tribe is presently composed by 53 species distributed in five genera: *Dorynota* Chevrolat, 1836, *Heteronychocassis* Spaeth, 1915, *Omoteina* Chevrolat, 1836, *Paranota* Monrós & Viana, 1949

and *Paratrikona* Spaeth, 1923; being the genus *Dorynota* composed by two other subgenus: *Dorynota s. str*. Chevrolat, 1836, *Dorynota* (*Akantaka*) Maulik, 1916 (Borowiec & Świetojańska, 2017).

Taxonomic history of the tribe Dorynotini

Chevrolat (in Dejean, 1836) first erected the genus *Dorynota* to include Neotropical cassids, previously described in the genus *Cassida* Linnaeus, adorned with an elytral post-scutellar projection. They were: *C. bidens* Fabricius, *C. pugionata* Germar, and *C. truncata* Fabricius.

However, most of the genera proposed in Dejean's catalogues were not used at that time. Despite being important works from a nomenclatural point of view, the catalogues of Dejean's beetle collection have created much confusion in the literature, since none of the names is formally described (Bousquet & Bouchard, 2013). Thus, in 1840 Hope described the genus *Batonota* and designated *C. bidens* as its genotype (=*Batonota bidens*); classification that was followed by subsequent authors (i.e., Boheman, 1854; Chapuis, 1875; Spaeth, 1914).

Later, Chapuis (1875) erected the tribe "Batonotites" to harbor the genus *Batanota* and its species. Batonotites was characterized by presenting a convex body; pronotum inserted in the sulcus on the anterior margin of elytra; prosternal collar slightly projected anteriorly; elytra with spiniform post-scutellar projection and metepisternum distinctly separated from the metepimeron by a stria, possessing simple pretarsal claws, basally approximated and thus, barely divergent.

In 1916, Maulik erected two additional genera, — *Akantaka* and *Trikona* — based on presence and shape of the post-scutellar projection on the elytra, and provided an identification

key, where the shape of the scutellum was also employed as a character to distinguish the three genera. Spaeth (1923) downgraded *Akantaka* to subgenus of *Batonota*, described new genera and provided key to the genera that composed *Batonotitae*: *Trikona* Maulik (=*Omoteina* Chevrolat); *Paratrikona* Spaeth; and *Batonota* Hope. In 1940, Barber & Bridwell reviwed the validity of Dejean's names and *Dorynota* was recognized as valid generic name for the taxon.

Monrós & Viana (1949) revalidate the group for which previous authors have used the name "Batonotites", by creating a new tribe Dorynotini, which he characterized on the disposition of the tarsal claws parallel and little divergent, with one of them being absent, pronotum inserted between the elytra and the last with a narrow and vertical tuberculum in the disc, next to the suture. In this same work, described the genus *Paranota* and recognized six more genera to the tribe: *Eremionycha*, Spaeth, 1911, *Omoteina* Chevrolat, 1836, *Heteronychocassis* Spaeth, 1915, *Dorynota* Chevrolat, 1836, *Paratrikona* Spaeth, 1923 and *Akantaka* Maulik, 1916.

In 1952, Hincks downgraded *Akantaka* to subgenus of *Dorynota* synonymized the genus *Trikona* with *Omoteina*, and recognized *Akantaka* as subgenus of *Dorynota*, classification that was accepted in herein works (Borowiec, 1999; Borowiec & Świętojańska, 2017). Borowiec (1999) transferred *Eremionycha* to the tribe *Cassidini* Gyllenhal, 1913, in his catalog resulting on the currently composition of the tribe.

Cladistic status of Dorynotini

Cladistic analysis based on adult morphology (Borowiec, 1995; Chaboo, 2007) and molecular data (12S mtDNA; Hsiao & Windsor, 1999), have supported the monophyly of the

Dorynotini. Members of the tribe are morphologically characterized by the disposition of tarsal claws parallel or little divergent, symmetric or asymmetric, pronotum inserted between the elytra and elytral suture distinctly adorned with a tubercle or a narrow vertical spine. The genera of the tribe were grouped mostly based on the presence or absence of the spine/tubercle, forming five conspicuous recognizable morphotypes. However, phylogenetic relationships among genera remain unresolved, and insight about the origin and function of the elytral spine/tubercle, remains poorly known.

Evolutionary scenarios proposed for the tribe

Across the clade, a latitudinal gradient in the size and shape of the post-scutellar tubercle/spine has been noted, with a posited increase in height and decrease in width associated with cooler areas of the tropics (Spaeth, 1923). The presence of this It was further suggested that environmental gradients across the clade's distribution drove the diversification of the clade (Spaeth, 1923). Geographically, the basal lineages are restricted to the Greater Antilles (*Omoteina* Chevrolat, 1836 and *Paratrikona* Spaeth 1923) and the Amazon Basin region (*Akantaka* Maulik 1916), whereas the most derived lineage occurs throughout the Neotropics, with its diversity concentrated in the southern part of the tribe's range. These patterns need to be examined in greater detail to illuminate influences of climatic factors on the clade's distribution, and to consider potential drivers of the group's morphological and ecological diversity.

In the chapters presented here, I provide a holistic approach to understand the mechanisms underlying the conspicuous morphological differentiation within the tribe, focusing on morphology, systematics and ecological biogeography.

In Chapter 1, 2, 3 and 4, species-level taxonomic revision of four genera of the tribe was conducted, to allow derive decisions about species delimitation; patterns of species distribution, morphology and ecology. The subgenus *Dorynota s. str*. Chevolat, and genera *Heteronychocassis* Spaeth, *Paranota* Monrós and Viana, and *Paratrikona* Spaeth are revised. Identification key, redescription of species and updated distributional records are provided, and to *Paranota* the morphology of the male and female genitalia of selected species are also supplied. As result of these revisions, *Paranota* now contains five species, with eleven new distributional records; *Dorynota s. str*. now includes eighteen species, three of which are newly described — *Dorynota* (*s. str*.) *monneorum* Simões & Sekerka 2016, *Dorynota* (*s. str*.) *borowieci* Simões & Sekerka 2016, and *Dorynota* (*s. str*.) *wappesi* Sekerka & Simões 2016 — with thirty-five new distributional records reported; and *Paratrikona* is now composed by seven species, with one newly described species described from Cuba — *Paratrikona blakeae* Simões, 2017— and two new distributional records.

In Chapter 1, the genus *Heteronychocassis*, that had never been revisited before, only mentioned in catalogs (Borowiec, 1999, Borowiec & Moragues, 2005, Borowiec & Świętojańska, 2014) and is only known from its type specimen is redescribed (Simões & Sekerka, 2014).

In chapter 2, the genus *Paranota* is revised, *P. apiculata* (Boheman 1854) comb. nov. was transferred from the genus *Dorynota*; *P. rugosa* (Wagener, 1881) stat. rev. et comb. nov. is resurrected from synonymy with *P. ensifera* (Boheman, 1854); and *P. parallela* (Blanchard, 1837) is found to not be a member Paranota and transferred to the genus *Dorynota*. Currently, *Paranota* contains five species. Ten new distributional records were provided for four species. Morphology of the male and female genitalia of selected species was reviewed in detail, and key to species

supplemented with color photographs of types and diagnostic characters were provided (Simões, 2014).

In chapter 3, the nominotypical subgenus of *Dorynota* was revised and now contains eighteen species. Three new species were described: *Dorynota* (s. str.) *moneorum* Simões & Sekerka, new species and *Dorynota* (s. str.) *borowieci* Simões & Sekerka, new species from Brazil, and *Dorynota* (s. str.) *wappesi* Sekerka & Simões, new species from Bolivia. Two new synonyms were proposed: *Dorynota* (s. str.) *aculeata* (Boheman, 1854) = *Dorynota* (s. str.) *pubescens* (Blake, 1939), new synonymy and *Dorynota* (s. str.) *cornigera* Boheman, 1854 = *Dorynota* (s. str.) *bellicosa* Boheman, 1854, new synonymy. *Dorynota* (s. str.) *pugnax* Boheman, 1854, restored status is resurrected from synonymy with *Dorynota* (s. str.) *nodosa* (Boheman, 1854). Thirty-five new country and region records were reported for ten species. A key to species, supplemented with color photographs of all species was provided (Simões & Sekerka, 2015)

In Chapter 4, the genus *Paratrikona* is revised. One new species is described from Cuba: *Paratrikona blakeae* Simões, 2017. An updated identification key to the species of the genus and new distributional records are also provided.

In Chapter 5, I present a phylogenetic reconstruction to investigate the homology of the elytral tubercle within the tribe Dorynotini. Our analyses include five of the six genera and subgenera of the tribe, and are based on 89 discrete morphological characters and DNA sequence data from three gene regions. Phylogenetic relationships were inferred using Bayesian methods, maximum likelihood and maximum parsimony. Both molecular and morphological analyses support the monophyly of Dorynotini as well as two of its six genera and subgenera (*Paranota* and subgenus *Akantaka*). The subgenus *Dorynota s. str*. is recovered as paraphyletic; and the inclusion of only a single species of *Paratrikona* did not allow a test of its monophyly. The

species endemic to the Greater Antilles were recovered as a monophyletic clade, composed of three distinct morphotypes and currently placed in separate genera. Our results indicate that the morphological characters that currently define dorynotine taxa are homoplastic and require re-evaluation guided by molecular analyses. Such a basis would allow for a more accurate classification and improved understanding of Dorynotini systematics and evolution.

Finally, in chapter 6 I test the only hypothesis posed y Spaeth (1923), to explain the morphological diversity within the group. In this chapter, I test whether the presence and size of the vertical spine is correlated with environment conditions. For that, I use an approach based on ecological niche modeling and morphological and environmental hypervolumes. The degree of overlap between the respective hypervolumes was assessed, and the correlation of matrix overlap values was quantified using Mantel tests. Degrees of niche similarity and conservatism at the genus level were also assessed using both Schoener's index and Hellinger distances. Results indicated that morphological divergence occurs along with high levels of environmental overlap; and perhaps historical biogeography, adaptive value for biotic, as opposed to abiotic, factors might have promoted the morphological diversification within the clade.

Chapter 1:

REDESCRIPTION OF *HETERONYCHOCASSIS ACUTICOLLIS* SPAETH, 1915 (COLEOPTERA: CHRYSOMELIDAE: CASSIDINAE)[1]

[1]Simões, M.V. and Sekerka, L. (2014) Redescription of *Heteronychocassis acuticollis* Spaeth, 1915 (Coleoptera: Chrysomelidae: Cassidinae). *The Coleopterists Bulletin*, 68, 407–410.

Abstract

The monotypic genus *Heteronychocassis* has never been redescribed, only mentioned in catalogs and is only known from its type specimen. In this note the species *H. acuticollis* is redescribed and its taxonomic placement discussed.

Introduction

Spaeth (1915) described the genus *Heteronychocassis* for a single species, *H. acuticollis* Spaeth, 1915. In his view, the genus is the closest relative of *Eremionycha* Spaeth, 1911 and that both belong to the group Batonotites (= Dorynotini Monrós and Viana, 1949). The genus has never been redescribed, only mentioned in catalogs (Borowiec 1999, Borowiec and Moragues 2005, Borowiec and Świętojańska 2014) and is only known from its type specimen. The exception is Monrós and Viana (1949), who made a key for genera of Dorynotini and placed *Heteronychocassis* in it, based on the primary description. In this note the species *H. acuticollis* is redescribed.

Results

Taxonomy

Heteronychocassis Spaeth, 1915

Heteronycocassis Spaeth, 1915: 285 (type species: *Heteronychocassis acuticollis* Spaeth, 1915 by monotypy); Blackwelder, 1946: 747 (catalog); Monrós and Viana, 1949: 425 (key to Dorynotini genera); Hincks, 1952: 334 (overview of Cassidinae tribes and genera); Seeno and Wilcox, 1982: 174 (catalog); Borowiec, 1999: 166 (catalog); Borowiec and Moragues, 2005: 263 (catalog).

Heteronychocassis acuticollis Spaeth, 1915
(Figs. 1.1–1.9)

Heteronychocassis acuticollis Spaeth, 1915: 286 (original description); Blackwelder, 1946: 747 (catalog); Monrós and Viana, 1949: 426 (catalog); Borowiec, 1999: 166 (catalog); Borowiec and Moragues, 2005: 263 (catalog).

Type material (Figs. 1–9). Holotype (by monotypy), glued: 'Guyane Française | Charvein [white, printed and cardboard label] || Type [pink, printed and cardboard label] || Archard | don. 14 || acuticollis | m. Typ. unic! | Spaeth det. [white, printed and cardboard label] || Manchester Museum | Holotype [pink, printed and cardboard label]'.

Type locality**.** Charvein (circa 5°34.5′ N, 53°53.7′ W, 10-30 m a.s.l.) is former French prison named Camp Carvein situated in Mana commune, arrondissement of Saint-Laurent-du-Maroni in French Guyana.

Redescription**.** Measurements. Total length: 8.7 mm; greatest elytral width: 7.7 mm; pronotum length: 2.0 mm; greatest width of pronotum: 5.5 mm.

Body (Figs. 1.1–1.2, 1.4) subtriangular, around 1.2 times longer than wide. Integument glabrous, except for extremely short setae and sparse setae on pronotum and ventral side. Ground color brown with anterior margin of pronotum, mid–region of elytral margin and elytral disc brownish–yellow and antennomeres V–XI dark–brown and I–IV light–brown.

Antenna with scape, pedicel, II-III glabrous with sparse long setae, antennomeres IV–XI with long and dense setae. Length ratio of antennal segments 100:40:60:84:68:76:85:68:68:84:132, with XI tapered towards apex. Inter–ocular distance 1.3 wider than widest width of eye. Coronal suture deep. Eyes (Fig. 1.5) subrounded, around 2.05 times longer than wider; Frontoclypeous (Fig. 15) as wide as long, open and elevated at the apex,

depressed medially with short, with complete epistomal suture and incomplete mid–suture; labrum (Fig. 1.5) medially elevated and sinuous anterior margin.

Pronotum (Fig. 1.1) trapezoidal, two times wider than long, with sharp sides; anterior margin continuous, covering the head completely in dorsal view; lateral margins sharp; basal margin bisinuate and posterior angle truncate; disc convex, with shallow depression close to posterior angle, and finally punctate. Prosternum with glabrous and smooth surface, with narrow elevation; process (Fig. 1.5) 1.5 times longer than wide, depressed and rounded apex.

Mesosternum glabrous; mesosternal process deeply notched; mesepimeron with exposed portion closing mesocoxae cavity. Scutellum appears to be triangular. Elytra continuous with pronotum, slightly longer than wide, with the widest region at the anterior third; basal margin smooth; antero–lateral angle rounded and projected anteriorly. Humeri smooth and round moderately protruded. Disc regularly convex, with two shallow principal impressions at anterior third close to suture; on dorsal view, coarse punctuation in discontinuous rows with fine and disordered punctuation in the intervals, denser close to suture and principal impressions; on lateral view, humeri followed by deep and straight notch and row of coarse punctures. Explanate margins moderately broad, in the widest part half the width of disc, smooth and shiny. Epipleura (Fig. 1.7) continuous, with two deep cavities, one short anteriorly to deep notch following the humeri, and another after, not reaching apex. Metasternum smooth, with mid-region elevated.

Sternites length ratio 100:66:60:60:66. Legs sparsely and finely setose at tibial apex; trochanters triangular, with sparse and short setae; femur slightly wider and grooved at anterior half, with sparse and long setae; tibia longer than femur, wider towards the apex, densely setose. Tarsomeres with long and dense setae; I with subparallel lateral margins, II–III bilobed, with

long and sparse setae. Proclaws (Fig. 1.8) with single large basal tooth, meso- and metaclaws (Fig. 1.9) asymmetrical, with inner claw half the length of outer.

Geographic Distribution. French Guyana (Spaeth 1915).

Figure 1. 1–1.9. *Heteronychocassis acuticollis* Spaeth, 1915 (holotype). 1.1, dorsal habitus; 1.2, ventral habitus; 1.3, labels; 1.4, lateral habitus; 1.5, ventral view of prosternum, arrows indicating frontoclypeus and labrum; 1.6, frontal view, anterior margin of elytra; 1.7, ventral view of elytra, arrow indicating epipleura; 1.8, claw of protarsus; 1.9, claw of mesotarsus.

Discussion and Conclusions

Chapuis (1875) erected the group Batonotites, composed of a single genus *Batonota* Hope, 1840, that later would be split into several genera (Spaeth 1923). He defined Batonotites as having the metepisternum distinctly separated from the metepimeron by a stria and possessing simple tarsal claws, basally approximated and thus barely divergent. The supplemental characters used by Chapuis included: a convex body; the pronotum inserted in the notch at the anterior margin of elytra; the prosternum slightly projected anteriorly; the elytra with a spinose projection; and the metepisternum distinct.

Maulik (1916) divided *Batonota* into three genera based on the general shape and form of the dorsal spine: *Batonota* (species with trapezoidal scutellum, long dorsal spine and lateral sides of the elytra concave), *Akantaka* Maulik, 1916 (species with trapezoidal scutellum, short dorsal spine and lateral sides of the elytra straight), and *Trikona* Maulik, 1916 (species with triangular scutellum and very deeply punctate elytra).

Spaeth (1923) summarized the characters which separate *Batonota* (*s. lato*), made note of the structure of tarsal claws as unique within all Cassidinae, and revised genera close to *Batonota*. As a result, he downgraded *Akantaka* to a subgenus of *Batonota* and additionally described a new genus *Paratrikona* Spaeth, 1923 for species included formerly in *Trikona* (later recognized as a junior objective synonym of *Omoteina* Chevrolat, 1836), with the exception of *T. humeralis* (Olivier, 1808), and provided a key to the genera.

Later, Monrós and Viana (1949) proposed a new substitute name, Dorynotini, for Batonotites because the latter was based on junior synonym and included seven genera: *Akantaka* Maulik, 1916 (now considered as a subgenus of *Dorynota*); *Dorynota* Chevrolat 1836 (senior objective synonym of *Batonota* Hope, 1840); *Eremionycha* Spaeth 1911;

Heteronychocassis Spaeth, 1915; *Omoteina* Chevrolat, 1836; *Paranota* Monrós and Viana, 1949; and *Paratrikona* Spaeth, 1923. Since that time, the name Dorynotini has had prevailing usage and was conserved by all subsequent authors (e.g. Hincks 1952, Borowiec 1999). Monrós and Viana (1949) characterized Dorynotini as having the following combination of characteristics: the head covered by the pronotum; the pronotum inserted in a notch at the anterior margin of the elytra; the epipleura projected; the elytra with tubercle or spine projection close to elytral suture; and tarsal claws parallel or slightly divergent, sometimes with one of them reduced or absent.

They also provided a key to the genera of the tribe. In the key, the genus *Heteronychocassis* was characterized by the following combination of morphological features: subtriangular body, with the widest body width close to humeri; the antennae with four basal antennomeres glabrous and seven pubescent apical antennomeres; head not visible from above; elytra without spinose projection; and each tarsus with a pair of non-divergent and asymmetrical claws. However, this does not correspond with the morphology of the type specimen of *H. acuticollis*, which shows protarsal claws with a single large basal tooth, while the meso- and metatarsal claws are paired, asymmetrical, with inner claw half the length of the outer. Almost certainly Monrós and Viana did not examine the actual type specimen, because the Spaeth collection was at that time inaccessible. So they placed *Heteronychocassis* in the key based on the original description, which does not describe the protarsal claw as single.

Hincks (1952) retained the genus within Dorynotini and used the structure of tarsal claws as the main characteristic to separate the tribe.

So far the genus is still known only from the holotype specimen, which was unfortunately heavily damaged during loan (Lech Borowiec and Dmitri Logunov, pers. comm.). One of the authors (LS) salvaged the specimen in 2008 and glued all parts together to get an idea about the

general shape and prevent future loss of fallen parts. Some legs and antennae were glued to a separate card pinned under specimen. Fortunately, the crucial morphological features for identification were preserved. The structure of tarsal claws is typical for Dorynotini with the meso- and metatarsi having two proximate claws, with the inner claw being shorter. The basally proximate asymmetrical tarsal claws are unique features within Cassidinae s. str. (otherwise present only in a several genera of Old World hispines) and thus most likely represents a synapomorphy for Dorynotini. Within Dorynotini *Heteronychocassis* is unique, as it is the only genus which lacks a postscutellar tuberculate or spiniform projection.

Bibliography

Blackwelder RE. 1946. Checklist of the coleopterous insects of Mexico, Central America, the West Indies and South America. Part 4. *Bulletin of the United States National Museum* 185: 551–763.

Borowiec L. 1999. A world catalogue of the Cassidinae (Coleoptera: Chrysomelidae). Biologica Silesiae, Wroclaw, Poland.

Borowiec L, Świętojańska J. 2014. World catalog of Cassidinae. Available from: <www.biol.uni.wroc.pl/Cassidinae/catalog%20internetowy/index.htm> (8th February 2014).

Borowiec L, Moragues G. 2005. Tortoise beetles of the French Guyana – a faunistic review (Coleoptera: Chrysomelidae: Cassidinae). *Genus* 16: 247–278.

Chapuis F. 1875. Famille des phytophages [pp. 1–420]. *In:* Histoire naturelle des insects, Genera des Coléoptères ou exposé méthodique et critique de tous les genres proposes jusqu ici dans cet order d'Insectes, Volume 2 (T. Lacordaire, editor). Roret, Paris.

Dejean PFMA. 1836. Catalogue des Coléoptères de la collection de M. le Comte Dejean. [Livraison 5]. Méquignon-Marvis, Paris, 361–443.

Hincks WD. 1952. The genera of the Cassidinae (Coleoptera: Chrysomelidae). *Transactions of the Royal Entomological Society of London* 103: 327–358.

Hope FW. 1840. The coleopterist's manual, part the third, containing various families, genera, and species of beetles, recorded by Linnaeus and Fabricius. Also, descriptions of newly

discovered and unpublished insects. J. C. Bridgewater, and Bowdery and Kereby, London, [5] + 191 pp. + 3 pls.

Maulik S. 1916. On Cryptostome beetles in the Cambridge University Museum of Zoology. *Journal of Zoology* 86: 567–589.

Monrós F, Viana MJ. 1949. Revision de las especies Argentines de Dorynotyni (Col. Cassidae) (Primera contribución al conocimiento de Cassidinae). Acta Zoologica Lilloana 8: 391–426.

Seeno TN, Wilcox JA. 1982. Leaf beetle genera (Coleoptera: Chrysomelidae). *Entomography* 1: 1–221.

Spaeth F. 1915. Neue Cassidinnen (Coleoptera). *Stettiner Entomologische Zeitung* 76: 265–290.

Spaeth, F. 1923. Ueber Batonota Hope. (Col. Cassid.). *Wiener Entomologische Zeitung* 40: 65–76.

Chapter 2:

TAXONOMIC REVISION OF THE GENUS *PARANOTA* MONRÓS & VIANA, 1949 (COLEOPTERA: CHRYSOMELIDAE: CASSIDINAE)[2]

[2]Simões, M.V. (2014) Taxonomic Revision of the Genus *Paranota* Monrós and Viana, 1949 (Coleoptera: Chrysomelidae: Cassidinae: Dorynotini). *The Coleopterists Bulletin*, 68, 631–655.

Abstract

The Neotropical genus *Paranota* Monrós and Viana, 1949 is revised and its species redescribed. *Paranota apiculata* (Boheman 1854) comb. nov. is transferred from the genus *Dorynota*, *P. rugosa* (Wagener, 1881) stat. rev. et comb. nov. is resurrected from synonymy with *P. ensifera* (Boheman, 1854), and *P. parallela* (Blanchard, 1837) is found to not be a member *Paranota* and transferred to the genus *Dorynota*. Following this revision, *Paranota* now contains five species. In addition, the morphology of the male and female genitalia of selected species is reviewed in detail. Identification key to species, updated distribution records, and maps are provided.

Introduction

The Neotropical tribe Dorynotini Monrós and Viana, 1949 is distributed from central Mexico to northern Argentina (Borowiec & Świętojańska, 2014). The tribe is well characterized by the narrow vertical spine that adorns the elytral suture (Monrós & Viana, 1949). It currently comprises 53 species distributed in five genera: *Dorynota* Chevrolat, 1836, *Heteronychocassis* Spaeth, 1915, *Omoteina* Chevrolat, 1836, *Paranota* Monrós and Viana, 1949, and *Paratrikona* Spaeth, 1923 (Borowiec & Świętojańska, 2014).

Paranota is among the most species-poor genera of the tribe, presently composed of only four described species, and a known distribution limited north to Bolivia and south to Argentina, though the genus is not known to be restricted to any specific biome (Borowiec & Świętojańska, 2014). Monrós and Viana (1949) characterized *Paranota* by having convex body, humeral angle less developed than in *Dorynota*, spine projection short and wide at base, but markedly distinguished by the asymmetrical tarsal claws, with the internal claw distinctly shorter than the external one, overpassing the tarsal pad.

Little is known about *Paranota* biology, with poor immature data available for only two species, *P. ensifera* and *P. spinosa* (Fiebrig, 1910; Świętojańska, 2009)**.** Host plant records for the genus indicate a close association with the plant family Bignoniaceae, mainly *Tabebuia* (Fiebrig, 1910; Monrós & Viana, 1949; Silva *et al.*, 1968; Marques *et al*., 2006), with three species recorded, *P. ensifera, P. parallela* and *P. spinosa*, being the latter also associated with the family Lecythidiaceae (Silva *et al.*, 1968). Following the work of Monrós & Viana (1949) the only treatments of *Paranota* were checklists and catalogs (Hincks, 1952; Seeno & Wilcox, 1982; Borowiec, 1999; Świętojańska, 2009; Borowiec & Świętojańska, 2014).

Taxonomic history of *Paranota*

In the first attempt to organize the multiplicity of forms within the genus *Cassida* Linnaeus, 1758, Hope (1839) erected six new genera, which differed considerably in the outward appearance: *Mesomphalia*, *Dolichotoma* (=*Cyclossoma* Guérin), *Selenis* (=*Acromis* Chevrolat), *Tauroma* (=*Omocerus* Chevrolat), *Desmonota* (=*Polychalca* Chevrolat) and *Batonota* (=*Dorynota* Chevrolat).

Cassida bidens Fabricius, 1781 was designated as the type species of *Batonota*, and *Cassida pugionata* Germar, 1824 was transferred to the genus, which was characterized by presenting prothorax with the anterior margin subrounded, elytra with anterior angles strongly expanded anteriorly, and the elytral disc with a spine projection medially at the suture. In his review of *Batonota,* Boheman (1854) transferred eleven species to the genus that had previously been placed in *Dorynota* or *Cassida*, and described fifteen new species, among them *B. ensifera*, and *B. spinosa*, totaling 28 species.

Subsequently, Boheman (1862) added six new species to the genus, with Wagener (1881) later described six additional new species, among them *B. minima* and *B. rugosa,* and provided an identification key to 45 recognized species of *Batonota*.

After the description of nine additional species by Champion (1893), Spaeth (1914) provided a list recognizing 45 species of *Batanota*. Two years later, Maulik (1916) divided the genus into three, including *Batonota*, *Akantaka* and *Trikona*, leaving *Batanota* with 19 species.

Monrós and Viana (1949) erected the genus *Paranota* in order to accommodate species under the genera *Batonota* Boheman and *Dorynota* Chevrolat. *Paranota ensifera* was designated

as the type species of the genus, and three more species were added, *P. minima* (Wagener, 1881), *P. parallela* (Blanchard, 1837) and *P. spinosa* (Boheman, 1854).

In this contribution, *Paranota* and its constituent species are redescribed, *P. apiculata* comb. nov. is transferred to the genus, *P. rugosa* (Wagener, 1881) stat. rev. et comb. nov., is resurrected from synonymy with *P. ensifera* (Boheman, 1854) and transferred to *Paranota*, and one species has its original combination is reinstated: *P. parallela* (Blanchard, 1837) = *Dorynota paralela* Blanchard, 1837 stat. rev.. The geographic range of the genus is expanded and detailed distribution maps are provided.

Materials and Methods

Specimens**.** A total of 894 adult specimens (including types) were examined for this study. Specimens were obtained from the following collections: Coleção de Entomolgia de Pe. Jesus S. Moure do Departamento de Zoologia, Universidade Federal do Paraná, Paraná, Brazil (DZUP); Department of Biodiversity and Evolutionary Taxonomy, University of Wrocław, Poland (DBET); The Manchester Museum, Manchester, U.K. (MM); Muséum National d'Histoire Naturelle, Paris, France (MNHN); Museu Nacional, Universidade Federal do Rio de Janeiro, Rio de Janeiro, Brazil (MNRJ); Museu de Zoologia da Universidade de São Paulo, São Paulo, Brazil (MZUSP); Swedish Museum of Natural History, Stockholm, Sweden (SMNH); National Museum of Natural History, Smithsonian Institution, Washington D.C., U.S.A. (USNM); Finnish Museum of Natural History, University of Helsinki, Helsinki, Finland (MZH).

Dissections and measurements. A thorough study of the exo- and endoskeleton structures of *Paranota ensifera* (Boheman, 1854) was conducted. All the species had its male and female

genitalia dissected; expect the female of *P. minima* and *P. apiculata* **comb. nov.,** due to lack specimens available for dissection. To prepare for the morphological examinations of the exo- and endoskeleton, wings, male and female terminalia were boiled in an aqueous solution of 10% potassium hydroxide (KOH) for about seven minutes. Measurements were taken from specimens in which the sex could be identified and are presented in millimeters.

Type material. The type material for all species was examined and photographed. Exact label data are given for all types; a double slash (//) divides data on different labels and a single slash (\) divides data in different rows; type localities are cited in the original spelling. The type-species is described in detail, followed by the others species in the same order as they appear in the key.

Figures and maps. Dissected structures were observed and line drawings created using an Olympus BX51 compound microscope equipped with a camera lucida. Photographs were taken using a Visionary Digital micro-photographic system with a Canon EOS 70D digital camera and Infinity K2 microscopic lens. Measurements were made with an ocular micrometer. Images were assembled using CombineZP (Hadley 2010) and plates created using Adobe Illustrator CS6. The distribution map was based on locality information provided by specimen labels and in literature records. The map was created using ArcGIS 9.0 software.

Terminology**.** Structural terminology follows Monrós & Viana (1949), Borowiec (2005) and Chaboo (2007), with exception to the following: hind wing venation, which follows Kukalová-Peck & Lawrence (2004); the metendosternite, which follows Crowson (1938) and Hübler & Klass (2013); male terminalia, which follows Mann (1988), and female terminalia, which follows Rodriguez (1994), Mann & Crowson (1996) and Borowiec & Opalińska (2007).

Results

Taxonomy

Paranota Monrós & Viana, 1949

Paranota Monrós & Viana 1949: 396; Hincks 1952: 334; Seeno & Wilcox 1982: 173; Borowiec 1999: 166.

Type species. *Batonota ensifera* Boheman, 1854 (by original designation).

Redescription. Body subquadrangular or elongate on dorsal view, with greatest width at humeral angle; short and dense setae on dorsum, except glabrous median longitudinal line on pronotum.

Head entirely concealed by pronotum. Coronal suture deep, extending to mid-frontal sulcus. Vertex depressed anteriorly, with coarse, dense punctation and sparse setae, with tumid region followed by antennal sockets. Frontoclypeus (Fig. 2.2) triangular. Eyes (Figs. 2.1–2.2) oval, 1.7 to 1.8 times longer than wide, surrounded by long and dense setae. Antennal sockets tangent to the eye margin. Antennae (Fig. 2.9) telescoped, not extending beyond the elytral length; shiny, with sparse long setae from escape to V; VI–XI with short and dense setae and XI with sparse long setae near and at the apex. Scape globose, 2.5 to 2.7 times longer than pedicel; antennomere III shortest; XI longest, 1.5 times the length of X, slightly wider medially, tapered towards apex.

Pronotum (Fig. 2.10) ellipsoidal, 1.5 to 1.8 times wider than long, with maximum at the median region; surface finely and densely punctate; anterior margin with tegument anastomosed, medially emarginated or rounded; lateral angles rounded and convergent posteriorly; posterior margin bisinuate with W-shaped posterior angle. Prosternum (Fig. 2.11) with antennal sulcus present; collar slightly protruding anteriorly with rounded edges, not covering mouth parts, followed by deep and short depression medially; process 1.5 times longer than wide, shiny, flat; lateral margins convex; apex obtuse and expanded laterally. Mesosternum (Fig. 2.13) glabrous; mesosternal process as wide as apex of prosternal process; notched medially, with truncate posterior angle; mesepimeron with exposed portion rectangular. Metasternum (Fig. 2.13) smooth and glabrous, 3.5 to 5 times longer than mesosternal process, with strong protuberance close to posterior margin. Metepisternum and metepimeron continuous; metepisternum rectangular approximately four times shorter than mesepimeron; metepimeron narrow medially, widening towards the base. Scutellum (Fig. 2.18) diamond-shaped with smooth surface.

Elytra (Figs. 2.18–2.21) ca. three times longer than prothorax; basal margin crenulate; anterior angle projected, reaching largest width of pronotum, laterally obtuse or rounded; humeral angle slightly projected anteriorly; disc with edge well-marked by coarse punctures and transverse grooves, and at the anterior third next to suture spine projection shorter than body height, flattened and ridged antero-posteriorly; lateral margins 1/3 the width of disc, with reflexed edges; apical margin subacuminated or rounded. On ventral view, epipleural ridge (Fig. 2.19) with denticle expansion projected over the metepisternum.

Legs (Figs. 2.23–2.25; 2.27–2.29; 2.31–2.33) long, slender, shiny, sparsely and finely setose at tibial apex; trochanters triangular, with sparse and short setae; femur fusiform, with smooth surface, grooved anteriorly, with sparse short setae, more concentrated at the ventral

region; tibia long and slender, slightly longer than femur, wider close to the rounded apex, apical third densely setose and with ventral distal surface broadly notched. Tarsomeres (Figs. 2.26; 2.30; 2.34; 2.37; 2.61) with sparse and long setae; I with subparallel lateral margins, II–III bilobed, with long and sparse setae; IV with parallel margins. Claws (Fig. 2.38) subparallel and asymmetrical, nails with same width, external nail distinctly longer than internal nail, directed ventrally.

Abdomen (Fig. 2.42) completely covered by elytra, shiny. Ventrite I ca. two times the length of II; III–IV subequal in size, ca. 1.5 shorter than II; V slightly longer than IV, with flat posterior margin.

Male terminalia. (Figs. 2.39–2.41; 2.52–2.56; 2.62–2.64; 2.72–2.77). Tergite VIII convex, well-sclerotized, apical margin rounded and basal margin with lateral apodemes; long dense setae. Tegmen (Figs. 2.40–2.41; 2.53–2.54; 2.63–2.64; 2.73–2.74) Y-shaped, sclerotized, with muscles completing the connection ca. base; manubrium, with truncate apex, and on lateral view, with sinuous base. Ejaculatory duct long, strongly coiled. Flagellum feebly sclerotized, with a short distal hook. Seminal vesicle slightly shorter than aedeagus. Median lobe (Figs. 2.32; 2.52; 2.62; 2.72) in a 90° angle with neck constricted dorsally; apex flat, subrounded with small projection medially, not arched ventrally or dorsally; basal orifice oval.

Female terminalia. Sternite VIII (Figs. 2.43; 2.65; 2.78) with apodeme as long as the width of sternite, narrow at base. Spermatheca (Figs. 2.44; 2.67; 2.80) U-shaped, strongly sclerotized and falcate, rounded at base, tapered continuously towards apex. Spermathecal duct long and strongly coiled.

Composition. *Paranota minima* (Wagener, 1881), *P. rugosa* (Wagener, 1881) stat. rev. et comb. nov., *P. ensifera* (Boheman, 1854); *P. spinosa* (Boheman, 1854); and *P. apiculata* (Boheman, 1854) comb. nov..

Discussion. Monrós and Viana (1949) characterized *Paranota* as showing convex body, humeral angle poorly developed, antennae with five basal antennomeres glabrous and six apical pubescent; claws not divergent and asymmetric, with the internal claw distinctly shorter than the external one, overpassing the tarsal pad.

Monrós and Viana (1949) compared *Paranota* to the genus *Dorynota* Chevrolat, and distinguished *Paranota* by having a more convex body, elytra with coarser punctures, humeral angles not as developed and spine projection with a wider base. However, some species of *Dorynota s. str.* have the same body shape, punctuation, and elytral spine projection aspect as *Paranota*, such as the one found in *D. aculeata* (Boheman, 1854), while in *Akantaka* the body is more expanded laterally, with more sparse and fine punctuation, humeral angles well developed, almost as wide as elytra, and the later with the disc adorned with a tubercle instead of a spine projection. Therefore, Monrós and Viana (1949) were probably referring to the subgenus *Akantaka*, and not *Dorynota* (*s. str.)*.

The subgenera of *Dorynota* are conspicuously different from each other. Maulik (1916) differentiated *Akantaka* from *Dorynota* (*s. str*.) by presenting short spine, and broadly explanated elytra with straight or convex lateral sides. While *Dorynota* (*s. str*.) shows a long and spine and lateral sides of elytra concave behind humeral angles. Due to the explanated elytra, *Akantaka* presents a flat shape, while *Dorynota* has a convex body shape.

Therefore, to be more accurate, *Paranota* should be compared to *Dorynota* (*s. str*.). Both present: convex body shape on lateral view; antennae with five basal antennomeres shiny and six

apical pubescent; antennal sulcus present; mesoscutum might be diamond-shaped; elytral disc with spine projection medially; epipleura deeply excavated anteriorly, and ridge with a denticle expansion projected over the metepisternum. However, *Paranota* differs from *Dorynota* for presenting pronotum slightly inserted in the internal margin the anterior elytral angle; scutellum might is exclusively diamond-shaped; tarsomere IV slightly overpassing III; claws asymmetrical and subparallel.

With the dissection of most of the species female genitalia it was possible to observe stability of this structure within the genus. Hence, I add the U-shaped spermatheca, strongly sclerotized and falcate, rounded at base, tapered continuously towards apex, as a characteristic that can contribute to the differentiation from *Dorynota*, which shows falcate spermatheca, with truncate base and posterior third abruptly tapering towards apex.

Paranota is mainly characterized by the following set of features: pronotum pentagonal, completely covering the head, with rounded lateral angles and posterior margin slightly inserted in anterior margin of elytra; prosternum with antennal sulcus present; elytra densely punctate with crenulate basal margin; scutellum diamond-shaped; antennal sulcus present, poorly-developed; prosternal collar slightly projected, followed by short deep depression; prosternal process with subparallel laterals and expanded apically; epipleural ridge with denticle expansion projected over the metepisternum; claws subparallel and asymmetrical. Plus, although only three species had the female genitalia dissected, it was possible to observe a pattern of U-shaped spermatheca within the genus.

List of examined species

Paranota ensifera (Boheman, 1854)

(Figs. 2.1–2.46, 2.99)

Batonota ensifera Boheman 1854: 166.

Batonota ensifera: Boheman 1856: 95, 1862: 238; Gemminger and Harold 1876: 3644; Wagener 1881: 46; Fiebrig 1910: 171; Spaeth 1914g: 66, 1923: 69, 1941a: 1061; Bruch 1915: 563; Maulik 1916: 583; Costa Lima 1936: 312.

Dorynota ensifera: Blackwelder 1946: 747; Borowiec 1996a: 181.

Paranota ensifera: Monrós and Viana 1949: 399, 424; Buzzi 1988: 567; Borowiec 1999d: 166, 2002a: 108, 2009f: 692; Sekerka 2004: 160; Borowiec and Moragues 2005: 275; Flinte *et al* 2009: 593; Borowiec and Takizawa 2011: 454.

Botonota gregaria: Boheman, 1854: 167, 1856: 95, 1862: 238; Gemminger and Harold 1876: 3645; Wagener 1881: 45; Spaeth 1923: 69; Monrós and Viana 1949: 399.

Batonota ensifera ab *gregaria*: Spaeth 1914g: 66.

Dorynota ensifera ab *gregaria*: Blackwelder 1946: 747.

Batonota bellator Chevrolat: Gemminger and Harold 1876: 3645 (nomen nudum).

Type material. Lectotype (Figs. 2.35–2.36): gregaria Dej.// Brasil // M. Wien // Type // Lectotype \ des. L. Borowiec // NHRS–JLKB \ 000020982 (SMNH). Paralectotype: Brasil // M. Wien // Paralectotype \ des. L. Borowiec // NHRS–JLKB \ 000020983 (SMNH).

Additional Material Examined. M. Berl. (1 spec., DBET); Instituto Oswaldo Cruz, Zona da N.O.B., Indio da Brasil, 17.X.1938 (1 spec., DBET); ARGENTINA: San Ignacio, Misiones, Letrou de L. Iguane, 1911, E. R. Wagener leg. (1 spec., MNHN); BRAZIL: “BRAZILIA”:

Dejean leg. (1 spec., DBET; 3 spec., MZH); Westerman leg. (1 spec., SMNH); Reich. Haag leg. (1 spec., MM); *Goiás*: Bananeira, 10.III.1937 (1 male, MNRJ); 10.I.1939, Zellibor-Hauff leg. (2 spec., MNRJ); Campinas (1 spec., DZUP); XII.1935, Borgmeier and S. Lopes leg. (1 female, MNRJ); Goiatuba, F. Justus Jor. leg. (1 spec., DZUP); II.1941 (2 spec., MNRJ); X.1941, J. Guerin leg. (1 spec., DZUP); II.1943, Campos Seabra leg. (1 female, MNRJ); I.1952, Campos Seabra leg. (1 spec., MNRJ); Jatahy, Donkier Coll. (5 spec., MM); Leopoldo Bulhões, XII.1933 (1 spec., MM); Minaçu, XII.1987, Monné and Roppa leg. (1 spec., MNRJ); *Mato Grosso*: Diamantina, Alto Rio Arinos, X.1983, B. Silva leg. (1 female, MNRJ); Murtinho, XI.1929, R. Spitz leg. (1 female, DZUP); Poconé, 4.XI.1988, J. Becker and O. Roppa leg. (1 male, 3 females, 3 spec., MNRJ); *Minas Gerais*: Ibiá, 20.X.1965, C.T. and C. Elias leg. (1 spec., DZUP); Passos, 28.XII.1962, Claudionor Elias leg. (1 female, 1 spec., DZUP); Pirapora, XI.1975, Seabra, Alvarenga, Roppa and Monné leg. (1 spec., MNRJ); Porto Alegre, (1 spec., DZUP); Rio Claro, IX.1947, J. C. M. Carvalho leg. (1 spec., MNRJ); Sertão da Diamantina, Faz. das Melancias, 10–11.1902, E. Gounelle leg. (7 spec., MM); Uberaba, (1 spec., DBET); VI.1924 (13 spec., DBET); *Rio de Janeiro*: Mendes, (2 spec., DBET); *São Paulo*: (2 spec., DBET); (1 spec., MM); Amparo, (1 spec., MNRJ); Engenho Coelho, 1920, A. Rionter leg. (2 males, MNRJ); BOLIVIA, Dept. Santa Cruz, Buena Vista, 400m, 1952, Campos Seabra leg. (1 spec., MNRJ); COLOMBIA, (1 spec., MM); FRENCH GUIANA, Saint–Laurent–du–Maroni (3 spec., DBET).

Measurements. Male/female. n=6/10. Total length: 9.8±10.3 / 10±11.5; greatest elytra width: 7.6±8.4 / 8.2±9.4; pronotum length: 2.7±3.0 / 3.0±3.2; greatest width of pronotum: 4.8±5.5 / 5.2±5.9.

Diagnosis. This species may be distinguished from other members of the genus by the ground color of dorsum ranging from yellowish–brown to reddish–brown, usually mottled; elytra

with humeral ridge interrupted medially; disc with dense and finer punctures, without rugose aspect.

Redescription. Body (Figs. 2.35–2.36) with ground color of dorsum ranging from yellowish–brown to reddish–brown, with pronotum always brighter and elytral disc mottled with yellow.

Head (Figs. 2.1–2.2) with inter–ocular distance 1.3 times as broad as widest width of eye. Vertex with long and short setae. Frontoclypeus tumescent, with deep punctures and long sparse setae; epistomal suture distinct and complete. Antennae (Fig. 2.9) with length ratio of segments 100: 36: 24: 44: 52: 100: 92: 76: 84: 84: 140. Mouth fossa (Fig. 2.2) with irregular shape, widest at mandibular articulating region, narrowed ventrally. Labrum (Figs. 2.3–2.4) well–sclerotized, 1.2 times wider than long; anterior half strongly flattened inward (or ventrally); anterior margin laterally indented and medially emarginated; midline ridge elevated, followed downward by two rounded shallow depressions and upward with a band of punctures ornate by setae, with striate surface, deeply and finely punctured with long sparse setae and striate. Mandible (Figs. 2.5–2.6) well sclerotized, short, robust and strongly concave; base with short and dense setae; apex with four teeth, three sharp vertically positioned at the front, and one dull horizontally positioned ventrally. Maxilla (Fig. 2.8) with cardo six times longer than wide, narrower medially; membranous lacinia, wider apically and expanded internally, with fringe-like pilosity at the apex; galea subcycilindrical, longer than lacinia, bearing dense long and short setae from base to apex, with greater concentration at the rounded apex. Maxillary palp well–developed, surpassing the galea, 4–segmented, palps with long and erect setae, palpomere I two times longer than wide, subcylindrical, 1.7 times smaller than II–III; II curved and strongly expanded apically, apex 1.5 times wider than base; III subcylindrical; IV slightly longer than III, widest medially and tapered

apex. Labium (Fig. 2.7) with post– and prementum well developed; postmentum subtrapezoidal; prementum subrectangular, with four long setae situated below labial palp; ligula well developed, semi–coriaceous, subrounded apical margin, with deep punctures and 14 long sparse setae; labial palp 3–segmented, with long sparse setae; palpomere I, shortest, 1.2 times shorter than II–III, cylindrical; II, strongly curved; III, wider medially and tapered towards the apex.

Prosternum (Fig. 2.10) with process with rare sparse and fine punctures, ca. two times longer than wide; apex medially angled and expanded laterally. Proendosternite (Fig. 2.12) sclerosed, developed with pointed projection towards the anterior region, and membranous, rounded apex projected towards posterior region of the body. Mesoscutellum (Fig. 2.18) flat, with deeply punctured close to the anterior margin; anterior lateral projections 1.25 times longer than mesoscutum; axillary cord long and straight. Mesosternum (Fig. 2.13) deeply notched with process thick, with rounded posterior margin, slightly notched. Mesendosternite (Figs. 2.14–2.15) sclerosed, with membranous and flat apex, obliquely directed to mesepimeron and fused at the apex to its internal wall. Metasternum (Fig. 2.13) smooth, with sparse and rare short setae, medially flat; metepisternum smooth anterior third with rounded lateral projection. Metendosternite (Figs. 2.16–2.17) five times wider than long; anterior tendon placed on distal dorsal wall of lamina; anterior lamina (anla) narrow and continuous; ventral lamina (vela) vestigial, ridge–like expansion along the entire posterior face of furcal arm; ventrally, with a double lobe–like tendon (vete), with base obliquely oriented, with anterolateral edge continuous with anterior edge of lamina; median ventral flange narrow and flattened laterally; stalk (stk) almost two times shorter than median region of metendosternite.

Elytra (Figs. 2.19–2.21) with anterior angle slightly obtuse externally; lateral margins subparallel; apical margin rounded; humeral ridge interrupted and poorly–marked; disc with

dense small punctures and three longitudinal ridges, two closer to suture departing from anterior margin, extending to apex, and one departing from humerus, extending to 1/3 of disc; lateral margins sub–parallel and posterior margin rounded; medially with spine projection (Figs. 20–21) 1.5 to 1.8 times shorter than the body height. On ventral view, epipleural ridge well developed with sharp projection at the anterior third, with longitudinal carena flattened and reduced at the median region. Hind wing (Fig. 2.22) with the length 2.7 times its greatest width, microtrichiate; Costa (C) reduced, restricted to basal region; Sub–costa (Sc) restricted to the wing basal third; Radius (R) only overlaps half of the wing; Radius cell closed with a subtriangular aspect; s–r evident, about as long as the radial cell; s–m vestigial; Cubitus (Cu) and Anterior Media (AM) developed, reaching the basal margin; Plical (P) developed, without ramifications; Empusal (E) united to 1st Anal (1A); transverse 2nd Anal a, Anal cell (Ac) and 2nd Anal b; Jugal (Ju) absent.

Legs (Figs. 2.23–2.34) subequal in length, slender, long, shiny, sparsely and finely setose except densely setose at tibial apex and ventral portion of tarsi. Tarsomere I short, ca. 1.5 times shorter than II; III ca. 1.5 times longer than II, and two times wider than IV. Claws (Fig. 2.38) with internal nails 1.4 times shorter than external. Abdomen (Fig. 2.42) sparsely setose, with higher concentration at the sternites V apex; sternites I–V with equal length decreasing in width towards apex and little evident ellipses depressions close to lateral margins; sternite V flattened posterior margin.

Male terminalia. (Figs. 2.39–2.41). Manubrium (Figs. 2.40–2.41) two times longer than arms, truncate apex, and on lateral view, with sinuous base. Ejaculatory duct long, strongly coiled.

Female terminalia. (Figs. 2.43–2.46) Sternite IX (Fig. 2.46) subdivided into two plates with long, erect setae at apical margin; Tergite X (Fig. 2.45) with two regions next to sclerotized

apical margin, densely setose, with a range of short and erect setae on the edge. Spermatheca (Fig. 2.44) with ampulla short and pointed. Duct of spermathecal gland 1.7 times longer than spermatheca, loose. Spermathecal gland short and narrow with output side of ampulla.

Host-plants. Recorded to *Tabebuia aurea* Benth and Hook (=*Tecoma argentea* Bureau and K. Schum), *Tabebuia impetiginosa* (Mart.) (=*Tabebuia ipe* (Mart.)) (Silva *et al.* 1968) and *Tabebuia ochracea* (Cham.) (Fiebrig 1910) (Bignoniaceae).

Remarks. Boheman (1854), in the original description, compared *Paronota ensifera* (Figs. 35–36) to *Batonota gregaria* Boheman, 1857, and differentiated it by the size and height of body, and punctuation on prothorax and elytra. Later**,** Monrós and Viana (1949) considered these differences to be intraspecific variations, and synonymized both species.

Wagener (1881) provided a key to identification of the genus *Batonota* Hope, and considered *P. ensifera* (=*Batonota ensifera* Boheman, 1854) similar to *P. spinosa* (Figs. 2.69–2.70) (=*Batonota spinosa* Boheman, 1854), but differentiate on the elytra sculpture, *P. ensifera* with carina elytra and *P. spinosa* with smooth elytra.

Monrós & Viana (1949) considered *P. spinosa* the most similar species to *P. ensifera* within the genus, differing from the latter by having robust and compact body shape, with uniform color and deep punctuation. However, although *P. ensifera* shows a more robust and compact body shape than *P. spinosa*, the deep punctuation on the dorsum is a feature of the genus, not unique to *P. ensifera*; plus, the dorsum color ranges from yellowish–brown to reddish–brown, with pronotum always brighter and elytral disc mottled with yellow, never uniform.

Paranota ensifera is similar to *P. rugosa* (Figs. 2.57–2.60) by having body not strongly convex on lateral view, elytra coarsely punctate, with anterior angle expanded and obtuse

laterally; anterior third with long spine projection, almost as long as body height. However, *P. ensifera* differs by having body with ground color of dorsum ranging from yellowish–brown to reddish–brown; epistomal suture complete; elytra with anterior angle slightly expanded laterally, and anterior half of lateral margin subparallel; humeral ridge interrupted medially; disc with dense and finer punctures, without rugose aspect; tarsomere III slightly longer than IV (Fig. 2.37), with apex almost three times wider than base. While, *P. rugosa* presents body with ground color of dorsum ranging from brownish–red to dark–red; epistomal suture incomplete; elytra with anterior angle strongly expanded laterally, and anterior half of lateral margin sinuous; humeral ridge incomplete; disc with coarser punctuation, with rugose aspect; tarsomere III as long as IV (Fig. 2.61), with apex ca. two times wider than base.

Distribution**.** Recorded to Argentina (Chaco, Corrientes, Misiones, Salta), Bolivia (Guarayos), Brazil (Goiás, Mato Grosso, Rio de Janeiro, São Paulo), Ecuador, Paraguay (Alto Parana, Cerro Cora, Dept. Central, Naranjo, Ybycui), and to Peru **(**Borowiec and Świętojańska 2014). New to Brazil (Minas Gerais), Colombia and French Guiana (Fig. 2.99).

Figures 2. 1–2.9. *Paranota ensifera* (Boheman, 1854) (male). 1–2, head: 1, dorsal view; 2, frontal view; 3–4, labrum: 3, dorsal view; 4, anterior margin; 5–6, mandibles: dorsal view; 6, lateral view; 7, labium, ventral view; 8, maxillae, dorsal view; 9, antenna. Scale bars = 1mm.

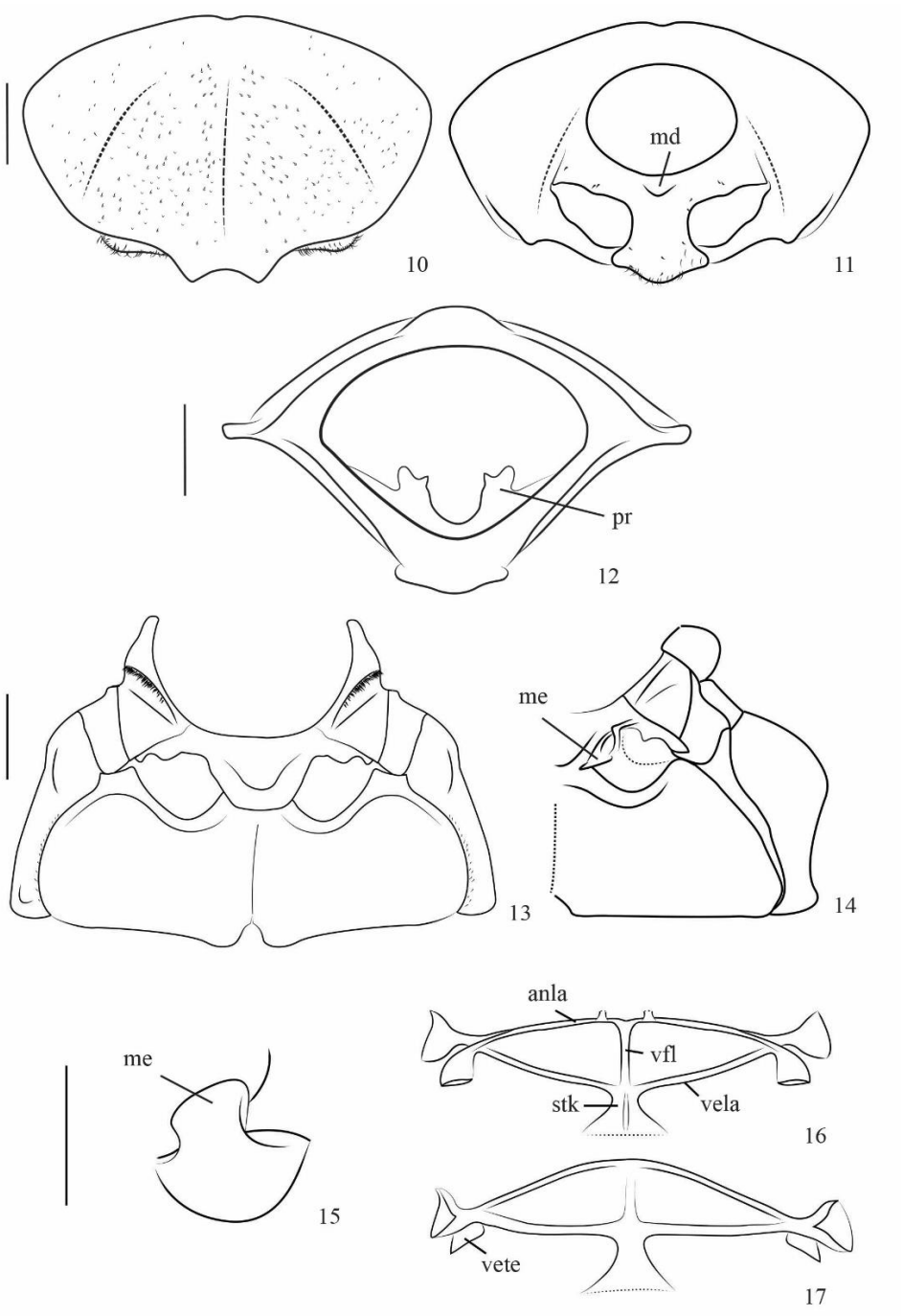

Figures 2.10–2.17. *Paranota ensifera* (Boheman, 1854) (male). 10–11, prothorax: 10, dorsal view; 11, ventral view; 12, proendosternite; 13, meso– and metasternum; 14–15, mesoendosternite: 14, general; 15, detail; 16–17, metendosternite: 16, dorsal view; 17, ventral view (anla, anterior lamina; md, median depression; me, mesendosternite; pr, proendosternite; stlk, stalk; vela, ventral lamina; vete, ventral tendon; vfl, median ventral flange). Scale bars = 1mm.

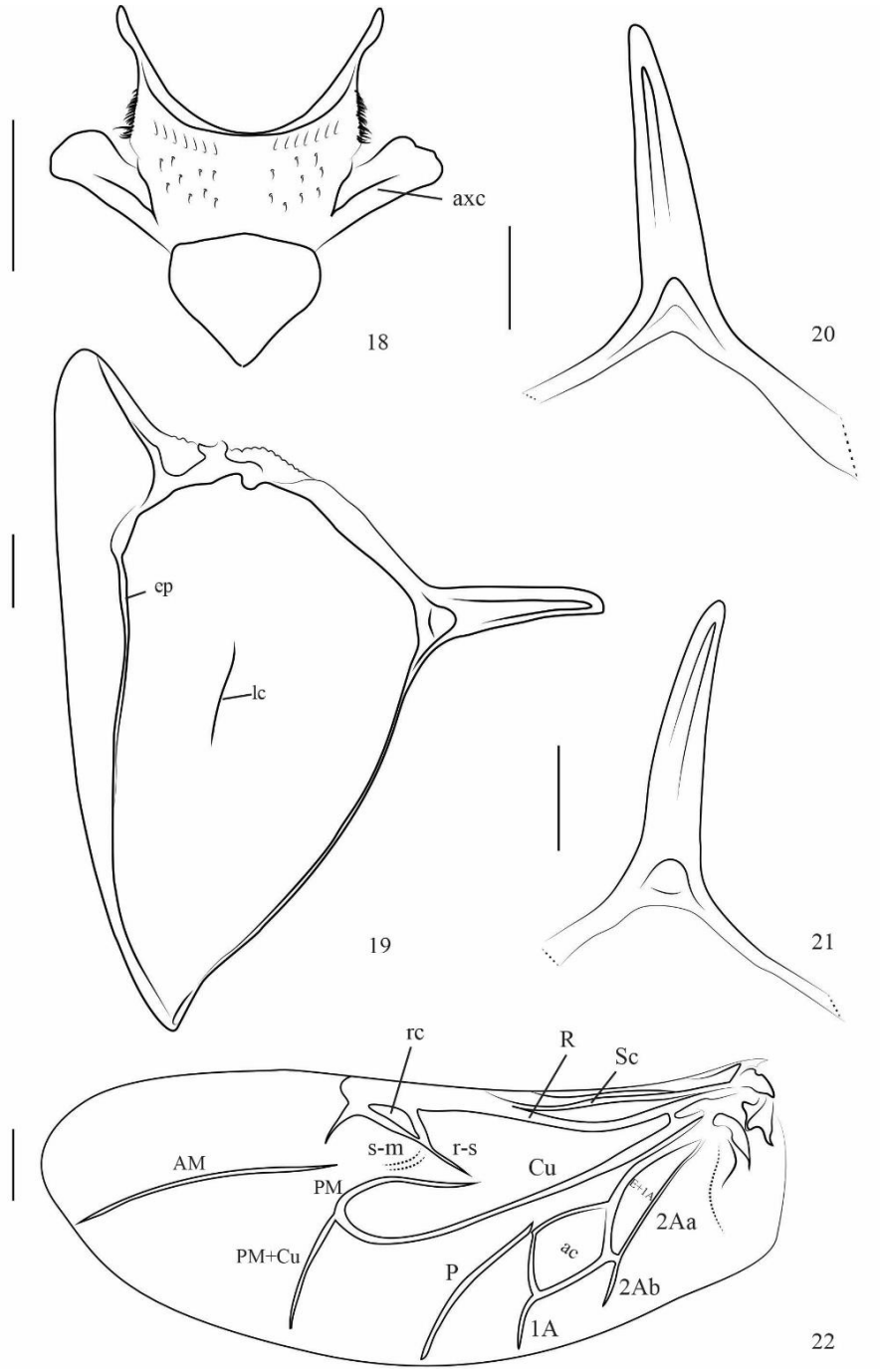

Figures 2.18–2.22. *Paranota ensifera* (Boheman, 1854) (male). 18, mesoscutum and scutelum, general aspect; 19–21, elytra: 19, ventral view; 20–21, spinose projection: 20, left internal view; 21, right internal view; 22, wing (ac, anal cell; AM, Anterior Media; axc, axillary cord; C, Costa; Cu, Cubitus; Ju, Jugal; lc, longitudinal carena; E, Empusal; ep, epipleura; PM, Posterior Media; P, Plical; R, Radial; rc, Radius cell; Sc, SubCosta; 1A, 1st anal; 2Aa, anterior branch of A; 2Ab, posterior branch of 2A). Scale bars = 1mm.

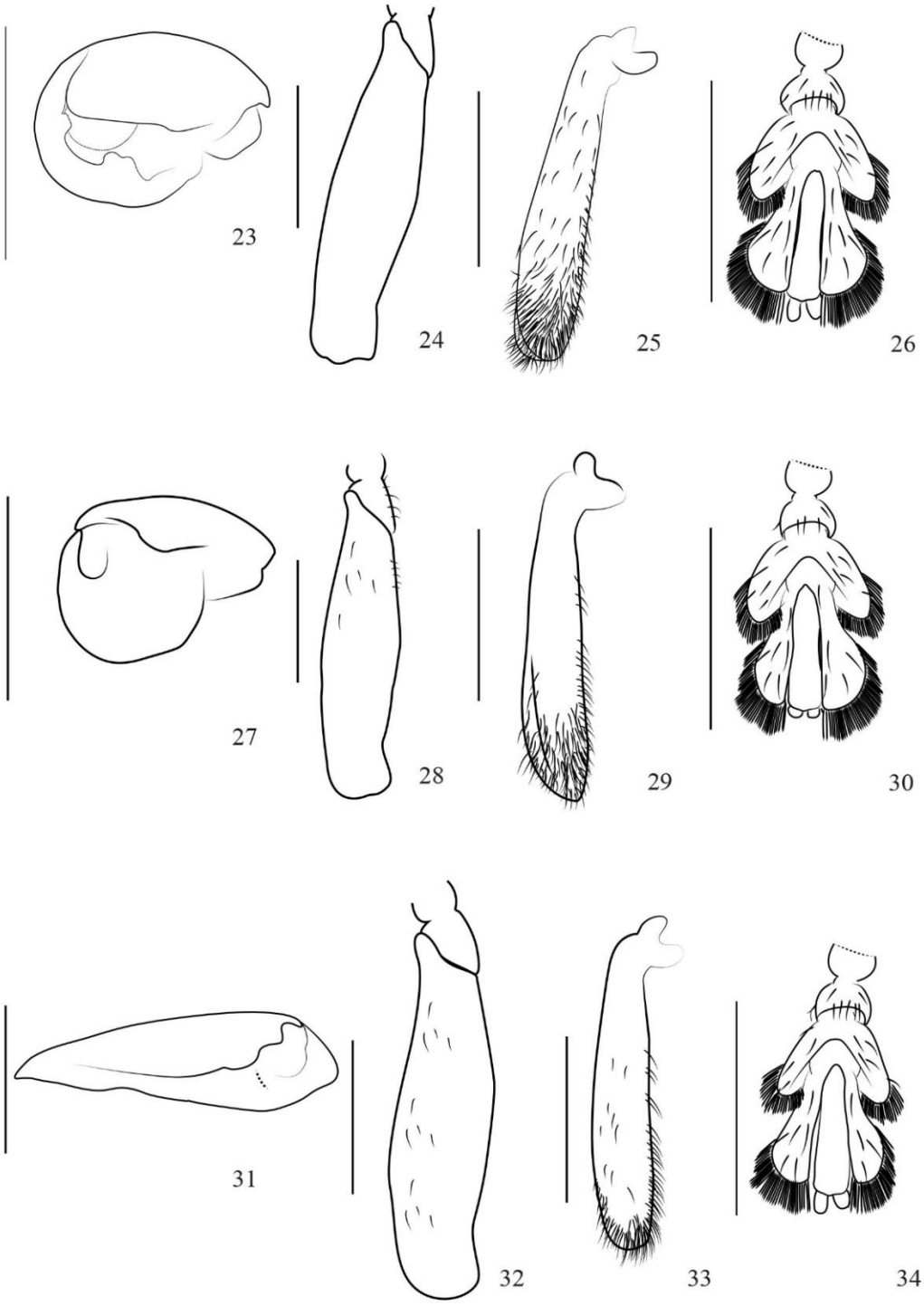

Figures 2..23–2.34. *Paranota ensifera* (Boheman, 1854) (male). 23, procoxa; 24, profemur; 25, protibia; 26, protarsomere; 27, mesocoxa; 28, mesofemur; 29, mesotibia; 30, mesotarsomere; 31, metacoxa; 32, metafemur; 33, metatibia; 34, metatarsomere. Scale bars = 1mm.

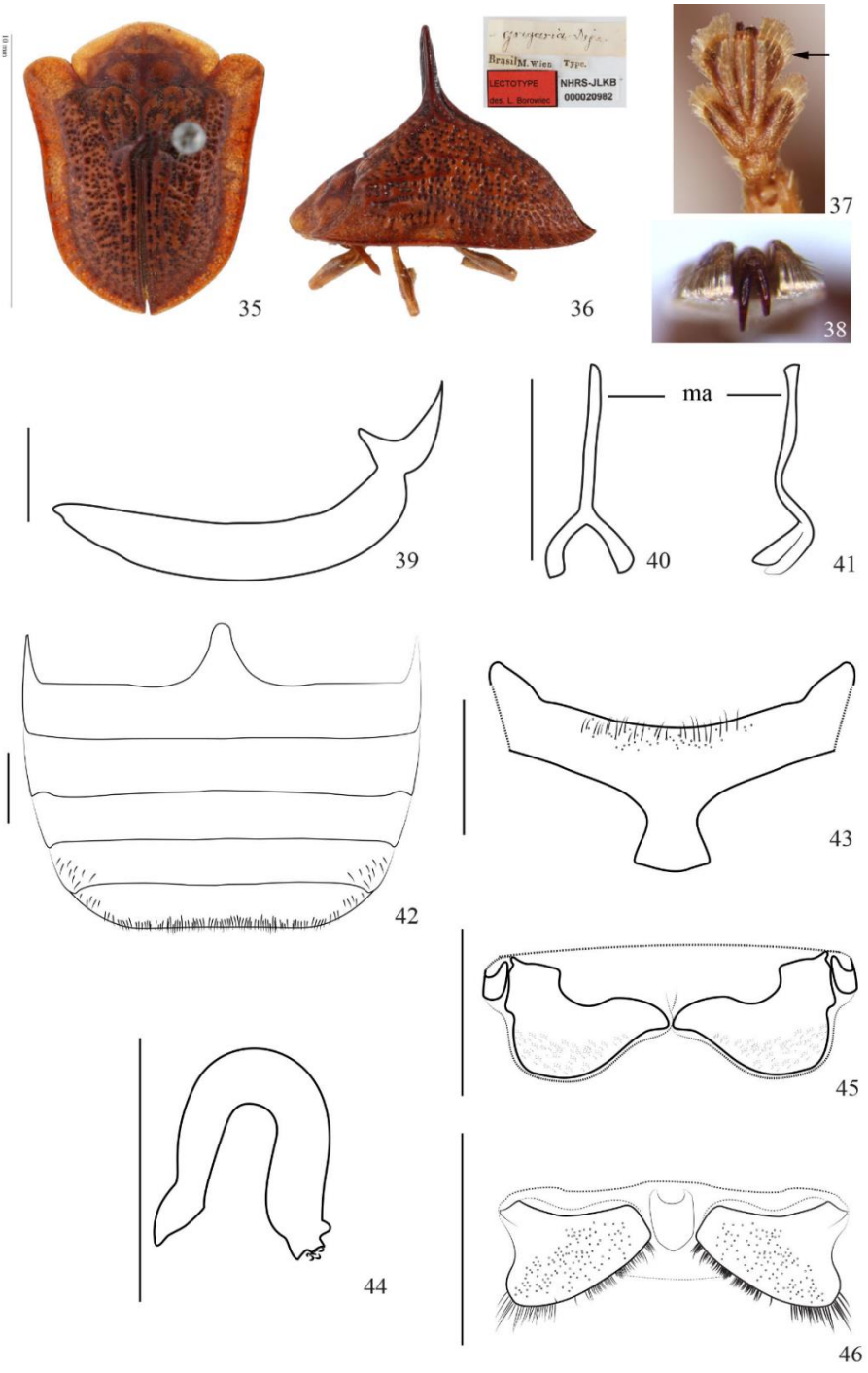

Figures 2.35–2.46. *Paranota ensifera* (Boheman, 1854). 35–36, lectotype: 35, dorsal view; 36, lateral view and labels; 37, protarsomere; 38, claws; 39, median lobe, lateral view; 40–41, tegmen: 40, dorsal view; 41, lateral view; 42, female abdomen; 43, sternite VIII; 44, spermatheca; 45, tergite X; 46, sternite IX. Scale bars = 1mm.

Paranota minima (Wagener, 1881)

(Figs. 47–56, 100)

Batonota minima Wagener 1881: 42, 46; Spaeth 1914g: 66 1923: 69; Maulik 1916: 583.

Dorynota minima: Blackwelder 1946: 747.

Paranota minima: Monrós and Viana 1949: 397, 425; Borowiec 1999d: 167.

Type material. Holotype (Figs. 49–51): Paraguay // Typus // minima \ coll. Wagener \ typus // Manchester Museum \ M/ CR MUS. SPAETH COLL. // Manchester Museum \ Syntype // F2019.2658 (MM).

Additional material examined**.** ARGENTINA, *Barrancas*: Provincia de Santiago del Estero, E.R. Wagner leg.(1 spc, MNHN); *Formosa*: Clorinda, IX.1949, A. Martinez leg. (1 male, USNM); PARAGUAY, (1 male, MM); *Monte Lindo*: XI.1993 (1 male, 1 female, DBET).

Measurements. Male/female. n=3/1. Total length: 6.9±7.5 / 9.0; greatest elytra width: 5.7±6.4 / 7.6; pronotum length: 1.7 / 2.6; greatest width of pronotum: 4.0±4.5 / 5.0.

Diagnosis. This species may be distinguished from other members of the genus by showing ground color dark–red, body of diminutive size and strongly convex on lateral view and humeral ridge complete and well–marked.

Redescription. Body (Figs. 47–50) strongly convex on lateral view, with shiny tegument, dark–red dorsally, except for half–moon black spots on posterior half of pronotum, and yellowish brown ventrally, except for antennomere VI–XI reddish brown, lateral margins of

prosternal process, lobe of hypomeron, mesepisternum, anterior and lateral margin of metasternum, metepimeron and anterior margin of sternites dark brown.

Head with inter–ocular distance 1.3 shorter than widest width of eye. Coronal suture depressed at the start. Vertex with short and sparse setae. Frontoclypeus flat, with mid–frontal and epistomal sulcus incomplete. Inter–antennal distance two times shorter than antennal sockets. Antennae with length ratio of antennal segments 100: 95: 25: 50: 65: 75: 75: 65: 80: 85: 105.

Prosternal process with apex 1.8 times wider than median region, notched medially, three times shorter than prosternal process, with truncate posterior angle. Mesepimeron with exposed portion rectangular, ca. two times wider than long.

Elytra with dense and coarse punctation; anterior angle strongly obtuse externally with reflexed margins; humeral ridge complete and well–marked; disc with three longitudinal ridges, two closer to suture, departing from anterior margin, meeting at the posterior third of disc and extending to posterior margin, and one departing from humerus, extending to 1/3 of disc. Lateral margins subparallel, ca. 1/5 width of disc, with reflexed edge; apical margin rounded. Disc with spine projection ca. 1.3 times shorter than body height. On ventral view, epipleural ridge well developed with rounded denticle projection at the anterior third.

Abdomen with sternites glabrous; III–V subequal in length 1.3 times shorter than II; V with flat posterior margin. Tarsomere II 1.3 times longer than I. Claws with left nail 1.6 times longer than right nail.

Male terminalia (Figs. 52–56) same as described to *P. ensifera* (Fig. 2.39), except for tegmen (Figs. 53–54) with manubrium, two times longer than arms.

Variation. The inter-ocular distance varies from 1.2 to 1.4 shorter than widest width of eye.

Remarks**.** Wagner (1881) and Monrós and Viana (1949) highlight the diminutive size and convex shape of the body, features that distinctly characterize the species from the others in the genus. Monrós and Viana (1949) compared it to *P. ensifera* (Figs. 35–36), and considered that the body color and elytra shape were similar. However, *P. minima* (Figs. 47–50) presents body ground color dark–red, and the most internal ridges of elytra meet at the posterior third of disc and extend to posterior margin. While *P. ensifera* presents body with ground color of dorsum ranging from yellowish–brown to reddish–brown; and the most internal ridges of elytra meet at the posterior third of disc and extend to posterior margin.

Paranota minima resembles *P. rugosa* (Wagener, 1881) stat. rev. et comb. nov. (Figs. 57–60) on its body color, prosternal process, humeral angle and ridge shape. Both present body ground color dark-red; prosternal process with apex distinctly expanded laterally; antero elytral angle strongly obtuse, with complete and well-marked ridge. However, *P. rugosa* (Wagener, 1881) stat. rev. et comb. nov. never has less than 10mm of body length, pronotum with wide and emarginated anterior margin; elytra punctuation dense, coarse and disordered, disc with rugose aspect; while *P. minima* never has more than 10mm of body length (Monrós and Viana 1949), pronotum with narrow and entire anterior margin; elytra punctuation dense and coarse forming longitudinal rows.

Distribution. Recorded to Argentina (Formosa) and Paraguay (Borowiec and Świętojańska 2014). A new locality record from Paraguay (Monte Lindo) is added (Fig. 2.100).

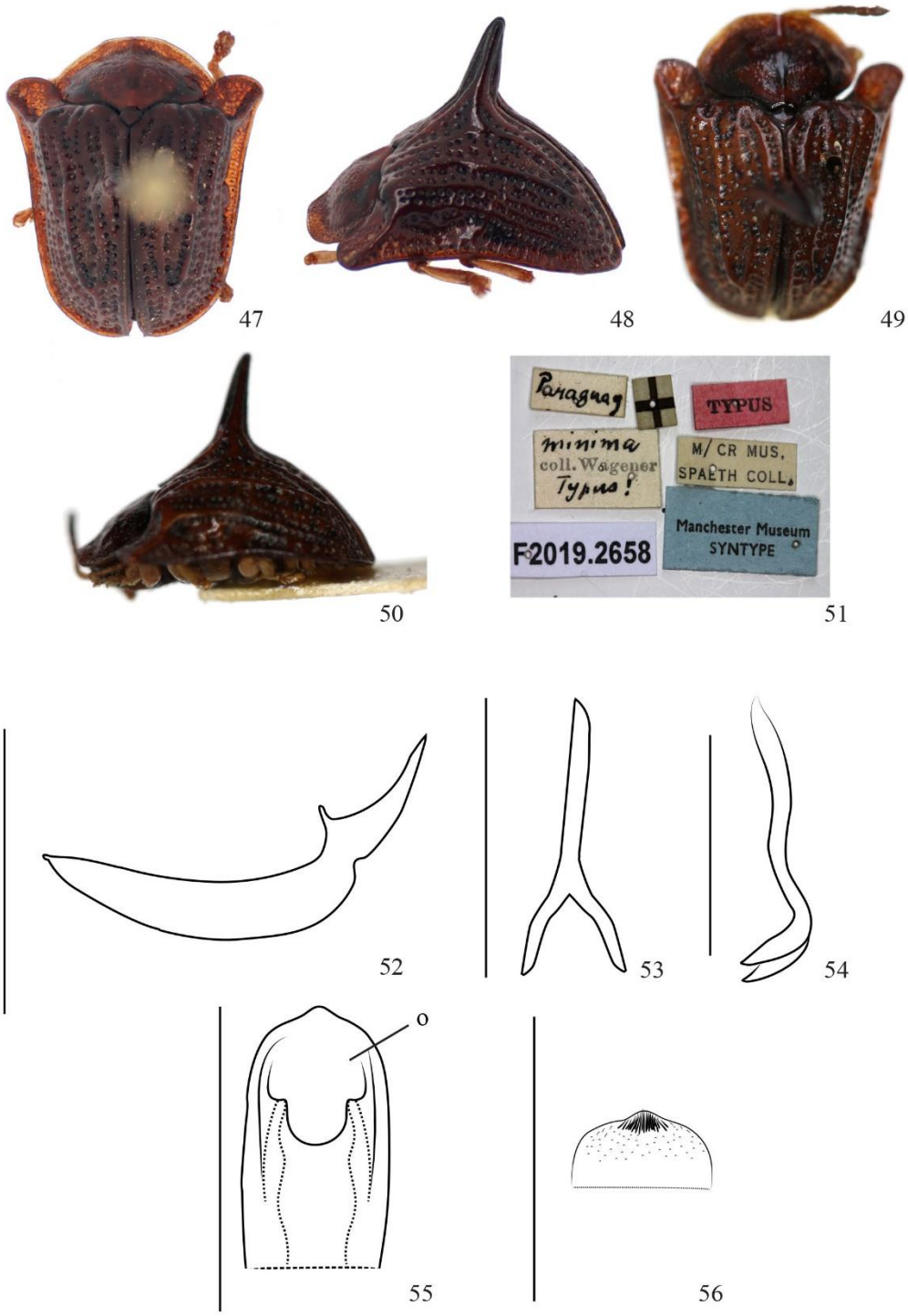

Figures 2.47–2.56. *Paranota minima* (Wagener, 1881) (male). 47, dorsal view; 48, lateral view; 49–51, holotype: 49, dorsal view; 50, lateral view; 51, labels; 52, median lobe, lateral view; 53–54, tegmen: 53, dorsal view; 54, lateral view; 55–56, apex of median lobe: 55, dorsal view; 56, ventral view (o, ostium). Scale bars = 1mm.

Paranota rugosa (Wagner, 1881) stat. rev. et comb. nov.

(Figs. 57–68, 101)

Batonota rugosa Wagener 1881: 41 (type locality: ‘Domingo’).

Type material. Holotype (Figs. 59–60): Domingo \ Reich // Typus // rugosa \ coll. Wagener \ typus // Manchester Museum \ syntype // ensifer \ Spaeth det. // F2010.2669 (MM).
Additional Material Examined**.**ARGENTINA: *Misiones*: Loreto, X.1954, A. Maller leg. (1 male, MNRJ); San Ignacio, I–IV.1910, E. R. Wagner leg. (1 spec., MNHN); 1910, E. R. Wagener leg. (1 spec., MNHN); BOLIVIA: Depart. Santa Cruz: Buena Vista, J. Steinbach leg. (1 spec., DBET); 1952, 400m, Campos Seabra leg. (1 male, MNRJ); BRAZIL: “BRAZILIA”: Jul. Moser Coll. (1 spec., DBET); *Mato Grosso*: Cáceres, 10.XI.1984, C. Elias leg. (1 female, DZUP); XI.1987, O. Roppa and P. Magno leg. (1 female, MNRJ); Corumbá, VII.1979, B. Silva leg. (1 female, MNRJ); *São Paulo*: Indiana, (1 male, DZUP); São Paulo, XII.1932, F. Campos (1 female, MNRJ); PARAGUAY: (1 spec., DBET); *Asunción*: 1915, E. Gounelle leg. (7 spec., MNHN); *Itapuá*: 1972, Pe. J. S. Moure leg. (1 female, DZUP); *Vega*: XII.1954, A. Maller leg. (3 females, MNRJ).

Measurements. Male/female. n=3/8. Total length: 10.3±10.5 / 11.3±11.7; greatest elytra width: 9.1±9.5 / 9.9±10.1; pronotum length: 3.0 / 2.5±3.1; greatest width of pronotum: 5.5±5.6 / 5.5±5.7; elytra length/ width: 0.80±0.83 / 0.81±0.94; length of pronotum/ greatest width of pronotum: 0.5 / 0.4±0.6**.**

Diagnosis**.** This species may be distinguished from other members of the genus by showing ground color of dorsum ranging from brownish–red to dark–red, elytra with anterior

angle strongly expanded laterally, with anterior half of lateral margin sinuous, and disc with coarse punctuation, creating a rugose aspect.

Redescription. Body (Figs. 57–60) dark red dorsally and yellowish brown or reddish brown ventrally, except apex of antennomere VI–XI yellow, and prosternal process, mesosternum, anterior margin of metasternum and metepimeron black. Inter–ocular distance as wide as widest width of eye, surrounded by long and dense setae. Vertex densely punctate and with dense, short setae; coronal suture deep, glabrous, extending to epistomal suture. Frontoclypeus, swollen with discernible and incomplete epistomal suture, with deep and sparse punctures. Inter–antennal distance ca. 1/3 width of antennal sockets. Antennae with length ratio of antennal segments 100: 33: 37: 33: 44: 93: 93: 81: 89: 74: 107.

Prosternal process ca.1.5 times longer than wide; apex obtuse and expanded laterally, 1.5 times wider than median region; mesosternal process, notched medially, four times shorter than prosternal process, with truncate posterior angle. Mesepimeron with exposed portion rectangular. Metasternum 3.6 times wider than long, smooth and glabrous, 3.5 times longer than mesosternal process, with posterior angle elevated to fit the metalegs and median longitudinal groove well marked. Metepimeron with long, dense and decumbent setae.

Elytra with dense and coarse punctation; anterior angle obtuse and reflexed, reaching largest width of pronotum; ridge thin well–marked and complete extending to anterolateral angle, followed by deep depression posteriorly. Disc edge well–marked, with three longitudinal keels, with deep punctures. Lateral margins sinuous, ca. 1/5 width of disc, with reflexed edge; apical margin subacuminated. Disc with vertical spine perpendicular to the body at the anterior third next to suture, flattened and ridged antero-posteriorly and narrow on lateral view, ca. 1.2

times shorter than body height. On ventral view, epipleural ridge well developed with sharp and sinuous projection at the anterior third.

Abdomen with sternites I–IV with short and sparse setae medially; V with long, dense and erect setae on posterior margin; I ca. twice the length of II; II–IV subequal in size, ca. 1.5 shorter than II; V slightly longer than IV, with flat posterior margin. Tarsomere I–III bilobed; tarsomere II 1.4 times longer than I; III two times longer than II and 1.2 times longer in length than IV. Claws with the left nail 1.4 times longer than right nail.

Male terminalia. (Figs. 62–64). Same as described to *P. ensifera* (Fig. 2.39), except for tegmen (Figs. 63–64) with manubrium, 1.7 longer than arms and ejaculatory duct long, uncoiled.

Female terminalia (Figs. 65–68). Same as described to *P. ensifera* (Figs. 43–46), except for sternite IX (Fig. 2.66) with sclerose region between the two plates; tergite X (Fig. 2.68) with sclerosed plates with sinuous anterior margin and posterior margin rounded and expanded.

Remarks. Wagener (1881) described *Batonota rugosa*, which was characterized mainly by the sculpture of the pronotum and elytra, with pronotum strongly punctuated and elytra with three longitudinal keels of different lengths: two departing from the anterior margin and one from the humerus angle, the most internal extending to the anterior third, and external extending to the median region, all with dense, coarse and irregular punctuation, and shiny wrinkles in between.

Spaeth (1914) cited the *B. rugosa* in his list of Chrysomelidae species and Maulik (1916) created a key to the species of *Batonota*, following Wagener`s table (1881), where he considered *B. rugosa* and *B. ensifera* as two different species. Later, Spaeth (1923) synonymized *B. rugosa* with *B. ensifera*, not offering justification or characters that would support the taxonomical change, and from then on, all later literature considered *B. rugosa* as synonym of *B. ensifera*.

Here, the status of *B. rugosa* is resurrected from synonym with *P. ensifera* (Boheman, 1854) and transference to the genus *Paranota* is proposed. For more comments see *P. ensifera.*

Distribution**.** Recorded to Argentina (Misiones), Bolivia (Santa Cruz), Brazil (Mato Grosso, São Paulo) and to Paraguay (Asunción, Itapuá, Vega) (Borowiec and Świętojańska 2014) (Fig. 2.101).

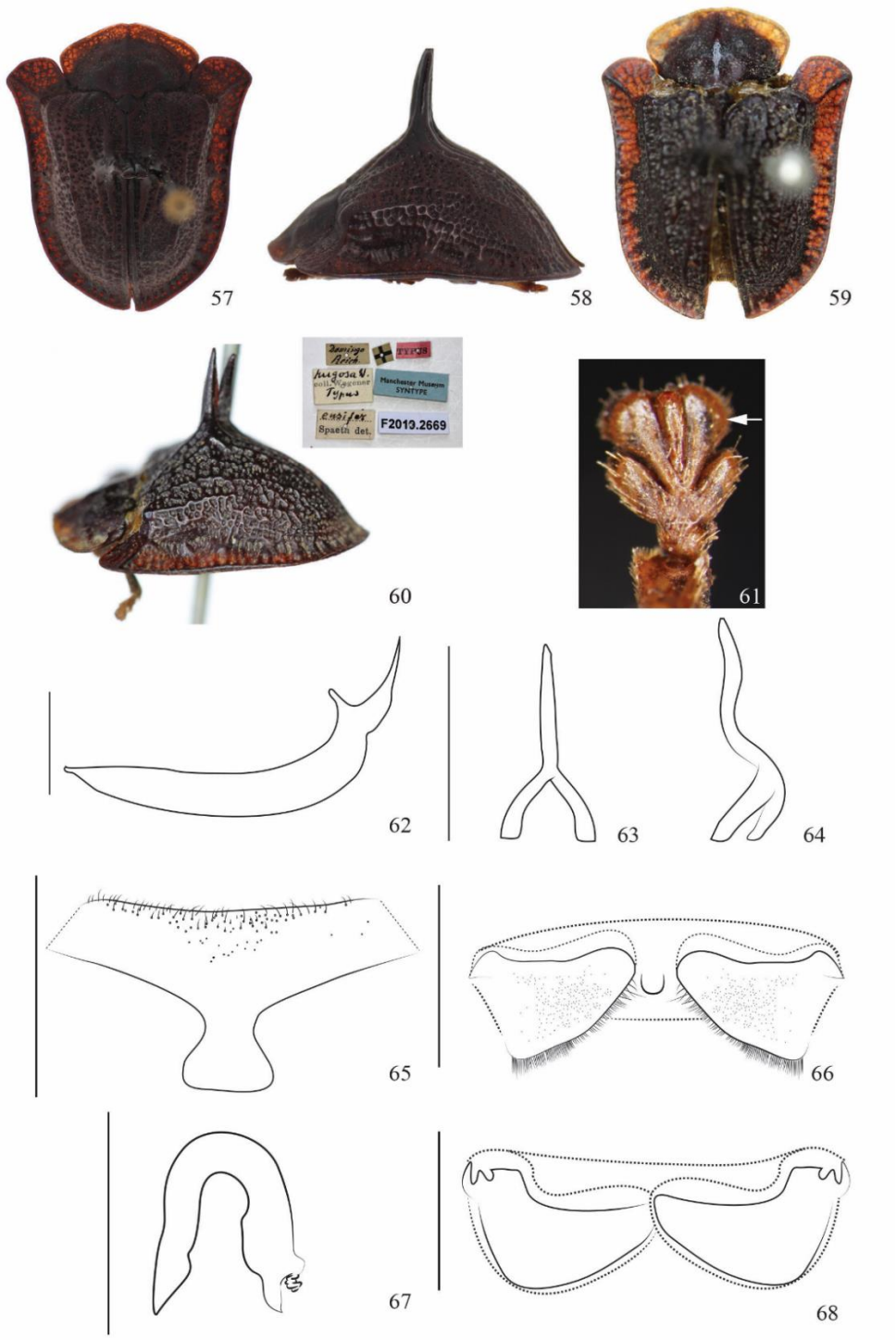

Figures 2.57–2.68. *Paranota rugosa* (Wagener, 1881) stat. rev. et comb. nov. (male). 57, dorsal view, 58, lateral view; 59–60, holotype: 59, dorsal view; 60, lateral view and labels; 61, protarsomere; 62, median lobe, lateral view; 63–64, tegmen: 63, dorsal view; 64, lateral view; 65, sternite VIII; 66, sternite IX; 67, spermatheca; 68, tergite X. Scale bars = 1mm.

Paranota spinosa (Boheman, 1854)

(Figs. 69–81, 102)

Batonota spinosa Boheman 1854: 168, 1856: 95, 1862: 238; Gemminger and Harold 1876: 3645; Wagener 1881: 45; Spaeth 1914g: 67, 1923: 69; Maulik 1916: 583; Węgrzynowicz and Wšsowska 1996: 40.

Dorynota spinosa: Blackwelder 1946: 747; Buzzi 1988: 566; Borowiec 1996a: 182.

Paranota spinosa: Monrós and Viana 1949: 401, 425; Borowiec 1999d: 167, 2002a: 108, 2009f: 692; Flinte *et al*. 2009: 594.

Type material. Lectotype (Figs. 69–70): Brasil // Type // Mhn // Lectotype \ des. L. Borowiec // NHRS–JLKB \ 000020987 (SMNH). Paralectotype: Brasil // Type // Mhn // Lectotype \ des. L. Borowiec (SMNH).

Additional Material Examined. (1 female, DZUP); ARGENTINA: Formosa, (1 female, 5 spec., DZUP); XI.1952, Dirings leg. (1 male, 1 female, MZUSP); XII.1953, Dirings leg. (3 spec., MZUSP); Gran Guardia, XII.1953, A., Maller leg. (2 female, 1 spec., DZUP); BOLIVIA: (2 spec., MNHN); *Chiquitos*: (1 spec**.,** DBET); BRAZIL: (1 spec., MM); *Goiás*: C. Elias leg. (1 spec., MM); Aragarças, I.1955, F.M. Oliveira leg. (1 female, MNRJ); I.1955, F.M. Oliveira leg. (1 male, 1 female, DZUP); Bananeiras, X.1938, B. Pohl leg. (1 spec., MZUSP); XII.1935, Campinas, Borgmeier and S. Lopes. leg. (4 spec**.,** DZUP); XII.1935, Borgmeier and S. Lopes. leg. (1 female, MNRJ); 1935, R. Spitz leg. (5 spec., DZUP); I.1936, Borgmeier and S. Lopes. leg. (2 spec., DZUP); I.1939, Dirings leg. (1 spec., MZUSP); Corumbá, Faz. Monjolinho,

14.VI.1949, F. Lane leg. (4 spec., DZUP); Goiatuba, (1 female, DZUP); Jataí, I.1955, P. Pereira leg. (1 spec., DZUP); Donckier leg. (2 spec., DBET); Leopoldo Bulhões, XII.1933, R. Spitz leg. (1 female, 2 spec., MM); XII.1933, R. Spitz leg. (1 spec., DZUP); XI.1937, Dirings leg. (3 spec., MZUSP); Minaçú, XII.1987, Monné and Roppa leg. (4 spec., DZUP); XII.1987, Monné and Roppa leg. (1 female, DZUP); *Mato Grosso*: II.1923 (1 female, DZUP); 2.XI.1961, F.M. Oliveira leg. (1 spec., DZUP); Barra do Tapirapé, XI.1964, B. Malkin leg. (2 females, 2 spec., DZUP); Cáceres, 13.XI.1984, Buzzi, Mielke, Elias and Casagrande leg. (3 females, DZUP); 9–11.XI.1984, C. Elias leg. (2 spec., DZUP); Chapada, (1 female, USNM); 27.X.1961, F.M. Oliveira leg. (1 female, 1 spec., DZUP); Corumbá, (2 spec., DBET); Cuiabá, 26.X.1953, C.R. Gonçalves leg. (1 spec., DZUP); Guaicurus, XI.1938 (3 female, 1 spec., DZUP); Murtinho, XII.1927, W. Meher leg. (1 spec., DZUP); XI.1929, R. Spitz leg. (1 male, 3 females, 4 spec., DZUP); XII.1939, W. Meher leg. (3 spec., DZUP); Porto Velho, Rio Tapirapé, 30.XII.1964, R. T. Lima leg. (1 spec., DZUP); Rio Varccaria, XII.1922, Lane leg. (8 spec., DZUP); I.24 (11 males, 11 females, DZUP); Rio Verde (1 female, MNRJ); XI. 1964, A. Maller leg. (3 spec., DZUP); XI. 1964, A. Maller leg. (1 female, MNRJ); X.1965, A. Maller leg. (1 spec., DZUP); Rondonópolis, XI.1950, Dirings leg. (2 spec., MZUSP); Rosário-Oeste, XI.1970, Dirings leg. (24 spec., MZUSP); III–II.1971, Dirings leg. (259 spec., MZUSP); XI.1971, Dirings leg. (31 spec., MZUSP); I–II.1972, Dirings leg. (35 spec., MZUSP); X.1973, Dirings leg. (41 spec., MZUSP); II.1974, Dirings leg. (9 spec., MZUSP); *Minas Gerais*: I.1916 (1 spec**.**, MM); Uberaba, (1 spec**.,** DBET); Pirapora, 1912, Garbe leg. (1 female, DZUP); *Pará*: Santarensinho, Rio Tapajós, II.1964, Dirings leg. (32 spec., MZUSP); *São Paulo*: Franca, (1 male, DZUP); Ihering. leg. (1 spec**.**, MM); XI.1911, Garbe leg. (7 spec**.**, DZUP); Mogi Guaçu, Fazenda

Campinha, 17–19.1967, H. Reichardt leg. (2 females, 3 spec., DZUP); PARAGUAY: Bruch leg. (3 spec., MM).

Measurements. Male/female. n=13/41. Total length: 9.3±10.0 / 10.1±11.5; greatest elytra width: 7.8±8.3 / 8.1±9.4; pronotum length: 2.8±3.0 / 2.9±3.5; greatest width of pronotum: 5.1±5.8 / 5.1±6.1.

Diagnosis**.** *Paranota spinosa* can be easily distinguished from the other species of the genus by showing ground color of body reddish–brown dorsally, with anterior margin of pronotum, post–humerus region yellow and disc mottled with reddish–brown and yellow, ventrally yellow, elytra with rounded anterior angle and humeral ridge absent.

Redescription. Body (Figs. 69–70) is reddish–brown dorsally, with anterior margin of pronotum, post–humerus region yellow and disc mottled with reddish–brown and yellow, ventrally yellow, except prosternal process, mesosternum, anterior margin of metasternum and metepimeron black. Inter–ocular distance as wide as widest width of eye. Vertex densely punctate and with long, dense setae; coronal suture deep, glabrous, extending to epistomal suture. Frontoclypeus triangular, swollen, with deep and sparse punctures, and discernible and incomplete epistomal suture. Inter–antennal distance half width of antennal sockets; antennae with length ratio of antennal segments 100: 40: 20: 40: 60: 104: 92: 80: 80: 88: 132. Mesosternal process, notched medially, 2.5 times shorter than prosternal process, with truncate posterior angle. Metasternum 3.5 times wider than long, smooth and glabrous, 5.3 times longer than mesosternal process. Metepimeron (Fig. 2.71) with deep depression apically and smooth surface; elytral disc with confluent and obscured punctuation on lateral view; epipleural ridge with sharp and curved denticle expansion projected over the metepisternum.

Elytra with dense, fine and disordered punctation clustered at the parascutellar disc; anterior angle rounded; humeral ridge absent; disc with two longitudinal ridges, one closer to suture, departing from anterior margin extending to third of disc, and one departing from humerus, extending to 1/3 of disc; spine projection ca. 1.5 times shorter than the body.

Tarsomere II 2.4 times longer than I; III two times longer than II and 1.2 times longer in length than IV. Claws with the internal nail 1.5 times longer than external nail.

Male terminalia. (Figs. 72–74). Same as described to *P. minima* (Figs. 52–56). Internal sac (Figs. 75–77) membranous, highly convoluted dorsally, with two bags bulging dorsally (Fig. 2.77); surface and inner walls armed with spicules, more concentrated distally, with two sclerites (sclt) and one short, slender flagellum (flg) medially at the apex.

Female terminalia (Figs. 78–81). Same as described to *Paranota*, except for sternite IX (Fig. 2.46) with sclerosed region between the two plates; tergite X (Fig. 2.45) with sclerosed plates with sinuous anterior margin and posterior margin rounded and expanded.

Host-plants. Recorded to *Tabebuia aurea* Benth and Hook (=*Tecoma argentea* Bureau and K. Schum) (Bignoniaceae) (Fiebrig 1910) and *Lecythis pisonis* (Lecythidiaceae) (Silva *et al.* 1968).

Remarks**.** Boheman (1854) described *P. spinosa* and compared it with *P. ensifera* (= *Batonota gregariae* Boheman 1854) (Figs. 35–36) and considered they very similar by presenting size, prothorax subtly punctate on the sides, anterior angle of elytra prominent and humeral ridge absent. However, *P. ensifera* presents anterior angle expanded laterally, forming oblique angle and humeral ridge poorly marked. While *P. spinosa* has the anterior angle rounded, not expanded laterally, and the humeral ridge absent.

In the key to the species of the genus *Botanota* Hope, Wagener (1881) differentiated *P. ensifera* (= *Batonota ensifera* Boheman, 1854) from *P. spinosa* by the presence of carina on disc, However, *P. spinosa* (= *Batonota spinosa* Boheman, 1854) present carina on the disc, but less marked than in *P. ensifera.*

Monrós and Viana (1949) differentiates *P. spinosa* from *P. ensifera* by presenting a longer and more convex body; elytra punctuation less coarse than *P. ensifera*; disc with brighter spot at the median region and spine projection not as long as the one in *P. ensifera*. I agree with Monrós and Viana (1949) and add that *P. spinosa* shows elytra with anterior angle rounded, with ridge not well-marked and incomplete; disc with two longitudinal ridges, one closer to suture, departing from anterior margin extending to third of disc, and one departing from humerus, extending to 1/3 of disc. While *P. ensifera* has elytra with anterior angle externally obtuse, with interrupted and poorly–marked ridge; disc with three longitudinal ridges, two closer to suture departing from anterior margin, extending to apex, and another one departing from humerus, extending to 1/3 of disc. For more comments see *P. ensifera*.

Here *Paranota spinosa* is considered to be quite similar to *P. apiculata* comb. nov. (Figs. 82–83). Both present anterior angle of elytra rounded and humeral ridge absent. However, *P. spinosa* present body elongate; prosternum with vestigial antennal sulcus; metepimeron with deep depression apically and smooth surface; elytral disc with confluent and obscured punctuation on lateral view; epipleural ridge (Fig. 2.71) with sharp and curved denticle expansion projected over the metepisternum. While *P. apiculata* comb. nov. presents body subquadrangular; prosternum with developed antennal sulcus; metepimeron elevated medially at the apex, with deep punctures close to anterior margin; elytral disc with not confluent and closely

arranged into rows on lateral view; epipleural ridge (Fig. 2.84) with blunt denticle expansion projected over the metepisternum.

Distribution. Recorded to Argentina (Misiones), Bolivia, Brazil (Mato Grosso, Minas Gerais, Pará, Rio de Janeiro), and to Paraguay (Asuncion, San Bernardino) (Borowiec and Świętojańska 2014). New state records to Brazil (Goiás, São Paulo) and to Argentina (Formosa) (Fig. 2.102).

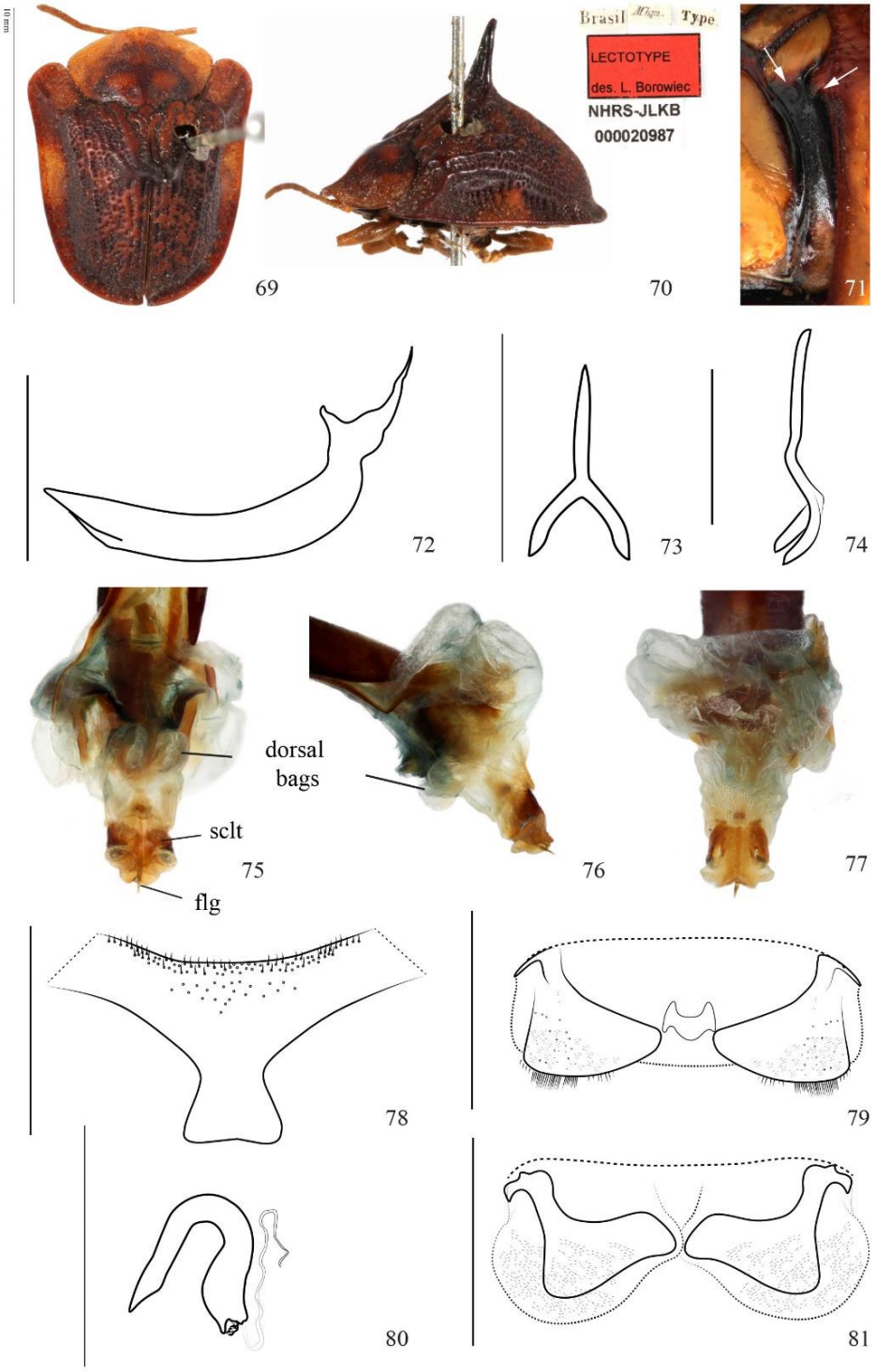

Figures 2.69–2.81. *Paranota spinosa* (Boheman, 1854) (male). 69–81, holotype: 69, dorsal view; 70, lateral view and labels; 71, metepimeron; 72, medium lobe, lateral view; 73–74, tegmen: 73, dorsal view; 74, lateral view; 75–77, internal sac: 75, dorsal view; 76, lateral view; 77, ventral view; 78, sternite VIII; 79, sternite IX; 80, spermatheca; 81, tergite X (flg, flagellum; sclt, sclerite). Scale bars = 1mm.

Paranota apiculata (Boheman, 1854) comb. nov.

(Figs. 82–84, 103)

Batonota apiculata Boheman 1854: 169, 1856: 95, 1862: 238; Gemminger and Harold 1876: 3644, Wagner 1881: 46; Spaeth 1914g: 65; Maulik 1916: 583.

Dorynota apiculata: Blackwelder 1946: 747, Monrós and Viana 1949: 420.

Dorynota (s. str.) *apiculata*: Borowiec 1999d: 161.

Type material. Lectotype (Figs. 82–83): Brasil // Type // M. Berl // Lectotype \ des. L. Borowiec // NHRS–JLKB \ 000020990 (SMNH).

Additional Material Examined. BRAZIL: *Goiás*: Campinas, XI.1984, T. Borgmeier leg. (1 spec., MNRJ); *Mato Grosso*: Chapada dos Guimarães, VII.1983, O. Roppa and M.A. Monné leg. (1 spec., MNRJ); *Pará*: Santarém, (1 spec., DBET); *Rondônia*: Colorado d'Oeste, Cabeça do Rio Pimenta, X.1988, J. Becker leg. (4 spec., MNRJ); XI.1961, F. M. Oliveira leg. (1 spec., DZUP).

Measurements**.** Female. n=2. Total length: 9.7±11.5; greatest elytra width: 8.0±10.0; pronotum length: 2.5±3.3; greatest width of pronotum: 5.5±6.0.

Diagnosis. This species distinguished from other members of the genus by its reduced size, body uniformly and mostly reddish-brown and elytra with deep punctures arranged in rows at the dorsum.

Redescription**.** Body is reddish–brown dorsally, with anterior margin of pronotum, reddish–yellow and elytral margin red; ventrally, yellow, except for the prosternal collar and

process, prosternum, mesosternum, metepimeron, posterior margin of metasternum, pro–, meso– and metacoxae reddish–brown.

Inter–ocular distance 1.5 times shorter than widest width of eye. Vertex densely punctate and with long, dense setae; coronal suture deep, glabrous, extending to epistomal suture. Frontoclypeus subtriangular, swollen, with deep and sparse punctures, and discernible and complete epistomal suture. Inter–antennal distance approximately half width of antennal sockets; antennae with length ratio of antennal segments 100: 31: 19: 37: 50: 100: 81: 75: 75: 87: 131. Mesosternal process, notched medially, 2.5 times shorter than prosternal process, with truncate posterior angle, narrower at apex. Metasternum three times wider than long, smooth and glabrous, 5.3 times longer than mesosternal process. Metepimeron with deep punctures close to anterior margin.

Elytra lateral angle rounded; humeral ridge absent; humeral angle slightly projected; lateral margins subparallel and posterior margin rounded; disc with dense and disordered punctures dorsally, clustered at the parascutellar disc and closely arranged into rows on lateral view. On ventral view, epipleural ridge well developed with blunt short projection at the anterior third over the metepimeron. Spine projection at anterior third of disc slightly bent posteriorly, ca. 1.6 times shorter than body height on lateral view.

Tarsomere II subequal in length to IV, two times longer than I; III slightly longer than II, strongly expanded laterally at apex; IV not overpassing III.

Remarks**.** Boheman (1850), in the original description, compared *Paranota apiculata* comb. nov. (= *Batonota apiculata* Boheman, 1854) (Figs. 82–83) to *P. spinosa* (Figs. 69–70) and considered the size and height of the body, regular elytra punctuation forming rows and shorter and sharper dorsal spine are similar between the two species. However, the body shape of *P.*

spinosa is elongate, although the male might show the body slightly subquadrangular when it has a reduced size, while *P. apiculata* comb. nov. is subquadrangular; and on lateral view, the punctuation of *P. apiculata* is arranged in rows, while *P. spinosa* presents elytral disc with punctuation not confluent and closely arranged into rows.

Wagener (1881) differentiated *P. apiculata* comb. nov. (= *Batonota apiculata* Boheman, 1854) from *P. spinosa* by showing humerus extended laterally, while in *P. spinosa* it is not. However, with the analysis of both species, it is possible to see that they share the feature of rounded anterior angle of elytra, not expanded laterally. For more comments see *P. spinosa.*

Distribution. Recorded to Brazil (São Paulo) (Boheman 1854). New state records to Brazil (Goiás, Mato Grosso, Pará, Rondônia) (Fig. 2.103).

Species excluded from the genus Paranota

Dorynota (*Dorynota*) *parallela* Blanchard, 1837 stat. rev.

(Figs. 85–97)

Dorynota (*Dorynota*) *parallela* Blanchard in D'Orbigny 1837: 212; Blackwelder 1946: 425; Monrós and Viana 1949: 425.

Batonota parallela: Boheman 1854: 165, 1856: 95, 1862: 238; Gemminger and Harold 1876: 3645; Wagener 1881: 46; Spaeth 1914: 66, 1923: 68; Maulik 1916: 583.

Batonota (*Botanota*) *parallela*: Spaeth 1942: 32

Paranota parallela: Monrós and Viana 1949: 425; Borowiec 1999: 167, 2002: 108, 2009: 692; Borowiec and Moragues 2005: 275; Marques *et al.* 2006: 22; Flinte *et al.* 594.

Batonota mucronotata Boheman, 1854: 164; 1856: 94, 1862: 237; Gemminger and Harold, 1876: 3645; Wagener, 1881: 45; Spaeth, 1914: 66, 1923: 68; Maulik, 1916: 583.

Dorynota mucronotata: Blackwelder, 1946: 747

Batonota monocera: Gemminger and Harold, 1876: 3645 (nomen nudum).

Type material. Lectotype: Brasil // Type // Mhn // NHRS–JLKB \ 000020986 // Lectotype \ des. L. Borowiec (SMNH); Paralectotype (Figs. 85–86): Museum Paris \ Bolivie \ (Chiquitos) \ D`Orbigny 1834 // 7316 \ 34 // Paralectotype \ des. L. Borowiec (MNHN).

Additional Material Examined. ARGENTINA: Misiones, V.1955, Dirings leg. (1 female, MZUSP); BOLIVIA: Reyes, Beni, 1–20.XII.1956, L. Pena leg. (1 spec., MNRJ); BRAZIL: "BRAZILIA": Dejean leg. (6 spec., ZMH); *Bahia:* G. Bondar leg. (13 spec., MNRJ); G. Bondar leg. (3 spec., USNM); *Goiás:* Anápolis, IX.1937 (1 spec., MNRJ); Campinas, (1 spec., DZUP); Goiatuba, II.1941 (1 spec., MNRJ); Leopoldo Bulhões, IX.1937, Nick leg. (1 spec., USNM); XI.1950, Dirings leg. (1 spec., MZUSP); Minaçu, XII.1987, Monné and Roppa leg. (2 spec., MNRJ); *Mato Grosso*: Cáceres, 10.XI.1984, C. Elias leg. (4 spec., DZUP); Chapada dos Guimarãs, 27.X.1961, F.M. Oliveira leg. (3 spec., DZUP); Cuiabá, 26.X.1953, C.R. Gonçalves leg. (4 spec., MNRJ); Poconé, 4.XI.1988, J. Becker and O. Roppa leg. (1 spec., MNRJ); Rio Paraná, X.1954, Dirings leg. (1 spec., MZUSP); Rosario Oeste, (1 spec., MNRJ); X.1973, Dirings leg. (12 spec., MZUSP); I–II.1972, Dirings leg. (10 spec., MZUSP); II.1970, Dirings leg. (1 spec., MZUSP); XI.1970, Dirings leg. (2 spec., MZUSP); XI.1970, Dirings leg. (4 spec.,

MZUSP); XI.1971, Dirings leg. (5 spec., MZUSP); II.1971, Dirings leg. (2 spec., MZUSP); X.1973, Dirings leg. (1 spec., MZUSP); *Minas Gerais*: Araguary, X.1931, R. Spitz leg. (1 spec., DZUP); Belo Horizinte, 19.X.1946, Pena Filho leg. (1 spec., MNRJ); Passos, XII.1962, C. Elias leg. (2 spec., DZUP); XI.1961, C. Elias leg. (1 spec., DZUP); Pedra Azul, XI.1972, F.M. Oliveira leg. (1 spec., MNRJ); XII.1970, F.M. Oliveira leg. (2 spec., MNRJ); Pirapora, (1 spec., MNRJ); XI.1975, Seabra, Alvarenga, Roppa and Monné leg. (16 spec., MNRJ); Rio Paraná, (1 spec., DZUP); Rosório Oeste, (1 spec., DZUP); *Pará*: Rio Tapajós, Santarenzinho, II.1964, Dirings (26 spec., MZUSP); *Santa Catarina*: Corupá, XI.1944, X.J.Guerín leg. (1 spec., USNM); *São Paulo*: (1 spec., DZUP); Anhangabau, XI.1924, R. Spitz (1 spec., MNRJ); Jundiaí, 21.X.1961, Werner col. (5 spec., MZUSP); Rio Claro, 13.XI.1980, Alejo Mesa leg. (1 spec., MZUSP).

Remarks. The description of *Dorynota parallela* by Blanchard (1837) was brief and highlighted only diagnostic features to the subgenus *Dorynota* (s. str.), such as punctate pronotum and elytra, and conspicuous spine projection at the median region of the elytra. Boheman (1854) redescribed the species, with further details of body color, elytra and pronotum shape and punctuation, and in its discussion, *P. parallela* was compared size-wise with *D. pugionata*, being slightly shorter and wider and with subequal in size to *P. ensifera* (Boheman, 1854) (= *P. gregariae* Boheman, 1854). Monrós & Viana (1949) transferred the species *P. parallela* to the genus and did not justify the taxonomical change.

After the examination of lectotype, paralectotype, 247 specimens identified as *Paranota parallela* obtained from the DZUP, LB, MM, MNHN, MNRJ, MZH, MZUSP and SMNH collections, male and female terminalia, it was observed that the species does not present diagnostic features of *Paranota*, and here its original combination is reinstated.

Dorynota parallela stat. rev. presents pronotum with anterior margin medially acuminated and elevated; scutellum slightly projected over posterior angle of pronotum; elytra spine projection slightly shorter than body height; claws (Fig. 2.38) parallel with the left nail slightly shorter than right nail; male terminalia (Figs. 88–93) with median lobe (Fig. 2.88) in a obtuse angle; tegmen (Figs. 89–90) not well–sclerotized, except for basal portion of manubrium, with arms flattened laterally, acuminate at apex; Internal sac (Figs. 91–93) membranous, highly convoluted dorsally, with two bags bulging dorsally (Figs. 91–92); surface and inner walls sparsely armed with spicules and two sinuous arms (Fig. 2.93) laterally to apex. Female terminalia (Figs. 2.94–2.97) with sternite VIII (Fig. 2.95), with apodeme 1.7 times longer than sternite width, narrow and with subparallel lateral margins medially; spermatheca (Fig. 2.94) falcate, with truncate base and posterior third abruptly tapering towards apex; spermathecal duct long and coiled.

In *Paranota* the pronotum presents anterior margin medially emarginated or rounded; scutellum not projected over posterior angle of pronotum; claws (Fig. 2.38) subparallel with the left nail distinctly shorter than right nail; male terminalia (Figs. 2.39–2.41, 2.52–2.56, 2.62–2.64, 2.72–2.74) with tegmen (Figs. 2.40–2.41, 2.53–2.54, 2.63–2.64, 2.73–2.74) well–sclerotized, with arms not flattened laterally, truncate apex; median lobe (Figs. 2.39, 2.52, 2.62, 2.72) in a 90° angle; female terminalia (Figs. 2.43–2.46, 2.65–2.68, 2.78–2.81); sternite VIII (Figs. 2.43, 2.65, 2.78) with apodeme as long as the width of sternite, narrow at base. Spermatheca (Figs. 2.44, 2.67, 2.80) U-shaped, rounded at base, tapered continuously towards apex. Spermathecal duct long and strongly coiled.

Distribution**.** Recorded to Argentina (Misiones), Bolivia (Beni, Guarayos, Velasco), Brazil (Pará, Goiás, Mato Grosso, Bahia, Minas Gerais, São Paulo, Rio de Janeiro, Santa

Catarina), Ecuador; Paraguay (Asunción, San Luis), and Peru (Vilcanota) (Borowiec and Świętojańska 2014).

Key to the species of the genus *Paranota* Monrós & Viana

1. Body shiny, strongly convex on lateral view. Elytra with humeral ridge continuous, well-marked and strongly elevated. (Figs. 2.47–2.56, 2.100). Paraguay, Argentina ……..... *P. minima* (Wagener, 1881).

- Body dull or only longitudinal ridges of elytra shiny, not strongly convex on lateral view. Elytra with humeral ridge absent or poorly-marked, slightly elevated, interrupted or incomplete .....……...……..…… 2.

2. Elytra with anterior angle expanded laterally, forming oblique lateral angle; humeral ridge present …….....… 3.

- Elytra with anterior angle rounded, not forming oblique lateral angle; humeral ridge absent ……..……... 4.

3. Ground color of dorsum ranging from dark-red to brownish-red. Elytra with strongly sinuous anterior half of lateral margin after humeral angle; anterior angle strongly expanded laterally; humerus ridge incomplete, not reaching anterior angle; disc with rugose aspect; tarsomere III slightly longer than IV, with apex almost three times wider than base. (Figs. 2.57–2.68, 2.101). Brazil (MT, GO, SP), Bolivia, Paraguay, Argentina

…….....……

……..... *P. rugosa* (Wagener, 1881) stat. rev. et comb. nov.

- Ground color of dorsum ranging from yellowish-brown to reddish-brown. Elytra with anterior half of lateral margin subparallel after humeral angle; anterior angle slightly expanded laterally; humerus ridge interrupted medially; disc punctuation dense and clustered, without rugose aspect; tarsomere III as long as IV, with apex ca. two times wider than base. (Figs. 2.1–2.46, 2.99). Ecuador, Peru, Brazil (MT, GO, RJ, SP), Bolivia, Paraguay, Argentina ..... *P. ensifera* (Boheman, 1854).

4. Body elongate; prosternum with vestigial antennal sulcus; metepimeron with deep depression apically and smooth surface; elytral disc with confluent and obscured punctuation on lateral view; epipleural ridge with sharp and curved denticle expansion projected over the metepisternum. (Figs. 2.69–2.81, 2.102). Brazil (PA, MT, GO, MG, RJ, SP), Bolivia, Paraguay, Argentina ..... *P. spinosa* (Boheman, 1854).

- Body subquadrangular; prosternum with developed antennal sulcus; metepimeron with deep punctures close to anterior margin; elytral disc with not confluent and closely arranged into rows on lateral view; epipleural ridge with blunt denticle expansion projected over the metepisternum. (Figs. 2.82–2.84, 2.103). Brazil (SP, RO, MT) ..... *P. apiculata* (Boheman, 1854) comb. nov.

Bibliography

Blackwelder RE. 1946. Checklist of the coleopterous insects of Mexico, Central America, the West Indies and South America. *Bulletin of the United States National Museum* 185: 551–763.

Blanchard É. 1837. Insectes de l'Amérique méridionale recueillis par Alcide d'Orbignyi. [pp. 60–222]. *In*: D'Orbigny A. 1837–45 (ed.): Voyage dans l'Amérique méridionale (Le Brésil, la République Orientale de l'Uruguay, la République Argentine, la Patagonie, la République du Chili, la République de Bolivia, la République du Pérou), exécuté pendant les années 1826, 1827, 1828, 1829, 1830, 1831, 1832 et 1833. Tome sixieme, 2e. partie: Insectes. Chez P. Bertrand, Paris, 222 pp.

Boheman CH. 1854. Monographia Cassididarum. Tomus secundus. Ex Officina Norstedtiana, Holmiae. 506 pp.

Boheman CH. 1856. Catalogue of Coleopterous Insects in the collection of the British Museum. Part IX. Cassidae.

Boheman, C.H. 1862. Monographia Cassididarum. Tomo. IV, Ex Officina Norstedtiana, Holmie, 504 pp.

Borowiec L. 1996. Faunistic records of Neotropical Cassidinae (Coleoptera: Chrysomelidae). *Polskie Pismo Entomologiczne* 65: 119–251.

Borowiec L. 1999. A world catalogue of the Cassidinae (Coleoptera: Chrysomelidae). Biologica Silesiae, Wroclaw, 476 pp.

Borowiec L. 2002. New records of Neotropical Cassidinae, with description of three new species (Coleoptera: Chrysomelidae). *Genus* 13: 43–138.

Borowiec L. 2005. Three new species of the genus *Dorynota* sgen. *Akantaka* Maulik, 1916 from Bolivia and Brazil (Coleoptera: Chrysomelidae: Cassidinae: Dorynotini). *Genus* 16: 29–41.

Borowiec L. 2009. New records of Neotropical tortoise beetles (Coleoptera: Chrysomelidae: Cassidinae). *Genus* 20: 615–722.

Borowiec L., Moragues G. 2005. Tortoise beetles of the French Guyana – a faunistic review (Coleoptera: Chrysomelidae: Cassidinae). *Genus* 16: 247–278.

Borowiec L., Opalińska S. 2007. The structure of spermathecae of selected genera of Stolaini and Eugenysini (Coleoptera: Chrysomelidae: Cassidinae) and its taxonomic significance. *Annales Zoologici* 57: 463–479.

Borowiec, L, Takizawa H. 2011. Neotropical tortoise beetles in the Amazon Insectarium, Tokyo, Japan with description of nine new species (Coleoptera: Chrysomelidae). *Genus* 22: 427–484.

Borowiec L., Świętojańska J. 2014. World catalog of Cassidinae. Available from: <http://www.cassidae.uni.wroc.pl/katalog%20internetowy/index.htm> (8th November 2014).

Bruch C. 1915. Catálogo systemático de los Coleópteros de la República Argentina. Pars IX. Familia Chrysomelidae 19: 346–441.

Buzzi ZJ. 1988. Biology of Neotropical Cassidinae. *In*: P. Jolivet, E. Petipierre, T.H. Hsiao, Biology of Chrysomelidae. Kluwer Academic Publishers, Dordrecht/ Boston/ London, 559–580.

Chaboo CS. 2007. Biology and phylogeny of the Cassidinae Gyllenhal *sensu lato* (tortoise and leaf–mining beetles) (Coleoptera: Chrysomelidae). *Bulletin of the American Museum of Natural History* 305: 1–250.

Costa Lima A.da. 1936. Terceiro Catalogo dos Insetos que vivem nas Plantas do Brasil. Rio de Janeiro pp 460.

Crowson RA. 1938. The metendosternite in Coleoptera: a comparative study. *Transactions of the Entomological Society of London* 87: 397–416.

Fiebrig K. 1910. Cassiden und Cryptocephaliden Paraguays. Ihre Entwicklungsstadien und Schutzvorrichtungen. *Zoologische Jahrbücher* 2: 161–264.

Flinte V, Borowiec L, de Freitas S, Viana JH, Fernandes FR, Nogueira de Sá F, de Macedo MV, Monteiro RF. 2009. Tortoise Beetles of the State of Rio de Janeiro, Brazil (Coleoptera: Chrysomelidae: Cassidinae). *Genus* 20: 571–614.

Gemminger M, Harold E. 1872. *Catalogus Coleopterorum hucusque descriptorum synonymicus et systematicus*, vol. 9. Gummi, Monachii.

Hadley A. 2010. CombineZP software package. Available from: <www.hadleyweb.pwp.blueyonder.co.uk/CZP/Installation.htm> (Accessed 20th February 2014).

Hincks WD. 1952. The Genera of the Cassidinae (Coleoptera: Chrysomelidae). *Transactions of the Royal Entomological Society of London* 103 327–358.

Hübler N, Klass KD. 2013. The morphology of the metendosternite and the anterior abdominal venter in Chrysomelidae (Insecta: Coleoptera: Chrysomelidae). *Arthropod Systematics and Phylogeny* 71: 3–41.

Kukalová-Peck J, Lawrence JF. 2004. Relationships among coleopteran suborders and major endoneopteran lineages. Evidence from hind wing characters. *European Journal of Entomology*, 101: 95–144.

Mann JS. 1988. Male genitalia of Chrysomelidae (Coleoptera) I. Subfamilies Cassidinae and Hispinae. *Journal of Animal Morphology and Physiology* 35, 123–130.

Mann J.S, Crowson RA. 1996. Internal sac structure and phylogeny of Chrysomelidae. *In*: Jolivet PHA, Cox ML, eds. Chrysomelidae Biology. Vol. 1: The Classification, Phylogeny and Genetics. The Netherlands: SPB Academic Publishing 291–316.

Marques OM, Schmidt CDS, Coutinho ML, Gil–Santana HR, Santana MJS. 2006. *Paranota parallela*: um insecto nocivo ao ipê amarelo no Estado da Bahia. *Revista Bahia Agrícola* 7: 22–23.

Maulik S. 1916. On Cryptostome beetles in the Cambridge University Museum of Zoology. *Journal of Zoology* 86: 567–589.

Monrós F, Viana MJ. 1949. Revision de las especies Argentines de Dorynotyni (Col. Cassidae) (Primera contribución al conocimiento de Cassidinae). *Acta Zoologica Lilloana* 8: 391–426.

Rodriguez V. 1994. The function of the spermathecal muscle in *Chelymorpha alternans* Boheman (Coleoptera: Chrysomelidae: Cassidinae). *Physiological Entomology* 19: 198–202.

Seeno TN, Wilcox JA. 1982. Leaf beetle genera (Coleoptera: Chrysomelidae). *Entomography* 1: 1–221.

Sekerka L. 2004. Species of Cassidinae and Hispinae contained in the Moravian Museum Collection in Brno (Coleoptera, Chrysomelidae). *Acta Entomologica Musei Nationalis Pragae* 89: 117–165.

Silva AGd'A, Gonçalves CR, Galvão DM, Gonçalves AJ, Gomes J, Silva M, de. Simoni, L. 1968. Quarto catálogo dos insetos que vivem nas plantas do Brasil. Seus parasitos e predadores. Ministério da Agricultura, Laboratório Central de Patologia Vegetal. Rio de Janeiro. Parte II, 1º Tomo, 622 pp.

Spaeth F. 1914. Chrysomelidae: 16. Cassidinae. *In*: Schenkling S. (ed.): Coleopterorum Catalogus, Pars 62, W. Junk, Berlin, 180 pp.

Spaeth F. 1923. Ueber *Batonota* Hope. (Col. Cassid.). *Wiener Entomologische Zeitung* 40: 65–76.

Spaeth F. 1941. Die Coleopteren der Deutschen Gran–Chaco–Expedition 1925/26. Cassidini (Chrysomelidae). *Mitteilungen der Münchner Entomologischen Gesellschaft* 31: 1059–1063.

Świętojańska J. 2009. The immatures of tortoise beetles with bibliographic catalogue of all taxa (Coleoptera: Chrysomelidae: Cassidinae). *Polish Taxonomical Monographs*, 16: 1–157.

Wagener B. 1881. Cassididae. *Mitteilungen der Münchener Entomologischen Vereins* 5: 17–85.

Węgrzynowicz P, Wššowska M. 1996. The type material of family Chrysomelidae (Coleoptera) in the Museum and Institute of Zoology PAS, Warsaw. *Bulletin of Museum and Institute of Zoology PAS* 1: 35–52.

Chapter 3:

TAXONOMIC REVISION OF THE NEOTROPICAL LEAF BEETLE SUBGENUS *DORYNOTA S. STR.* CHEVROLAT (COLEOPTERA: CHRYSOMELIDAE: CASSIDINAE)[3]

[3]Simões, M.V. and Sekerka, L. (2015) Review of the Neotropical Leaf Beetle Subgenus *Dorynota* s. str. Chevrolat (Coleoptera: Chrysomelidae: Cassidinae: Dorynotini). *The Coleopterists Bulletin*, 69, 231–254.

Abstract

A review of *Dorynota* s. str. is presented in which eighteen species are included in the subgenus. Three new species are described: *Dorynota* (s. str.) *monneorum* Simões and Sekerka, new species and *Dorynota* (s. str.) *borowieci* Simões and Sekerka, new species from Brazil, and *Dorynota* (s. str.) *wappesi* Sekerka and Simões, new species from Bolivia. Two new synonyms are proposed: *Dorynota* (s. str.) *aculeata* (Boheman, 1854) = *Dorynota* (s. str.) *pubescens* (Blake, 1939), new synonymy and *Dorynota* (s. str.) *cornigera* Boheman, 1854 = *Dorynota* (s. str.) *bellicosa* Boheman, 1854, new synonymy. *Dorynota* (s. str.) *pugnax* Boheman, 1854, restored status is resurrected from synonymy with *Dorynota* (s. str.) *nodosa* (Boheman, 1854). Thirty-five new country and region records are reported for ten species. A key to species and color photographs of all species are provided.

Introduction

Chevrolat (in Dejean, 1836) first proposed the genus *Dorynota* for twelve Neotropical cassids with a postscutellar spine. Of these, only three were previously described in the genus *Cassida* Linnaeus, 1758: *D. bidens* (Fabricius, 1781), *D. pugionata* (Germar, 1824), and *D. truncata* (Fabricius, 1781) with the remaining names represent nomina nuda. Hope (1840) described the genus *Batonota* and designated *Cassida bidens* Fabricius, 1781 as its genotype. Later, Duponchel and Chevrolat (1842) designated *C. bidens* as the genotype of *Dorynota*, thus *Batonota* became a younger objective synonym of *Dorynota*. However, most of the genera proposed in Dejean's catalogues were not used at that time consequently subsequent authors gave priority to *Batonota* (i.e. Boheman 1854, Chapuis 1875, Spaeth 1914). The validity of Dejean's names was clarified by Barber and Bridwell (1940), and since then *Dorynota* has been considered the valid generic name for this taxon.

Maulik (1916) erected the genus *Akantaka* for species of *Batonota* (=*Dorynota* Chevrolat, 1836) with a short postscutellar spine, thus appearing rather gibbous than spinose and with broadly explanate elytra with straight or convex lateral sides. Spaeth (1923) lowered *Akantaka* to a subgenus of *Batonota* and provided a key to related genera and species groups. Monrós and Viana (1949) considered *Akantaka* as valid genus and designated *Batonota viridisignata* Boheman, 1854 as its type species. Hincks (1952) again lowered *Akantaka* to subgenus of *Dorynota*, which still accepted (Borowiec 1999).

Dorynota is distributed from Mexico to northern Argentina, with its highest diversity in tropical areas of South America. The genus currently includes 16 species in the nominotypical subgenus and 24 in the subgenus *Akantaka*. Host plants are known for only nine species, with

most all being associated with the diverse genus *Tabebuia* Gomes ex A. P. de Candolle (Bignoniaceae). A few associations have also been recorded from *Tecoma* Juss. (Monrós and Viana 1949), which has its history of generic delimitations, intricately interwoven with that of the genus to *Tabebuia* (Gentry 1969). Based on our recent extensive fieldwork, at least 21 *Dorynota* species are associated with *Tabebuia* Gomes ex A.P. de Candolle, 1838 and its related genera (Windsor and Sekerka unpubl. data).

Recently we had the opportunity to examine extensive material of *Dorynota* and found several new species and numerous new country and province records. The present paper deals with the nominotypical subgenus, which has never been reviewed, with the exception of a key to species provided by Wagener (1881) and the review of the Argentinean species by Monrós and Viana (1949).

Material and Methods

All identifications were made according to comparison with respective type specimens.

Distributions are given by countries and their major administrative divisions. The information generally follows a summary by Borowiec and Świętojańska (2014). However, we verified all original sources of the distributional information for the species here discussed and replaced localities with their respective provinces or departments to provide consistent data. For species with very few records, we cite also the original source(s). For brevity and to reduce duplication, we include only new unpublished faunistic records in the "Additional Material Examined" section though significantly more material was examined.

Label data for studied type specimens are cited verbatim: a vertical bar (|) separates data on different rows and a double vertical bar (||) separates different labels. Additional information about the label or explanatory notes is given in square brackets. The following abbreviations are used to describe the labels as necessary: b – blue, bb – black frame, cb – cardboard; cd – g – green, gl – glued; hw – handwritten, p – printed, r – red, sl – soft label, tr – triangle; w – white.

Distribution maps were made based on locality information from specimen labels and literature records. They are provided for every species, except for *D. rufomarginata* (Wagener, 1881) and *D. nodosa* (Boheman, 1854) for which no detailed locality data is known.

Institutional abbreviations cited in the text follow Evenhuis (2014): American Museum of Natural History, New York, U.S.A. (AMNH); Coleção de Entomolgia de Pe. Jesus S. Moure do Departamento de Zoologia, Universidade Federal do Paraná, Paraná, Brazil (DZUP); Collection of Lukáš Sekerka, Prague, Czech Republic (LSC); Department of Biodiversity and Evolutionary Taxonomy, University of Wrocław, Poland (DBET); Finnish Museum of Natural History, Helsinki, Finland (MZH); Instituto Nacional de Biodiversidad, Costa Rica (INBIO); Museu de Zoologia da Universidade de São Paulo, São Paulo, Brazil (MZUSP); Museu Nacional, Universidade Federal do Rio de Janeiro, Rio de Janeiro, Brazil (MNRJ); Museum fur Naturkunde de Humboldt Universität, Berlin, Germany (ZMHB); Muséum National d'Histoire Naturelle, Paris, France (MNHN); National Museum of Natural History, Smithsonian Institution, Washington D.C., U.S.A. (USNM); Natural History Museum, London, U.K. (BMNH); Swedish Museum of Natural History, Stockholm, Sweden (SMNH); Texas A and M University, Texas, U.S.A. (TAMU) and the Manchester Museum, Manchester, U.K. (MMUE); Zoological Museum, University of Copenhagen, København, Denmark (ZMUC).

Terminology for the structures follows those commonly used in Chrysomelidae and/or Coleoptera and female terminalia are described as in Rodriguez (1994), Chaboo (2007) and Borowiec and Opalińska (2007).

References cited for each species are limited only to primary descriptions and additional works which include taxonomic changes. For a complete list of references see Borowiec (1999) and Borowiec and Świętojańska (2014).

Results

Examined species

Dorynota (s. str.) aculeata (Boheman, 1854)

(Figs. 3.1–3.2, 3.43)

Batonota aculeata Boheman, 1854: 170 (type locality: 'Insula St. Domingo').

Batanota pubescens Blake, 1939: 234 (type locality: 'Constanza, Dom. [inican] Rep. [ublic]'). New synonymy.

Type material. *Batonota aculeata*, lectotype (designated by Borowiec (1999)), pinned: 'Domingo. [w, p] || Mhn. [w, p, cb] || Type. [w, p, cb] || LECTOTYPE | des. L. Borowiec [r, p, cb]' (SMNH); Paralectotype, pinned: 'Domin | go. [w, p, s] || Mhm. [w, p, cb] || NHRS-JLKB | 000020989 [w, p, cb] || PARALECTOTYPE | des. L. Borowiec [r, p, cb]' (SMNH). *Batonota pubescens*, holotype,

pinned: ‘Constanza | Aug. ’38, Dom.Rep. | 3-4000ft | Darlington [w, p, cb] || MCZ | Type No 23634 [r, cb, hw] || M.C.Z. | Type | 23634 [r, p, cb] || Batonota | pubescens | type Blake [cd, hw]’ (MCZ). Additional material examined (28). Without additional locality data: (1 spec., DBET; 1 spec., MZH); DOMINICAN REPUBLIC: St. Domingo[1] (2 spec., MMUE; 3 spec., MZH), 1985, A. Salle (4 spec., MNHN); HAITI: Without additional locality data: (1 spec., DBET); *Port-au-Prince*: East Pétionville, 24.V.1973 (1 spec., DBET).

Diagnosis**.** *Dorynota aculeata* is a very distinctive species, as it is among the two species of the subgenus possessing a triangular scutellum, the second one being *D. ohausi* (Spaeth, 1916). It has coarse punctation with finely punctate elytral intervals as in *D. hastifera*, *D. parallela* and *D. pugionata*. However, these differ by possessing wider intervals between punctuations, which are not or only weakly costate, while *D. aculeata* presents narrow and costate intervals.

Remarks**.** Boheman (1854) described *B. aculeata* based on an unknown number of specimens. However, he must have had at least two, as he listed a length span. Blake (1939) described *D. pubescens* based on 16 specimens collected in Constanza, Dominican Republic and compared it to *D. aculeata* (Boheman, 1854), previously described from Hispaniola. She probably had not examined type specimens of *D. aculeata* and her comparative notes were based on the original description.

Blake (1939) used the color of dorsum, presence or absence or elytral pubescence and form of the elytral sculpture as the primary distinguish characters between the species. As its name

[1] We included these specimens under Dominican Republic, however they were not necessarily collected in the capital Santo Domingo. In the past, the island of Hispaniola was referred to as ‘Insula Santo Domingo’, not only the capital, as it is today.

suggests, pubescence of the elytra is particularly distinct and this was probably the main reason why she described *D. pubescens*, as Boheman's (1854) description does not mention this feature.

We examined the holotypes of both names as well as the type series and 28 additional specimens and found them to be conspecific. We observed great variability in body color, pubescence distribution, and elytra ridging in the analysed series of both taxa. The dorsal color ranges from yellowish brown to dark red, with punctures always darker than the background dorsal color, and venter with pro-, meso-, metasternum, and abdomen always darker than distal portion of legs, ranging from blackish red, with legs yellow distally, to blackish-brown with legs yellowish-brown distally. The pubescence varies with the conservation of the specimen, being more conspicuous and distinct in well-preserved material than in older specimens. Both types of *D. aculeata* possess short but clearly seen elytral pubescence. We have also observed that freshly eclosed specimens of many *Dorynota* species have more conspicuous pubescence than older ones. The sculpture of the elytra is similar in both taxa, with the punctation becoming more irregular on the second half of the disc.

Based on the examined material, we consider that the assigned characteristics by Blake (1939) to differentiate the two taxa constitute intraspecific variation. Thus we synonymize *D. pubescens* with *D. aculeata*.

Distribution**.** Dominican Republic and Haiti (Borowiec and Świętojańska 2014) (Fig. 3.43).

Dorynota (s. str.) aurita (Boheman, 1862)

(Figs. 3.3–4, 43)

Batonota aurita Boheman, 1862: 237 (type locality: 'Costa Rica').

Type material. Holotype (by monotypy), pinned: '14264 [w, p, sl] || aurita | N. | Costa | Rica. Wagn. [g, hw, cb] || HOLOTYPE | des. L. Borowiec [r, p, cb] || HOLOTYPUS | Batonota | aurita | Boheman, 1854 | des. L. Borowiec [r, p, cb, bb]' (ZMHB).

Additional material examined *(*10). COSTA RICA: *Guanacaste*: Santa Rosa National Park, D. H. Janzen lgt. (2 spec., TAMU); MEXICO: Aguacera, 16 Km, W. Ocozocautla, 6.VI.1987, D.B. Thomas lgt. (1 spec., TAMU); *Chiapas:* La Sepultura, 26.VI.1988, DB and AM Thomas lgt. (1 spec., TAMU); *Durango:* Ventanas, Godman-Salvin Coll., Biol. Centr-Amer. (8 spec., BMNH); *Guerrero:* Acapulco, Godman-Salvin Coll., Biol. Centr-Amer. (1 spec., TAMU); 18.2miles, 3,000ft, 5.VII.1987 Kovarik, Schaffner lgt. (1 spec., TAMU); Ixtapa, 17–20.VII.1985, J. E. Wappes lgt. (1 spec., TAMU); *Oaxaca*: 4 Km, E. Ventosa 50m, 12. VII. 1992 C. Bellamy lgt. (2 spec., TAMU); PANAMA: *Los Santos*: Laboratorio Los Achotines, 3 km, 23. VI. 1996, Gillogly and Schaffner lgt. (8 spec., 2 LSC, 6 TAMU).

Diagnosis. *Dorynota aurita* is readily characterized by presence of a long spine, impunctate elytral intervals, yellow dorsum, and U-shaped elytra. Most similar externally is *D. ohausi*, from Ecuador, which differs in absence of the humeral carina, while *D. aurita* has a large and high humeral carina. Other similar species such *D. rileyi*, *D. wappesi* or *D. monneorum* differ in having a subtriangular (first two) or shield shaped body (the last one) and maculate explanate margin of elytra (first and last one). For summary of distinguishing characters see Table 3.2 under *D. monneoroum*.

Remarks**.** The Panamanian specimens fully match the holotype. Based on the distribution data, the species is probably restricted to seasonally dry Pacific forest which, unfortunately, has been mostly destroyed in Panama.

Distribution**.** Costa Rica, Mexico (Durango, Guerrero, Jalisco, Puebla), and Nicaragua (Chontales) (Borowiec and Świętojańska 2014). Also included in the material examined are specimens which represent a new country record for Panama (Los Santos) and a new province record for Costa Rica (Guanacaste) (Fig. 3.43).

Dorynota (s. str.) bidens (Fabricius, 1781)

(Figs. 3.5–3.6, 3.43)

Cassida bidens Fabricius, 1781: 112 (type locality: 'Brasilia').

Type material. Syntype (? holotype), pinned: 'Cassida bidens | Fabr. Spec. 112. n. 32 [w, hw, cb, bb]' (BMNH).

Additional material examined (30). BRAZIL: *Bahia*: without additional locality data (1 spec., ZMUC); 'Cachimbo', 1890 Ch. Pujol lgt. (12 spec., MNHN; 3 spec., LSC); Conceição de Almeida (Interceção B. Rios e Rio Jaguaripe), 21.VII.1979, J. Becker lgt. (1 spec., MNRJ); Itamaraju, 26.X.1985, J. Becker lgt. (1 spec., MNRJ); Porto Villa Victoria, 1890, Ch. Pujol lgt. (1 spec., MNHN); *Espírito Santo*: without additional locality data (3 spec., DBET; 1 spec., LSC; 2 spec. MMUE, 1 spec. ZMUC); Linhares (1 spec., MNRJ); *Pernambuco*: without additional locality data, L. L. Castro lgt. (1 spec., MNRJ); *São Paulo*: Rio Piracicaba, II.1885, P. Germain lgt. (1 spec., MNHN); FRENCH GUIANA: *Cayenne*: Cayenne (3 spec., DBET).

Diagnosis. *Dorynota bidens* is one of the two species in the subgenus with a black dorsum. The other species, *D. nigra*, differs in that the elytra are uniformly black with a dark green metallic tint and a shorter dorsal spine, while *D. bidens* has a dull black body with a small dark red spot

around the midlength of the lateral slope of each elytron. Externally, *D. bidens* resembles *D. monoceros* and differs except for the color in having finer and sparser punctation of the elytra, particularly in apical half, and the presence of relatively dense and long pubescence around the red elytral spot, at the base of the elytra and on the pronotum.

Remarks**.** Fabricius (1781) did not state how many specimens he examined, mentioning only that *D. bidens* was described from the Joseph Banks collection, currently deposited at the BMNH. There is just a single specimen in the Banks collection, and quite likely it is the sole specimen used for the description. Moreover, the collection is pinned in the original drawers and there is a single hole after the pin under this species.

The record from Paraguay was made by Spaeth (1914) in the *Coleopterorum Catalogus* without specification of specimens or locality. We were not able to find any specimen from Paraguay and consider this record to be dubious. Based on the distribution data known to us, *D. bidens* seems to be a species occurring rather along the eastern coast of South America in regions influenced by the Atlantic ocean than in the interior dry areas.

Distribution**.** Brazil (Minas Gerais, Rio de Janeiro), Paraguay and Trinidad and Tobago (Borowiec and Świętojańska 2014). New country record to French Guiana, and four new states record to Brazil (Bahia, Espírito Santo, Pernambuco and São Paulo) (Fig. 3.43).

Dorynota (s. str.) borowieci Simões and Sekerka, 2015

(Figs. 3.7–3.8, 3.43)

Type locality. Brazil, Ceará State, Serra do Baturité (Fig.43).

Type material. Holotype, pinned: ‘Serra do Baturité | (Ceará) | Gounelle 1.1895 [w, p, cb] || Museum Paris | Coll. E. Gounelle 1915 [g, p, cb]’ (MNHN). Three paratypes, pinned: same data as holotype, deposited: 2 in LSC and 1 in MNHN. All specimens provided an additional label: ‘HOLOTYPE [or PARATYPE respectively] | Dorynota | borowieci sp. nov. | M. Simões and L. Sekerka des. 2014 [r, p, cb]’.

Diagnosis**.** *Dorynota* (s. str.) *borowieci* belongs to the species group characterized by the uniformly brownish-red body, except humerus black dorsally, and subtriangular or U-shaped habitus, with the anterior 1/3 of the elytra lateral margins abruptly wider than the posterior 2/3. The new species is quite similar in appearance to four species: *D. monoceros* (Germar, 1824), *D. pugnax* (Boheman, 1854), *D. nigra* (Boheman, 1856) and *D. bidens* (Fabricius, 1871), by presenting the U-shaped body, but it can be easily separated mainly by its conspicuous uniform brownish-red dorsal color, except for the black humerus. While, *D. nigra* and *D. bidens* are entirely dark-colored dorsally. In general appearance including color and structure of elytral disc the new species is most similar to *D. monoceros* and *D. pugnax*. The main diagnostic characters to distinguish *D. monoceros*, *D. pugnax* and *D. borowieci* are summarized on Table 3.1.

Description**.** Measurements (n = 4). Body length: 12.5–14.0 mm, body width: 11.5–12.5 mm, body length/width ratio: 1.1, length of pronotum: 3.0–3.5 mm, width of pronotum: 6.5–7.1 mm, pronotum width/length ratio: 2.0. Body subtriangular, U-shaped, with anterior 1/3 of the elytra lateral margins abruptly wider than the posterior 2/3.

Integument opaque; glabrous, except for short yellow sparse setae on pronotum, abdominal sternites and legs. Ground color brownish-red, except for antennomeres VI–XI, mouth parts, basal margin of elytra and humerus black.

Antennae with scape and pedicel glabrous, antennomeres III–V with short and sparse setae and VI–XI densely setose with ventromarginal groove. Length ratio of antennal segments 100:37:33:50:67:108:108:83:100:100:133, with XI tapered towards apex. Pronotum approximately 2 × wider than long, elliptical, with the maximum width in the middle, disc finely and densely punctate; anterior margin sinuous; lateral margins rounded; posterior angles W-shaped. Prosternum with collar projected laterally, not covering mouth parts; process flat, with concave lateral margins, and acuminate apex expanded laterally. Scutellum rhomboidal, impunctate, smooth and shiny.

Elytra with poorly-marked crenulate basal margin, lateral and sutural margins flat. Humeral angles strongly expanded anteriorly, reaching to midlength of pronotum laterally, with anterior margin truncate and oblique corner angle. Disc with coarse, large and shallow punctures arranged in rows on the first third and disordered on apical 2/3; intervals distinct, approximately as wide as puncture diameter, smooth, impunctate; explanate margin converging posterad, finely and densely punctate, and distinctly bordered from disc by marginal row of puncture, the latter extending from humeral callus to apex of elytra. Dorsal spine acute, as long as the body height, on lateral view tilted posteriorly, with base 2x wider than apex.

Table 3. 1. Diagnostic characters distinguishing *D. monoceros*, *D. pugnax* and *D. borowieci*.

Diagnostic character/ Species	*D. monoceros*	*D. pugnax*	*D. borowieci*
Dorsal spine	High, 2.6x longer than its base	Low, 1.6x longer than its base	Low, 1.25x longer than its base
Humeral carina	Elevated and sharp	Not elevated and obtuse	Elevated and sharp

Prosternal collar followed by depression	Present	Present	Absent
Prosternal process	Depressed medially	Depressed medially	Flat

Etymology**.** The species is dedicated to Dr. Lech Borowiec (DBET, Wrocław, Poland), a leading specialist in the Cassidinae.

Figures 3. 1–3.8. *Dorynota* (s. str.) species: 1–2, *D.aculeata* (Boheman, 1854) form Dominican Republic (St. Domingo), paralectotype: 1, dorsal view; 2, lateral view and labels; 3–4, *D. aurita* (Boheman, 1862) from Mexico (Durango): 3, dorsal view; 4, lateral view; 5–6, *D. bidens* (Fabricius, 1781) from Brazil (Minas Gerais): 5, dorsal view; 6, lateral view; 7–8, *D. borowieci* Simões and Sekerka, new species**,** holotype: 7, dorsal view; 8, lateral view.

Dorynota (s. str.) cornigera (Boheman, 1854)

(Figs. 3.9–3.10, 3.43)

Batonota cornigera Boheman 1854: 162 (type locality: ‘Brasilia’).

Batonota bellicosa Boheman, 1854: 159 (type locality: ‘Brasilia’). New synonym

Type material. *Batonota cornigera*, lectotype (designated by Borowiec (1999)), pinned: ‘Brasil. [w, p, cb] || Mhn. [w, p, cb] || Type. [w, p, cb] || LECTOTYPE | des. L. Borowiec [r, p, cb]’ (SMNH). *Batonota bellicosa*, holotype (by monotypy), pinned: ‘14262 [w, p, sl] || bellicosa | Boh.* | Brasil. Sello. [g, hw, cb, bb] || HOLOTYPE | des. L. Borowiec [r, p, cb] || HOLOTYPUS | Batonota | bellicosa | Boheman, 1854 | des. L. Borowiec [r, p, cb, bb]’ (ZMHB).

Additional material examined (36). ARGENTINA: *Misiones*: XI.1941, A. Maller lgt. (1 spec., MNRJ); BRAZIL: without additional locality data (2 spec., DBET; 3 spec., MMUE); XII.1964 (2 spec., MNRJ); *Goiás*: Jatahy (1 spec., MMUE); *Mato Grosso*: (1 spec., LSC; 1 spec., ZMHB); *Minas Gerais*: Pedra Azul, XII.1970, F.M. Oliveira lgt. (1 spec., MNRJ); Poços de Caldas, Morro de Ferro Poços de Caldas (Morro de Ferro), I.XI.1970, J. Becker lgt. (1 spec., MNRJ); *Rio de Janeiro*: without further locality data (1 spec., DBET); Corcovado, I.1962, Alvarenga and Seabra lgt. (1 spec., MNRJ); *Rio Grande do Sul*: without additional locality data (1 spec., MMUE); Porto Lucena, (1 spec., MMUE); *São Paulo*: without further locality data (1 spec., DBET, 1 spec., ZMUC); Rosana (Porto Primavera), 11.XII.1998, A. Brescov lgt. (1 spec., MZUSP); *Santa Catarina*: Curupá (Hansa), XI.1939 (2 spec., MNRJ); Joinville (2 spec., MMUE); Pinhal, XII.1953, A. Maller lgt. (1 spec., MNRJ); Rio Vermelho, XII.1948, Dirings lgt. (2 spec., MZUSP); I.1949, A. Maller lgt. (2 spec., AMNH); Rio Vermelho, III.1952 (1 spec., MNRJ); XII.1955, A.

Maller lgt. (1 spec., MNRJ); Rio Negrinho, XI.1925, A. Maller lgt. (1 male, 1 female, MNRJ); PARAGUAY: without additional locality data (2 spec., DBET); *Cordillera*: San Bernardino, W. Elsenlohr V. [endor] (1 spec., DBET), P. Sladhorn lgt. (1 spec., LSC).

Diagnosis**.** *Dorynota cornigera* is very variable species with regards to coloration, but can be easily distinguished by the presence of conspicuous acute humeral angles. *Dorynota hastifera* and some specimens of *D. pugionata* possess the humeral angles shaped as such, but also have punctate elytral intervals, while in *D. cornigera*, they are impunctate.

Remarks**.** Boheman (1854) described *D. cornigera* and *D. bellicosa* from an unknown number of specimens. However, for *D. cornigera* information on length span and variation was provided, and he cited 'A Dom. Com. Mannerheim et e Mus. Imp. Wienn. ad describendum communicata', therefore he must have had at least two specimens. Borowiec studied Boheman's that is now deposited at the SMNH and found a single specimen of this species, which he designated as the lectotype. Other specimens, if found, shall be designated as paralectotypes.

Dorynota bellicosa was also described from an unknown number of specimens. However, as Boheman gave a single length measurement and stated 'Dom. Sellow. Mus. Reg. Berol.', we assume he must have had a single specimen, as in many other species described by him. The ZMHB holds a single specimen of this species, and only one specimen is mentioned in the historical collection`s catalog, therefore it is considered as the holotype by monotypy.

Boheman (1854) compared both taxa to *D. pugionata* (Germar, 1824), based on general body appearance and the presence of long dorsal spine. By reading the primary descriptions, the main characters used to separate these two species were size and body coloration, with *D. bellicosa* presenting as darker in form with partly black ventrites and *D. cornigera* as a pale form with yellowish ventrites.

We examined types of both taxa, as well as 36 additional specimens and found that both taxa are conspecific. *Dorynota bellicosa* represents an extreme form, differing from *D. cornigera* in dark yellowish-brown elytra, and somewhat sparser and slightly smaller elytral punctation. The examined series of specimens display great variability in dorsal as well as ventral color. Dorsum is always with a variegated pattern ranging from yellow to brown or evenly black with lateral slopes and margin darker than the central part of the disc. Coloration of the pronotum is also variable and the black pattern can be completely reduced in extreme forms. Punctation of the elytra is also variable, as noticed by Monrós and Viana (1949), and is dependent on the size of specimen. Small specimens with smaller surface of elytra present more condensed punctuation, while large specimens with larger surface present sparser punctuation.

As both taxa were described in the same publication, we chose to retain the name *D. cornigera* as valid for this taxon, since it has been applied correctly and *D. bellicosa* was unknown to subsequent cassidine workers (following the First Reviser Principle, Article 24.2.1. of the Code; ICZN 1999).

Distribution**.** Argentina (Entre Ríos, Salta, Chaco), Brazil (Distrito Federal, Goiás, Minas Gerais, Santa Catarina, São Paulo); Paraguay (Asunción) (Borowiec and Świętojańska 2014). Three new state records to Brazil (Mato Grosso, Rio de Janeiro, Rio Grande do Sul), new province records to Argentina (Misiones) and Paraguay (Cordillera) (Fig. 43).

Dorynota (s. str.) hastifera (Spaeth, 1923)

(Figs. 3.11–3.12, 3.44)

Batonota hastifera Spaeth, 1923: 71 (type locality: ‘Bahia’).

Type material. Holotype, pinned: ‘Bahia [hw by Spaeth] | Brasil [w, p, cb] || ex coll. | v d. Poll [w, p, cb] || hastifera [hw] | Typus [hw] | Spaeth det. [w, p, cb] || TYPUS [pink, p, cb] || M/ CR MUS. | SPAETH COLL. [w, p, cb] || Manchester Museum | SYNTYPE [b, p, cb]’ (MMUE). Additional material examined. Known only from the two type specimens.

Diagnosis**.** See diagnosis under *D. pugionata*.

Remarks**.** Spaeth (1923) described *D. hastifera* from two specimens, one from Bahia and the other from Colombia. As the second specimen is conspecific with the holotype, but does not have more precise locality data and as no species of this group occur in Colombia, we consider this record as dubious and quite likely the specimen was mislabeled.

Distribution. Brazil (Bahia) and Colombia[?] (Spaeth 1923 (Fig. 3.44).

Dorynota (s. str.) monneorum Simões & Sekerka, 2015

(Figs. 3.15–3.20, 3.44)

Type locality. Costa Rica, Puntarenas Province, Osa Peninsula, Carara Biological Reserve, Estacíon Quebrada Bonita, approximately 09°46′ N, 84°36′ W 50 m a.s.l. (Fig. 44).

Type material. Holotype, pinned: ‘Est. Queb. Bonita, 50m, Res. Biol. | Carara, Prov. Punt., COSTA | RICA, Abr 1993, R. Guzmán. | L-N-194500, 469850 [w, p, cb] || Costa Rica INBIO | CR1001 | 370598 [w, p, cb]’. Four paratypes, two females and two with undetermined sex pinned: female, with dissected genitalia in vial, with label data: ‘female [w, hw, cb] || Rancho Quemado, 200m, | Península de Osa, Prov, | Puntarenas, Costa Rica | D. Brenes, Abr 1992 | L-S 292500, 511000 [w, p, cb] || Costa Rica INBIO | CR1000 | 495202 [w, p, cb] || Dorynota | A.

Mora D`93 [w, bb, hw, cb]'; female, dissected with abdomen and three apical antennomeres from right antenna mounted on white triangle, with label data: 'female [w, hw, cb] || Rancho Quemado, Penín- | sula de Osa, 200m. Prov, | Punt., COSTA RICA, | F. Quesada, Nov 1991, | L-S 292500, 511000 [w, p, cb] || Costa Rica INBIO | CR1000 | 45202 [w, p, cb]'; unsexed specimen: 'Rancho Quemado, 200m, | Península de Osa, Prov. Punt., | COSTA RICA, Jul 1991. F. | Quesada. L-S-292500, 511000 [w, p, cb] || Costa Rica INBIO | CR1001 | 407485 [w, p, cb] || Dorynota | sp. | det. Chaboo 2000 [w, bb, hw, cb]'; unsexed specimen: 'glued leg [w, p, cb] || Brasil AM, Benjamin | Constant VIII. | 1979 A.C. Domingos leg. [w, hw, cb]'. Holotype and two paratypes deposited in INBIO, one in LSC and one in MNRJ. All specimens provided with additional label: 'HOLOTYPE [or PARATYPE respectively] | Dorynota | monneorum sp. nov. | M.V.P. Simões and L. Sekerka des. 2014 [r, p, cb]'.

Diagnosis. *Dorynota* (*s. str*.) *monneorum* belongs to a species group that is characterized by impunctate elytral intervals and pronotum at most finely punctate, but can be distinguished by its shield-shaped body with bisinuate lateral margins of the elytra, a feature so far unique for this taxon. It can be also easily separated from other species by the regularly convex surface of the humeral angles, which is without the carina present in all remaining *Dorynota* s. str. with the exception of *D. ohausi* (Spaeth, 1915). The latter can be easily separated by uniformly yellowish or reddish-brown dorsum, while *D. monneorum* has pronotum and elytra with extensive black pattern and the explanate margin of elytra with two transverse maculae. In general appearance, including colour and structure of elytral disc, the new species is most similar to *D. rileyi* Borowiec, 1994 and *D. monoceros* (Germar, 1824), the only two other *Dorynota* s. str. species with maculae on the explanate margin of elytra. The diagnostic characters to distinguish *D. rileyi* and *D. monneorum* are summarized in Table 2.

Description. Measurements (n = 5). Body length: 9.1–11.5 mm, body width: 8.1–9.2 mm, body length/width ratio: 1.2, length of pronotum: 2.9–3.3 mm, width of pronotum: 4.9–5.7 mm, pronotum width/length ratio: 1.7. Body slightly longer than wide, shield-shaped, with anterior half wider and sinuate, and posterior half chalice-like, converging posteriad.

Integument opaque, except for transparent anterior margin of pronotum and explanate margin of elytra; glabrous, except for short setae on pronotum and ventral side. Ground color of dorsum yellow; pronotum with black pattern on disc (Fig. 3.15) and with narrow lateral spots on marginalia; elytra with extensive black pattern as in Fig. 3.15, explanate margin with narrow posthumeral and wide posterolateral transverse spots; five distal antennomeres brownish-yellow, rest yellow; ventral surface brownish-black except of two anterior thirds of prosternum, anterior half of metasternum, legs and sternites I–V yellow.

Antennae with five basal glabrous antennomeres and distal antennomeres with short setae; scape almost 3x longer than pedicel; tapered towards apex. Length ratio of antennomeres: 100:33:27:47:60:67:67:53:67:63:100.

Pronotum about 1.8x wider than long, elliptical, with maximum width medially, disc finely and sparsely punctate; anterior margin sinuous; lateral margins rounded; posterior angles truncate. Prosternum with prosternal collar projected anteriorly, not covering mouth parts; process flat, with acuminate and elongate apex. Scutellum rhomboidal, impunctate, smooth and shiny.

Elytra with basal margin crenulate, lateral and sutural margins elevated. Humeral angles expanded anteriorly reaching to midlength of pronotum, anterior margin obliquely truncate, with outer margin of humeral corner slightly projected laterally, followed by sinuous lateral margin. Disc with coarse punctures arranged in discontinuous rows; intervals distinct, approximately as

wide as puncture diameter, smooth and slightly forming carina: two posthumeral (on first and second interval), one reaching ½ and other ¼ of disc, and two dorsal (on third and fourth interval), stretching from basal ¼ of disc to apical ¾; explanate margin converging posterad, with fine and sparse punctures, distinctly bordered from disc by marginal row of puncture, extending from humeral callus to apex of elytra, interrupted by two transverse ridges around midlength; surface of humeral angle regularly convex without carina. Dorsal spine acute, almost 1.5x shorter than body height, in posterior view, base 2.5x wider than apex.

Female terminalia (Figs. 17–20). Sternite VIII (Fig. 17) somewhat sclerotized with median setae at medially at the apical margin, shortening laterally; lateral arms membranous, fused to sternite IX, forming transverse membranous sacs; apodemes as long as width of apical region. Sternite IX (Fig. 20) subdivided into two plates with long, erect setae at apical margin. Tergite X (Fig. 18) with two regions next to sclerotized apical margin, densely setose, with a range of short and erect setae on the edge. Spermatheca (Fig. 3.19) strongly sclerotized and curved, with apex parallel to base, 2x wider than second 1/3, and apex abruptly tapered. Duct of spermathecal gland strongly coiled and long, ca. 6x longer than spermatheca.

Table 3. 2. Diagnostic characters to distinguish *D. aurita, D. monneorum, D. rileyi* and *D. monneorum*.

Diagnostic character	*D. aurita*	*D. rileyi*	*D. wappesi*	*D. monneorum*
Body shape	U-shaped	elongate-triangular	elongate-triangular	escutcheon-shaped
Anterior margin of pronotum	sinuate	truncate	truncate	sinuate
Outline between pronotum and elytra	discontinuous	discontinuous	discontinuous	continuous
Anterior margin of humeral angles	truncate horizontally	truncate horizontally	oblique	sinuate
Humeral carina	strongly elevated	low	low	absent

Outer humeral angle	rounded, on the same level as inner	subacuminate, on the same level as inner one	rounded, situated lower than inner one	subacuminate, situated lower than inner one
Explanate margin of elytra	immaculate	maculate	immaculate	Maculate
Lateral margin of elytra	sinuate behind humeral angles, followed by straight an parallel outline	sinuate behind humeral angles, followed by straight oblique outline	sinuate behind humeral angles, followed by straight oblique outline	bisinuate
Apex of prosternal process		subrounded	acuminate	acuminate

Etymology**.** The species is named after Dr. Miguel Monné and Dra. Marcela Monné, Museu Nacional/Universidade Federal do Rio de Janeiro.

*Dorynota (s. str.) monoceros (*Germar, 1824)

(Figs. 3.13–3.14, 3.44)

Cassida monoceros Germar, 1824: 536 (type locality: 'Brasilia').

Batonota gladiator Boheman, 1856: 94 (type locality: 'Guayra'); Spaeth, 1914: 66 (synonymy).

Type material. *Cassida monoceros*: lectotype (designated by Borowiec (1999)), pinned: '14255 [w, p, s] || LECTOTYPE | des. L. Borowiec [r, p, cb] || monoceros | Boh.* | Caffid. Monoceros | Germ. | S. Paul. Sello [g, hw, cb, bb] || PARALECTOTYPUS | Cassida | monoceros | Germar, 1824 | des. L. Borowiec [r, p, cb, bb]' (ZMHB); two paralectotypes, pinned: 'PARALECTOTYPE | des. L. Borowiec [r, p, cb] || PARALECTOTYPUS | Cassida | monoceros | Germar, 1824 | des. L. Borowiec [r, p, cb, bb]' (ZMHB). *Batonota gladiator*: syntype, pinned: 'Guayra [w, hw, s] || Deyrolle [w, p, s] || Gladiator Bhn. [w, Boheman hw, s] || NHRS-JLKB |

000020993 [w, p, cb]' (SMNH); syntype, pinned: 'Type | Guayra [w, Baly's hw, cb] || Type [w, p, s, circle label with red frame] || Guayra. [hw] | ex Deyrolle [hw] | Baly Coll. | 1905—54. [w, p, cb] || Batonota | gladiator, Bhn | ?Type [w, C. J. Gahan's hw, cb]' (BMNH).

Additional material examined (26). BRAZIL: *Bahia*: without additional locality data, G. Bondar lgt. (2 spec., MMUE; 1 spec., MNRJ); *Espírito Santo*: Linhares (Reserva Biologica Sooretama), XII.1964, F. M. Oliveira lgt. (1 spec., MNRJ); *Mato Grosso*: Rosário-Oeste, II.1972, (1 spec., MZUSP), X.1973, Dirings lgt. (2 spec., MZUSP), II.1974 (1 spec., MZUSP); *Minas Gerais*: Lagoa Santa, Reinhardt lgt. (4 spec., ZMUC); Matozinho, 3–4 trimestre 1885, E. Gounelle lgt. (1 spec., MNHN); *Pará*: Santarém (Santarenzinho, Rio Tapajós), II.1964, Dirings lgt. (7 spec., MZUSP); *São Paulo*: without additional locality data (1 spec., DBET); Bananal (Serra da Bocaína), I.1937, D. Mendes lgt. (1 spec., MNRJ); Peruíbe, 20.XII.1936 (1 spec., MNRJ); COLOMBIA: 'Kolombian', (1 spec., MMUE); PARAGUAY: *Central*: San Antonio (Rio Paraguay), 8.X.1936 (1 spec., DBET); *Itapuá*: Vega, XII.1954, Dirings lgt. (3 spec., MZUSP); URUGUAY: *Paysandú*: 'Paysandu' (1 spec., LSC); VENEZUELA: *Distrito Federal*: Caracas (1 spec., MMUE).

Diagnosis. *Dorynota monoceros* is characterized by the elytra with a long dorsal spine, the impunctate elytral intervals, humeri strongly expanding laterally with low but distinct carina and pale colored dorsum. A similar combination of characters is also found in *D. pugnax*, which differs by having a short elytral spine (1.0–1.5x longer than width of its base) while *D. monoceros* has a long spine (at least 2.0x longer than width of its base). *Dorynota borowieci* is the most similar species, but it differs in having a uniformly yellow explanate margin of the elytra and less impressed and somewhat sparser punctation of the elytra, while *D. monoceros* has the explanate margin laterobasally with a black margin, and a black spot posteriorly on the

underside, and the punctation is very dense and strongly impressed, particularly on latero-apical slope of the elytra.

Remarks**.** Among other records, we found a single specimen from Colombia, in the MMUE collection, that unfortunately does not have precise locality data and could be easily mislabeled. Therefore we do not consider it as a new country record until more accurately labeled specimens become available.

Boheman (1856) described *D. gladiator*, which was later synonymized with *D. monoceros* by Spaeth (1914). *Dorynota gladiator* differs from the types of *D. monoceros* in that it has slightly less coarse and sparser punctation of elytra, by the presence of black spot on apical slope of elytra, and the rust-colored ventral side.

Monrós and Viana (1949) were the first who listed Bolivia in the species distribution, however, they did not mention any particular specimen in examined material. We do not know why they did so, as we were unable to find any published record of either species from Bolivia and thus consider this record as dubious. On the other hand, the species might occur in Bolivia as it is found in the neighboring regions.

Also problematic is the interpretation of the type locality of *B. gladiator*, since Guayra can refer to different places. Boheman (1856) provided just a brief description and mentioned that he obtained the material from Deyrolle. Boheman (1862), in the supplement to his monograph, included description of *B. gladiator* again and mentioned 'Guayra. Dom. Deyrolle. Venezuela Dom. Baly.', what might suggest that the type locality he referred to was the city La Guaira in Venezuelan state of Vargas.

On the other hand, there are no accurately labeled specimens of *Dorynota* from Venezuela, thus it also could refer to Guairá department of Paraguay that would also be in the

species distribution. The third option is two Brazilian municipalities named Guaíra. One situated in the state of Paraná and the other in São Paulo. It is known that Baly purchased many syntypes of species described by Boheman (1856, 1862) from Deyrolles material, thus the BMNH specimen of *B. gladiator* is considered as a syntype. We do not consider the specimen from Venezuela in Baly's collection as a syntype because it was not mentioned in 1856. Both syntypes have a long spine and morphology similar to specimens distributed in the southern part of the range, thus the type locality probably rather refers to Paraguay than to Venezuela. Generally, it is questionable whether the species is truly present in Venezuela, as only old and poorly labeled specimens with data ‘Caracas’ or ‘Venezuela’ are available. The Baly's specimen from Venezuela has a short dorsal spine and less expanded and broadly rounded humeral angles and probably belongs to *D. pugnax*.

Distribution**.** Argentina (Corrientes, Misiones), ? Bolivia, Brazil (Rio de Janeiro, Santa Catarina), Paraguay (Asunción, Caazapá, Concepción, Guairá, Paraguarí), Venezuela [?] (Borowiec & Świętojańska, 2014). New country record to Uruguay (Paysandú), six new state records to Brazil (Bahia, Espírito Santo, Mato Grosso, Minas Gerais, Pará, São Paulo), two new departments to Paraguay (Central, Itapuá) and new locality record to Venezuela (Distrito Federal) (Fig. 3.44).

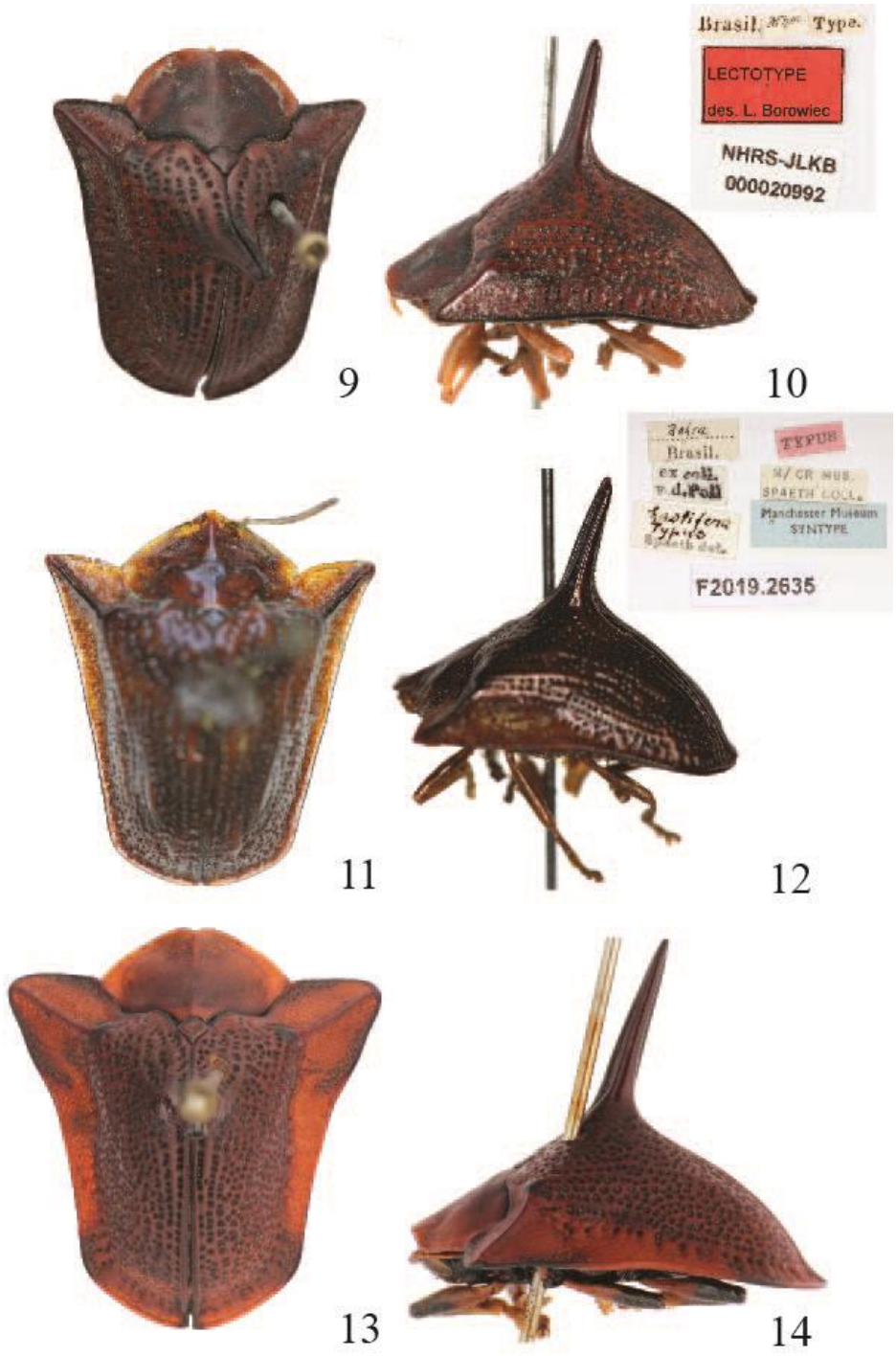

Figure 3. 9–14. *Dorynota* (s. str.) species: 9–10, *D. cornigera* (Boheman, 1854), lectotype: 9, dorsal view; 10, lateral view and labels; 11–12, *D. hastifera* (Spaeth, 1923), holotype: 11, dorsal view; 12, lateral view and labels; 13–14, *D. monoceros* (Germar, 1824) from Brazil (Bahia): 13, dorsal view; 14, lateral view.

Dorynota (s. str.) nigra (Boheman, 1856)

(Figs. 3.21–3.22, 3.44)

Batonota nigra Boheman, 1856: 93 (type locality: ‘Peruvia’).

Type material. Lectotype (designated by Borowiec (1999)), pinned: ‘Peru [w, p, cb] || Deyrolle [w, p, cb] || Type. [w, p, cb] || Lectotype | des. L. Borowiec [r, p, cb]’ (SMNH). Paralectotype, pinned: ‘Peru [g, hw, cb] || Type | C: Deyrolle [w, J. S. Baly’s hw, cb] || Type [w, p, s, circle label with red frame] || Peru. [hw] | ex Deyrolle [hw] | Baly Coll. | 1905—54. [w, p, cb] || Batonota | nigra, Bhn | Type ! [w, C. J. Gahan’s hw, cb]’ (BMNH).

Additional material examined. COLOMBIA: *Arauca*: Tame, 21.–29.VI.1976, M. Cooper lgt. (1 spec., BMNH).

Diagnosis**.** *Dorynota nigra* is a well-characterized species, the only of the nominotypical subgenus with elytra with a metallic tint. The similarly dark colored *D. bidens* differs in that the elytra are dull black without a metallic tint and longer dorsal spine.

Remarks. Boheman (1856) did not state how many specimens he examined, however we can assume he had at least two, as he provided two type localities in his description and also described var. a. Borowiec (1999) examined the specimen in SMNH and designated it as a lectotype. We recently examined another specimen from the Baly collection (ex. Deyrolle material) deposited in the BMNH, which thus becomes as a paralectotype according to the Code (ICZN 1999). The typical form was described from Peru, while the variants are from Caracas. The types were almost certainly mislabeled and only the locality for the variants is correct, as we

do not know any other specimens of this species from Peru and the species seems to be restricted to northern coast of South America.

Distribution**.** Trinidad and Venezuela (Aragua, Distrito Federal) (Borowiec and Świętojańska 2014). New country record to Colombia (Fig. 3.44).

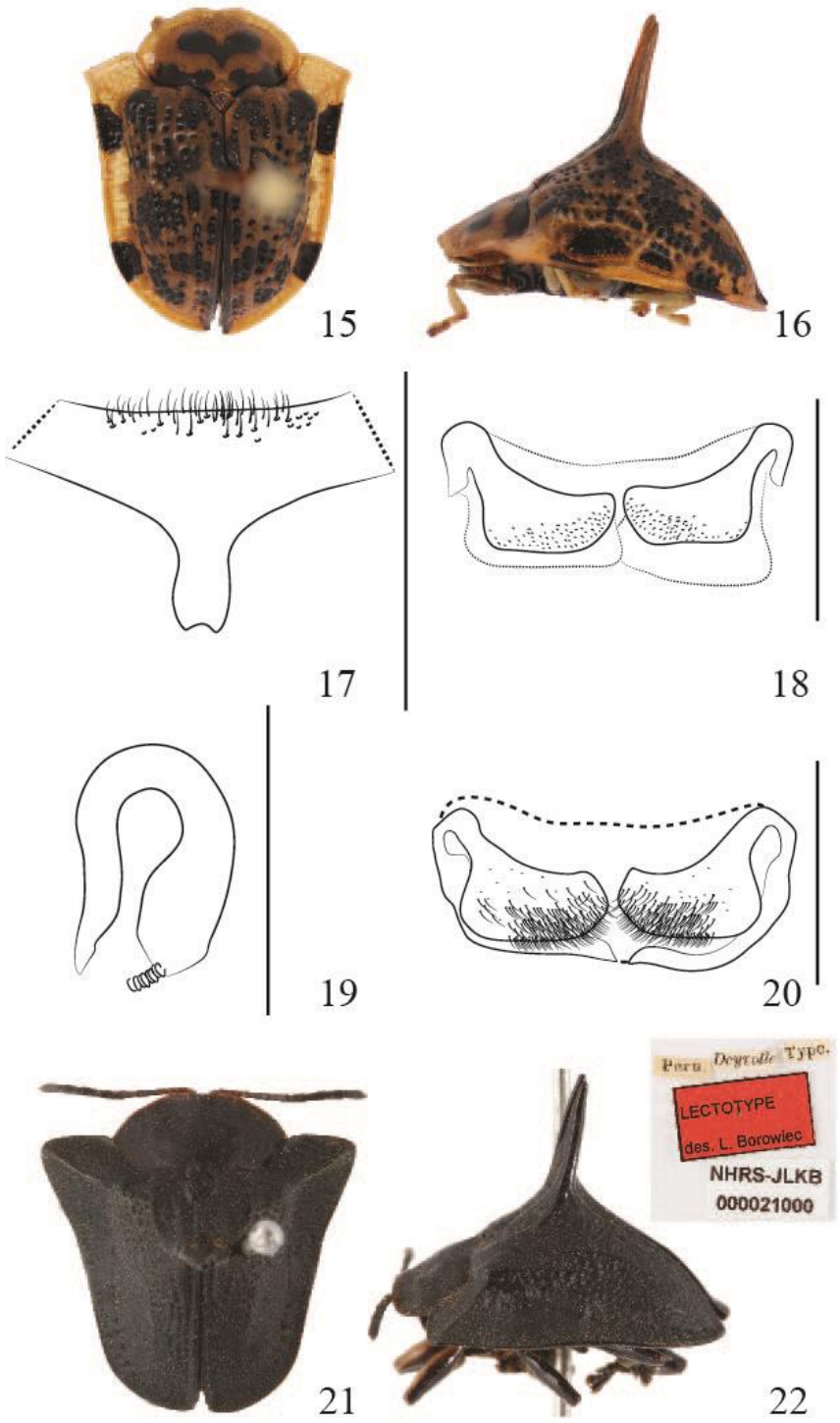

Figure 3.15–22. *Dorynota* (s. str.) species: 15–20, *D. monneorum* Simões and Sekerka, new species: holotype: 15, dorsal view; 16, lateral view; 17, sternite VIII; 18, tergite X; 19, spermartheca; 20, sternite IX; 21–22, *D. nigra* (Boheman, 1856), lectotype: 9, dorsal view; 10, lateral view and labels.

*Dorynota (s. str.) nodosa (*Boheman, 1854)

(Figs. 3.23–3.25)

Batonota nodosa Boheman, 1854: 160 (type locality: ‘Columbia’).

Type material. Syntype, pinned: ‘292 | [illegible] [g, sl, hw on underside of a circle label] || MUSÉUM PARIS | Colombie ? [hw] [g, p, cb]’ (MNHN); syntype, pinned: ‘MUSEUM PARIS | COLOMBIE | C. PARZUDAKI 1840 [g, p, cb] || 2899 | 40 [g, sl, hw on underside of a circle label]’ (MNHN).

Diagnosis**.** *Dorynota nodosa* and *D. rufomarginata* are the only two species of the nominotypical subgenus that have a very short spine reminiscent of *Akantaka* species, which is triangular in frontal view and not projecting above the base. All *Akantaka* species can be easily separated by the following combination of characters: the lateral sides of elytra straight not concave behind the humeral angles and dorsal spine in lateral view with apex not markedly narrower than base, followed by gradual and continuous slope. Both species are externally quite similar but *D. nodosa* has elytra with a thin black outer margin with the lateral sides more concave, while *D. rufomarginata* has a uniformly pale elytral margin and lateral sides less concave and subparallel.

Remarks**.** *Dorynota nodosa* (Boheman, 1854) had been misidentified in the past with some populations of *D.* (*Akantaka*) *insidiosa* (Boheman, 1854) from Central America because no author examined the type specimen deposited in the MNHN collection. It has short spine and distinctly concave lateral margins of elytra, thus certainly belongs to the nominotypical subgenus. All Mesoamerican specimens we have seen so far have straight or slightly convex

lateral margins of elytra and even lower spine thus belong to yet probably undescribed species of *Akantaka*. Spaeth (1923) synonymized *D. pugnax* with *D. nodosa* and since then the species was considered a synonym. We have examined type of *D. pugnax* and found that it is quite different from *D. nodosa*, rather similar to *D. monoceros* thus is removed here from synonymy (see remarks under *D. pugnax*). Published records of *D. nodosa* (i.e. Champion 1893 and Chaboo 2002) quite likely belong to other species, therefore we retain only Colombia in distribution of *D. nodosa*.

Distribution**.** Colombia (Boheman 1854).

*Dorynota (s. str.) ohausi (*Spaeth, 1916)

(Figs. 3.26–3.27)

Batonota Ohausi Spaeth, 1916: 284 (type locality: 'Ecuador').

Type material. Syntype, pinned: 'Ecuador | Buckley [w, hw, cb, circular label] || Ohausi [hw] | m. Typus [hw] | Spaeth det. [w, p, cb, Spaeth's hw] || coll. Baly [w, p, cb] || TYPE [r, p, cb] || M/CR MUS | SPAETH COLL. [w, p, cb] || Manchester Museum | SYNTYPE [b, p, cb]' (MMUE).
Additional material examined. ECUADOR: *Loja*: without additional locality data, A. Gaujon lgt. (1 spec., LSC; 3 spec., MNHN).

Diagnosis**.** *Dorynota ohausi* can be easily separated from other species by the regularly convex humeral angles which lack a carina. The only other species with this character is *D.*

monneorum, but it differs from this species in the escutcheon body shape and black-patterned dorsum, while *D. ohausi* is uniformly yellow with a subtriangular body.

Remarks**.** So far this species has been considered as being described in 1915, however, the description was published in the second issue of 1915 volume of the Stettiner Entomologische Zeitung which was released on 31st March 1916. Therefore the year of publication must change to 1916.

Distribution**:** Ecuador (Zamora-Chinchipe) (Borowiec 2002). New province record for Ecuador (Loja) (Fig. 44).

Dorynota (s. str.) parallela Blanchard, 1846

(Figs. 3.28–3.29)

Dorynota parallela Blanchard, 1846: 212 (type locality: ‘Guarayos (Bolivia)’).

Type material. Paralectotype (designated by Borowiec (1999)), pinned: ‘MUSEUM PARIS | BOLIVIE | (CHIQUITOS) | D`Orbigny 1834 [w, p, cb, bb] || 7316 | 34 [circle label] || PARALECTOTYPE | des. L. Borowiec [r, p, cb, bb]’ (MNHN).

Additional material examined (49). ARGENTINA: *Misiones*: without additional locality data, V.1955, Dirings lgt. (1 female, MZUSP); BRAZIL: *Bahia*: without additional locality data, G. Bondar lgt. (13 spec. MNRJ, 3 spec., USNM); *Pará*: Santarém (Santarenzinho, Rio Tapajós), II.1964, Dirings lgt. (26 spec., MZUSP); *São Paulo*: without additional locality data (1 spec., DZUP); Vale do Anhangabaú, XI.1924, R. Spitz lgt. (2 spec., MNRJ); Rio Claro, 13.XI.1980, Alejo Mesa lgt. (1 spec., MZUSP); *Santa Catarina*: Corupá, XI.1944, J. Guerín lgt. (1 spec.,

USNM); BOLIVIA: *Beni*: Reyes, 1–20.XII.1956, L. Peña lgt. (1 spec., MNRJ); *Santa Cruz:* Chiquitos, Santiago, 730m, XI.2008, W. D. Edmonds and T. Vidaurre (4 spec., TAMU).

Diagnosis**.** *Dorynota parallela* can be easily distinguished from other species as having densely punctate intervals of the elytra and rounded humeral angles. *Dorynota pugionata* and *D. hastifera* have acute humeral angles and more sparsely and more finely punctate intervals. The elytral disc is also nearly regular without elevated ribs. *Dorynota aculeata* differs in that it has very finely and sparsely punctate intervals and humeral angles which are not expanded laterally.

Remarks**.** The species was until now considered as being described in 1837. However, d'Orbigny's voyage was published in many separate issues and the volume containing a greater part of the beetles (including the subfamily Cassidinae) was published as late as 1846 (Sherborn and Woodward 1901) thus the year of publication must be revised to reflect this.

Monrós and Viana (1949) revised Argentinean species of Dorynotini and transferred *B. parallela* to a newly formed genus *Paranota* Monrós and Viana, 1949. Recently, Simões (in press) revised the genus *Paranota* and transferred *P. parallela* to *Dorynota* (s. str.) on the basis of the structure of the anterior margin of pronotum, scutellum, tarsal claws and male terminalia.

Spaeth (1914) recorded the species from Ecuador and Borowiec (1996) reported it from French Guiana. However, both records must be considered as erroneous. The first one was published by Spaeth (1914) in the *Coleopterorum Catalogus* where he cited Ecuador as part the species' distribution and since then it was followed. It is questionable whether Spaeth had seen some specimen(s) from Ecuador, (there are none in his collection) or perhaps the record is the result of an error. Borowiec (1998) considered the record an error as well. Borowiec (1996) recorded the species as new to French Guiana, based on old specimens from Bas Maroni,

however, these specimens were most likely mislabeled, as pointed out later by Borowiec and Moragues (2005).

Distribution**.** Brazil (Goiás, Mato Grosso, Minas Gerais, Rio de Janeiro); Bolivia (Santa Cruz); Peru (Vilcanota); Paraguay (Asunción, Concepción) (Borowiec and Świętojańska 2014). New country record to Argentina (Misiones), four new state records to Brazil (Pará, Bahia, São Paulo, Santa Catarina), new department record to Bolivia (Beni) (Fig. 3.44).

*Dorynota (s. str.) pugionata (*Germar, 1824)

(Figs. 3.30–3.31, 3.44)

Cassida pugionata Germar, 1824: 537 (type locality: 'Brasilia').

Batonota Ballista Boheman, 1854: 157 (type locality: 'Brasilia'); Spaeth, 1914: 66 (synonymy).

Type material. Lectotype (designated by Borowiec (1999)), pinned: '14261 [w, p, s] || LECTOTYPE | des. L. Borowiec [r, p, cb] || pugionata / Boh.* / S. Joao d. R. Sello. [g, hw, cb, bb]' (ZMHB); five paralectotypes without labels but according to the register coming from the same series as the lectotype, pinned (ZMHB). All specimens were provided with an additional label: 'LECTOTYPUS [or PARALECTOTYPUS] | Cassida | pugionata | Germar, 1824 | L. Borowiec des. [r, p, cb, bb]'. *Batonota ballista*: lectotype (designated by Borowiec (1999)), pinned: 'Brasil. [w, p, cb] || M. Berl [w, p, cb] || Type. [w, p, cb] || Ballista Bhn. [w, hw, s, Boheman's hw] || LECTOTYPE | des. L. Borowiec [r, p, cb] || NHRS-SRAH | 000000105 [w, p, cb]' (SMNH).

Additional material examined (5). BRAZIL: *Pará*: Cachimbo, 1890, Ch. Pujol lgt. (1 spec., MNHN); BOLIVIA: *Santa Cruz*: Chiquitos, 1834, d`Orbigny lgt. (2 spec., MNHN); PARAGUAY: *Asunción*: without additional locality data (1 spec., ZMHB); *Paraguarí*: 'Paraguari' (1 spec., MMUE).

Diagnosis**.** *Dorynota pugionata* is characterized by the following combination of characters: elytral intervals punctate, humeral angles acuminate and elytra smooth, without ribs. *Dorynota aculeata* and *D. parallela* differ in their rounded humeral angles and the elytra with at least partly with elevated intervals. The most similar species is *D. hastifera,* which differs in that it has less coarsely punctate intervals, a much narrower explanate margin of the elytra and a dorsum which is mostly pale, with only the humeral carina being black.

Remarks. Boheman (1854) described *B. ballista* from an unknown number of specimens, however, he mentioned a length span and two depositories: 'Mus. Reg. Holm. A Dom. Germar ad conferendum etiam misa'. Borowiec (1999) designated the lectotype from a specimen Boheman obtained from Germar and a paralectotype from a second specimen, originally from Stål. In our opinion the second specimen is not a part of the type series, since Boheman did not mention Stål among depositories nor was Stål mentioned as a collector/depository in any of the species described in the *Monographia Cassididarum*. The specimen was most likely collected by J. W. Stål in southern Brazil and was certainly received after publishing the description, therefore we remove the specimen from the type series.

The MMUE specimen from Paraguay is quite likely the one published by Spaeth (1923) as a first record for this country, but without specified locality data.

Distribution**.** Argentina (Misiones), Brazil (Bahia, Espírito Santo, Goiás, Mato Grosso, Minas Gerais, Paraná, Rio Grande do Sul, Rio de Janeiro, São Paulo, Santa Catarina); Paraguay

(Concepción, Puerto Elisa) (Borowiec and Świętojańska 2014). New country record to Bolivia, new state record to Brazil (Pará) and two new province records to Paraguay (Asunción, Paraguarí) (Fig. 3.44).

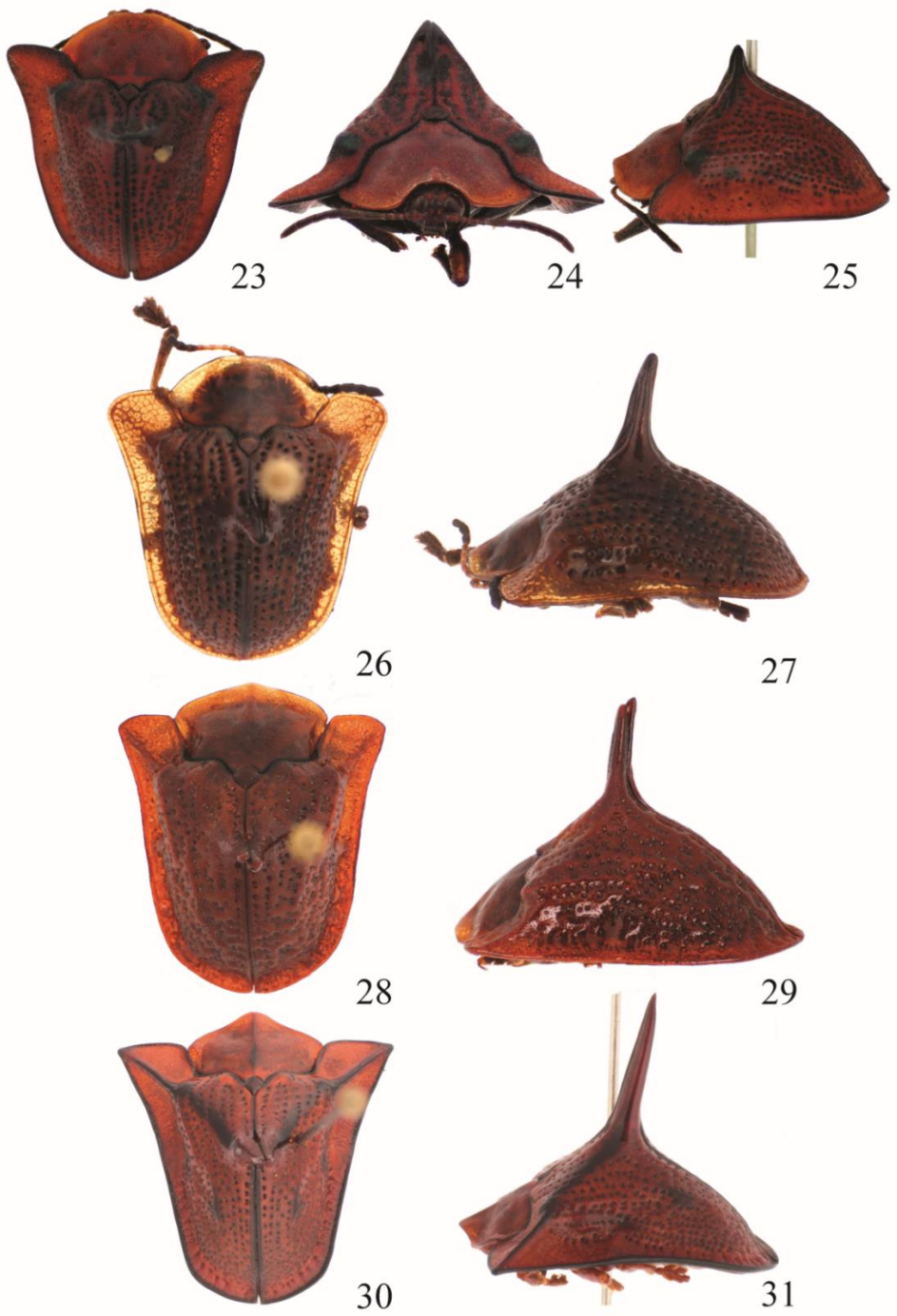

Figure 3. 23–31. *Dorynota* (s. str.) species: 23–25, *D. nodosa* (Boheman, 1854) from Colombia: 23, dorsal view; 24, frontal view; 25, lateral view; 26–27, *D. ohausi* (Spaeth, 1916) from Equator (Zamora-Chinchipe): 26, dorsal view; 27, lateral view; 28–29, *D. parallela* Blanchard, 1846 from Brazil (Goiás): 28, dorsal view; 29, lateral view; 30–31, *D. pugionata* (Germar, 1824) from Brazil (Rio de Janeiro): 30, dorsal view; 31, lateral view.

Dorynota (s. str.) pugnax (Boheman, 1854), restored status

(Figs. 3.32–3.33, 3.45)

Batonota pugnax Boheman, 1854: 161 (type locality: ‘Columbia’).

Type material. Holotype (by monotypy), pinned: ‘E. Coll. | Chevt. [w, p, cb] || Type [w, p, s circle label with red frame] || 44 [g, p, s] || Batonota | pugionata | Bhn | Columbia [w, s hw by Chevrolat] || 67•56 [w, p, sl]’ (BMNH).

Additional material examined (3). COLOMBIA: ‘Columbia’, (1 spec., LSC); PANAMA: Chiriqui (1 spec., DBET; 1 spec., MMUE); VENEZUELA: ‘Venezuela’, (1 spec., BMNH ex coll. J. S. Baly and published by Boheman (1862) as *D. gladiator*).

Diagnosis**.** See diagnosis under *D. monoceros* and Table 1 under *D. borowieci*.

Remarks. Boheman (1854) did not state the precise number of specimens, however, he mentioned ‘Mus. Dom. Chevrolat’ as the depository and gave a single length and width measurements. In such a case, Boheman always had a single specimen and because there is only a single specimen in the Chevrolat collection, we consider it a holotype fixed by monotypy. The precise labeling and type status will be clarified in the catalog of Boheman’s types housed in SMNH (Sekerka, in prep.).

The species was synonymized with *D. nodosa* (Boheman, 1854) by Spaeth (1923) based on the primary description. However, examination of the type revealed that this species is actually morphologically close to *D. monoceros* (Germar, 1824) and not to *D. nodosa*. The latter distinctly differs in that it has a very short dorsal spine, which is barely longer than width of its base, elytra strongly emarginate and more protruding behind the humeral angles. Therefore, we

restore specific status of *D. pugnax*. It can be separated from *D. monoceros* by its shorter elytral spine, less dense and finer punctation of the elytra, and the elytra with mostly distinct intervals, while *D. monoceros* has very coarse and dense elytral punctation with very narrow intervals and punctures nearly touching each other.

The species is also probably found in Venezuela as the specimen reported by Boheman (1862) under *D. gladiator* and cited here most likely belong to *D. pugnax*.

Distribution. Colombia (Boheman 1854), Venezuela [?] (Boheman 1862). New country record to Panamá (Fig. 45).

Dorynota (s. str.) rileyi Borowiec, 1994

(Figs. 3.34–3.35, 3.45)

Dorynota rileyi Borowiec, 1994: 161 (type locality: 'Parag.[uay] Central: Asuncion').

Type material. Paratype, pinned: 'PARAG: CENTRAL | Asuncion, Jardin | Botanico: II-6-| 83: E.G.Riley [w, p, cb] || PARATYPTE | des. L. Borowiec [r, p, cb] || Dorynota | rileyi n. sp. | L. Borowiec, 1994 [w, p, cb, bb]' (DBET).

Additional material examined. BOLIVIA: *Santa Cruz*: Potrerrilo del Guenda, 17°40.3′S, 63°27.4′W, 22.IX–12.XII.2005, B. K. Dozier lgt. (1 spec., LSC).

Diagnosis**.** This is a well-characterized species and is the one of three species with a maculate explanate margin of the elytra. The other species is *D. monneorum*, which differs in the escutcheon body shape and absence of humeral carina. Externally, it is also similar *D. wappesi*,

which differs in having the explanate margin of elytra uniformly yellow. For further characters see diagnosis under *D. wappesi* and Table 2 under *D. monneorum*.

Distribution. Paraguay (Asunción) (Borowiec 1994). New country record to Bolivia (Fig. 45).

*Dorynota (s. str.) rufomarginata (*Wagener, 1881)

(Figs. 3.36–3.38)

Batonota rufomarginata Wagener, 1881: 41 (type locality: 'Brasilia').

Type material. Holotype, pinned: 'Brasil [w, hw, cb] || rufomargin. [hw] | coll. Wagener | Typus ! [hw] [w, p, cb] || TYPUS [pink, p, cb] || M/ CR MUS. | SPAETH COLL. [w, p, cb] || Manchester Museum | SYNTYPE [b, p, cb] || F2019.2722 [w, p, cb]' (MMUE).

Additional material examined. Known only from the holotype.

Diagnosis**.** See diagnosis under *D. nodosa*.

Remarks**.** The species is very close to *D. nodosa* and perhaps representative of just a local form. Unfortunately, both species are known only from types thus it is very difficult evaluate them. Until we have an opportunity to study more material, we will leave *D. rufomarginata* as a valid species close to *D. nodosa*. It is also uncertain whether the specimen was actually collected in Brazil or was mislabeled.

Distribution. Brazil (Wagener 1881).

Dorynota (s. str.) wappesi Sekerka and Simões, 2015

(Figs. 3.39–3.40, 3.45)

Type locality. Bolivia, Santa Cruz Department, Florida Province, road to Amboró National Park above Achira, 18°07.43′ S, 63°47.98′ W, 1940 m a.s.l.(Fig. 45).

Type material**.** Holotype: 'BOLIVIA Santa Cruz dpt. | Florida pr. 1940 m | Rd. to Amboro above Achira | 14–15.x.2006 (cut/burn area) | 18°07.43'S, 63°47.98'W | Wappes, Nearns and Eya lgt. [w, p, cb]' (LSC). Specimen provided with additional label: 'HOLOTYPUS | Dorynota (s. str.) | wappesi sp. nov. | L. Sekerka and | M. Simões des. 2014 [r, p, cb]'.

Diagnosis**.** *Dorynota* (s. str.) *wappesi* belongs to a group of species characterized by impunctate elytral intervals, a pronotum which is at most finely punctate, a high postscutellar elytral spine, humeral angles with a costa and moderately expanded laterally, and with a rather narrow explanate margin of elytra. The group is comprised of *D. aurita* (Boheman, 1862) and *D. rileyi* Borowiec, 1994. *Dorynota aurita* differs in that it has a U-shaped body and a strongly elevated humeral carina, while *D. wappesi* has an elongate-triangular body and a low humeral carina. *Dorynota rileyi* has a similar body shape and formation of the humeri, but differs in that the explanate margin of the elytra is maculate, the antennae are uniformly yellow with only the terminal antennomeres slightly infuscate, the prosternal process is much more widened apically, and the scutellum is regularly rhomboidal, while *D. wappesi* has an immaculate explanate elytral margin, infuscate seven distal antennomeres, the prosternal process weakly widened apically, and the scutellum subrhomboidal with a convex anterior margin. For the main diagnostic characters to distinguish *D. wappesi* from other related species, see Table 2 under *D. monneorum*.

Description. Measurements (n = 1). Body length: 11.5 mm, body width: 7.5 mm, body length/width ratio: 1.5, length of pronotum: 2.5 mm, width of pronotum: 5.3 mm, pronotum width/length ratio: 2.2. Body elongate-triangular, regularly converging from base to apex.

Integument shiny, disc of elytra and pronotum opaque with transparent explanate margins; pronotum and elytral disc with short and sparse yellow setae, denser ventrally. Ground color of dorsum yellow; pronotum with M-shaped spot on disc (Fig. 37) and basal margin black; elytral punctures with black fovea, suture, and humeral calli, explanate margin uniformly yellow only apex somewhat darkened ventrally (Fig. 38); three basal antennomeres yellow, remaining infuscate brownish-black; ventral side yellow with basal margin of abdomen, posterior half of metathorax and areas around coxae black.

Antennae with five basal glabrous antennomeres and six densely setose distal antennomeres; scape ca. 3x longer than pedicel; tapered towards apex. Length ratio of antennomeres: 100:33:27:47:60:67:67:53:67:63:100. Pronotum semicircular, with maximum width approximately in the middle, disc finely and sparsely punctate, except anterior half with coarse punctures; anterior margin strongly emarginate but this could be an artifact due to inadequate hatching as in other *Dorynota* species; lateral margins rounded and convex; posterior angles truncate. Explanate margin moderately broad, smooth, shiny, sparsely punctate, transparent and with honey-comb structure. Prosternum with prosternal collar projected antreiorly, not covering mouthparts; process flat, weakly constricted and with shortly rhomboidal apex, surface smooth, shiny and sparsely pubescent with long setae. Scutellum subrhomboidal, impunctate, smooth and shiny, with convex anterior margin.

Elytra strongly convex and projecting in sharp postscutellar spine. Dorsal spine 3.5 mm long, 2x longer than its base and 1.4x longer than height of elytra. Base of elytra much wider

than base of pronotum, strongly emarginated due to projecting humeral angles; basal margin serrate in emargination, denticles obtuse and swollen. Humeral angles strongly projecting anterad and reaching midlength of pronotum, with oblique carina extending from humeral callus to outer corner, truncate anterior margin, obtuse corners, outer corners slightly expanding laterally and situated slightly posteriorly to inner ones. Disc coarsely and partly irregularly punctate, sutural and five lateral rows regular; intervals distinct, mostly narrower than puncture diameter, only 2nd interval slightly wider than puncture diameter, smooth, shiny, impunctate, and sparsely pubesent with extremely short and barely visible adherent setae. Punctures deeply impressed, foveolate, fovea micro-reticulate thus semiopaque. Due to strongly impressed punctures intervals appear to form low ribs, particularly 1st behind dorsal spine, and 4th and 6th in nearly whole length. Marginal row of punctures distinct in whole length, interrupted by two vacancies around midlength, its punctures with smaller diameter than those on disc but more deeply impressed. Ultimate interval slightly wider than remaining lateral ones. Explanate margin converging posterad, smooth finely and sparsely punctate, micro-reticulate but shiny, its outer margin swollen thus appears slightly canaliculate.

Etymology**.** The species is named in honor of the collector of the holotype, Jim Wappes (San Antonio, Texas), friend and a specialist in Bolivian Cerambycidae.

*Dorynota (s. str.) yucatana (*Champion, 1893)

(Figs. 3.41–3.42, 3.45)

Batonota yucatana Champion, 1893: 162 (type locality: ‘Mexico, Temax in North Yucatan’).

Type material. Syntype, pinned: ‘Temax, | N. Yucatan | Gaumer. [w, p, cb] || Batonota | yucatana, | Champ. [w, hw, cb, G. C. Champion's hw] || Sp. figured. [w, p, cb] || Godman-Salvin | Coll., Biol. | Centr.-Amer. [w, p, cb]’ (BMNH); six syntypes, pinned: ‘Temax, | N. Yucatan | Gaumer. [w, p, cb] || Batonota | yucatana, | Ch. [w, hw, cb, Champion's hw] || Godman-Salvin | Coll., Biol. | Centr.-Amer. [w, p, cb]’ (BMNH); three syntypes, pinned: ‘Temax, | N. Yucatan | Gaumer. [w, p, cb] || Godman-Salvin | Coll., Biol. | Centr.-Amer. [w, p, cb]’ (BMNH); syntype, pinned: ‘Temax, | N. Yucatan. | Gaumer. [w, p, s] || Batonota | yucatana, | Champ [w, Champion hw, cb] || NHRS-JLKB | 000022144 [w, p, cb]’ (SMNH).

Additional material examined. BELIZE: *Cayo*: without additional locality data, B. Davis lgt. (1 spec., BMNH).

Diagnosis**.** *Dorynota yucatana* can be readily characterized by its very small body, which is less than 8 mm long, while all other species are at least 11 mm long. Additionally, the pronotum is transverse, much broader than wide and broadly rounded, with laterally projecting humeral angles with high carinae. Champion (1893) mentioned that the punctures of the elytral intervals are visible only under strong lens. We have studied most of the type series and the intervals are microreticulate without distinct punctation.

Remarks**.** The specimen mentioned above is the only specimen known to us besides those of the type series. The specimen originally came from the collection of G. C. Champion, however, Champion most likely received it after the completion of the Cassidinae volume in *Biologia Centrali Americana*, as it was not included there (Champion 1893). It bears an original identification label from Champion, which reads ‘Batonota sp.’. In our opinion, the specimen belongs to *D. yucatana* because it is similar in size, shape and formation of humeri. It only differs in its slightly coarser punctation and darker color. This variation is quite normal for Mesoamerican

Cassidinae, as in southern populations of one species there is a gradient toward a more sculptured and darker form.

Distribution. Mexico (Yucatán) (Champion 1893). New country record to Belize (Fig. 3.45).

Figure 3. 32–42. *Dorynota* (s. str.) species: 32–33, *D. pugnax* (Boheman, 1854), restored status: 32, dorsal view; 33, lateral view; 34–35, *D. rileyi* Borowiec, 1994 from Paraguay (Asunción): 34, dorsal view; 35, lateral view and labels; 36–38, *D. rufomarginta* (Wagner, 1881): 36, dorsal view; 37, frontal view; 38, lateral view; 39–40, *D. wappesi* Sekerka and Simões, new species, holotype: 39, dorsal view; 40, lateral view; 41–42, *D. yucatana* (Champion, 1893) from Mexico (Yucatán, Temax): 41, dorsal view; 42, lateral view.

Figure 3.43. Map of geographic distribution of the following *Dorynota* species: *D. aculeata* (Boheman, 1854); *D. aurita* (Boheman, 1862); *D. bidens* (Fabricius, 1781); *D. borowieci* Simões and Sekerka, new species and *D. cornigera* (Boheman, 1854).

Figure 3. 44. Map of geographic distribution of the following *Dorynota* species: *D. ohausi* (Spaeth, 1915); *D. nigra* (Boheman, 1856); *D. monoceros* (Germar, 1824); *D. monneorum* Simões and Sekerka, new species and *D. hastifera* (Spaeth, 1923).

Figure 3. 45. Map of geographic distribution of the following *Dorynota* species: *D. parallela* Blanchard, 1837; *D. pugionata* (Germar, 1824); *D. pugnax* Boheman, 1854, restored status; *D. riley* Borowiec, 1994; *D. yucatana* (Champion, 1893) and *D. wappesi* Sekerka and Simões, new species.

Key to the species of the subgenus *Dorynota s. str.*

1. Lateral sides of elytra concave behind humeral angles; dorsal spine in lateral view with at least apical half 2x narrower than basal half, followed by steep and abrupt slope … 2 (*Dorynota* spp.)

- Lateral sides of elytra straight or convex around midlength; dorsal spine in lateral view with apex not markedly narrower than base, followed by gradual and continuous slope …… *Akantaka* Maulik, 1916.

2. Dorsal spine in frontal view broadly triangular and not projecting from its base with straight lateral margins …… 3.

- Dorsal spine in frontal view elongate and projecting from its base with sinuous lateral margins at the base ……..……. 4.

3. Body with dark red outline and lateral margins subparallel; elytral disc in lateral view with low elevation under humeral angle and two clusters of punctation, medially and close to apical third, markedly darker than rest of disc (Figs. 3.36–3.38) …. *D. rufomarginata* (Wagener, 1881).

- Body with black outline and lateral margins slightly sinuous in anterior half; elytral disc with low elevation under humeral angle, with punctation distributed uniformly (Figs. 3.23–3.25) ……...…...……. *D. nodosa* (Boheman, 1854).

4. Pronotum densely and coarsely punctate; elytral intervals punctate …….. 5.

- Pronotum smooth, impunctate, or with several sparsely arranged punctures; elytral intervals impunctate ……..……... 8.

5. Scutellum rhomboidal; dorsum at most with sparse and very short pubescence; South America. .....…..... 6.

- Scutellum triangular; dorsum usually with long and dense pubescence; endemic to Hispaniola (Figs. 3.1–3.2) ……... *D. aculeata* (Boheman, 1854).

6. Body appearing strongly triangular, with strongly explanate humeral angles and subacuminate apex of elytra; elytral surface smooth, intervals not elevated; dorsum with black pattern …….. 7.

- Body nearly oval with weakly explanate humeral angles and rounder elytal apex; elytra appear rugose due to more or less elevated intervals; dorsum reddish brown without black spots (Figs. 3.28–3.29) ……..…….. *D. parallela* (Blanchard, 1837).

7. Explanate margin of elytra broad; outer margin of elytral suture, oblique ridge from spine to humerus, latero-apical spot, scutellum, and midline of pronotum black; elytral intervals densely and coarsely punctate (Figs. 3.30–3.31) …….. *D. pugionata* (Germar, 1824).

- Explanate margin of elytra narrow; black color limited to humeral angles; elytral intervals moderately punctate (Figs. 3.11–3.12) ..... *D. hastifera* (Spaeth, 1923).

8. Dorsum black, with or without a metallic tint …… 9.

- Dorsum yellow to reddish or brown, but never with a metallic tint. ……..……... 10.

9. Dorsum opaque black, sides of pronotum and lateral slope around midlength with more or less visible reddish spot; dorsum densely pubescent with long setae; dorsal spine long, approximately 1.2x shorter then body height (Figs. 3.5–3.6) ……. *D. bidens* (Fabricius, 1781).

- Dorsum uniformly black, usually with dark green metallic luster; dorsum covered with short setae, and at first glance appears bare; dorsal spine short, approximately 2x shorter then body height (Figs. 3.21–3.22) …… *D. nigra* (Boheman, 1856).

10. Humeral angles without carina ……... 11.

- Humeral angles with sharp carina ……..… 12.

11. Body subtriangular, with rounded apex; dorsum uniformly yellow; endemic to Ecuador (Figs. 3.26–3.27) ……..... *D. ohausi* (Spaeth, 1915).

- Body escutcheon-shaped, with acuminate apex; dorsum with extensive black pattern; Costa Rica (Puntarenas) and Brazil (Amazonas) (Figs. 3.15–3.16)

…….. *D. monneorum* Simões and Sekerka, new species.

12. Body large, at least 11 mm long; humeral angles straight and truncate; South American species, only one in Mesoamerica. ……..... 13.

- Body small, length below 8mm; humeral angles rounded and directed backwards; endemic to Yucatan peninsula in Mexico (Figs. 3.41–3.42) …….. *D. yucatana* (Champion, 1893).

13. Humeral angles broad, moderately protruding laterally. …….…..... 14.

- Humeral angles very broad, strongly protruding laterally. ……... 16.

14. Dorsum yellow with black pattern; humeral carina low; outer humeral angle obtuse; apex of elytra subangulate; explanate margin for elytra moderately broad; Bolivia and Paraguay …..... 15.

- Dorsum amber yellow with indistinct yellowish-brownish pattern; humeral carina strongly elevated; outer humeral angle rounded; apex of elytra rounded; explanate margin of elytra very narrow; Mesoamerican species (Figs. 3.3–3.4) ……..... *D. aurita* (Boheman, 1862).

15. Explanate margin of elytra with transverse black spots; antennae uniformly yellow, only terminal antennomere slightly infuscate; scutellum rhomboidal; lowland species; Bolivia and Paraguay (Figs. 3.34–3.35) ……..... *D. rileyi* Borowiec, 1994.

- Explanate margin of elytra uniformly yellow; antennomeres IV–XI infuscate; scutellum subrhomboidal, with convex anterior margin; montane species; Bolivia (Figs. 3.39–3.40)

…….…… *D. wappesi* Sekerka and Simões, new species.

15. Humeral angles rounded; lateral margin of elytra broadly explanate; punctation of elytra coarse and dense with intervals narrower than puncture diameter; elytra yellowish red to reddish brown, but the color always uniform; pronotum the same color as elytra and always immaculate …… 16.

- Humeral angles sharply triangular; explanate margin of elytra narrow; punctation of elytra coarse but sparsely arranged with intervals 1–2x wider than puncture diameter; elytra yellowish-brown variegated; pronotum usually with black maculation (Figs. 3.9–3.10) ……. *D. cornigera* (Boheman, 1854).

16. Outer margin of elytra black, at least on humeri ……..… 17.

- Explanate margin of elytra uniformly yellow (Figs. 3.7–3.8) …… *D. borowieci* Simões and Sekerka, new species.

17. Dorsal spine long, at least 2x longer than width of its base; punctation of elytra very dense with narrow intervals with punctures nearly touching each other (Figs. 3.13–3.14) …….. *D. monoceros* (Germar, 1824).

- Dorsal spine short, approximately 1.0–1.5x longer than width of its base; punctation moderate with distinct intervals, at least as wide as puncture diameter (Figs. 3.32–3.33) ……..… *D. pugnax* Boheman, 1854, restored status.

Bibliography

Barber HS, Bridwell JC. 1940. Dejean catalogue names (Coleoptera). *Bulletin of the Brooklyn Entomological Society* 35: 1–12.

Blake DH. 1939. Eight new Chrysomelidae (Coleoptera) from the Dominican Republic. *Proceedings of the Entomological Society of Washington* 41: 231–239.

Blanchard É. 1846. Insectes de l'Amérique méridionale recueillis par Alcide d'Orbignyi [pp. 60–222]. *In*: Voyage dans l'Amérique méridionale (Le Brésil, la République Orientale de l'Uruguay, la République Argentine, la Patagonie, la République du Chili, la République de Bolivia, la République du Pérou), exécuté pendant les années 1826, 1827, 1828, 1829, 1830, 1831, 1832 et 1833. Tome sixieme, 2e. partie: Insectes (A. d'Orbigny, 1837–45, editor). Chez P. Bertrand, Paris, France.

Boheman CH. 1854. *Monographia Cassididarum. Tomus secundus*. Ex Officina Norstedtiana, Holmiae, Sweden.

Boheman CH. 1856. Catalogue of Coleopterous Insects in the collection of the British Museum. Part IX. Cassidae. Printed by order of the trustees, London, UK.

Boheman CH. 1862. *Monographia Cassididarum. Tomus quartus* (Supplementum). Ex Officina Norstedtiana, Holmie, Sweden.

Borowiec L. 1994. *Dorynota rileyi* n. sp. from Paraguay (Coleoptera: Chrysomelidae: Cassidinae). *Genus* 5: 161–164.

Borowiec L. 1996. Faunistic records of Neotropical Cassidinae (Coleoptera: Chrysomelidae). *Polskie Pismo Entomologiczne* 65: 119–251.

Borowiec L. 1998. Review of the Cassidinae of Ecuador, with a description of thirteen new species. *Genus* 9: 155–246.

Borowiec L. 1999. A world Catalogue of the Cassidinae (Coleoptera: Chrysomelidae). Biologica Silesiae, Wrocław, Poland.

Borowiec L. 2002. New records of Neotropical Cassidinae, with description of three new species (Coleoptera: Chrysomelidae). *Genus* 13: 43–138.

Borowiec, L, Moragues G. 2005. Tortoise beetles of the French Guyana – a faunistic review (Coleoptera: Chrysomelidae: Cassidinae). *Genus* 16: 247–278.

Borowiec L, Opalińska S. 2007. The structure of spermathecae of selected genera of Stolaini and Eugenysini (Coleoptera: Chrysomelidae: Cassidinae) and its taxonomic significance. *Annales Zoologici* 57: 463–479.

Borowiec L, Świętojańska J. 2014. World catalog of Cassidinae. <www.biol.uni.wroc.pl/Cassidinae/catalog%20internetowy/index.htm> (Accessed 10 January 2014).

Champion GC. 1893. Fam. Cassididae [pp. 125–164]. *In*: *Biologia Centrali-Americana*. Insecta. Coleoptera. Vol. VI. Part 2. Phytophaga (part) (F. D. Godman and O. Salvin, editors). Taylor and Francis, London, UK.

Chapuis MF. 1875. Tome onzième. Famille des Phyttophages. *In*: Histoire Naturelle des Insectes. Genera des Coléoptères ou exposé méthodique et critique de tous les genres proposés jusqu'ici dans cet ordre d'insectes (T. Lacordaire and F. Chapuis, editors). A la Librairie encyclopédique de Roret, Paris, France.

Dejean PFMA. 1836. Catalogue des Coléoptères de la collection de M. le Comte Dejean. [Livraison 5]. Méquignon-Marvis, Paris, France.

Duponchel P, Chevrolat LAA. 1842. Cassidaires [pp. 210–211]. *In*: Dictionaire Universel d'histoire Naturelle. Tome troisième (C. d'Orbigny, editor). Bureau Principal des Éditeurs, Paris, France.

Evenhuis NL. 2014. Abbreviations for insect and spider collections of the World. <hbs.bishopmuseum.org/codens/codens-inst.html> (Accessed 10 January 2014).

Fabricius JC. 1781. *Species insectorum eorum differentias specificas, synonyma auctorum, loca natalia, metamorphosis adiectis observationibus, descriptionibus*. Carol. Ernest. Bohnii, Hambvrgi et Kilionii, Germany.

Gentry AH. 1969. *Tabebuia*: The tortuous history of a generic name (Bignon.). *Taxon* 21: 113–114.

Germar EF. 1824. *Insectorum species novae aut minus cognitae, descriptionibus illustratae*. Volumen primum, Coleoptera. J. C. Hendelii et Filii, Halae, Germany.

Hincks WD. 1952. The genera of the Cassidinae (Coleoptera: Chrysomelidae). *Transactions of the Royal Entomological Society of London* 103: 327–358.

Hope FW. 1840. The coleopterist's manual, part the third, containing various families, genera, and species of beetles, recorded by Linnaeus and Fabricius. Also, descriptions of newly discovered and unpublished insects. J. C. Bridgewater, and Bowdery and Kereby, London, UK.

ICZN 1999. International Code of Zoological Nomenclature. Fourth edition. The International Trust for Zoological Nomenclature, London, UK.

Maulik S. 1916. On Cryptostome beetles in the Cambridge University Museum of Zoology. *Journal of Zoology* 86: 567–589.

Monrós F, Viana MJ. 1949. Revisión de las especies Argentinas de Dorynotyni (Col. Cassidae) (1a contribución al conocimiento de Cassidinae). *Acta Zoologica Lilloana* 8: 391–426.

Sekerka L,. Barclay MVL. 2014. Fabrician types of Cassidinae (Coleoptera: Chrysomelidae) deposited in the Natural History Museum, London. A*cta Entomologica Musei Nationalis Pragae* 54: 657-684.

Sherborn CD, Woodward BB. 1901. Notes on the dates of publication of the natural history portions of some French voyages. Part. I. 'Amérique médidionale'; 'Indes orientales'; 'Pôle Sud' ('Astrolabe' and 'Zélée'); 'La Bonite'; 'La Coquille'; and 'L'Uranie et Physicienne'. *The Annals and Magazine of Natural History* 7: 388–392.

Rodriguez V. 1994. The function of the spermathecal muscle in *Chelymorpha alternans* Boheman (Coleoptera: Chrysomelidae: Cassidinae). *Physiological Entomology* 19: 198–202.

Simões MVP. 2014. Taxonomic revision of the genus *Paranota* Monrós and Viana, 1949 (Coleoptera: Chrysomelidae: Cassidinae: Dorynotini). *The Coleopterists Bulletin* 68: 631-655.

Spaeth F. 1914. Chrysomelidae: 16. Cassidinae. *In*: *Coleopterorum Catalogus, Pars* 62 (S. Schenkling, editor). W. Junk, Berlin, Germany.

Spaeth F. 1916. Neue Cassiden (Coleoptera). *Stettiner Entomologische Zeitung* 76: 265–290

Spaeth F. 1923. Ueber *Batonota* Hope. (Col. Cassid.). *Wiener Entomologische Zeitung* 40: 65–76.

Wagener B. 1881. Cassididae. *Mittheilungen des Münchener Entomologischen Vereins* 5: 17–85.

Chapter 4:

TAXONOMIC REVISION OF THE GREATER ANTILLES GENUS *PARATRIKONA* SPAETH (COLEOPTERA: CHRYSOMELIDAE: CASSIDINAE: DORYNOTINI)[4]

[4]Simões, M.V. (2017) Taxonomic revision of the Greater Antilles genus *Paratrikona* Spaeth, 1923 (Coleoptera: Chrysomelidae: Cassidinae: Dorynotini). *Zootaxa*, 4238, 417–425.

Abstract

The Greater Antilles genus *Paratrikona* is revised. One new species is described from Cuba: *Paratrikona blakeae* Simões new species. An updated identification key to the species of the genus and new distributional records are provided.

Introduction

The Greater Antilles genus *Paratrikona* Spaeth, 1923 is currently composed by seven rarely collected species, two endemic to Cuba and five endemic to Hispaniola (Borowiec and Świętojańska, 2016). Spaeth (1923) erected the genus for two species previously classified under *Batanota* Hope, 1840 (= *Dorynota* Chevrolat, 1836), *P. turrifera* (Boheman, 1854) and *P. lerouxii* (Boheman, 1854), and characterized by possessing elytra with coarse and regular puncturation and a short postscutellar tubercle.

In subsequent years, the genus was poorly studied and most of its species were described by the Chrysomelidae researcher Doris Holmes Blake (e.g., Blake, 1937; 1938; 1939), based on specimens collected by Philip Jackson Darlington as result of his expeditions to the West Indies. During this period Blake was active at the United States National Museum, she described four new species in the genus: *P. turritella* Blake 1937, *P. ovata* Blake 1938, *P. variegata* Blake 1939 and *P. rubescens* Blake 1939. Later, Monrós and Viana (1949) revised the Argentine species of Dorynotini and designated *P. turrifera* as the genus type species. Borowiec (2009) described *P. albomaculata* and provided an identification key to the species of the genus. However, Sekerka (2016) synonymized it with *P. rubescens*, maintaining its total of six described species. Species of this genus are extremely rare in the field and in collections, usually known from short series of specimens, as previously observed by P. J. Darlington in Blake (1939), and Borowiec (2009).

Recently, I had the opportunity to examine extensive material of *Paratrikona* from several institutions, and conducted fieldwork in the Dominican Republic. Here I report the results of the examination of this material, provide diagnoses to all species, an updated identification key and distribution data.

Material and Methods

All identifications were made by comparing relevant type specimens. Distributions are given by countries and their major administrative divisions. The information generally follows the summary by Borowiec and Świętojańska (2016).

Label data for studied type specimens are cited verbatim: a vertical bar (|) separates data on different rows and a double vertical bar (||) separates different labels. Additional information about the label or explanatory notes are given in square brackets. The following abbreviations are used to describe the labels as necessary: bb – black frame; cb – cardboard; gl – glued; hw – handwritten; p – printed; r – red; sl – soft label; tr – triangle; w – white. Institutional abbreviations cited in the text follow Evenhuis (2014): Private Collection of Lukáš Sekerka, Liberec, Czech Republic (LSPC); Department of Biodiversity and Evolutionary Taxonomy, University of Wrocław, Poland (DBET); Muséum National d'Histoire Naturelle, Paris, France (MNHN); Manchester Museum, Manchester, UK (MMUE). References cited for each species are limited only to primary descriptions and additional works which include taxonomic changes. For a complete list of references, see Borowiec (1999) and Borowiec and Świętojańska (2016).

Results

Taxonomy

Paratrikona lerouxii (Boheman, 1854)

(Figs. 4.1–4.3)

Batonota lerouxii Boheman, 1854:183 (type locality: ‘Cuba’).

Type material. *Batonota lerouxii*, lectotype (unsexed), pinned: ‘Cuba [hw, sl] || Duquet [hw, sl] || Type [p, sl] || LECTOTYPE | des. L. Borowiec [r, cb, p, bb]’ (NRS). Paralectotype (unsexed), pinned: ‘Cuba [hw, sl] || Guérin [hw, sl] || PARALECTOTYPE | des. L. Borowiec [r, cb, p, bb]’ (NRS).

Additional material examined (1). HAITI**:** Pt. au Prince, R.J. Crew (1 specimen, MNHN).

Diagnosis**.** *Paratrikona lerouxii* is one of two species in the genus with the elytral disc uniformly opaque yellow, sometimes with a small reddish spot at the top of the postscutellar tubercle. The other species, *P. blakeae* sp. nov., differs in that the elytra have the anterior angle slightly truncate, exceeding the widest region of the pronotum, lateral margin opaque, coarse and denser punctures on disc and laterally, and hump followed by a convex slope. While *P. lerouxii* has elytra with the anterior angles rounded, not exceeding the widest region of the pronotum, lateral margin transparent, coarse and moderately punctured on disc and laterally, postscutellar elevation followed by straight slope.

Externally, *P. lerouxii* resembles *P. turritella* that is also endemic to Cuba. Both share a similar body shape, yellow ground color of body, pronotum with irregular callosities on both sides and elytra deeply punctate. The similarity between both species was also pointed out by Blake (1937), who observed that *P. turritella* has elytra with hump below scutellum before the middle, more produced than in *P. lerouxii*. After analyzing a larger series of specimens, I can add that *P. lerouxii* has pronotum around 1.8 X wider than long, with truncate posterior angle, elytra with smooth lateral margin and poorly developed humeral ridge. In contrast, *P. turritella* has

body with pronotum around 1.7 X wider than long, with sinuous posterior angle, elytra with rugose lateral margin and humeral ridge absent. The main diagnostic characters to distinguish *P. lerouxii*, *P. blakeae*, and *P. turritella* are summarized in Table 4.1.

Table 4. 1. Diagnostic characters distinguishing *P. lerouxii*, *P. blakeae* and *P. turritella*.

Diagnostic character/ species	*P. lerouxii*	*P. blakeae*	*P. turritella*
Pronotum	ca. 1.8 X wider than long	depressed medially	ca. 1.7 X wider than long
Pronotum posterior angle	truncate	truncate	sinuous
Elytra puncturation	as wide as intervals	2 x smaller than intervals	wider than intervals
Elytral lateral margin	smooth	smooth	rugose
Elytral postscutellar elevation	present, low and obtuse	present, low and obtuse	present, high and angulate
Elytral postscutellar elevation followed by	straight slope	convex slope	concave slope
Humeral angles	rounded, not exceeding mid-length of pronotum	slightly truncate, exceeding mid-length of pronotum	rounded, not exceeding mid-length of pronotum
Humeral ridge	present	present	absent

Distribution. Cuba (Boheman, 1854). New country record for Haiti.

Paratrikona blakeae Simões, 2017

(Figs. 4.4–4.6)

Type locality. Cuba.

Type material. Holotype (unsexed), pinned: ‘Cuba [hw] | Coll. Geittner [p, cb] || Lerouxii D. | (M. Hung. d) [p, cb, bb] || M/ CR MUS. | SPAETH COLL. [w, p, cb] || ‘HOLOTYPE | Paratrikona | blakeae sp. nov. | M. Simões des. 2016 [r, p, cb]’ (MMUE). Two paratypes (unsexed), pinned: "Cayamas | Cuba, Baker [w, p, cb]" (LSPC).

Diagnosis**.** *Paratrikona blakeae* is readily characterized by humeral angles expanded anteriorly, surpassing mid-length of pronotum, and elytra strongly convex with angulate apex in lateral view, with disc densely and regularly punctate in longitudinal rows, intervals smooth, shiny, impunctate and distinct, wider than puncture diameter.

Description**.** Measurements (holotype): Body length 12.5 mm, body width 10.5 mm, body length/width ratio 1.9, pronotal length 2.9 mm, pronotal width 5.9 mm, pronotal width/length ratio: 2.03. Body elongate-triangular, regularly converging from base to apex. Integument yellow opaque, except for antennomers VI-XI and punctures of elytral disc light brown, posterior margin of pronotum and basal margin of elytra black.

Antennae with 5 basal antennomeres glabrous, 6 distal antennomeres densely setose; scape ca. 2.25 X longer than pedicel, tapered towards apex. Length ratio of antennomeres: 100:44:50:66:55:55:83:72:66:72:94. Pronotum trapezoidal, with maximum width before middle, anterior margin concave, disc coarsely rugose, lateral margins subparallel and sinuous following wider region; posterior angle truncate. Explanate pronotal margin moderately broad. Prosternum glabrous with prosternal collar projecting anteriorly with angulate anterior margin, not covering mouthparts, concave laterally, followed by deep and short depression. Prosternal process with subparallel lateral margins, angulate apex, surface with two longitudinal sulci and rugose apex. Scutellum triangular, impunctate, smooth and shiny. Elytra with basal margin serrate in emargination, denticles obtuse and swollen, strongly convex in lateral view with angulate apex;

humeral angles expanded anteriorly, surpassing mid-length of pronotum, with anterior margin slightly truncate, followed by continuous concave lateral margin. Humeral angles slightly projected laterally with oblique elevation extending from humeral callus to outer corner, followed by deeply punctate depression. Disc densely, deeply and regularly punctate in longitudinal rows, intervals distinct, 2 x wider than diameter of puncture, smooth, shiny, impunctate. Marginal row of punctures distinct in entire length, interrupted once after humeral callus oblique elevation and before mid-length. Explanate elytral margin converging posterad, smooth, finely and densely punctate, shiny. Mesosternal process short c. 1.5x longer than wide, convex laterally with truncate apex.

Distribution**.** Cuba (Caymans).

Etymology**.** The species is dedicated to Chrysomelidae researcher Doris Holmes Blake (1892-1978). Entomologist specialized in the study of Chrysomelidae, and contributed extensively to broaden the knowledge of the genus *Paratrikona*.

Paratrikona ovata Blake, 1938

(Figs. 4.7–4.9)

Paratrikona ovata Blake 1938: 51 (type locality: 'Haiti, Grande Rivière').

Type specimen. Holotype (unsexed), pinned: 'M.C.Z. | Type | 23159 [p, r, cb] || Grande Riviere | W.M. Mann Haiti [p, sl] || Paratrikona | ovata | Blake [hw, sl] || MCZ Type | 23159 [hw, sl]' (USNM).

Additional specimens examined. Known only from the two type specimens.

Diagnosis**.** As the name suggests, *P. ovata* is readily characterized by the conspicuously oval body shape in dorsal view, dorsal ground color yellow with brown posterior margin of pronotum and coarse and irregular punctures on elytra, ventral ground color dark brown, except for antennomeres I–IX, tibiae and tarsomeres. In lateral view, with high and conical postscutellar tuberculum followed by slightly sinuous slope.

Blake (1938) indicated that the most similar species to *P. ovata* within the genus is *P. turrifera*, differing by presenting elytra with no 'spine' (= postscutellar tuberculum) and less regular and dense puncturation. I add that *P. turritella* has body elongate, with ventral color yellow, pronotum 1.7 X wider than long, elytral punctures rounded and anterior slope to postcutellar tuberculum straight. Conversely, *P. ovata* has body oval, with ventral ground color dark brown, except for antennomeres I–IX, tibiae and tarsomeres, pronotum 2.1 X wider than long, with posterior margin strongly sinuous, elytral punctures quadrangular, and anterior slope to postscutellar tuberculum sinuous.

Distribution**.** Haiti (Grande Rivière) (Blake, 1938).

Paratrikona rubescens Blake, 1939

(Figs. 4.10–4.12)

Paratrikona rubescens Blake 1939: 238 (type locality: 'Jarabacoa, Dom. [inican] Rep. [ublic]')
Paratrikona albomaculata Borowiec, 2009: 567 (type locality: 'Jarabacoa, Rep. Dominikana'); Sekerka, 2006: 300 (synonymy).

Type specimens. *Paratrikona rubescens*, holotype (male), pinned: 'triangle with aedeagus glued [gl, tr] || Jarabacoa | Aug.'38, Dom. Rep. | 1,500-4,000 ft. | Darlington [w, p, cb] || MCZ | Typ. No | 23636 [w, hw, cb] || Paratrikona | rubescens | type Blake [w, hw, cb] || Jan.-Jun. 2003 | MCZ Image | Database [w, p, bb] || M.C.Z. | Type | 23636 [r, cb, p]' (MCZ). Paratype, pinned: 'Jarabacoa | Aug.'38, Dom. Rep. | 1,500-4,000 ft. | Darlington [w, p, cb] || M.C.Z. | Paratype | 23636 [r, cb, p]' (MCZ). *Paratrikona albomaculata*, holotype (unsexed), pinned: 'Rep. Dominikana | 5-7. 5. 2001 | Jarabacoa env. | lgt. Z. Martinová [w, cb, p] || HOLOTYPE | des. L. Borowiec [r, cb, p, bb] || Paratrikona | albomaculata n. sp. | HOLOTYPUS | des. L. Borowiec 2009 [w, p, cb, bb]' (DBET).

Additional specimens examined (3). DOMINICAN REPUBLIC: Barahona, 1700 m, 22.VI.2015, Carlos Molinari lgt. (1 male, 2 females, SEMC).

Diagnosis**.** *Paratrikona rubescens* is readily characterized by the pronotum with large brownish-black M-shaped spot and elytra with red ground color. Males, when alive, present elytra with conspicuous irregularly scattered chalk-white spots, which lose their brightness when dry. Females, whether alive or as dry specimens, have a well-marked semicircular spot around postscutellar tubercle, two large spots on slope and spots on explanate margin.

Morphologically, the closest species to *P. rubescens* within the genus is *P. variegata*. Blake (1939) indicated that *P. variegata* has elytra with deep red color, glabrous, slightly larger, and wider with fewer, coarser punctures and with a postscutellar tubercle higher than in *P. rubescens*. While I was able to confirm most of these characters, I did not observe pubescence on the elytra in any of the specimens in the series of *P. rubescens.* This may be due to the age of the specimens. In addition, I observed that *P. rubescens* has punctuate humeral angle, conspicuous poorly developed humeral ridge, and a postscutellar tubercle in lateral view followed by gradual

and uniform slope. In contrast, *P. variegata* has impunctate humeral angle, humeral ridge absent and postscutellar tubercle in lateral view followed by abrupt, sinuous slope.

Remarks**.** Blake (1939) described *P. rubescens* based on two specimens collected in Jarabacoa, Dominican Republic, by P. J. Darlington. The dried male specimen dissected by Blake has elytra deep red with faint white spots around the postscutellar tubercle and on the slope, while the second specimen has a slight trace of white markings close to the postscutellar tubercle only and one at the margin. In the remarks of its description, Blake (1939) indicated that Dr. Darlington observed that when alive, *P. rubescens* has red coloration with conspicuous white blotches irregularly arranged, however, only a slight trace of the white markings are detectable on dried specimens.

Borowiec (2009) described *P. albomaculata* based on two unsexed specimens from Jarabacoa, Dominican Republic. He considered the species very distinct from others in the genus, mainly due to its conspicuous bicolor dorsal aspect, by showing elytra with large chalk-white relief forming incomplete ring around postscutellar tubercle and spots on explanate margin. However, Sekerka (2016) considered that both species share puncturation pattern, elytra convexity, and black M-shapped pattern of pronotum, and that the white-chalk mark on the elytra was a character present in both species, but in specimens used to describe *P. rubescens* it was indicated only slightly. Based on these remarks he considered those specimens to be conspecific and synonymized *P. albomaculata* with *P. rubescens.*

During recent fieldwork in the Dominican Republic, I collected two females and one male that fit the description of the former *P. albomaculata* and *P. rubscens,* respectively. The females (Figs. 4.16–4.17) have elytra with strong chalk-white markings, while the male (Figs. 4.18–4.21) has slightly less distinct marks. However, when both specimens dried, the male lost

the white marking and acquired a rather red coloration of the elytra, retaining faint white marks, similar to the holotype of *P. rubescens*. Based on these observations, I affirm the conclusion of Sekerka (2016) that *P. albomaculata* is a synonym of *P. rubescens* and this variation observed by him is actually sexual dimorphism within the species.

Distribution**.** Dominican Republic (Barahona, Jarabacoa) (Blake, 1939; Borowiec 2009).

Figure 4. 1 Figures 1–12. 1–3, *Paratrikona lerouxii* (Boheman, 1854), lectotype: 1, dorsal view; 2, lateral view; 3, labels; 4–6, *Paratrikona blakae* new species, holotype: 4, dorsal view; 5, lateral view, 6, labels; 7–9, *Paratrikona ovata* Blake, 1938, holotpe: 7, dorsal view; 8, lateral view; 9, labels; 10–12, *Paratrikona rubescens* Blake, 1939, paratype: 10, dorsal view; 11, lateral view; 12, labels.

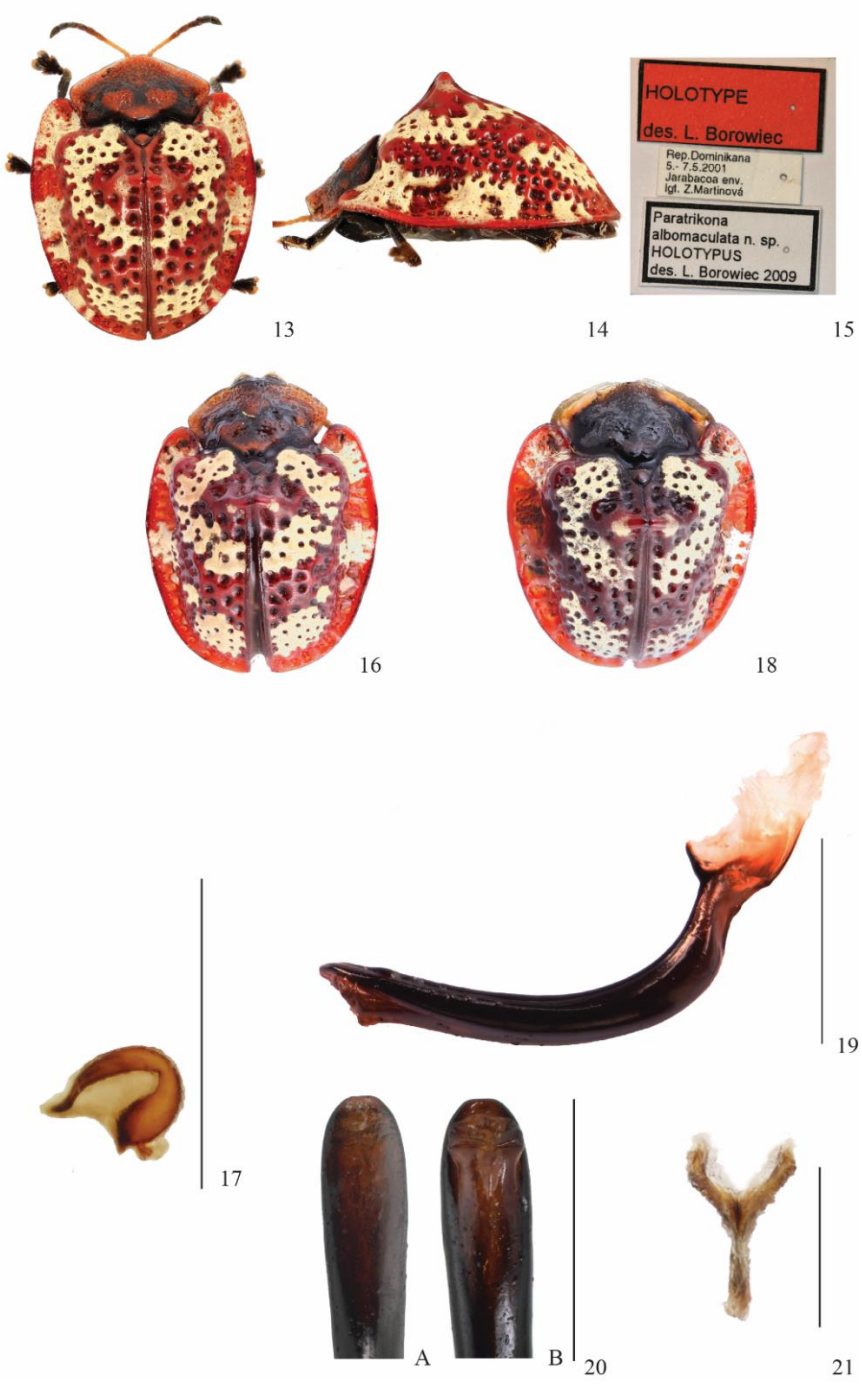

Figure 4. 2Figures 13–15. *Paratrikona albomaculata* Borowiec, 2005, holotype: 13, dorsal view; 14, lateral view; 15, labels; 16–21, female and male of *P. rubescens* Blake, 1939 collected during field work in Dominican Republic: 16, female, dorsal view: 17, spermatheca; 18, male, 19, median lobe, lateral view; 20A, dorsal view of the apex; 20B, ventral view of the apex; 21, tegmen, dorsal view. No pictures of living specimens were taken, specimens were preserved in alcohol which might have contributed to the preservation of the faded white marks on the elytra in the male.

Paratrikona turrifera (Boheman, 1854)

(Figs. 4.22–4.24)

Batonota turrifera Boheman, 1854: 171 (type locality: ‘St. Domingo’, Dominican Republic).

Type specimen. *Batonota turrifera*, lectotype, pinned: ‘St. Domin | go [hw, sl] || Mhm [hw, sl] || Type [p, sl] || LECTOTYPE | des. L. Borowiec [r, cb, p, bb]’ (NRS).

Additional specimen examined (1). CUBA: *Cayana*: XI.1941, Relle v. lgt. (1 spec., MMUE).

Diagnosis**.** *Paratrikona turrifera* is unique and conspicuously characterized by presenting body in quadrangular shape on dorsal view, elytra coarsely punctate, puncturation fovea-like as wide as, or wider than intervals, postscutellar tuberculum high and conical and lateral margin slightly wider proximally to humeral callus.

Distribution**.** Dominican Republic (Santo Domingo) (Boheman, 1854). New country record for Cuba (Cayamas).

Paratrikona turritella Blake, 1937

(Figs. 4.25–4.27)

Paratrikona turritella Blake, 1937:76 (type locality: ‘Sierra Maestra, Oriente Province, Cuba’).

Type specimen. Holotype (male), pinned: ‘Sierra Maestra, Cuba | Julio 10-20 de 1922 | Col. C. H. Ballou y | S. C. Bruner Alt. | 1100-1300 m [sl, p] || Paratrikona | turritella | Blake [cb, hw] || Type No. | 51837 | USNM [r, cb, p,]” (USNM).

Diagnosis**.** *Paratrikona turritella* is characterized by the yellow tegument, pronotum rugose, elytra with coarse puncturation, wider than intervals, with postscutellar elevation present, high and angulate followed by concave slope.

Remarks**.** This species is known only from the type specimen. Further remarks under *P. lerouxii*.

Distribution**.** Cuba (Sierra Maestra) (Blake, 1937).

Paratrikona variegata Blake, 1939

(Figs. 4.28–4.30)

Paratrikona variegata Blake, 1939: 236 (type locality: 'Constanza, Dom. [inican] Rep. [ublic]').

Type specimen. *Paratrikona variegata*, holotype (male), pinned: 'MCZ | Type No | 23635 [hw, sl] || Constanza | Aug.' 38, Dom. Rep. | 3-4,000ft | Darlington [p, cb] || Paratrikona | variegata | Type Blake [hw, sl] | M.C.Z | Type | 23635 [r, p]' (MCZ).

Diagnosis**.** See diagnosis under *P. rubescens*.

Remarks. See remarks under *P. rubescens.*

Figure 4. 3Figures 22–24. *Paratrikona turrifera* (Boheman, 1854), lectotype: 22, dorsal view; 23, lateral view; 24, labels; 25–27, *Paratrikona turritella* Blake, 1937, holotype: 25, dorsal view; 26, lateral view, 27, labels; 28–30, *Paratrikona variegata* Blake, 1939, paratype: 28, dorsal view; 29, lateral view; 30, labels.

Key to species of the genus *Paratrikona* Spaeth

1. Body widest at the anterior half of elytra; prothorax not emarginated anteriorly; head not visible from above; elytral anterior angle rounded; claws not divergent (Paratrikona Spaeth, 1923) …..……...…… 2

- Body widest at middle of elytra; prothorax emarginated anteriorly, head visible from above; elytra with anterior angle narrowed; claws weakly divergent …… *Omoteina* Chevrolat, 1836.

2. Body quadrangular; elytra with postscutellar tuberculum well-developed and conical ……..……...……. *P. turrifera* (Boheman, 1854).

- Body oval, ellipsoid or triangular; elytra with postscutellar tuberculum absent or poorly developed ..... 3.

3. Body dorsal ground color yellow ……..…….…….. 4.

- Body dorsal ground color red …..……..…….…… 7.

4. Body opaque yellow …….……..……....……... 5.

- Body transparent yellow …….……..….. *P. turritella* Blake, 1937.

5. Body ellipsoid, triangular or elongate-triangular with punctures dark yellow to brown, small, round and organized in regular longitudinal rows ……... 6.

- Body oval; elytra with punctures brown, coarse, irregular shaped and displaced ..……..……...……..……... *P. ovata* Blake, 1938.

6. Elytra with anterior angle slightly truncate, exceeding the widest region of the pronotum, lateral margin opaque and in lateral view, hump slightly followed by concave slope ……..…... *P. blakeae* Simões, new species.

- Elytra with anterior angle rounded, not exceeding the widest region of the pronotum and in lateral view, postscutellar elevation followed by straight slope ……..……..…... *P. lerouxii* (Boheman, 1854).

7. Elytra with punctuate and conspicuous and poorly developed humeral ridge, postscutellar tubercle in lateral view followed by gradual continuous slope ……..…….. *P. rubescens* Blake, 1939.

- Elytra with impunctate humeral angle, humeral ridge absent and postscutellar tubercle in lateral view followed by abrupt, sinuous slope ……...…..… *P. variegata* Blake, 1939.

Bibliography

Blake DH. 1937. Ten new species of West Indian Chrysomelidae (Coleoptera). *Proceedings of the Entomological Society* 39: 67–78.

Blake DH. 1938. Eight new species of West Indian Chrysomelidae (Coleoptera). *Proceedings of the Entomological Society* 40: 44–42.

Blake DH. 1939. Eight new Chrysomelidae (Coleoptera) from the Dominican Republic. *Proceedings of the Entomological Society* 41: 231–239.

Boheman CH. 1854. Monographia Cassididarum. Tomus secundus. Ex Officina Norstedtiana, Holmiae. 506 pp.

Borowiec L. 2009. *Paratrikona* albomaculata, a new species from the Dominican Republic (Coleoptera: Chrysomelidae: Cassidinae: Dorynotini). *Genus* 20: 567–570.

Borowiec L., Świętojańska J. (2016). World catalog of Cassidinae. Available from: <www.biol.uni.wroc.pl/Cassidinae/catalog%20internetowy/index.htm> (Accessed 20th of March 2016).

Spaeth F. 1923. Ueber Batonota Hope. (Col. Cassid.). *Wiener Entomologische Zeitung* 40: 65–76.

Sekerka L. 2016. Taxonomic and nomenclatural changes in Cassidinae (Coleoptera: Chrysomelidae). *Acta Entomologica Musei Nationalis Pragae* 56: 275–344.

Chapter 5:

A THORNY SITUATION: DNA AND MORPHOLOGY ILLUMINATE THE EVOLUTION OF THE LEAF BEETLE TRIBE DORYNOTINI (COLEOPTERA: CHRYSOMELIDAE)

Abstract

The tribe Dorynotini is an endemic Neotropical lineage of large and charismatic leaf beetles characterized by an elytral suture conspicuously adorned with a tubercle or narrow vertical spine. The form and size of this tubercle/spine, along with other characters, has been used to define and differentiate the six genera and subgenera in the tribe, forming five conspicuous recognizable morphotypes. However, the systematic relationships among these taxa and the origin of the pronounced tubercle remains unknown, thus allowing speculation regarding its adaptive function for members of the tribe. Here we present a phylogenetic reconstruction to investigate the homology of the elytral tubercle within the tribe Dorynotini. Our analyses include five of the six genera and subgenera of the tribe, and are based on 89 discrete morphological characters and DNA sequence data from three gene regions. Phylogenetic relationships were inferred using Bayesian methods, maximum likelihood and maximum parsimony. Both molecular and morphological analyses support the monophyly of Dorynotini as well as two of its six genera and subgenera (*Paranota* and subgenus *Akantaka*). The subgenus *Dorynota s. str*. is recovered as paraphyletic; and the inclusion of only a single species of *Paratrikona* did not allow a test of its monophyly. The species endemic to the Greater Antilles were recovered as a monophyletic clade, composed of three distinct morphotypes and currently placed in separate genera. Our results indicate that the morphological characters that currently define dorynotine taxa are homoplastic and require re-evaluation guided by molecular analyses. Such a basis would allow for a more accurate classification and improved understanding of Dorynotini systematics and evolution.

Introduction

Cassidinae *sensu lato*, commonly known as tortoise beetles, are the second largest subfamily of leaf beetles with ca. 6300 described species worldwide (Borowiec & Świętojańska, 2017). The tribe Dorynotini Monrós & Viana, 1949 is an exclusively Neotropical clade of cassidines (Chaboo, 2007) distributed from central Mexico to northern Argentina, including the Greater Antilles (Borowiec & Świętojańska, 2017). The tribe currently contains 53 species distributed in five genera: *Dorynota* Chevrolat, 1836, *Heteronychocassis* Spaeth, 1915, *Omoteina* Chevrolat, 1836, *Paranota* Monrós & Viana, 1949 and *Paratrikona* Spaeth, 1923. The diverse genus *Dorynota* is further split into two subgenera: *Dorynota s. str.* and *Akantaka* Maulik, 1916 (Bouchard *et al.*, 2011; Borowiec & Świętojańska, 2017).

Chevrolat (in Dejean, 1836) first proposed the genus *Dorynota* for Neotropical cassidines with a post-scutellar spiniform projection. Later, Maulik (1916) erected two additional genera, *Akantaka* and *Trikona*, based on presence and shape of the post-scutellar projection on the elytra and provided an identification key, where the shape of the scutellum was also employed as a character to distinguish the three genera. Monrós & Viana (1949) revalidated the group for which previous authors have used the name "Batonotites", by creating the tribe Dorynotini, characterized by (i) the presence of insertion pockets (for the posterior margin of the pronotum) on the anterior margin of the elytra, (ii) presence and shape of vertical post-scutellar spine/tubercle on the elytral suture, and (iii) symmetry and angle between pretarsal claws. The genera of the tribe were grouped mostly based on the presence or absence and shape of the elytral spine/tubercle, forming five conspicuous, recognizable morphotypes (Figs 5.1, 5.2). In this same work, the authors described the genus *Paranota* and recognized six more genera within the tribe: *Akantaka*, *Dorynota*, *Heteronychocassis*, *Omoteina*, *Paratrikona* and *Eremionycha*, Spaeth, 1911.

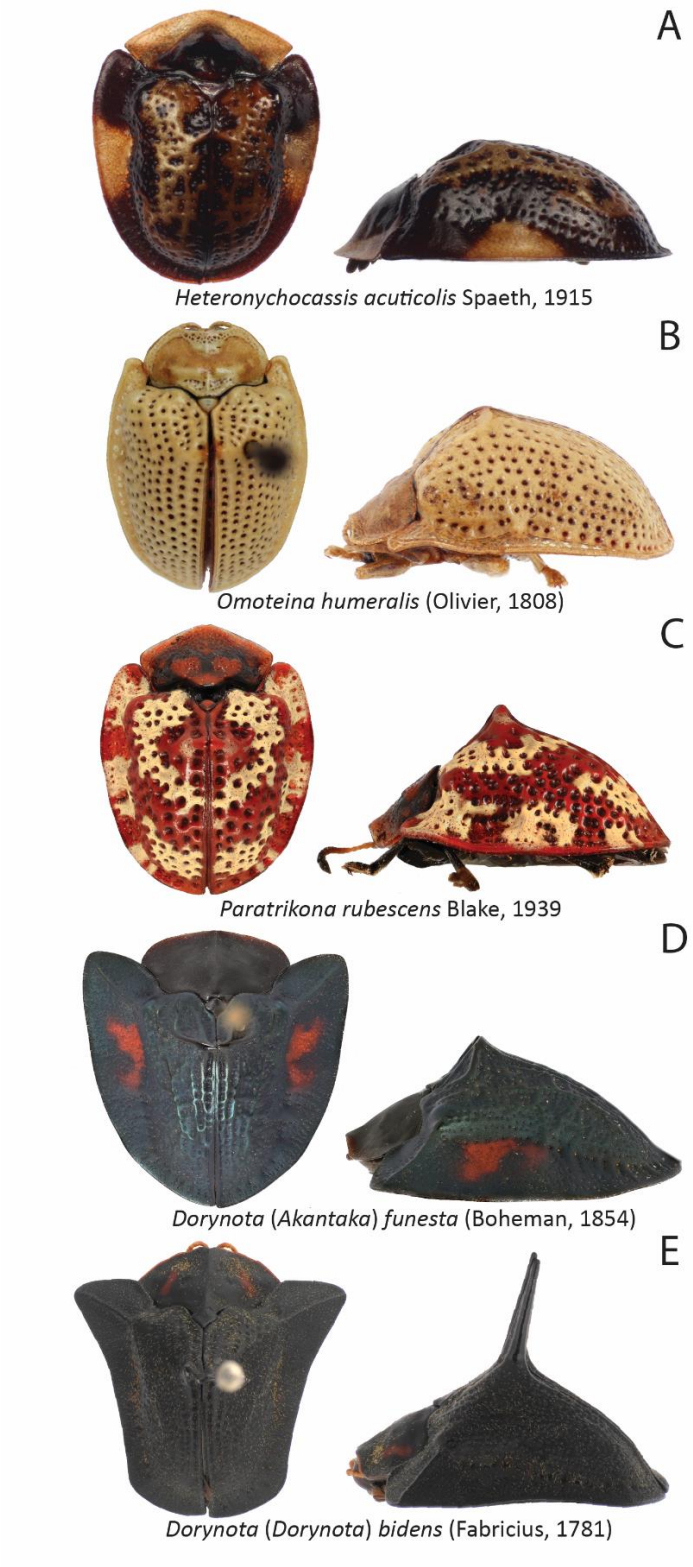

Figure 5. 1A–E. Dorsal and lateral habitus of the five morphotypes found within the tribe Dorynotini.

Figure 5. 2A–C. Adult dorynotine. A, male and female of *Dorynota* (*s. str.*) *pugionata* (Germar) copulating; B, *Omoteina humeralis* (Olivier); C, *Dorynota* (*Akantaka*) *funesta* (Boheman). (Photo: 2A by Victor Chaves Machado; 2C by alapi973 (Flickr: https://www.flickr.com/people/83287919@N00/).

Hincks (1952) downgraded *Akantaka* to a subgenus of *Dorynota* and synonymized the genus *Trikona* with *Omoteina*, a classification that was accepted in later works (Borowiec, 1999; Borowiec & Świętojańska, 2017). In 1999, Borowiec transferred *Eremionycha* to the tribe Cassidini Gyllenhal, resulting in the current composition of Dorynotini.

Multiple cladistic analyses based on adult morphology (Borowiec, 1995; Chaboo, 2007) and molecular data (12S mtDNA; Hsiao & Windsor, 1999) have supported the monophyly of the Dorynotini. However, phylogenetic relationships among genera remain unresolved, and insight about the homology and function of the elytral spine/tubercle is still lacking.

Spaeth (1923) observed that members of the tribe lacking the post-scutellar projection or with a tubercle-shaped projection, were restricted to the Greater Antilles (*Omoteina* and *Paratrikona*) and the Amazon Basin region (*Akantaka*), whereas species with a spiniform post-scutellar projection occur throughout the Neotropics, with its diversity concentrated in the southern part of the tribe's range. Based on this distribution pattern, he suggested that the presence of the post-scutellar projection would be correlated with environmental gradients across

the clade's distribution, allowing the species with the spine to invade cooler areas of the Neotropics. Simões *et al.* (2017) rejected the hypothesis posed by Spaeth (1923), concluding that morphological divergence occurs along with high levels of environmental overlap, and suggested that the presence of the post-scutellar projection could be related to biotic interactions, perhaps favoring camouflage to guard against predation instead.

The tribe Dorynotini was last reviewed by Monrós & Viana (1949), and no systematic work has been conducted on the tribal level since. Here, we combine morphological and molecular data to (1) test the monophyly of the tribe, (2) test the monophyly and relationships among the tribe's genera, (3) elucidate biogeographical patterns, and (4) investigate the homology and evolution of the elytral post-scutellar projection and other key characters using ancestral character state reconstruction. This is the explicitly phylogenetic analysis to resolve relationships among dorynotine lineages, allowing further insight to their intriguing evolution and morphology.

Material and Methods

Taxon sampling

For morphological and molecular datasets we sampled 16 species of Dorynotini, including five of the six genera and subgenera (Table S1). We were unable to include the monotypic genus *Heteronychocassis,* which is known only from the heavily damaged holotype (Simões & Sekerka, 2014). Although sampling is limited in the number of in-group species, our efforts were directed towards covering the diversity of genera within the tribe, in which species are extremely

rare in the field and in collections, usually known from short series of specimens only (Blake, 1939; Borowiec, 2009; Simões, 2017).

We sampled a broad selection of outgroup taxa as the relationships among tribes of Cassidinae remain contentious (Borowiec, 1995; Hsiao & Windsor, 1999; Chaboo, 2007). In general, Cassidini Gyllenhal, 1813 and Ischyrosonychini Chapuis, 1875 are consistently recovered as potential sister-tribes to Dorynotini by both morphological (Borowiec, 1995; Chaboo, 2007) and molecular (Hsiao & Windsor, 1999) datasets. However, the monophyly of Ischyrosonychini is weakly supported (Borowiec, 1995) and Cassidini have been recovered as paraphyletic in previous studies (Borowiec, 1995; Chaboo, 2007). We sampled 15 species representing these two tribes as well as Mesomphaliini Chapuis, 1875, to root the tree. Specimens for sequencing were obtained by MS during field collections in Brazil and the Dominican Republic (2015), and by DW in Panama, Bolivia and French Guiana.

Morphological characters

Eighty-nine phylogenetically informative adult morphological characters were selected to assess interspecific morphological differences and build a discrete data matrix (Appendix S1, Table S4). They include 85 external anatomical characters and four internal anatomical characters (Appendix S1).

To prepare the morphological examinations of the exo- and endoskeleton and wings, specimens were placed in a heated aqueous solution of 10% potassium hydroxide (KOH) for seven minutes. Structural terminology follows Monrós & Viana (1949), Borowiec (2005) and Chaboo (2007), with the following exceptions: hind wing venation, which follows Suzuki

(1994); the metendosternite, which follows Crowson (1938) and Hübler & Klass (2013). All character states were treated as unordered in all analyses. Missing characters states were scored as '?'.

DNA extraction and gene sequencing

Total genomic DNA was extracted from legs or thoracic tissue of specimens preserved in 96% ethanol using a Qiagen DNeasy extraction kit (Valencia, California). We used the primers listed in Table 5.1 to amplify and sequence one mitochondrial gene, cytochrome oxidase subunit 1 (CO1, 588 bp); and two nuclear genes, 28S (995 bp) and carbamoylphosphate synthetase (CAD, 723 bp).

Table 5. 1. List of primers and PCR conditions used to amplify the gene fragments.

Gene	Location	Primer	Direction	Sequence	Reference
CO1	Mitochondrial	Jerry	Forward	CAACAYTTATTTTGATTTTTTGG	Simon et al. (1994)
CO1	Mitochondrial	Pat	Reverse	ATCCATTACATATAATCTGCCATA	Simon et al. (1994)
28S	Nuclear	NLF184–21	Forward	ACCCGCTGAAYTTAAGCATAT	Van der Auwera et al, (1994)
28S	Nuclear	LS1041R	Reverse	TACGGACRTCCATCAGGGTTTCCCCTGACTTC	Maddison (2008)
CAD	Nuclear	CD439F	Forward	TTC AGT GTA CAR TTY CAY CCH GAR CAY AC	Wild & Maddison (2008)
CAD	Nuclear	CD688R	Reverse	TGT ATA CCT AGA GGA TCD ACR TTY TCC ATR TTR CA	Wild & Maddison (2008)

Polymerase chain reactions consisted of the following cycling steps: initial denaturation for 4 min at 95–98 °C; 30–40 cycles of denaturation at 30 s for 95–98 °C, annealing for 30 s with different temperatures depending on the primer pair (see below), and extension for 1–1.5 min at 72 °C; final extension for 5–10 min at 72 °C. The annealing temperatures for each gene fragment were as follows: 50–51 °C for CO1 and 50 °C for 28S. Fragment 1 of CAD was generated using a touchdown PCR with the following conditions: initial denaturation at 95 °C (3.5 min); 6 cycles of 95 °C (30 s), 50 °C (30 s) and 72 °C (1 min); 10 cycles of 95 °C (30 s), 51 °C (30 s) and 72 °C (1 min); 10 cycles of 95 °C (30 s), 52 °C (30 s) and 72 °C (1 min); 6 cycles of 95 °C (30 s), 53 °C (30 s) and 72 °C (1 min); 4 cycles of 95 °C (30 s), 54 °C (30 s) and 72 °C (1 min); 4 cycles of 95 °C (30 s), 55 °C (30 s) and 72 °C (1 min); 4 cycles of 95 °C (30 s), 56 °C (30 s) and 72 °C (1 min); 6 cycles of 95 °C (30 s), 57 °C (30 s) and 72 °C (1 min). Genbank accession numbers, specimen voucher numbers and collection data are provided in Supporting Information, Table S2.

Sequence alignment and phylogenetic analysis

Sequence alignment

Sequence data were aligned and concatenated using Geneious R 9.0.5 (Biomatters, http://www.geneious.com/). Protein-coding gene fragments (COI, CAD) were aligned using MUSCLE (Edgar, 2004), and the ribosomal gene fragment (28S) was aligned using MAFFT 7.017 (Katoh & Standley, 2013) with default settings (Algorithm: Auto; Scoring matrix: 200

PAM/k = 2; Gap open penalty: 1.53; Offset value: 0.123). The reading frames of protein-coding gene fragments CO1 and CAD were checked in Geneious R 9.0.5 to ensure the absence of stop codons or other alignment problems.

Phylogenetic analyses

We performed analyses using three combinations of data: morphology only, molecular only and a third with both molecular and morphological datasets combined. For the morphology-only dataset, we conducted an equal weight maximum parsimony analysis in TNT (Goloboff *et al.*, 2008) using a New Technology Search with 10,000 trees held in memory, and 1000 parsimony ratchet iterations performed (Nixon, 1999), followed by 100 cycles of tree drifting and 100 rounds of tree fusing (Goloboff, 1999). Branch support was calculated with the parsimony bootstrap (PB, nona: 1000 replications, option 'mult*100; hold/100') and Bremer support (BrS, nona: 'bsupport 10000'). A PB $\geq$ 70 is considered as indicating strong support for a given node (Felsenstein, 1985); Bremer support values are also reported (Bremer, 1994).

For the molecular-only and total-evidence datasets, phylogenetic relationships were investigated using maximum likelihood (ML) and Bayesian inference (BI). The molecular dataset was partitioned *a priori* by codon positions for protein coding gene fragments and by gene for ribosomal gene fragments, resulting in a total of seven partitions. Optimal partitioning schemes (Table S3) and models for BI analyses were estimated with PartitionFinder v2.1.1 (Lanfear *et al*., 2012) using the search scheme '*greedy*', and '*mrbayes*' set of models based on the Bayesian information criteria (BIC); for ML analyses, we used the Auto function in IQ-

TREE (Nguyen *et al.*, 2015). For the total-evidence dataset, the morphological partition was analyzed using the MK model (Lewis, 2001).

The BI analyses were conducted in MrBayes 3.2.6 (Ronquist *et al*., 2012) using two runs of eight MCMC chains each (one cold and seven incrementally heated) running for 20 million generations, sampling every 1000 cycles. After checking for convergence of the runs in Tracer 1.5 (http://BEAST.bio.ed.ac.uk/Tracer) and applying a conservative burn-in of 25%, we used the command *sump* in MrBayes to calculate the posterior probabilities (PPs) and *sumt* to produce a 50% majority rule consensus tree.

The ML analyses were carried out in IQ-TREE as implemented in W-IQ-TREE (http://iqtree.cibiv.univie.ac.at/, Trifinopoulos *et al.*, 2016). We performed 1000 ultrafast bootstrap replicates (MB, Minh *et al.*, 2013) to investigate nodal support across topologies. A posterior probability PP $\geq$ 0.95 and a MB $\geq$ 95 was recognized as indicating strong support for a given node (Hillis & Bull, 1993; Erixon *et al*., 2003).

Ancestral character state reconstruction (ACSR)

The analysis of character evolution was conducted through ancestral character state reconstruction (ACSR) with Mesquite v. 3.10 (Maddison & Maddison, 2015) over the ML tree. The parsimony approach was used, on account for the incompleteness of sampling within the representatives of the tribe (Joy *et al*., 2016). The reconstructed characters states were: antennal calli (absent; present, poorly-developed; and present, well-developed; character 28); shape of scutellum (triangular or diamond-shaped; character 46); anterior margin of elytra with insertion pocket (character 49); shape of lateral margins (concave or convex/straight; character 53);

presence of post-scutellar projection (character 56), and its shape (conical-shaped tubercle, triangular-shaped tubercle, and spiniform; character 57); angle formed at the base of pretarsal claws (obtuse, straight, acute and subparallel with no angle near the base; character 82); and their symmetry (symmetrical, inconspicuously asymmetrical and conspicuously asymmetrical; character 83).

Results

Phylogenetic analyses

The molecular matrix comprised 2291 aligned base pairs (bp). Analyses of the morphological partition, individual genes alone and total-evidence (both under ML or BI) produced topologies with low nodal support. All gene trees and total-evidence analyses recovered broadly similar phylogenetic patterns, nonetheless with lower nodal support (see Figs S89–S96). Hence, here we used the concatenated molecular dataset to integrate and maximize the amount of information, and ensure the consistency of our prediction with higher nodal support (Fig. 5.3).

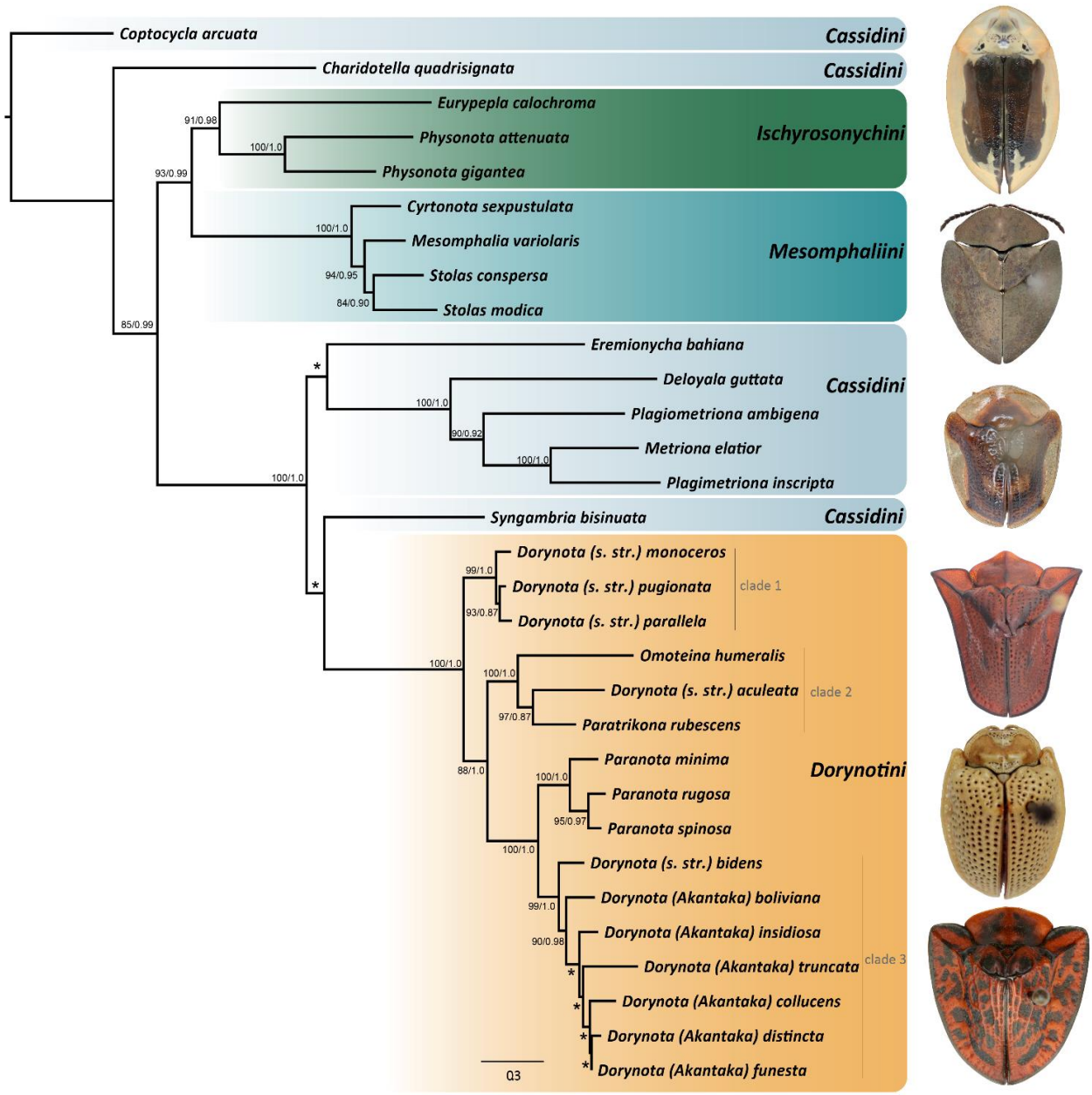

Figure 5. 3**.** Phylogeny of Dorynotini from maximum likelihood analysis of concatenated molecular dataset of two nuclear (28S, CAD) and one mitochondrial gene (CO1). Support values represent maximum likelihood and posterior probabilities of the Bayesian analysis are plotted on the nodes, conflicting values are indicated by "*". Branch lengths represent relative number of changes. Adult cassidinae photographs (top to bottom): *Physonota gigantea* Boheman; *Stolas modica* (Boheman); *Eremiocycha bahiana* (Boheman); *Dorynota* (*s. str.*) *pugionata* (Germar); *Omoteina humeralis* (Olivier); *Dorynota* (*Akantaka*) *pugionata* (Fabricius).

Both analyses (ML and BI) recovered Cassidini as the sister group to Dorynotini with strong support (MB = 100, PP = 1.0). Cassidini is decisively paraphyletic as previous reconstructions have shown (Chaboo, 2007). However, a representative of the tribe were always recovered as sister taxon to Dorynotini, *Syngambria bisinuata* (Boheman, 1855) in the ML analysis, and *Eremionycha bahiana* (Boheman, 1855) in the BI analysis (Fig. 5.4).

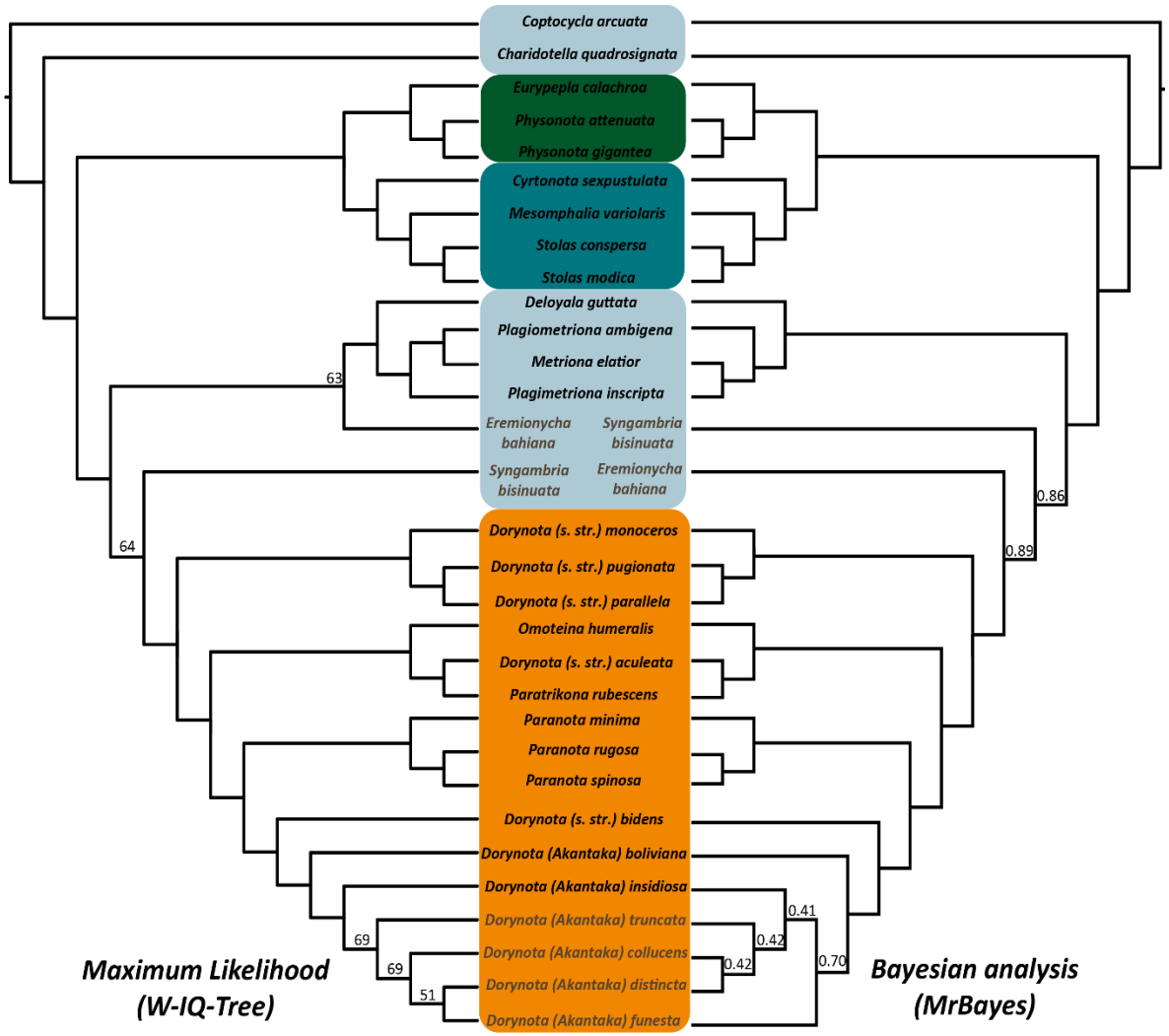

Figure 5. 4. Mirrored topologies recovered through maximum likelihood (left) and Bayesian inference (right). Conflicting nodes between both analyses and respective support values, represented in the tree.

Dorynotini was strongly supported as monophyletic in all analyses (MB = 100, PP = 1.0). The genus *Paranota* was recovered as monophyletic with strong support and congruent internal topologies in all analyses (MB = 100, PP = 1.0). The genus *Dorynota* was recovered as polyphyletic in all analysis, though there was some consistent structuring within the genus. The subgenus *Akantaka* was recovered as monophyletic with strong support (MB = 100, PP = 1.0; MB = 99, PP = 0.98, respectively), though the internal relationships of the subgenus were recovered with low support and exhibited areas of conflict between different analyses (Fig. 4). The subgenus *Dorynota s. str.* was recovered as paraphyletic with respect to other genera, with its members emerging in three different clades within the tree: first, a strongly supported monophyletic clade of South American *Dorynota s. str.* species ('clade 1'; MB = 99, PP = 1.0) was recovered as sister to the rest of Dorynotini (MB = 88, PP = 1.0); second, *Dorynota (s. str.) aculeata*, was recovered as sister to *Paratrikona* (MB = 97, PP = 0.87), together with *Omoteina* forming a clade endemic to the Greater Antilles, with high support ('clade 2'; MB = 100, PP = 1.0); and finally, *Dorynota* (*s. str*.) *bidens* was recovered as sister to the *Akantaka* clade, also with high support ('clade 3' MB = 99, PP = 0.99) (Fig. 3).

The parsimony analysis based on morphological data (Fig. S95) recovered a well-resolved strict consensus tree, collapsed from 16 shortest trees [length = 319, consistency index (CI) = 0.418, retention index (RI) = 0.752]. The topology recovered is partially congruent to results of the molecular dataset analyses. The tribe Dorynotini, the genus *Paranota* and subgenus *Akantaka* were recovered as monophyletic, with high nodal support (PB = 98, BrS = 10; PB =80, BrS = 4; PB = 49, BrS = 1, respectively); and clades 2 and 3 were strongly supported (PB = 82, BrS = 6; PB = 80, BrS = 4, respectively). *Dorynota s. str*. was recovered as paraphyletic, with representatives emerging independently in two clades along the tree: first, within clade 2, with

high nodal support (PB = 82, BrS = 6); second, in a poorly supported clade (PB = 13, BrS =?), including the subgenera *Dorynota s. str*. and *Akantaka*, where *D.* (*s. str.*) *pugionata* and *D.* (*s. str.*) *parallela* are recovered as a clade, sister to *D.* (*s. str*.) *monoceros* and clade 3.

Ancestral character state reconstruction (ACSR)

For Dorynotini, the diamond-shaped scutellum and the spiniform post-scutellar projection were recovered as synapomorphies. The diamond-shaped scutellum exhibits a single reversal to triangular-shaped in the Greater Antillean clade (Figs S3, S51), and the spiniform post-scutellar projection was lost in *O. humeralis* and underwent transitions in *Paratrikona rubescens* and *Akantaka* to conical or triangular-shaped tubercles (Figs 5.5A–B). The straight angle between the pretarsal claws was recovered as the plesiomorphic state within Dorynotini, which evolved into subparallel once in *Dorynota (s. str.) pugionata* + *Dorynota (s. str.) parallela*, and acute angle between pretarsal claws in the clades *Dorynota (s. str.) aculeata* + *Paratrikona rubescens* and *Paranota*. Based on our results, the symmetry and angle at the base of the pretarsal claws are correlated characters within Dorynotini: subparallel claws inconspicuously asymmetric, acute angled base of claws are distinctly asymmetric and obtuse angled base of claws are symmetric (Fig. 5C). The presence of well-developed antennal calli was recovered as a synapomorphic character for the tribe, instead of genera, with one reversal to being poorly-developed in *Paranota* + clade (3).

The ancestral character state reconstruction analysis also revealed other characters that appear to have a phylogenetic significance as a potential synapomorphies for the tribe, they are: w-shaped posterior angle of pronotum (character 25); presence of insertion pocket in the anterior

margin of the elytra (character 49); presence of humeral ridge on the elytra (character 50); presence of locking system at the elytral suture (character 64); epipleural ridge tooth (character 65); metasternum with elevated posterior margin (character 74); and protibial apex depressed on internal margin (character 40) (Appendix 3). The morphological characters traditionally used for diagnosing genera of the tribe were not recovered as synapomorphies, but represent plesiomorphies or convergent characters. These characters include the scutellum shape, presence and shape of a post-scutellar spine/tubercle, and the disposition and asymmetry of the pretarsal claws.

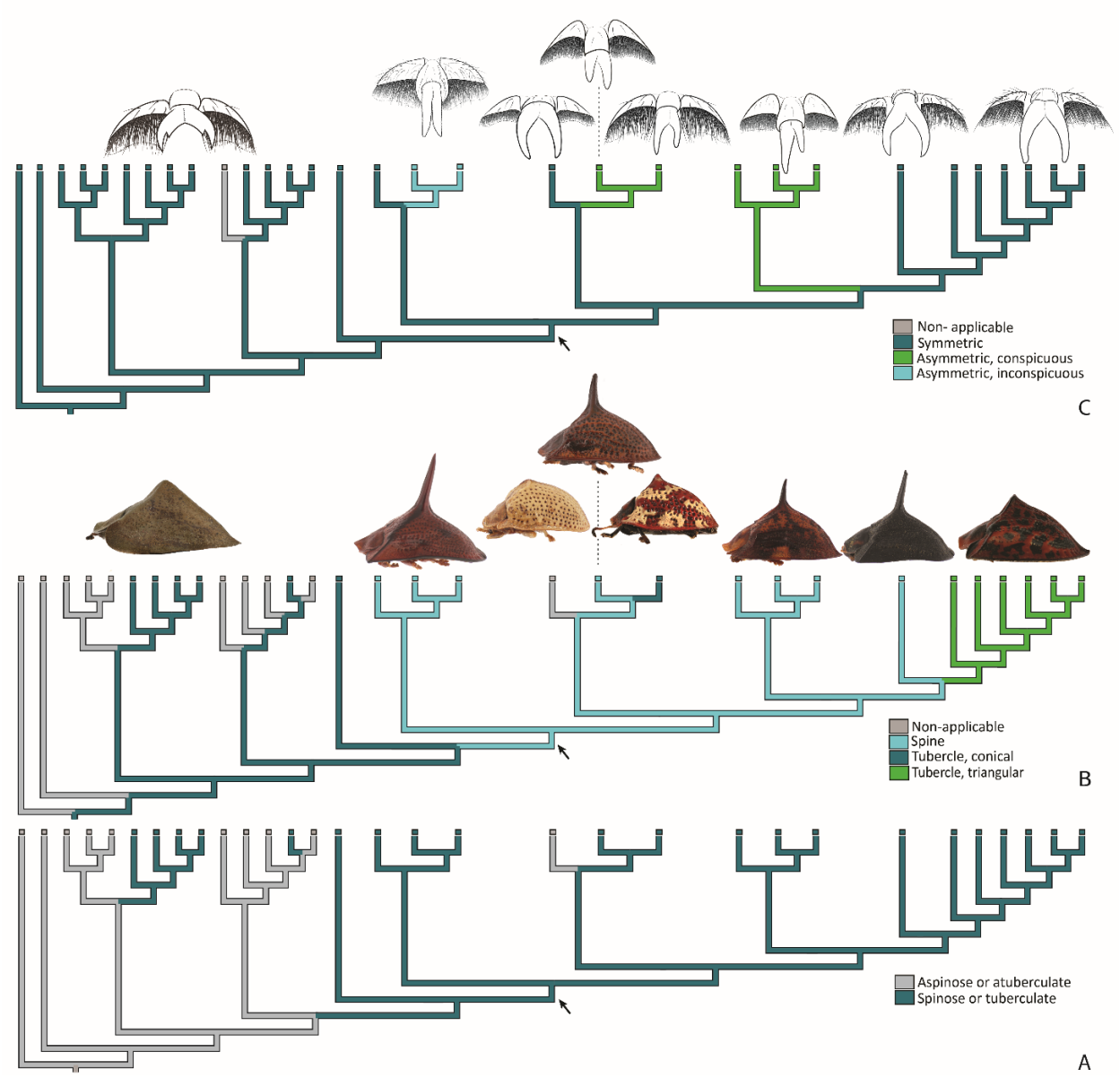

Figure 5. 5A–C. Ancestral character state reconstruction (ACSR) of selective characters traditionally used to classify different genera of Dorynotini. Tribe stem node indicated by arrow. Branch color represents parsimony reconstruction. A, elytra dorsum with post-scutellar projection (character 56). B, shape of post-scutellar projection (character 57); C, symmetry of pretarsal claws (character 83). Adult cassidinae species represented (left to right): *Stolas modica* (Boheman); *Dorynota* (*s. str.*) *pugionata* (Germar); *Dorynota* (*s. str.*) *parallela* Blanchard; *Omoteina humeralis* (Olivier); *Dorynota* (*s. str.*) *parallela* (Boheman); *Paratrikona rubescens* Blake; *Paranota minima* (Wagener); *Dorynota* (*s. str.*) *bidens* (Fabricius); *Dorynota* (*Akantaka*) *funesta* (Boheman); *Dorynota* (*Akantaka*) *collucens* (Spaeth).

Discussion

Monophyly and systematic placement of Dorynotini within Cassidinae

Borowiec (1995) was the first to provide a cladistic test of the tribal relationships within the subfamily Cassidinae, based on 19 adult morphological characters that were previously used by Hincks (1952). In this seminal work, Borowiec (1995) recovered Dorynotini as part of a polytomy with the tribes Cassidini and Ischyrosonychini; he did not provide additional discussion on its placement or possible relationships with other tribes. Hsiao & Windsor (1999) used molecular data (12S DNAmt) to test the relationships between Hispinae and Cassidinae; however, only one species of Dorynotini was included, which was recovered as nested within the Cassidini. Chaboo (2007) conducted a phylogenetic analysis of Cassidinae *sensu lato*, based on morphological data of adults and immatures, including *Dorynota* and *Paratrikona*; her analysis recovered Dorynotini + Ischyrosonychini as sister to Stolaini (= Mesomphaliini Chapuis, 1875).

Here, the species conflicting as most related to Dorynotini, in the results either of BI or ML, are currently placed within Cassidini: *Eremionycha bahiana* (Boheman, 1855) and *Syngambria bisinuata* (Boheman, 1855). Both species present different morphologies regarding the presence of the post-scutellar tubercle. Given the results of the parsimony ACSR on the ML tree, the most recent ancestor of Dorynotini had a cone-shaped tubercle post-scutellar projection (Figs 5.5A–B), and the presence of the spiniform post-scutellar projection is an synapomorphic state for the tribe, which suffered one secondary loss in *O. humeralis*, and convergent reduction of the spine to a tubercle in *P. rubescens* (conical-shaped) and *Akantaka* (triangular-shaped). The

sister taxon of Dorynotini, as recovered by our ML analysis, is *S. bisinuata*, which has a conical tubercle post-scutellar projection, allowing for speculations on the transition to the elongate process within the stem-Dorynotini. In the BI analysis, *E. bahiana* is recovered as sister to Dorynotini, and although previously placed within the tribe, its morphology does not offer support for such placement.

Based on the ACSR, we observed characters that should be further investigated regarding their phylogenetic significance as synapomorphies for the tribe, including: w-shaped posterior angle of pronotum (character 25), the protibial apex depressed on the internal margin (character 40), the presence of insertion pocket in the anterior margin of the elytra (character 49), the presence of humeral ridge on the elytra (character 50), presence of a locking system at the elytral suture (character 64), the presence of the epipleural ridge tooth (character 65) and the elevated posterior margin of the metasternum (character 74) (see Appendix 3, Figures S98, S101, S104–S105, S109, S110, S113).

The w-shaped posterior angle of the pronotum varied from well-marked to soft-marked states in our analysis. The shape of the posterior angle of the pronotum is generally associated with the presence of a diamond-shaped scutellum, a synapomophy for the tribe, and the development of both characters are likely to be associated. The depressed internal margin of the protibia is possibly involved in antennal rubbing, as observed in other groups of insects, where the foreleg rubs along the antenna in mid-air anterior or lateral to the head (Valentine, 1973). The presence of the insertion pocket in the anterior margin of the elytra helps accommodate the pronotum, as the anterior margin of the elytra is expanded anteriorly and laterally, which also contributes to the formation of the conspicuous humeral angles. The locking system observed in the elytral suture could potentially be associated with the plesiomorphic spiniform post-scutellar

projection in the tribe, as it is found in all its species and not in the outgroup. Monrós & Viana (1949) described the epipleural ridge tooth in the diagnosis of the genus *Dorynota* — "*dentículo elitral*" (= elytral tooth). In this study, all Dorynotini members show this character, varying from conspicuous to poorly-conspicuous, and it could be another character contributing the elytral locking mechanism. The elevated posterior margin of the metasternum is another feature that could potentially have a connection to defense mechanisms, facilitating the accommodation of retracted meso- and metalegs. Despite the suggested functions, characters mentioned above are in need of further investigation to determine their adaptive function for members the tribe.

Conflicts over morphological characters used for taxonomic classification within the tribe Dorynotini

In light of currently available evidence, and based on DNA sequences, our results conflict with the morphological taxonomic system of Monrós & Viana (1949). This suggests that the morphological characters currently used for taxonomical classification, are highly homoplastic, rendering them inapplicable for characterizing natural clades.

The genus *Paranota* and the subgenus *Akantaka* were recovered as monophyletic in our study. *Paranota* was characterized by having antennae with five glabrous basal antennomeres, six pubescent apical antennomeres, and asymmetric, parallel or subparallel pretarsal claws (Monrós and Viana, 1949). Simões (2014) compared the genus to the subgenus *Dorynota s. str.* and concluded that instead, *Paranota* should be characterized as presenting the following: slightly inserted pronotum in the internal margin of the anterior elytral angle; diamond-shaped scutellum; tarsomere IV slightly extending past III; and asymmetrical and subparallel claws.

Based on our ACSR, we could not recover any of those characters as synapomorphies to the genus.

The subgenus *Akantaka* was described based on the presence of straight or convex lateral elytral margins and triangular-shaped post-scutellar projection. Based on the ACSR, we recovered the triangular-shaped post-scutellar projection as a synapomorphy for the subgenus.

Omoteina, as a monotypic genus, is characterized by presenting gibbous elytra, deeply punctuate (Maulik, 1916), triangular scutellum, and divergent symmetric claws (Monrós & Viana, 1949). Based on ACSR, the triangular-shaped scutellum was a reversal from the diamond shape found within Dorynotini, and symmetric claws are a plesimorphic in the tribe.

Paratrikona species are rare in the field and in collections, usually known from short series of specimens (Simões, 2017). The genus is characterized by possessing elytra with coarse and regular punctuation and a short tubercle-like post-scutellar projection. Here, the genus is represented by a single species, so its monophyly could not be tested. Results from the ACSR indicate that the coarse and regular punctuation are not diagnostic; however, the tubercle post-scutellar projection is unique among Dorynotini. Based in our ACSR, it is a modification of the plesiomorphic spiniform post-scutellar projection found within the tribe.

The subgenus *Dorynota s. str.* was diagnosed by showing spiniform post-scutellar projection, pronotum partially inserted in the elytral anterior margin and subequal pretarsal claws (Monrós & Viana, 1949). In our analysis, we recover the subgenus *Dorynota s. str.* as paraphyletic, emerging in three clades (Fig. 5.3). Clade 1 is recovered as sister to all other Dorynotini, grouping species that show a wide distribution throughout central and southwest South America. The ancestral character state reconstruction did not recover any potential synapomorphies for the clade. However, its internal sister taxa, *D.* (*s. str*.) *parallela* + *D.* (*s. str*.)

pugionata, share two synapomorphies: mesoescutellum with transversal ridges poorly developed (character 44) (see Appendix 3, Fig. S102); and parallel asymmetric pretarsal claws. Clade 2 is composed of species endemic to the Greater Antilles, *O. humeralis*, *D.* (*s. str.*) *aculeata* and *P. rubescens* (see discussion below). Clade 3 is composed of *D* (*s. str.*) *bidens* sister to the subgenus *Akantaka*. Based on the ACSR, clade 3 shares many convergent characters with clade 1 (e.g., depressed surface of scutellum), and *D.* (*s. str.*) *bidens* and the subgenus *Akantaka* share characters that are plesiomorphic for the tribe (e.g., elevated posterior margin of metasternum). The lack of recovered synapomorphies for clade 3 represents the demand for further investigation of morphological characters and taxon sampling, as despite being recovered in every analysis, *Akantaka* still composes a clade, delineated by the triangular elytral post-scutellar projection synapomorphy.

The Greater Antillean clade

Clade 2 was consistently recovered as monophyletic in all analyses with high nodal support (Fig. 5.3). It is composed of the three species endemic to the Greater Antilles, *O. humeralis*, *D.* (*s. str.*) *aculeata* and *P. rubescens*. Based on ACSR, this clade presents a general pattern of reversal of states considered plesiomorphic within Dorynotini. They are, antennomere V wider at apex (character 8), pronotum with truncate posterior angle (character 25), absence of hypomeron depression (character 36), triangular-shaped scutellum (character 46), epipleural ridge tooth not conspicuously elevated (character 67), large deep elytral punctuation (character 71) and metasternum strongly elevated (character 74) (see Appendix 3, Figures S99–S100, S103, S111–S113).

The Greater Antillean clade is also markedly characterized by exhibiting three of the four possible states of the post-scutellar projection among its representatives: absent, found in *O. humearlis*; conical-shaped tubercle, found in *P. rubescens*; and spiniform, found in *D.* (*s. str.*) *aculeata*. The presence of the pronounced spine was seen as a possible convergence with the spines of other South-American dorynotines. However, results of the ancestral character state reconstruction indicate that the presence of the spine is the plesiomorphic state for all Dorynitini and was lost, or transformed in two of the three lineages of the Greater Antilles clade.

The genus *Omoteina* is monotypic and characterized by showing an oval body, elytra with coarse punctuation without post-scutellar projection, triangular scutellum and divergent pretarsal claws (Oliver 1808; Monrós & Viana, 1949). The ancestral character state reconstruction recovered the coarse punctuation on the elytra as a synapomophy of the genus in regard to the tribe. The ancestral character state reconstruction recovered the absence of a post-scutellar projection and the triangular scutellum as a reversal, and the divergent pretarsal claws is a retention of the plesiomorphic state found in the tribe. No synapomorphy for the genus was recovered.

The internal relationship of clade 2, recovers *D.* (*s. str*.) *aculeata* as sister-species to *P. rubescens*. Monrós & Viana (1949) previously suggested these two species would be closely related based on the presence of the triangular-shaped scutellum, which was recovered as a synapomophic state of the Greater Antillean clade, in regard to the tribe's plesiomorphic state of diamond-shaped scutellum. Despite being incorrect in regard to the character, Monrós & Viana (1949) were correct about the cladistic relationship between species, and our results based on the ancestral character state reconstruction recovered the pronotum with a rugose aspect as the synapomorphy for the clade (character 18).

Field observations by MS and literature indicate a difference of abundance of these species in natural habitats (Blake, 1939; Borowiec, 2009; Simões, 2017). Most common species, however, present a well-developed spine (*Dorynota* (*s. str.*) *aculeata*) or are non-bearing of a post-scutellar projection (*O. humeralis*). The most diverse group of Dorynotini in the Greater Antilles, is the genus *Paratrikona* (seven species), which has all of its representatives adorned with a short tubercle, but they are extremely rare and known only from short series of specimens. This asymmetry of diversification patterns, and morphological characters that might have shaped such patterns, should be further investigated in a broader taxa sampling scenario.

Conclusions

This study represents the first attempt to investigate relationships within Dorynotini in a phylogenetic framework. With the molecular phylogenetic data collected in this study, it is clear that a revision of the taxonomic system of Dorynotini and a re-evaluation of the traditional morphological diagnostic characters guided by molecular analyses is needed. The fact, that almost all characters traditionally used for classifying genera in the tribe, do not follow the pattern of the recognized genera, undermines this necessity. We show that the presence of the post-scutellar spine – the most conspicuous character of Dorynotini – is a synapomorphy of the tribe and has been reduced and transformed in some of its lineages.

Finally, it is important to note that our study has relatively limited morphological phylogenetic power, because we have evidence of relatively few gains and losses due to limited representation of the groups in here. Better taxon sampling and larger amounts of molecular data

than the present one are required to improve the understanding of the Dorynotini systematics and evolution.

Bibliography

Blake DH. 1939. Eight new Chrysomelidae (Coleoptera) from the Dominican Republic. *Proceedings of the Entomological Society* 41: 231–239.

Borowiec L. 1995. Tribal classification of the cassidoid Hispinae (Coleoptera: Chrysomelidae). In: Pakaluk J, Ślipiński SA, Crowson RA, eds. *Biology, Phylogeny, and Classification of Coleoptera: Papers Celebrating the 80th Birthday of Roy A. Crowson*. Warszawa: Muzeum i Instytut Zoologii PAN, 541–558.

Borowiec L. 2005. Three new species of the genus *Dorynota* sgen. *Akantaka* Maulik, 1916 from Bolivia and Brazil (Coleoptera: Chrysomelidae: Cassidinae: Dorynotini). *Genus* 16: 29–41.

Borowiec L. 2009. New records of Neotropical tortoise beetles (Coleoptera: Chrysomelidae: Cassidinae). *Genus* 20: 615–722.

Borowiec L, Świętojańska J. 2014. Cassidinae Gyllenhal, 1813. In: Leschen RAB, Beutel RG, eds. *Handbook of Zoology: Coleoptera, Beetles Volume 3: Morphology and Systematics (Phytophaga)*. Berlin/New York: deGruyter Press, 198–217.

Borowiec, L. & Świętojańska, J. (2017) World catalog of Cassidinae. Wrocław, Poland. <http://www.cassidae.uni.wroc.pl/katalog%20internetowy/index.htm> (8th November 2017).

Bouchard P, Bousquet Y, Davies AE, Alonso-Zarazaga MA, Lawrence JF, Lyal CHC, Newton AF, Reid CAM, Schmitt M, Ślipiński SA, Smith ABT. 2011. Family-group names in Coleoptera (Insecta). *ZooKeys* 88: 1–972.

Bremer K. 1994. Branch support and tree stability. *Cladistics* 10: 295–304.

Chaboo CS. 2007. Biology and phylogeny of the Cassidinae Gyllenhal *sensu lato* (tortoise and leaf-mining Beetles) (Coleoptera: Chrysomelidae). *Bulletin of the American Museum of Natural History*: 1–250.

Crowson RA. 1938. The metendosternite in Coleoptera: a comparative study. *Transactions of the Royal Entomological Society of London* 87: 397–415.

Dejean PFMA. 1833. *Catalogue des Coléoptères de la collection de M. le Comte Dejean. [Livraison 5]*. Méquignon-Marvis, Paris, France.

Edgar RC. 2004. MUSCLE: Multiple sequence alignment with high accuracy and high throughput. *Nucleic Acids Research* 32: 1792–1797.

Erixon P, Svennblad B, Britton T, Oxelman B. 2003. Reliability of Bayesian posterior probabilities and bootstrap frequencies in phylogenetics. *Systematic Biology* 52: 665–673.

Felsenstein J. 1985. Confidence limits on phylogenies: an approach using the bootstrap. *Evolution* 39: 783–791.

Goloboff P. 1999. Analyzing large data sets in reasonable times: solutions for composite optima. *Cladistics* 15: 415–428.

Hillis DM, Bull JJ. 1993. An empirical test of bootstrapping as a method for assessing confidence in phylogenetic analysis. *Systematic Biology* 42: 182–192.

Hincks WD. 1952. The genera of the Cassidinae (Coleoptera: Chrysomelidae). *Transactions of the Royal Entomological Society of London* 103: 327–358.

Hsiao TH, Windsor DM. 1999. Historical and biological relationships among Hispinae inferred from 12S mtDNA sequence data. In: Cox ML, ed. *Advances in Chrysomelidae Biology 1*. Leiden, The Netherlands: Backhuys, 39–50.

Hübler N, Klass KD. 2013. The morphology of the metendosternite and the anterior abdominal venter in Chrysomelinae (Insecta: Coleoptera: Chrysomelidae). *Arthropod Systematics and Phylogeny* 71: 3–41.

Joy JB, Liang RH, McCloskey RM, Nguyen T, Poon AFY. 2016. Ancestral Reconstruction. *PLoS Computational Biology* 12: 1–20.

Katoh K, Standley DM. 2013. MAFFT multiple sequence alignment software version 7: improvements in performance and usability. *Molecular Biology and Evolution* 30: 772–780.

Lanfear R, Calcott B, Ho SYW, Guindon S. 2012. PartitionFinder: combined selection of partitioning schemes and substitution models for phylogenetic analyses. *Molecular Biology and Evolution* 29: 1695–1701.

Lewis PO. 2001. A likelihood approach to estimating phylogeny from discrete morphological character data. *Systematic Biology* 50: 913–925.

Minh BQ, Nguyen MAT, Von Haeseler A. 2013. Ultrafast approximation for phylogenetic bootstrap. *Molecular Biology and Evolution* 30: 1188–1195.

Monrós F, Viana MJ. 1949. Revision de las especies Argentines de Dorynotyni (Col. Cassidae). *Acta Zoologica Lilloana*: 391–426.

Nguyen LT, Schmidt HA, Von Haeseler A, Minh BQ. 2015. IQ-TREE: A fast and effective stochastic algorithm for estimating maximum-likelihood phylogenies. *Molecular Biology and Evolution* 32: 268–274.

Nixon K. 1999. The parsimony ratchet, a new method for rapid parsimony analysis. *Cladistics* 15: 407–414.

Ronquist F, Teslenko M, Van Der Mark P, Ayres DL, Darling A, Höhna S, Larget B, Liu L, Suchard MA, Huelsenbeck JP. 2012. Mrbayes 3.2: Efficient Bayesian phylogenetic inference and model choice across a large model space. *Systematic Biology* 61: 539–542.

Shin C. 2015. Systematics and morphology of Ischyrosonychini, with an investigation of color change in the Geiger tortoise beetle (Coleoptera: Chrysomelidae). Unpublished D. Phil. Thesis, University of Kansas.

Simões MVP, Sekerka L. 2014. Redescription of *Heteronychocassis acuticollis* Spaeth, 1915 (Coleoptera : Chrysomelidae : Cassidinae). *The Coleopterists Bulletin* 68: 407–410.

Simões MVP. 2017. Revision of the Greater Antilles genus *Paratrikona* Spaeth, 1923 (Coleoptera: Chrysomelidae: Cassidinae: Dorynotini). *Zootaxa* 4238: 417–425.

Simões MVP, Lieberman BS, Soberón J, Peterson AT. 2017. Testing environmental correlates of clines in clades: an example from cassidine beetles. *Insect Conservation and Diversity*: 1–11.

Simon C, Frati F, Beckenbach A, Crespi B, Liu H, Flook P. 1994. Evolution, weighting, and phylogenetic utility of mitochondrial gene sequences and a compilation of conserved polymerase chain reaction primers. *Annals of the Entomological Society of America* 87: 651–701.

Spaeth F. 1923. Ueber Batonota Hope (Col. cassid). *Wiener entomologische Zeitung* 40: 65–76.

Suzuki K. 1994. Comparative morphology of the hindwing venation of the Chrysomelidae (Coleoptera). *Novel Aspects of the Biology of Chrysomelidae, Series Entomologica*: 337–354.

Trifinopoulos J, Nguyen LT, von Haeseler A, Minh BQ. 2016. W-IQ-TREE: a fast online phylogenetic tool for maximum likelihood analysis. *Nucleic Acids Research* 44: W232–W235.

Valentine BD. 1973. Grooming Behavior in Coleoptera. *The Coleopterist Bulletin* 27: 63–73.

Van der Auwera G, Chapelle S, De Wächter R. 1994. Structure of the large ribosomal subunit RNA of *Phytophthora megasperma*, and phylogeny of the oomycetes. *FEBS Letters* 338: 133–136.

Wild AL, Maddison DR. 2008. Evaluating nuclear protein-coding genes for phylogenetic utility in beetles. *Molecular Phylogenetics and Evolution* 48: 877–891.

Chapter 6

TESTING ENVIRONMENTAL CORRELATES OF CLINES IN CLADES: AN EXAMPLE FROM CASSIDINE BEETLES[6]

[6]Simões, M.V., Lieberman, B., Soberón, J. and Peterson, T. (2017) Testing envirionmental correlates of clines in clades: an example from Cassidinae beetles. *Insect Conservation and Diversity*, 68, 407–410.

Abstract

Phenotypic change across environmental gradients has been an important topic in evolutionary biology. Members of the tortoise beetle tribe Dorynotini are characterized by an elytral suture adorned with either a tubercle or a large, vertical spine.Overall spine height across species had previously been posited to exhibit a latitudinal gradient of increasing height and decreasing width towards the southern extreme of the tribe's range, and this pattern had been linked to environmental variation. We explore the evidence behind such a cline by testing associations between climate and morphology across the clade's geographic distribution using an approach based on ecological niche modeling and morphological and environmental hypervolumes. The degree of overlap between the respective hypervolumes was assessed, and the correlation of matrix overlap values was quantified using Mantel tests. Degrees of niche similarity and conservatism at the genus level were also assessed using both Schoener's index and Hellinger distances. Overall, we observed that characters defining our morphological hypervolumes were informative, and capable of grouping taxa into discrete units in morphospace. In contrast, environmental hypervolumes were largely homogeneous across the tribe, with high overlap among taxa. No significant correlations were found between environmental and morphological hypervolumes. Our results indicate that morphological divergence occurs along with high levels of environmental overlap; perhaps historical biogeographic factors along with sexual selection may have promoted its diversification. Our approach based on ENM and statistical comparisons between environmental and morphological hypervolumes can provide a useful approach to testing the existence of gradients and clines.

Introduction

The impact of environmental gradients on morphology has been an important topic in ecology and evolutionary biology, as geographic variation in environmental conditions may be a major factor involved in diversification (Schulter, 2000; Pincheira-Donoso *et al.*, 2008). As such, phenotypic gradients (clines) associated with environmental gradients are worth investigating and understanding in greater detail (Conover *et al.*, 2009). Occasionally, these clines have been classified as 'ecogeographic rules': consistent and concordant responses of organisms to the environment (McDowall, 2008). Among these patterns are Bergmann's (1847) rule (latitudinal variation in body size); Allen's (1878) rule (geographic variation in appendage size); Gloger's (1883) rule (geoclimatic variation in pelage color); and Jordan's (1892) rule (latitudinal variation in number of vertebrae in marine fish) (see also Lomolino *et al.*, 2006).

The existence of clines in general, and rules in particular, has been posited both within and among species in diverse ecosystems spanning multiple geographic regions and clades (Anderson and Handley, 2002; Clegg and Owens, 2002; McNab, 2002; Boback, 2003; Schmidt and Jensen, 2003, 2005; Lomolino, 2005; McClain *et al.*, 2006; Benton *et al.*, 2010; Koski and Ashman, 2015; Valenzuela-Sánchez *et al.*, 2015; Ficetola *et al.*, 2016). However, those rules and clines are not omnipresent in nature (Millien *et al.*, 2006) because geographic disjunctions can exist between populations of species, and because many other factors may influence morphology, including genetic drift and biotic interactions (Chown and Gaston, 1999). Several studies have re-evaluated the generality and underlying causation of these 'rules' (Ashton *et al.*, 2000; Meiri and Dayan, 2003; Meiri *et al.*, 2004; Pincheira-Donoso *et al.*, 2008; Feldman and Meiri, 2014; Slavenko and Meiri, 2015; Bülbül *et al.*, 2016), and have shown that such rules are

not as pervasive as had been believed. One of the problems with such a 'cline-centered' approach to explaining organismal morphology is that traits are not independently formed; instead, organisms should be viewed as integrated wholes (Gould and Lewontin, 1979; Murren, 2002; Kleyer and Minden, 2015). In particular, different studies have focused on single characters instead of suites of characters that might be correlated. The more characters involved, the more difficult it is to relate changes to single selective forces; indeed, a latitudinal diversity gradient itself might not result from the action of a single selective force (Saupe *et al.*, 2015). Further, in some early studies, trait values were averaged across all species of a community (e.g., community-weighted means) or only a few species were selected to test correlations with environmental conditions or ecosystem properties, which led to spurious conclusions (Kleyer and Minden, 2015).

As such, our focus is on testing perceived morphological gradients across clades and their possible associations with environmental gradients in the cosmopolitan subfamily Cassidinae (Insecta: Coleoptera). Cassidines rank among the most diverse lineages of leaf beetles, with ca. 6400 species worldwide (Borowiec and Świetojańska, 2017). We focus on the exclusively Neotropical tribe Dorynotini Monrós and Viana, 1949, which ranges from Mexico to Argentina, with 53 species in 5 genera (Borowiec and Świetojańska, 2017). Members of this tribe are characterized by an elytral suture adorned with a tubercle or narrow vertical spine (Fig. 6.1A-B); more basal lineages have smaller spines (effectively just tubercles), whereas derived lineages possess longer and thinner spines.

Across the clade, a latitudinal gradient in the size and shape of this tubercle/spine has been noted, with a posited increase in height and decrease in width associated with cooler areas of the tropics (Spaeth, 1923). It was further suggested that environmental gradients across the

clade's distribution drove the diversification of the clade (Spaeth, 1923) (Appendix S1, Fig. S1). Geographically, the basal lineages are restricted to the Greater Antilles (*Omoteina* Chevrolat, 1836 and *Paratrikona* Spaeth, 1923) and the Amazon Basin region (*Akantaka* Maulik, 1916), whereas the most derived lineage occurs throughout the Neotropics, with its diversity concentrated in the southern part of the tribe's range. These patterns need to be examined in greater detail to illuminate influences of climatic factors on the clade's distribution, and to consider potential drivers of the group's morphological and ecological diversity.

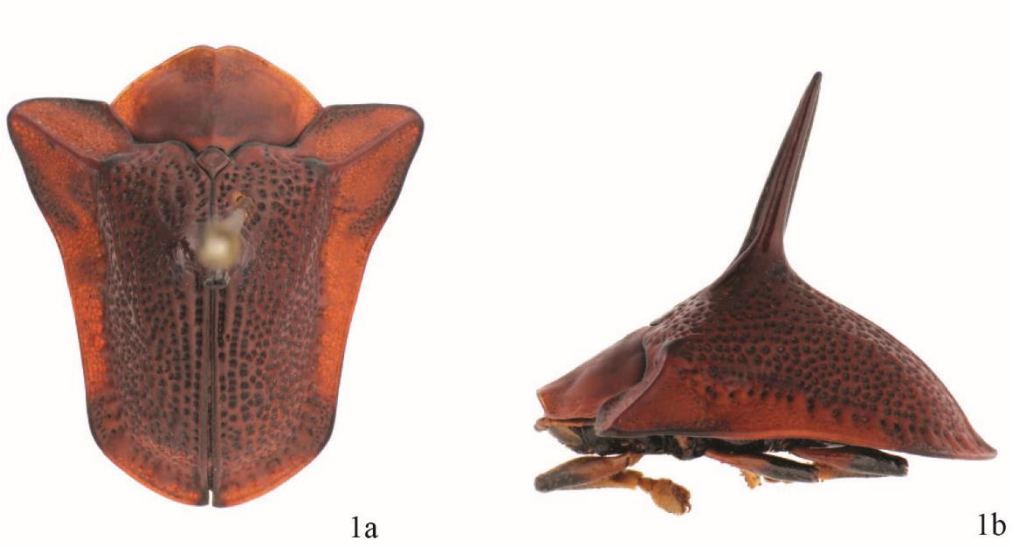

Figure 6. 1**Figure 1.** A representative specimen of Cassidinae, Dorynotini, *Dorynota monoceros* (Germar, 1824), shown in (A) dorsal and (B) lateral views.

In particular, in this study, we test the only hypothesis posed thus far to explain the morphological diversity within the group. We test whether the size of the vertical spine is correlated with environment conditions (Spaeth, 1923), and whether environmental factors are driving the morphological traits in closely related species of this monophyletic clade (for more information on Dorynotini see Simões, 2014, 2017; Simões and Sekerka, 2015). We use an ecological niche modeling (ENM) approach, in conjunction with data on distribution and

morphology; we compare environmental and morphological hypervolumes of taxa in the tribe at two levels: species and monophyletic genera. The *n*-dimensional hypervolumes that Hutchinson (1957) used to describe the set of environments that allows a species to maintain populations can be defined at different scales (species, communities) and for different axes (climate variables, traits) (Blonder *et al.*, 2014). Multidimensional analysis, such as the use of hypervolumes, can measure associations of functional traits with environmental characteristics, enabling inferences about how ecological and evolutionary processes structure diversity (Mouillot *et al.*, 2005; Lamanna *et al.*, 2014). Here, we introduce an approach that combines ENM tools with a comparison of hypervolumes to understand the causes of interspecific morphological differences within the Dorynotini.

Material and Methods

Specimen data

*Morphological Data***.** For a list for specimens examined and their institutional repositories, see Supporting Information (Table S1). To quantify aspects of cassidine morphology pertinent to the cline in dorsal spine characteristics, the following measurements (in millimeters) were made using an ocular micrometer: pronotum width and length; elytra width at humeral angle; elytra width at median region; elytra length; and total body height (which includes the spine) (Appendix S1, Fig. S2, and Appendix S2, Tables S2 and S3). This group does not appear to exhibit much sexual dimorphism, as in most cassidine beetles (Jolivet, 1999).

Occurrence data

Occurrence data were obtained from the specimens in the aforementioned institutions and from a literature review (Boheman, 1854, 1862; Wagner, 1881; Champion, 1893; Spaeth, 1923; Blake, 1937, 1938, 1939; Borowiec, 1994, 1996, 2002, 2009; Borowiec and Świętojańska, 2017; Simões, 2014, 2017; Simões and Sekerka, 2015). The first author also made field collections in Brazil (December-February 2015) and the Dominican Republic (June 2015); these localities corresponded to taxa and regions less well represented in museums and the literature. Specimens were georeferenced using the Global Gazetteer (http://www.fallingrain.com) and Google Earth (Google, Mountain View, CA, USA). In total, 185 occurrence records were assembled to characterize the known distributions of species in the tribe.

Environmental data

Environmental data were obtained from WorldClim (version 1.3, http://www.world-clim.org; for details, see Hijmans *et al.*, 2005). WorldClim contains climate data (i.e., monthly precipitation, and monthly mean, minimum, and maximum temperatures) at a spatial resolution of 5' (ca. 10 x 10 km resolution), obtained by interpolation among climate-station records from 1950 to 2000. These data were used to derive biologically meaningful bioclimatic variables representing annual trends, seasonality, and extreme conditions (Hijmans *et al.*, 2005). Of the total of 19 variables in WorldClim, 15 were used herein; four were excluded (mean temperature of wettest quarter, mean temperature of driest quarter, and precipitation of warmest and coldest quarters), owing to presence of anomalies and odd discontinuities between neighboring pixels.

To reduce dimensionality and collinearity, a principal components analysis (PCA) was applied to the matrix of environmental variables using the "*princomp*" routine in R (R Core Team, 2017). This transformation rotates all extracted measures in a new space to capture the most variance, in decreasing order. To create the environmental hypervolume (see below) we used the first 3 principal components, which explained 87% of overall environmental variance.

Hypervolume calculations

To measure morphological differentiation, we calculated the volume and overlap of trait and environmental spaces, and their respective centroid distances using the R package Hypervolume (Blonder *et al.*, 2014). The package allows for the fitting of kernel densities to points, and uses those kernels to estimate volume and overlap. Following protocols in Blonder (2016), each hypervolume was constructed using a Silverman bandwidth estimator and a 0% quantile threshold with 1000 Monte Carlo samples per data point. The bandwidth axis was estimated for each axis individually, using the *estimate bandwidth* function, which measures the tradeoff between variance in the data and sample size (Blonder *et al.*, 2016). After finding the intersection between the two hypervolumes, overlap values were calculated between individual pairs of taxa (2 × shared volume/summed volume) (Blonder *et al.*, 2014), analogous to the Sørensen coefficient. Comparisons between Euclidean distances from the taxon hypervolume centroids were also made.

Morphological (or other) hypervolumes can only be estimated when the number of observations (*m*) and dimensionality (*n*) are greater than two. Therefore, in the species-level analyses, species known from only one (i.e., the holotype) or no specimens (i.e., types lost) had

to be excluded from morphological analyses. There is no evidence, however, that excluding these species influenced the results retrieved (Appendix S1, Fig. S2). A similar phenomenon applies to environmental hypervolumes: species for which distributional data were limited ($m < 3$) had to be excluded from analysis. Because hypervolumes can be compared only if they are constructed using the same axes (Blonder *et al.*, 2014), damaged specimens, (e.g., lacking elytra or pronotum) were also excluded from analyses. With these considerations, we analyzed 42 species at the genus level, and 16 at the species level in four genera; sample sizes range 7–90 individuals.

As mentioned above, analyses were carried out for genera and species, to test for differences in patterns between taxonomic levels. At the genus level, all specimens available within each genus were treated as a unit, totaling 672 specimens across the four genera. For the species-level analysis, only species from genera with spines were considered; 16 of 22 species had enough morphological and environmental data to allow comparisons of overlap matrices. All analyses, unless otherwise specified, were conducted in R, version 3.0.2 (R. Core Team, 2014).

Morphological hypervolumes

To examine whether certain aspects of morphology might be unduly influencing the calculation of morphological hypervolumes, analyses were conducted with and without the total body height variable, and also on both raw data and natural log-transformed data. Note that body size and spine height were correlated ($r = 0.86$; $p < 0.0001$), thus necessitating our use of principal components analysis (see Supporting Information, Figure S4). Results did not differ, so

only analyses of raw data and including body height are presented here. For the purposes of brevity and clarity; the other analyses are provided in Supporting Information, Appendix S3. As with the environmental variables, a principal components analysis (PCA) was carried out on the morphological data matrix using the *princomp* routine in R (v. 3.2.2 Core Team, 2014) to reduce dimensionality and multicollinearity. We explored different aspects of the principal components to assess robustness of the results. In particular, one analysis included all principal components derived from the morphological data. Another excluded the first principal component since it explained 88%–93% of the variance (depending on whether the variable 'total body height' was included and whether the data were natural log-transformed or not), and thus might be influencing results disproportionately and swamping out other signals. A third analysis considered only components 2, 3, and 4, to reduce dimensionality and further avoid the potential dominant influences of component 1. In particular, according to Blonder (2014, http://www.benjaminblonder.org/hypervolume_faq.html), high dimensionality can lead to hypervolumes with disjunct data points that could potentially confound comparisons, owing to lack of sufficient data points.

Environmental Hypervolumes.

Niche models were developed using the maximum entropy algorithm Maxent 3.3.3.k (Phillips *et al.*, 2006), which computes a measure related to probability of presence using the Gibbs probability distribution with the maximum entropy based on the aforementioned environmental variables and occurrence data. Following standard protocols, empirical averages of environmental variables were used (Phillips *et al.*, 2004); specific settings employed were a

bootstrap with 100 replicates and a random seed. The calibration area was determined for each taxon individually, based on its known distribution and biogeographic patterns (Barve *et al.*, 2011). Environments potentially suitable for each taxon identified via Maxent were projected and explored in geographic space using ArcGIS 10.2, and validated using a jackknife approach specifically designed for situations of small sample sizes (Pearson *et al.*, 2007).

Maps from ENMs were initially converted into integer grids, retaining three significant digits (i.e., multiply by 1000), and reclassified as either "0" (unsuitable area) or "1" (suitable area) using the highest threshold that includes 90% of occurrence data used in calibration (Peterson, 2014). The final area was randomly sampled, using the function *spsample* available in the R package *sp* (Pebesma *et al.*, 2012), and these spatial points were used to extract values from the first three principal components rasters using the function *extract* available in the R package *raster* (Hijmans *et al.*, 2015). Extracted values were assembled (Appendix S2, Tables S4 and S5) and used to estimate environmental hypervolume for each genus and species.

According to Blonder *et al.*, (2014), increasing the number of points in the dataset enables use of smaller kernel bandwidths, which can help remove problematic, irregular edges of hypervolumes that may result from low dimensionality. To reduce the problem of irregular edges in our analyses of hypervolume, we increased sampling for the environmental hypervolume analysis through estimation of each species' potential distribution. This area was then used as an extended representation of their preferred environmental space, from which more points could be randomly sampled.

Statistical Methods. To test correlations between environment and morphology, a non-parametric Mantel test with 999 permutations was calculated using the R package *Vegan*

(Oksanen *et al*., 2012). In this case, the overlap between the environmental distance matrix and morphological distance matrix was calculated. The test statistic was the Pearson product-moment correlation coefficient *r*; probabilities were calculated using a two-tailed test, based on comparisons with a null distribution derived from randomization of the rows of the matrices.

Background Similarity Tests. The background similarity test was performed using ENMTools (Warren *et al.*, 2008). Lacking extensive data for all species, we only tested the null hypothesis of niche similarity between genera. We cast many random points, equal to the sample size available for each genus x 100, across the model calibration area; this is equivalent to M, ('Mobility') in the BAM diagram (Soberón and Peterson, 2005). Based on those points, we created 100 random replicates with which to calculate niche models, later used for niche similarity estimation. Each taxon pair was evaluated by comparing the observed similarity between the two niche models, against the background similarity (= niche model of one species against background models for the other; Warren *et al.*, 2008). The null hypothesis of niche similarity was rejected if observed *D* or *I* values fell below the 5^{th} percentile in the random-replicate distribution after a correction for multiple comparisons, for the taxon pair in question.

Results

Body height varied with geography (Fig. 6.2), but not in the way Spaeth (1923) predicted, i.e., increasing spine height and decreasing width towards the southern extreme of the tribe's range in association with different climatic niches.

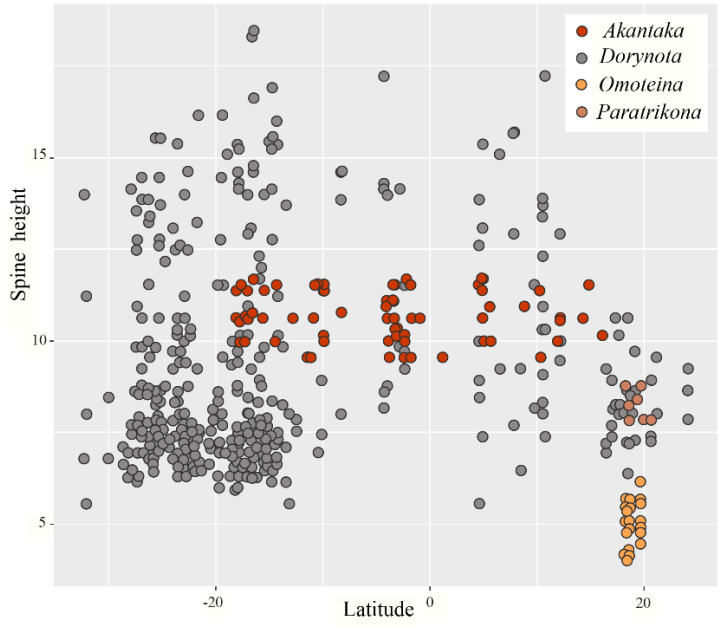

Figure 6. 2**.** Scatterplot showing distribution of elytra height (x) for the four Dorynotini genera at different latitudes (y).

Pairwise comparisons between climatic niches of observed and random points of pairs of species showed that neither of the tests were able to reject the null hypothesis of niche conservatism among genera in the tribe. Indeed, all comparisons showed striking similarity in overall characteristics, since observed *D* or *I* values fell *above* the 5th percentile of *D* or *I* values in the null distributions before correction for multiple comparisons (Table 1).

Table 6.1. Results of background similarity tests between observed and background niche models of different genera. Niche overlap values were based on Schoener's *D*/ Hellinger's *I* metrics of similarity, and values presented are proportions of null values falling below the observed, and as such are probability values associated with the null hypothesis of niche similarity.

	Akantaka	*Dorynota*	*Paratrikona*	*Omoteina*
Akantaka		0.76 / 0.90	0.1 / 0.49	0.17 / 0.46
Dorynota	0.67 / 0.66		0.04 / 0.10	0.22 / 0.16
Paratrikona	0.32 / 0.34	0.77 / 0.28		0.78 / 0.58
Omoteina	0.5 / 0.44	0.45 / 0.44	0.63/ 0.46	

The environmental hypervolumes showed high levels of overlap across genera and species (Fig. 6.3A–B). At the genus level, *Dorynota* showed the highest overlap with other

genera, probably owing to its broad geographic distribution: it showed ca. 72% overlap with *Paratrikona* and ca. 60% with *Akantaka*. By contrast, *Omoteina* had lower levels of overlap with other genera (17%–31%), probably reflecting its constrained distribution in both geographic and environmental spaces. At the species level, overlap was higher: they were never below ca. 30% and reached as high as 80%.

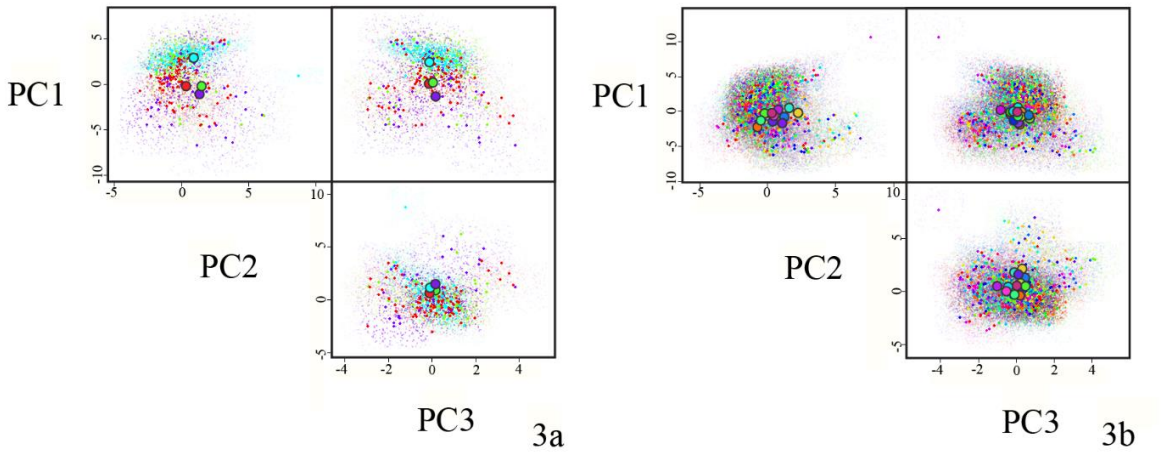

Figure 6. 3. Environmental hypervolumes of genera (A) and species (B), each showing a high degree of overlap across the taxa considered. Key to colors of genera: *Dorynota* in red; *Paratrikona* in green; *Omoteina* in blue; and *Akantaka* in purple. Key to colors of species: *D. aculeata* (Boheman, 1854) in red; *D. aurita* (Boheman, 1862) in orange; *D. bidens* (Fabricius, 1781) in light yellow; *D. cornigera* (Boheman, 1854) in bright yellow; *D. monneorum* Simões & Sekerka, 2015 in yellow green; *D. parallela* Blanchard, 1846 in lime green; *D. pugionata* (Germar, 1824) in light sea green; *D. rileyi* Borowiec, 1994 in turquoise; *D. yucatana* (Champion, 1893) in aqua; *D. monoceros* (Germar, 1824) in steel blue; *D. ensifera* (Boheman, 1854) in blue; *D. apiculata* in blue violet; *D. minima* (Wagner, 1881) in pink; *D. rugosa* (Wagener, 1881) in magenta; and *D. spinosa* (Boheman, 1854) in coral. Taxon centroids are shown as larger dots.

In contrast, morphological hypervolumes indicated low levels of overlap at both taxonomic levels. For instance, at the genus level (Fig.6. 4), mean overlap was less than ca. 3%, with only the overlap between *Omoteina* and *Paratrikona* being somewhat higher (10.7%). At the species level (Fig. 6.5), overlap values were slightly higher, ranging between 0% and 22%. This result suggests that traits selected for measurement were effective at delineating taxa, and therefore were reasonable candidates for constructing morphological hypervolumes. The Mantel

test comparing environmental and morphological hypervolumes found no correlation between these attributes ($r \sim 0$; $p >> 0.05$) (Tables 2 and Appendix S3, Tables S32 and S58), generally matching the pattern shown on the right side of Fig. 2, i.e., Spaeth's (1923) original hypothesis is not supported.

Table 6.2. Results of Mantel tests, comparing genus and species morphological and environmental hypervolumes. The columns indicate the principal components used to calculate the morphological hypervolumes. First, we used all principal components of the morphological dataset; second, we used all components except PC1; third, we used only components 2, 3, and 4.

r (*p*-value)		Principal components (all)	Principal components (all except PC1)	Principal components (only PC's 2, 3 & 4)
Species	With spine	-0.002 (0.527)	-0.052 (0.611)	0.127 (0.266)
	No spine	-0.081 (0.797)	-0.046 (0.609)	-0.051 (0.629)
Genus	With spine	-0.387 (0.833)	-0.496 (0.833)	-0.730 (1)
	No spine	-0.183 (0.541)	-0.332 (0.958)	-0.776 (1)

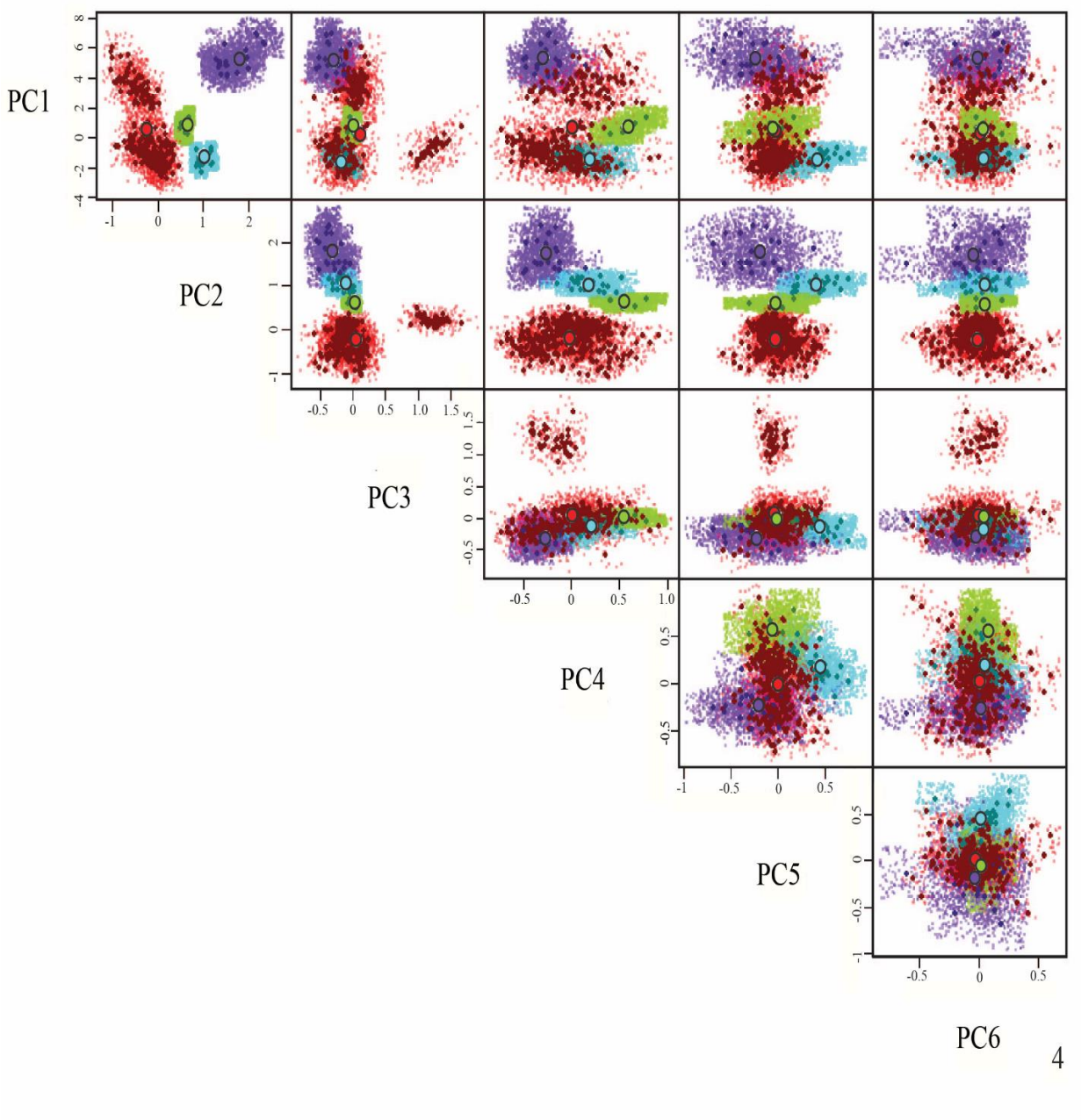

Figure 6. 4. Morphological hypervolumes of genera within the Cassidinae: Dorynotini, showing that different genera can be distinguished based on the morphological variables chosen. Key to colors of

represented genera: *Dorynota* in red; *Paratrikona* in green; *Omoteina* in blue; and *Akantaka* in purple. Taxon centroids are shown as larger dots.

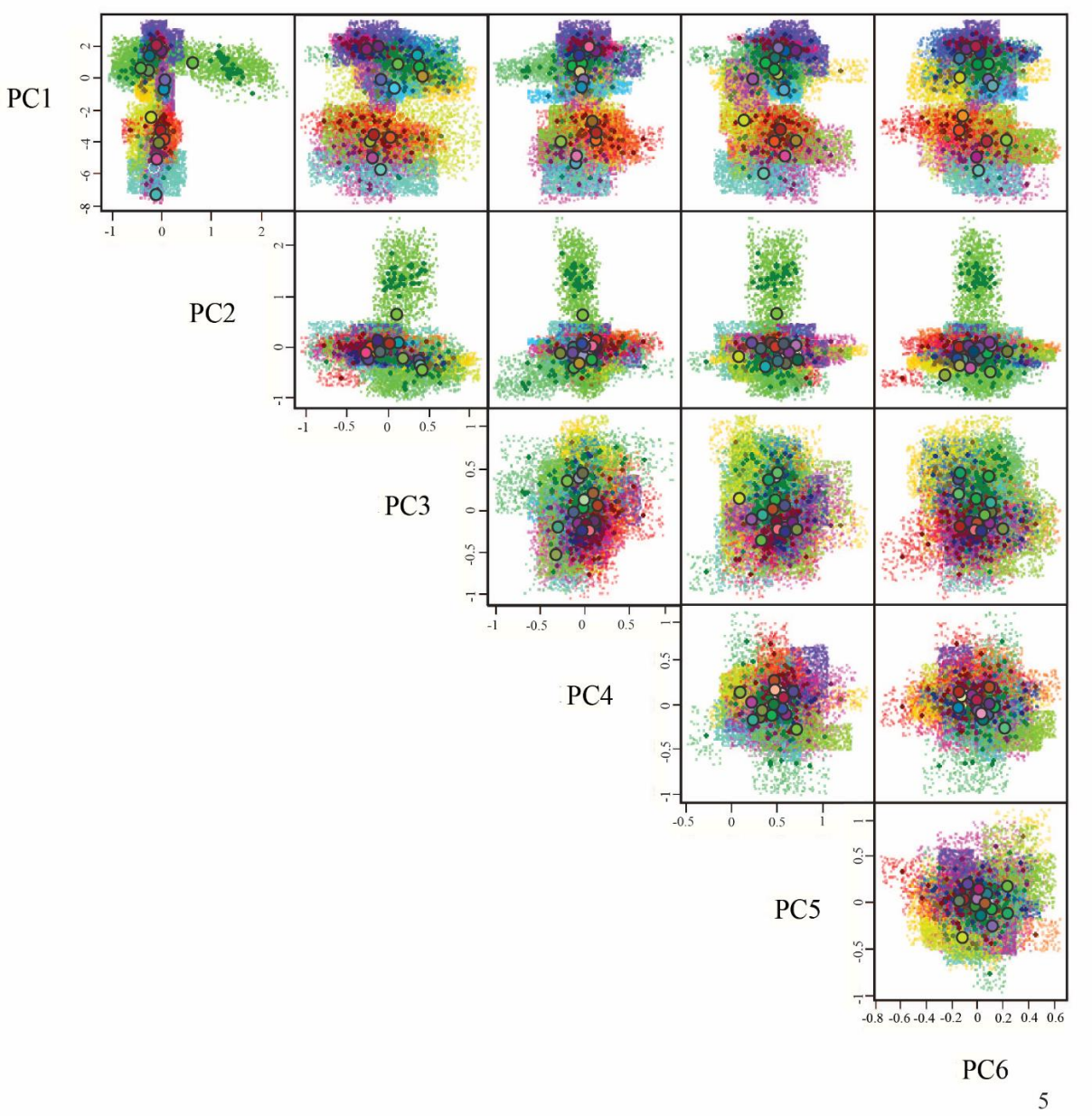

Figure 6. 5**.** Morphological hypervolume of species within the Cassidinae: Dorynotini, showing that different species can generally be distinguished based on the morphological variables chosen, though not to the same extent as genera. Key to colors of the represented species: *D. aculeata* in red; *D. aurita* in orange; *D. bidens* in light yellow; *D. cornigera* in bright yellow; *D. monneorum* in yellow green; *D. parallela* in lime green; *D. pugionata* in light sea green; *D. rileyi* in turquoise; *D. yucatana* in aqua; *D. monoceros* in steel blue; *D. ensifera* in blue; *D. apiculata* in blue violet; *D. minima* in pink; *D. rugosa* in magenta; and *D. spinosa* in coral. Taxon centroids are shown as larger dots.

Discussion

The *n*-dimensional hypervolume concept, when used to create and compare morphological and environmental spaces, and implemented following Blonder *et al.*, (2014), provides a potentially useful way to explore correlations relevant to biogeography and ecology. It is especially valuable in allowing simultaneous comparisons of different variables, which makes it possible to consider how different effects interact. Such a situation is quite pertinent when it comes to evaluating hypothesized ecomorphological patterns, like the one posited by Spaeth (1923) for the cassidine beetle clade across environmental space. In particular, while the size of the dorsal spine does vary across the range of the clade (Fig. 6.2; Appendix S1, Fig. S5), the suspected correlation between morphology and environment does not truly exist, and these characteristics seem to vary independently within the group (see also Barton *et al*., 2011 for an interesting discussion and means of testing these issues).

Despite the great morphological diversity within the clade, and distinct distributional patterns that suggest high correlations between environment and morphology, the results of the Mantel test indicated no correlations between overlap matrices of environmental and morphological hypervolumes. This outcome is supported by the niche background similarity test: all genera had higher levels of niche overlap than expected by chance, contradicting the hypothesis posited by Spaeth (1923), that ecological speciation was the main process promoting the clade's diversification.

It is worth noting that, even though high levels of environmental overlap and potential niche conservatism exist among taxa, different genera could readily be distinguished morphologically, with low degrees of overlap among morphological hypervolume matrices. This

result shows that morphological diversity exists in the clade despite potential niche conservatism. This suggests that generally there might not be a one to one relationship between the morphology of an organism and the niche it occupies (see Harmon *et al.*, 2005 and Soberón and Martínez-Gordillo, 2012 for additional discussion). Of course, to document niche conservatism more fully, a phylogeny of the group is necessary. However, at this point in time, it is clear that we are dealing with closely related species in a monophyletic clade (Simões, 2014, 2017; Simões and Sekerka, 2015).

Within the subfamily, it is generally difficult to differentiate males and females, although females tend to be at least 20% longer than males (Jolivet, 1999). Only in a few taxa is sexual dimorphism conspicuous, as in the genus *Acromis* (Chevrolat, 1836), where the male has strongly anteriorly projecting humeral angles of the elytra; these features are often adorned by holes gained during male-male combat for females (Windsor, 1987). Sexual dimorphism is generally even less prominent in Dorynotini, with only small differences in size observed. However, it is present in *Akantaka*: males often differ in coloration, making species identifications challenging without additional *in situ* observations (e.g., males can have metallic green bodies, with expanded humeral angles and sinuous lateral margins of elytra, whereas females are black and have both rounded humeral angles and rounded lateral margins of elytra). This dimorphism may suggest sexual selection played a role in promoting diversification within the clade. Dispersal capacity might also have played a role in diversification of this group. In particular, most species are relatively large (i.e., 10–15 mm) and their capacity for flight is limited, such that they are restricted to areas where host plants are present (Simões, pers. observ.), making the group more susceptible to distributional isolation and speciation processes.

Our results also suggest that the striking morphological trait seen within different genera of the clade, the tubercle/spine on the elytra, could be of adaptive value for biotic, as opposed to abiotic, factors. The first author encountered in the field a specimen of *Dorynota ensifera* (Boheman, 1854) (Fig. 6) which appears to show the dorsal spine mimicking the gall of its host plant. This behavior was observed in only one species within the larger clade. Further, we cannot be sure that this is typical of that species, or even truly constitutes using the spine to blend in with the gall for the purposes of camouflage from predators. However, it at least suggests another potential function for the tubercle/spine.

It is also conceivable that other factors related to population biology might be playing a role in this phenomenon. Unfortunately, relatively little is known about population biology of cassidines across latitudinal gradients, although some aspects of population biology in the group are documented: regarding life cycle, population abundance correlates with host plants utilization (see Nogueira-De-Sá and Vasconcellos-Neto, 2003 and Gomes *et al.*, 2012). At this point is hard to ascribe the causes of the patterns in this clade, but work is currently underway to explore the possible roles of these and other factors; more information about the natural history of this group would be invaluable. One important caveat to these conclusions is that the environmental hypervolumes constructed and compared herein might in fact reflect aspects of the realized niche, and not the fundamental niche, although our understanding of this problem is that it will bias results away from finding conservatism (Soberón and Peterson, 2011). Furthermore, the identified similarities of environmental overlap might be a consequence or artifact of the environmental layers used in the analysis herein; conceivably, other variables might better serve to differentiate taxa. Still, the variables chosen constitute the types of variables that Spaeth (1923) was considering when he documented the cline in the clade. It is conceivable, however,

that different variables might be more relevant to consider in analyses of clinal phenomena at smaller spatial scales. Irrespective of this constraint, exploring further how hypervolumes can be used to make multidimensional comparisons relevant to biogeographic, ecological, and evolutionary research will be fruitful. Indeed, new methodological developments continue to be made regarding analysis of hypervolumes (Blonder, 2016), such that this methodology will constitute a rewarding area of research.

Bibliography

Anderson RP, Handley CO. 2002. Dwarfism in insular sloths: biogeography, selection, and evolutionary rate. *Evolution* 56: 1045–1058.

Ashton KG, Tracy MC, Queiroz A de. 2000. Is Bergmann's Rule Valid for Mammals? *The American Naturalist* 156: 390–415.

Barton PS, Gibb H, Manning AD, Lindenmayer DB, Cunningham SA. 2011. Morphological traits as predictors of diet and microhabitat use in a diverse beetle assemblage. *Biological Journal of the Linnean Society* 102: 301–310.

Barve N, Barve V, Jiménez-Valverde A, Lira-Noriega A, Maher SP, Peterson AT, Soberón J, Villalobos F. 2011. The crucial role of the accessible area in ecological niche modeling and species distribution modeling. *Ecological Modelling* 222: 1810–1819.

Benton MJ, Csiki Z, Grigorescu D, Redelstorff R, Sander PM, Stein K, Weishampel DB. 2010. Dinosaurs and the island rule: The dwarfed dinosaurs from Haţeg Island. *Palaeogeography, Palaeoclimatology, Palaeoecology* 293: 438–454.

Blake D. 1937. Ten new species of West Indian Chrysomelidae (Coleoptera). *Proceedings of the Entomological Society of Washington* 39: 67–78.

Blake D. 1938. Eight new species of West Indian Chrysomelidae. *Proceedings of the Entomological Society of Washington* 40: 44–52.

Blake D. 1939. Eight new Chrysomelidae (Coleoptera) from the Dominican Republic. *Proceedings of the Entomological Society of Washington* 41: 231–239.

Blonder B. 2016. Do Hypervolumes Have Holes? *The American Naturalist* 187: E93–E105.

Blonder B, Lamanna C, Violle C, Enquist BJ. 2014. The n-dimensional hypervolume. *Global Ecology and Biogeography* 23: 595–609.

Boback SM. 2003. Body size evolution in snakes: evidence from island populations. *Copeia* 2003: 81–94.

Boheman C.H. 1854. *Monographia cassididarum*. *Tomus secundus.* ex officina Norstedtiana, Holmiae.

Boheman C.H. 1862. *Monographia cassididarum*. *Tomus quartus (Supplementum).* ex officina Norstedtiana, Holmiae.

Borowiec L. 1994. *Dorynota rileyi* n. sp. from Paraguay [Coleoptera: Chrysomelidae: Cassidinae]. *Genus* 5: 161–164.

Borowiec L. 1996. Faunistic records of Neotropical Cassidinae (Coleoptera: Chrysomelidae). *Polskie Pismo Entomologiczne* 65: 119–251.

Borowiec L. 2002. New records of Neotropical Cassidinae, with description of three new species (Coleoptera: Chrysomelidae) *Genus* 13: 43–138.

Borowiec L. 2009. *Paratrikona albomaculata*, a new species from the Dominican Republic (Coleoptera: Chrysomelidae: Cassidinae: Dorynotini) *Genus* 20: 567–570.

Borowiec L., Świetojańska J. 2017. World catalog of Cassidinae. Wrocław, Poland. <http://www.cassidae.uni.wroc.pl/katalog%20internetowy/index.htm> (8th November 2017).

Champion, G.C. (1893) Fam. Cassididae. *Biologia Centrali-America*, Insecta, Coleoptera. Vol. VI. Part 2. Phytophaga (ed. by F.D. Godman. and O. Salvin), pp. 125–164. Taylor &

Francis, U.K.

Chown SL, Gaston KJ. 1999. Exploring links between physiology and ecology at macro-scales: the role of respiratory metabolism in insects. *Biological Reviews of the Cambridge Philosophical Society* 74: 87–120..

Clegg SM, Owens PF. 2002. The 'island rule' in birds: medium body size and its ecological explanation. *Proceedings of the Royal Society B: Biological Sciences* 269: 1359–1365.

Conover DO, Duffy TA, Hice LA. 2009. The covariance between genetic and environmental influences across ecological gradients: Reassessing the evolutionary significance of countergradient and cogradient variation. *Annals of the New York Academy of Sciences* 1168: 100–129.

Eroğlu Aİ, Kurnaz M, Koç H, Bülbül U, Kutrup B. 2016. Age and growth of the red-belied lizard, Darevskia parvula. *Animal Biology* 66: 81–95.

Feldman A, Meiri S. 2013. Length-mass allometry in snakes. *Biological Journal of the Linnean Society* 108: 161–172.

Ficetola GF, Colleoni E, Renaud J, Scali S, Padoa-Schioppa E, Thuiller W. 2016. Morphological variation in salamanders and their potential response to climate change. *Global Change Biology* 22: 2013–2024.

Gomes PA., Prezoto F., Frieiro-Costa FA. 2012. Biology of *Omaspides pallidipennis* Boheman, 1854 (Coleoptera: Chrysomelidae: Cassidinae). *Psyche: A Journal of Entomology* 2012: 1–8.

Gould SJ, Lewontin RC. 1979. The spandrels of San Marco and the panglossian paradigm: a critique of the adaptationist programme. *Proceedings of the Royal Society B: Biological Sciences* 205: 581–598.

Harmon LJ, Kolbe JJ, Cheverud JM, Losos JB. 2005. Convergence and the multidimensional niche. *Evolution* 59: 409–421.

Hijmans RJ, Cameron SE, Parra JL, Jones PG, Jarvis A. 2005. Very high resolution interpolated climate surfaces for global land areas. *International Journal of Climatology* 25: 1965–1978.

Jolivet P. 1999. Sexual behavior among Chrysomelidae. *Advances in Chrysomelidae Biology 1*: 391–409. Leiden, Backhuys, the Netherlands.

Kleyer M, Minden V. 2015. Why functional ecology should consider all plant organs: an allocation-based perspective. *Basic and Applied Ecology* 16: 1–9.

Koski MH, Ashman TL. 2015. Floral pigmentation patterns provide an example of Gloger's rule in plants. *Nature Plants* 1: 14007.

Lamanna C a, Blonder B, Violle C, Kraft NJB, Sandel B, Simova I, Donoghue II JC, Svenning J christian, Mcgill BJ, Boyle B, Buzzard V, Dolins S, Jørgensen PM, Marcuse-kubitza A, Morueta-holme N, Peet RK, Piel W, Regetz J, Schildhauer M, Spencer N, Thiers BM, K WS, Enquist BJ. 2014. Functional trait space and the latitudinal diversity gradient. *Proceedings of the National Academy of Sciences of the United States of America* 111: 13745–13750.

Lomolino M V. 2005. Body size evolution in insular vertebrates: Generality of the island rule. *Journal of Biogeography* 32: 1683–1699.

Lomolino M V., Sax DF, Riddle BR, Brown JH. 2006. The island rule and a research agenda for studying ecogeographical patterns. *Journal of Biogeography* 33: 1503–1510.

Maulik S. 1916. On Cryptostome beetles in the Cambridge University Museum of Zoology. *Journal of Zoology* 86: 567–589.

McClain CR, Boyer AG, Rosenberg G. 2006. The island rule and the evolution of body size in the deep sea. *Journal of Biogeography* 33: 1578–1584.

McDowall RM. 2008. Jordan's and other ecogeographical rules, and the vertebral number in fishes. *Journal of Biogeography* 35: 501–508.

McNab BK. 2002. Minimizing energy expenditure facilitates vertebrate persistence on oceanic islands. *Ecology Letters* 5: 693–704.

Meiri S, Dayan T. 2003. On the validity of Bergmann's rule. *Journal of Biogeography* 30: 331–351.

Meiri S, Dayan T, Simberloff D. 2004. Body size of insular carnivores: little support for the island rule. *The American Naturalist* 163: 469–479.

Millien V, Kathleen Lyons S, Olson L, Smith FA, Wilson AB, Yom-Tov Y. 2006. Ecotypic variation in the context of global climate change: Revisiting the rules. *Ecology Letters* 9: 853–869.

Mouillot D, Stubbs W, Faure M, Dumay O, Tomasini JA, Wilson JB, Chi T Do. 2005. Niche overlap estimates based on quantitative functional traits: a new family of non-parametric indices. *Oecologia* 145: 345–353.

Murren CJ. 2002. Phenotypic integration in plants. *Plant Species Biology* 17: 89–99.

Nogueira-De-Sá F, Vasconcellos-Neto J. 2003. Host plant utilization and population abundance of three tropical species of Cassidinae (Coleoptera: Chrysomelidae). *Journal of Natural History* 37: 681–696.

Oksanen J, Blanchet F, Kindt R, Legendre P, O'Hara R. 2016. Vegan: community ecology package. *R package 2.3-3*. <https://cran.r-project.org/web/packa> (8th November 2017).

Pearson RG, Raxworthy CJ, Nakamura M, Townsend Peterson A. 2007. Predicting species distributions from small numbers of occurrence records: A test case using cryptic geckos in Madagascar. *Journal of Biogeography* 34: 102–117.

Pebesma E, Bivand R, Rowlingson B, Gomez-Rubio V, Hijmans RJ, Sumner M, MacQueen D, Lemon J, Brien J. 2016. Package 'sp'. *R*: 118.

Phillips SJ, Anderson RP, Schapire RE. 2006. Maximum entropy modeling of species geographic distributions. *Ecological Modelling* 190: 231–259.

Pincheira-Donoso D, Hodgson DJ, Tregenza T. 2008. The evolution of body size under environmental gradients in ectotherms: why should Bergmann's rule apply to lizards? *BMC Evolutionary Biology* 8: 68.

R Core Team 2017. R: Language and Environment for Statistical Computing. R Foundation for Statistical Computing, Vienna, Austria. <http://R-project.org/> (8th November 2017).

Saupe EE, Qiao H, Hendricks JR, Portell RW, Hunter SJ, Soberón J, Lieberman BS. 2015. Niche breadth and geographic range size as determinants of species survival on geological time scales. *Global Ecology and Biogeography* 24: 1159–1169.

Schluter D. 2000. The ecology of adaptive radiation. *Oxford Series in Ecology and Evolution*: 300.

Schmidt NM, Jensen PM. 2003. Changes in Mammalian Body Length over 175 Years—Adaptations to a Fragmented Landscape? *Conservation Ecology* 7: 6.

Schmidt NM, Jensen PM. 2005. Concomitant patterns in avian and mammalian body length changes in Denmark. *Ecology and Society* 10: 5.

Simões MVP. 2014. Taxonomic revision of the genus *Paranota* Monrós and Viana, 1949 (Coleoptera: Chrysomelidae: Cassidinae: Dorynotini). *The Coleopterists Bulletin* 68: 631–655.

Simões MVP. 2017. Revision of the Greater Antilles genus *Paratrikona* Spaeth, 1923 (Coleoptera: Chrysomelidae: Cassidinae: Dorynotini). *Zootaxa* 4238: 417–425.

Simões MVP, Sekerka L. 2015. Review of the Neotropical leaf beetle subgenus *Dorynota s. str.* Chevrolat (Coleoptera : Chrysomelidae : Cassidinae : Dorynotini). *The Coleopterists Bulletin* 69: 231–254.

Slavenko A, Meiri S. 2015. Mean body sizes of amphibian species are poorly predicted by climate. *Journal of Biogeography* 42: 1246–1254.

Soberón J, Martínez-Gordillo D. 2012. Occupation of environmental and morphological space: climatic niche and skull shape in *Neotoma* woodrats. *Evolutionary Ecology Research* 14: 503–517.

Soberón J, Peterson AT. 2005. Interpretation of models of fundamental ecological niches and species' distributional areas. *Biodiversity Informatics* 2: 1–10.

Soberón J, Peterson AT. 2011. Ecological niche shifts and environmental space anisotropy: a cautionary note. *Revista Mexicana de Biodiversidad* 82: 1348–1355.

Valenzuela-Sánchez A, Cunningham AA, Soto-Azat C. 2015. Geographic body size variation in ectotherms: effects of seasonality on an anuran from the southern temperate forest. *Frontiers in Zoology* 12: 37.

Warren DL, Glor RE, Turelli M. 2010. ENMTools: A toolbox for comparative studies of environmental niche models. *Ecography* 33: 607–611.

Wiens JJ, Ackerly DD, Allen AP, Anacker BL, Buckley LB, Cornell H V., Damschen EI, Jonathan Davies T, Grytnes JA, Harrison SP, Hawkins BA, Holt RD, McCain CM, Stephens PR. 2010. Niche conservatism as an emerging principle in ecology and conservation biology. *Ecology Letters* 13: 1310–1324.

Windsor DM. 1987. Natural history of a subsocial tortoise beetle, *Acromis sparsa* Boheman (Chrysomelidae, Cassidinae) in Panama. *Psyche (New York)* 94: 127–150.

Appendix I

Table S1. Material examined and institutions, for morphological coding of characters (Chapter 5)

Abbreviation for institutions: Coleção Entomológica Prof. José Alfredo Pinheiro Dutra, Departamento de Zoologia, Instituto de Biologia (DZRJ); Coleção de Entomolgia de Pe. Jesus S. Moure do Departamento de Zoologia, Universidade Federal do Paraná, Parana Brazil (DZUP); Department of Biodiversity and Evolutionary Taxonomy, University of Wrocław, Poland (DBET); Collection of Lukáš Sekerka, Prague, Czech Republic (LSC); Manchester Museum, Manchester, UK (MMUE); Muséum National d'Histoire Naturelle, Paris, France (MNHN); Museu de Zoologia da Universidade de São Paulo, São Paulo, Brazil (MZUSP); Museu Nacional, Universidade Federal do Rio de Janeiro, Rio de Janeiro, Brazil (MNRJ); National Museum of Natural History, Smithsonian Institution, Washington D.C., U.S.A. (USNM); Natural History Museum, London, U.K. (BMNH); Swedish Museum of Natural History, Stockholm, Sweden (SMNH); Texas A & M University, Texas, U.S.A. (TAMU); Manchester Museum, Manchester, U.K. (MMUE); Zoological Museum, University of Copenhagen, København, Denmark (ZMUC); Finnish Museum of Natural History, Helsinki, Finland (MZH); and the working collection of Donald Windsor (DWC).

Tribe	Genus	Species	Specimen used to code morphological characters
Cassidini	*Coptocycla*	*arcuata*	**Brazil:** Rio de Janeiro, Parque Nacional do Itatiaia (PNI), 1250m, 14-15-X.2011, Simões, M.V.P. lgt. (2 spec., MNRJ).
Cassidini	*Charidotella*	*quadrisignata*	
Cassidini	*Deloyala*	*guttata*	**Dominican Republic:** St. Domingo, 23.VI.2015, Simões, M.V.P. lgt. (2 spec., MNRJ).
Cassidini	*Eremionycha*	*bahiana*	**Brazil:** Rio de Janeiro, Cachoeiras de Macacu, Trilha Amarela, 09.X.2013, Sekerka lgt. (2 spec., DZRJ).
Cassidini	*Metriona*	*elatior*	**Brazil:** São Paulo, Cunha, 19.I.2015, Simões, M.V.P. & Assis, C. lgt. (2 spec., MNRJ).
Cassidini	*Plagiometriona*	*ambigena*	**Brazil:** Rio de Janeiro, Parque Nacional do Itatiaia (PNI), 1250 m, 22–25.IX.2011, Simões, M.V.P. lgt. (1 spec., MNRJ).
Cassidini	*Syngambria*	*bisinuata*	**Brazil:** Minas Gerais, Itanhandú, 25.I.2015, Simões, M.V.P. & Assis, C. lgt. (1 spec., MNRJ).
Dorynotini	*Dorynota*	*pugionata*	**Brazil:** Rio de Janeiro, Guapimirim, IV.1984, B. Silva lgt. (1 spec., MNRJ); Espíro Santo, Vitória, Morro Moscoso, III.1980, B. Silva lgt. (MNRJ).
Dorynotini	*Dorynota*	*aculeata*	Without additional locality data: (1 spec., DBET; 1 spec., MZH); **Dominican Republic:** San Critobal, 24.VI.2015, Simões, M.V.P. lgt. (6 spec., MNRJ); St. Domingo (2 spec., MMUE; 3 spec., MZH), 1985, A. Salle lgt. (4 spec., MNHN).
Dorynotini	*Dorynota*	*bidens*	**Brazil:** Rondônia, Colorado do Oeste, Cabide Rio Pimenta, 18.X.1988, Becker, J. lgt. (1 spec., MNRJ); Pernambuco: without additional locality data, L. L. Castro lgt. (1 spec., MNRJ); 'Cachimbo', 1890 Ch. Pujol lgt. (12 spec., MNHN); Conceição de Almeida (Interceção B. Rios e Rio Jaguaripe), 21.VII.1979, Becker, J. lgt. (1 spec., MNRJ); Itamaraju, 26.X.1985, Becker, J. lgt. (1 spec., MNRJ); Porto Villa Victoria, 1890, Ch. Pujol lgt. (1 spec., MNHN); Espírito Santo: without additional locality data (3 spec., DBET; 2 spec., MMUE); Linhares (1 spec., MNRJ); Rio de Janeiro, Itaguaí, Km 47, 13.V.1970, Sudo, S. lgt. (1 spec., MRNJ); São Paulo, Rio Piracicaba, II.1885, P. Germain lgt. (1 spec., MNHN).

Dorynotini	*Dorynota*	*boliviana*	**Bolivia:** Santa Cruz, Amboro National Park Los Volcanes, 20.XI–12.XII.2004, 1000 m, S 18°06'; W 63°36', Mendel, H. & Barclay, M.V.L. lgt. (1 spec., BMNH); Caranavi, 1–25.VI.2010, 1300 m, I. Callegari lgt. (1 spec., DBET)
Dorynotini	*Dorynota*	*collucens*	**Bolivia:** without additional locaity data, 67-56 (1 spec., BMNH)
Dorynotini	*Dorynota*	*distincta*	**Ecuador:** Baly col. 1905-54, Syntype (BMNH)
Dorynotini	*Dorynota*	*funesta*	**French Guiana:** "Cacao Degrad Kwata s Cirque Bagot", IX.1996, D. Rignon lgt. (DBET); **Brazil:** Pará, Óbidos, Canta Galo, Dirings lgt. (5 spec., MZUSP); Rio Trompetas, Le Moult lgt.(1 spec, DBET)
Dorynotini	*Dorynota*	*insidiosa*	**Ecuador:** Bolívar, Chimbo, 1891, M. de Mathan lgt. (1 spec., MNHN); La Chima [= Río La Chima, tributary of Río de Las Juntas, approx. 01°52'S, 79°10'W], I.-VI.1893, 28 spec., M. de Mathan lgt. (24 spec., MNHN; Guayas, Guayaquil (3 spec., MNHN).
Dorynotini	*Dorynota*	*monoceros*	**Brazil:** Bahia: without additional locality data, G. Bondar lgt. (2 spec., MMUE; 1 spec., MNRJ); Espírito Santo, Linhares (Reserva Biologica Sooretama), XII.1964, F. M. Oliveira lgt. (1 spec., MNRJ); Mato Grosso: Rosário-Oeste, II.1972, (1 spec., MZUSP), X.1973, Dirings lgt. (2 spec., MZUSP), II.1974 (1 spec., MZUSP); Minas Gerais: Lagoa Santa, Reinhardt lgt. (4 spec., ZMUC); Matozinho, 3–4 trimestre 1885, E. Gounelle lgt. (1 spec., MNHN); Pará: Santarém (Santarenzinho, Rio Tapajós), II.1964, Dirings lgt. (7 spec., MZUSP); São Paulo: without additional locality data (1 spec., DBET); Bananal (Serra da Bocaína), I.1937, D. Mendes lgt. (1 spec., MNRJ); Peruíbe, 20. XII.1936 (1 spec., MNRJ); **Colombia:** 'Kolombian', (1 spec., MMUE); **Paraguay:** Central: San Antonio (Rio Paraguay), 8.X.1936 (1 spec., DBET); Itapuá: Vega, XII.1954, Dirings lgt. (3 spec., MZUSP); **Uruguay:** Paysandú: 'Paysandu' (1 spec., LSC); **Venezuela:** Distrito Federal: Caracas (1 spec., MMUE).
Dorynotini	*Dorynota*	*parallela*	**Argentina:** Misiones: without additional locality data,V.1955, Dirings lgt. (1 spec., MZUSP); **Brazil:** Bahia, Monrós, F. lgt. (1 spec., USNM); Goiás, Leopoldo Bulhões, XI.1937, Dr. Nick lgt. (1 spec., USNM); Minas Garais, Pirapora, XI.1975, Seabra, Alvarenga, Roppa & Monné lgt. (1 spec, MNRJ); Bahia: without additional locality data, G. Bondar lgt. (13 spec. MNRJ, 3 spec., USNM); Pará: Santarém (Santarenzinho, Rio Tapajós), II.1964, Dirings lgt. (26 spec., MZUSP); São Paulo: without additional locality data (1 spec., DZUP); Vale do Anhangabaú, XI.1924, R. Spitz lgt. (2 spec., MNRJ); Rio Claro, 13.XI.1980, Alejo Mesa lgt. (1 spec., MZUSP); Santa Catarina: Corupá, XI.1944, J. Guerín lgt. (1 spec., USNM); BOLIVIA: Beni: Reyes, 1–20.XII.1956, L. Peña lgt. (1 spec., MNRJ); Santa Cruz: Chiquitos, Santiago, 730m, XI.2008, W. D. Edmonds & T. Vidaurre lgt. (4 spec., TAMU).
Dorynotini	*Dorynota*	*truncata*	**French Guiana:** Saint Jean du Maroni, Le Moult lgt. (1 spec., MNRJ); Brazil, Pará, Itaituba (Rio Tapajós), Dirinos lgt. (1 spec., MZUSP); Cayenne, Dejean Col. (MZH); Amapá, Serra do Navio, 4.VI. 1964, N. Virkki lgt. (1 spec., TAMU)
Dorynotini	*Omoteina*	*humeralis*	**Haiti:** Grand Riviere, Mann lgt. (10 spec., MCZ)
Dorynotini	*Paranota*	*minima*	**Paraguay:** Pres. Hayes, 42Km, NW Benjamin Aveval, 31.I.1983, E. G. Riley lgt. (1 spec., TAMU); **Argentina:** Barrancas: Provincia de Santiago del Estero, E.R. Wagner lgt. (1 spec., MNHN); Formosa: Clorinda, IX.1949, A. Martinez lgt. (1 spec.,
Dorynotini	*Paranota*	*rugosa*	**Brazil:** Mato Grosso, Corumbá, VII. 1979, B. Silva (MNRJ); **Argentina:** Misiones, Loreto, X.1954, Col. A. Maller (MNRJ)
Dorynotini	*Paranota*	*spinosa*	**Brazil:** Mato Grosso, Cáceres, 13.XI.1984, Buzzi, Mielke, Elias & Casagrande col (DZUP); ARGENTINA: Formosa: (1 spec., 5 spec., DZUP); XI.1952, Dirings lgt. (2 spec., MZUSP); XII.1953, Dirings lgt. (3 specimens, MZUSP); Gran Guardia, XII.1953, A., Maller lgt. (3 spec., DZUP); Goiás: C. Elias lgt. (1 spec., MMUE); Aragarças, I.1955, F.M. Oliveira lgt. (1 spec., MNRJ); I.1955, F.M. Oliveira lgt. (2 spec., DZUP); **Bolivia:** Chiquitos: (1 spec., DBET); Brazil (1 spec., MMUE).
Dorynotini	*Paratrikona*	*rubescens*	**Dominica Republic:** Jarabacoa, VIII.1938, 1,500–4,000 ft., Darlington col, (Typ. No 23636) (1 spec., MCZ); Barahona, 1700m, 22.VI.2015, Carlos Molinari lgt. (1 spec., KUcollections).
Mesomphaliini	*Cyrtonota*	*sexpustulata*	**Brazil:** Rio de Janeiro, 25.I.2015, Simões, M.V.P. & Assis, C. lgt. (1 spec., MNRJ)
Mesomphaliini	*Mesomphalia*	*variolaris*	**Brazil:** Bahia, Belmonte, Barrolândia, VIII.1978, G. Bondar & J. Becker (1 spec., MNRJ); II.1947, J. Becker (1 spec., MNRJ); Ilhéus, 1920 (1 spec., MNRJ).
Mesomphaliini	*Stolas*	*conspersa*	**Brazil:** Minas Gerais, Itanhandu, 25.I.2015, Simões, M.V.P. & Assis, C. lgt. (2 spec., MNRJ)
Mesomphaliini	*Stolas*	*modica*	**Brazil:** Minas Gerais, Itamonte, Est. Capivar, 22° 15840' S, 900m, 21.IIII.2008, Paula, A . A. Gomes (1 spec., MNRJ)
Physonotini	*Eurypepla*	*calachoroa*	
Physonotini	*Physonota*	*attenuata*	
Physonotini	*Physonota*	*gigantea*	

Appendix II

Table S2. List of specimens used in this study. Classification follows Borowiec & Świetojańska (2017). GenBank accession codes for each successfully sequenced or downloaded gene fragments will be provided once the paper is accepted. (Chapter 5).

Tribe	Genus	Species	Code	Locality	CO1	CAD	28S
Cassidini	*Coptocycla*	*arcuata*	MVPS32B	Brazil, Rio de Janeiro	XXXXX	XXXXX	XXXXX
Cassidini	*Charidotella*	*quadrisignata*	MVPS22B	Brazil, Rio de Janeiro	XXXXX	XXXXX	XXXXX
Cassidini	*Deloyala*	*guttata*	MVPS28B	Dominican Republic, Santo Domingo	XXXXX	XXXXX	XXXXX
Cassidini	*Eremionycha*	*bahiana*	MVPS13B	Brazil, Rio de Janeiro	XXXXX	XXXXX	XXXXX
Cassidini	*Metriona*	*elatior*	MVPS08B	Brazil, Rio de Janeiro	XXXXX	XXXXX	XXXXX
Cassidini	*Plagiometriona*	*ambigena*	MVPS35B	Brazil, Rio de Janeiro	XXXXX	XXXXX	XXXXX
Cassidini	*Syngambria*	*bisinuata*	MVPS31B	Brazil, Minas Gerais	XXXXX	XXXXX	XXXXX
Dorynotini	*Dorynota*	*pugionata*	MVPS09B	Brazil, Minas Gerais	XXXXX	XXXXX	XXXXX
Dorynotini	*Dorynota*	*aculeata*	MVPS17B	Dominican Republic, Barahona	XXXXX	XXXXX	XXXXX
Dorynotini	*Dorynota*	*bidens*	MVPS16B	Brazil, Rio de Janeiro	XXXXX	XXXXX	XXXXX
Dorynotini	*Dorynota*	*boliviana*	MVPS01B	Bolivia, Andres Ibanez	XXXXX	XXXXX	XXXXX
Dorynotini	*Dorynota*	*collucens*	MVPS05B	Bolivia, Florida	XXXXX	XXXXX	XXXXX
Dorynotini	*Dorynota*	*distincta*	MVPS11B		XXXXX	XXXXX	XXXXX
Dorynotini	*Dorynota*	*funesta*	DW7829	French Guiana	XXXXX	-	-

Dorynotini	*Dorynota*	*insidiosa*	MVPS04B	Panama, Chiriqui	XXXXX	XXXXX	XXXXX
Dorynotini	*Dorynota*	*monoceros*	DW0515		XXXXX	XXXXX	-
Dorynotini	*Dorynota*	*parallela*	MVPS20B	Brazil, Minas Gerais	XXXXX	XXXXX	XXXXX
Dorynotini	*Dorynota*	*truncata*	MVPS06B		XXXXX	XXXXX	XXXXX
Dorynotini	*Omoteina*	*humeralis*	MVPS18B	Dominican Republic, Barahona	XXXXX	XXXXX	XXXXX
Dorynotini	*Paranota*	*minima*	MVPS07B	Bolivia, Andres Ibanez	XXXXX	XXXXX	XXXXX
Dorynotini	*Paranota*	*rugosa*	MVPS14B	Brazl, Mato Grosso	XXXXX	XXXXX	XXXXX
Dorynotini	*Paranota*	*spinosa*	MVPS15B	Brazl, Mato Grosso	XXXXX	-	XXXXX
Dorynotini	*Paratrikona*	*rubescens*	MVPS19B	Brazl, Mato Grosso	XXXXX	XXXXX	XXXXX
Mesomphaliini	*Cyrtonota*	*sexpustulata*	MVPS41B	Brazil, Rio de Janeiro	XXXXX	XXXXX	XXXXX
Mesomphaliini	*Mesomphalia*	*variolaris*	MVPS46B	Brazil, Bahia	XXXXX	-	XXXXX
Mesomphaliini	*Stolas*	*conspersa*	MVPS44B	Brazil, Rio de Janeiro	XXXXX	XXXXX	XXXXX
Mesomphaliini	*Stolas*	*modica*	MVPS43B	Brazil, Rio de Janeiro	XXXXX	XXXXX	XXXXX
Physonotini	*Eurypepla*	*calachoroa*	MVPS56B	USA, Florida	XXXXX	XXXXX	XXXXX
Physonotini	*Physonota*	*attenuata*	MVPS53B	Nicaragua, Granada	XXXXX	XXXXX	XXXXX
Physonotini	*Physonota*	*gigantea*	MVPS52B	Nicaragua, Granada	XXXXX	XXXXX	XXXXX

Appendix III

Table S3. Optimal partitioning schemes and models for BI analyses estimated with PartitionFinder (Chapter 5).

Subset	Best model	#sites	Partition names
1	GTR+G	191	CO1_Position 1
2	HKY+I+G	432	CO1_Position 2; CAD_Position2
3	HKY+I+G	191	CO1_Position 3
4	GTR+G	241	CAD_Position 1
5	HKY+G	241	CAD_Position 3
6	SYM+G	995	28S

Appendix IV

Appendix S1. Morphological characters (Chapter 5)

Table S4. Data matrix. DATA MATRIX.

Missing data indicated by question marks (?); inapplicable data by hyphens (-).

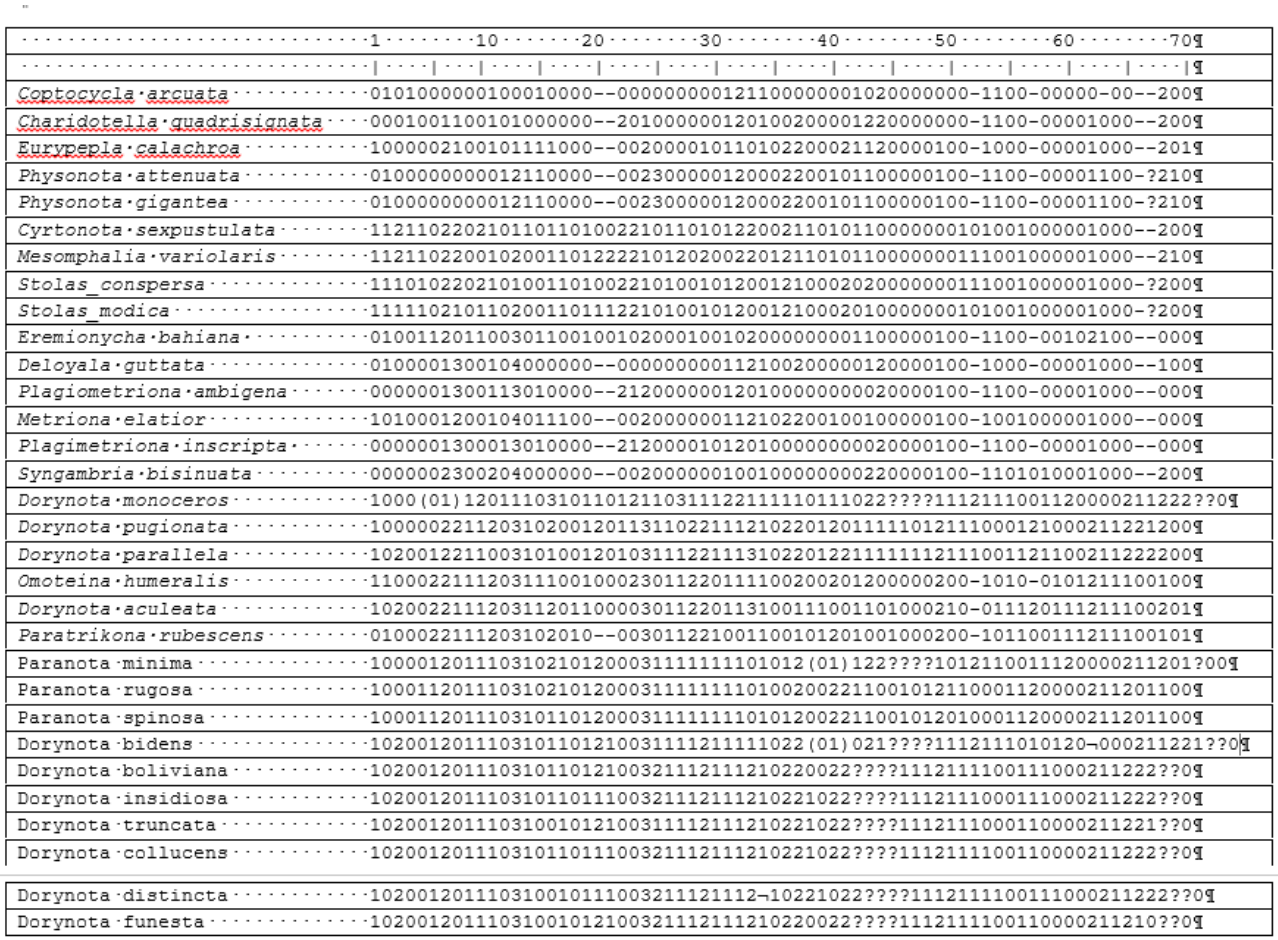

	1 10 20 30 40 50 60 70
Coptocycla arcuata	0101000000100010000--0000000001211000000001020000000-1100-00000-00--200
Charidotella quadrisignata	0001001100101000000--2010000001201002000001220000000-1100-00001000--200
Eurypepla calachroa	1000002100101111000--0020000101101022000211200000100-1000-00001000--201
Physonota attenuata	0100000000012110000--0023000001200022001011000000100-1100-00001100-?210
Physonota gigantea	0100000000012110000--0023000001200022001011000000100-1100-00001100-?210
Cyrtonota sexpustulata	1121102202101101101002210110101220021101011000000010100100000100--200
Mesomphalia variolaris	1121102200102001101222210120200220121101011000000011100100000100--210
Stolas_conspersa	1110102202101001101002210100101200121000202000000011100100000100-?200
Stolas_modica	1111102101102001101112210100101200121000201000000010100100000100-?200
Eremionycha bahiana	0100112011003011001001020001001020000000001100000100-1100-00102100--000
Deloyala guttata	0100001300104000000--0000000001121002000001200000100-1000-00001000--100
Plagiometriona ambigena	0000001300113010000--2120000001201000000000020000100-1100-00001000--000
Metriona elatior	1010001200104011100--0020000001121022001001000000100-1001000001000--000
Plagimetriona inscripta	0000001300013010000--2120000101201000000000020000100-1100-00001000--000
Syngambria bisinuata	0000002300204000000--0020000001001000000000220000100-1101010001000--200
Dorynota monoceros	1000(01)120111031011012110311122111110111022????111211100112000021122??0?
Dorynota pugionata	1000002211203102001201131102211121022012011111012111000121000211221200
Dorynota parallela	1020012211003101001201031112211131022012211111112111001121100211222200
Omoteina humeralis	1100022111203111001000230112201111002002012000002200-1010-01012111001000
Dorynota aculeata	1020022111203112011000030112201131001110011010002l0-0111201112111002010
Paratrikona rubescens	0100022111203102010--0030112210011001012010010002200-1011001112111001010
Paranota minima	1000012011103102101200031111111101012(01)122????101211001112000021120l?00
Paranota rugosa	1000112011103102101200031111111101002002211001012110001120000211201100
Paranota spinosa	1000112011103101101200031111111101012002211001012010001120000211201100
Dorynota bidens	1020012011103101101210031111211111022(01)021????1112111010120-000211221??0
Dorynota boliviana	1020012011103101101210032111211121022022????111211110011100021122??0
Dorynota insidiosa	1020012011103101101110032111211121022102????111211100011100021122??0
Dorynota truncata	1020012011103100101210031111211121022102????111211100011000021122l??0
Dorynota collucens	1020012011103101101110032111211121022102????111211110011000021122??0
Dorynota distincta	1020012011103100101110032111211121-1022102????111211110011100021122??0
Dorynota funesta	1020012011103100101210032111211121022002????111211110011000021121l??0

```
                                71        81        89¶
                                |    |    |    |    |¶
Coptocycla arcuata              0000-100111100000000¶
Charidotella quadrisignata      0100-100111100002000¶
Eurypepla calachroa             0000-100021000000000¶
Physonota attenuata             0000-101121001201000¶
Physonota gigantea              0000-101121001201000¶
Cyrtonota sexpustulata          0100-101101100202010¶
Mesomphalia variolaris          0000-101101101202010¶
Stolas_conspersa                0000-101001101202010¶
Stolas_modica                   0000-101001101202110¶
Eremionycha bahiana             0-00-111120--0002110¶
Deloyala guttata                0100-100201100202000¶
Plagiometriona ambigena         0-00-100001101002000¶
Metriona elatior                0-00-101001101002100¶
Plagimetriona inscripta         0-00-100001101002000¶
Syngambria bisinuata            0000-1000011010020?0?¶
Dorynota monoceros              0?110110?21100?????¶
Dorynota pugionata              0111111102131110200¶
Dorynota parallela              0111011102131111201¶
Omoteina humeralis              1112101122110110211¶
Dorynota aculeata               1112111012122010211¶
Paratrikona rubescens           1112111002122110211¶
Paranota minima                 0?111111?2122?????¶
Paranota rugosa                 0111111102122111201¶
Paranota spinosa                0111111102122111201¶
Dorynota bidens                 0?110110?21100?????¶
Dorynota boliviana              0?110110?21100?????¶
Dorynota insidiosa              0?110111?21100?????¶
Dorynota truncata               0?110110?21100?????¶
Dorynota collucens              0?110110?21100?????¶
Dorynota distincta              0?110110?21100?????¶
Dorynota funesta                0?110110?21100?????¶ Section Break (Next Page)
```

List of morphological characters used in the maximum parsimony analysis

Body

1. Outline, dorsal view: (0) continuous (Fig. S1); (1) discontinuous (Fig. S2). [Character 22 in Chaboo (2007)].

Note: Dorynotini members are characterized by presenting discontinuous (triangular or oval) body shape, as the elytral humeral angle is laterally or anteriorly expanded.

2. Outline, widest region, dorsal view: (0) elytra, humeral angle; (1) elytra, posterior to humeral angle; (2) pronotum, antero-lateral angle; (3) pronotum, posterior lateral margin.

Note: Monrós & Viana (1949) used this character in the key to Dorynotini genera. Members of the tribe are characterized by presenting the body widest region at the humeral angle on species with triangular or subtriangular body shape (Fig. S2), or posterior to the humeral angle on species with oval body shape (Fig. S3).

Head

3. Supraorbital region: (0) with no marks (Fig. S4); (1) with single round macule at the apex of coronal suture (Fig. S5); (2) with paired round macules, one on each side of the coronal sulcus (Fig. S6).

4. Frons (Frs): (0) frons flat or slightly projected anteriorly (Fig. S7); (1) frons strongly projected anteriorly (Fig. S8).

Note: This is a modified version of character 67 in Chaboo (2007), which characterizes the frons (=frontoclypeus; Chaboo 2007) as flat or protuberant. The frons (*Frs*) is triangular

or pentagonal and clearly defined in most tortoise beetles; it is laterally limited by the frontal sulci (occasionally indistinct) and ventrally by the clypeus (*Cl*) (Shin, 2015). The frons in Dorynotini species is flat or slightly projected (Figs S7, S9).

5. Head. Frons: (0) frons smooth (Fig. S9); (1) Frons punctuated (Fig. S7). [Character 17 in Shin (2015)].

6. Head. Labrum, antero-median sinuosity: (0) concave, conspicuous (Fig. S8); (1) concave, not conspicuous (Fig. S7); (2) truncate (Fig. S9). [Character 78 in Chaboo (2007)].

7. Antenna. (0) filiform; (1) telescoped, only apical antennomeres (Fig. S10); (2) telescoped, entire antenna (Fig. S11).

Note: This is a modified version of character 06 in Borowiec (1995), which recognizes only two states, telescoped or not. On telescoped antenna, antennomeres are compactly placed upon each other (Borowiec, 1995), while non-telescoped antenna are filiform, with discrete antennomeres. Here we add that antenna might present a telescoped aspect only on apical antennomeres, represented in outgroup species (Fig. S10) or entirely telescoped, exclusively found in members of the Dorynotini tribe (Fig. S11).

8. Antenna. (0) all antennomeres uniform in width; (1) antennomeres V−X wider at apex ; (2) antennomeres VI−X wider at apex; (3) antennomeres VII−X wider at apex.

Note: This is a modified version of character 60 in Chaboo (2007) — "*Antennomere, shape: Apex wider than base = 0; Apex as wide as base = 1".* In our study, we specify which antennomeres are wider at the apex.

9. Antenna. Apex of antennomeres VI−VII: (0) setose; (1) glabrous.

10. Antenna. Antennomeres VI−VII. (0) simple (Fig. S10); (1) slightly projected laterally; (2) strongly projected laterally (Fig. S12).

Note: This character is a modified version of character 37 in Shin (2015, Fig. 24), which defines antennomeres III-X as slightly serrate (laterally projected) or quadrate (with no lateral projections). In our study, we restricted the characterization to antennomeres VI−VII, as in Dorynotini these are the most conspicuously projected.

11. Antenna. Size of antennomere I and antennomere XI ratio: (0) I longer than XI; (1) I shorter than XI; (2) antennomere I subequal in length to antennomere XI.

12. Antenna. Surface of all antennomeres: (0) opaque, with evident microsculpture; (1) smooth and shiny.

13. Antenna. (0) long uniformly distributed setae in all antennomeres; (1) short dense setae starting on antennomere IV; (2) short dense setae starting on antennomere V; (3) short dense setae starting on antennomere VI; (4) short dense setae starting on antennomere VII.

14. Antenna. Setae aspect on apical antennomeres: (0) bristle-like (Fig. S13); (1) scale-like (Fig. S14).

15. Antenna. Antennomere IV and V length ratio: (0) antennomere IV longer or shorter than antennomere V; (1) antennomere IV as long as antennomere V.

Prothorax

16. Pronotum. Surface aspect: (0) smooth, impunctate (Fig. S15); (1) punctate, fine (Fig. S22); (2) punctate, coarse (Fig. S16 and S17).

17. Pronotum. Surface: (0) smooth; (1) microreticulate.

18. Pronotum. Surface: (0) deeply punctated, without irregular callosities (Fig. S16); (1) deeply punctated, with irregular callosities (Fig. 17).

Note: Blake (1937) and Simões (2017) used this character to describe species of the genus *Paratrikona* Spaeth.

19. Pronotum. Setae: (0) absent (Fig. S23); (1) present (Fig. S20).

Note: This is a modified version of character 25 in Chaboo (2007), which features the dorsal surface of the whole body, while in our study, we refer only to the surface of the pronotal disc.

20. Pronotum. Setae: (0) rare (Fig. S18); (1) sparse (Fig. S19); (2) dense (Fig. S20).

21. Pronotum. Setae: (0) short, scale-like (Fig. S16); (1) short, bristle-like (Fig. S20); (2) long, bristle-like (Fig. S21).

22. Pronotum. Lateral margin: (0) rounded; (1) acute; (2) truncate.

23. Pronotum. Anterolateral margin: (0) convex (Fig. S18); (1) straight (Fig. S23); (2) concave (Fig. S22).

Note: This is a modified version of character 91 in Chaboo (2007), which defines whether the anterolateral angle is broadly expanded or not. In our study, we characterize the shape of it.

24. Pronotum. Shape of basal line of pronotal disc: (0) convex (Fig. S23); (1) straight (Fig. S19); (2) sinuate (Fig. S15); (3) bisinuate (Fig. S16). [Character 94 in Chaboo (2007)].

25. Pronotum. Shape of posterior angle: (0) truncate (Fig. S22); (1) w-shaped, well-marked (Fig. S16); (2) w-shaped, poorly-marked (Fig. S24); (3) rounded (Fig. S15).

Note: This is a modified version of character 96 in Chaboo (2007), interpreted as showing three states— "*Pronotum, posterior angle: Straight or slightly convex = 0; Concave = 1; Acuminate or rounded = 2*". In our study, we consider four states, as the state "w-shaped", might be well- or poorly-marked within Dorynotini species.

26. Pronotum. Posterior angle. (0) poorly-developed (Fig. S18); (1) conspicuous (Fig. S16).

27. Prosternum. Prosternal collar followed by depression. (0) absent (Fig. S25); (1) present, short (Fig. S26); (2) present, transverse sulcus (Fig. S27).

Note: Prosternal collar is the anterior expanded portion of the prosternum (Chaboo, 2007).

28. Prosternum. Antennal calli: (0) absent (Fig.S28); (1) present, poorly-developed (Fig. S29); (2) present, well-developed (Fig. S30).

Note: Antennal calli are antennal groves are found between the prosternum and head cavity.

29. Prosternum. Prosternal collar continuity: (0) uniform, from one side to the other (Fig. S25); (1) not-uniform, not conspicuous (Fig. S32); (2) not-uniform, conspicuous (Fig. S31). [Character 87 in Shin (2015)].

30. Prosternum. Prosternal collar, mid region: (0) curved (Fig. S31); (1) flat (Fig. S32).

31. Prosternum. Prosternal collar, lateral view: (0) exceeds eye line (Fig. S34); (1) does not exceed eye line (Fig. S35).

Note: This is a modified version of character 105 in Chaboo (2007), which describes the anterior expansion of prosternal collar in regard to the coverage of mouthparts, while here we describe its anterior expansion in regard to the eye line.

32. Prosternum. Prosternal process: (0) truncate (Fig. S36); (1) medially expanded, forming V angle (Fig. S32); (2) rounded (Fig. S25).

Note: This is a modified version of character 111 in Chaboo (2007), in which four states describing the apex are considered— tuberculate laterally, rounded and angular. In our study, we add the truncate state, found in the in- and outgroup.

33. Prosternum. Depressed medially: (0) flat (Fig. S33); (1) shallow depression medially (Fig. S31); (2) sulcus single (Fig. S36); (3) sulcus double (Fig. S37).

Note: This is a modified version of character 112 in Chaboo (2007) that describes the surface of prosternal process flat or presenting an angular depression. In our study, we focus on describing the depression found on the process surface, which might be a shallow medial depression, sulcate medially or with two parallel sulcus.

34. Prosternum. Tergosternal suture: (0) absent (Fig. S36); (1) present (Fig. S37).

35. Prosternum. Tergosternal suture region depressed laterally: (0) absent (Fig. S41); (1) present (Fig. S39).

36. Prosternum. Hypomeron depression: (0) absent (Fig. S38); (1) present, not conspicuous (Fig. S40); (2) present, conspicuous (Fig. S41).

37. Prosternum. Prosternal process, lateral margins: (0) parallel (Fig. S36); (1) subparallel (Fig. S26); (2) curved (Fig. S25).

38. Proleg. Protocanter with white spot: (0) absent (Fig. S43); (1) present (Fig. S42).

39. Proleg. Protibia, apical spurs on apical posterior margin. (0) absent (Fig. S45); (1) present (Fig. S44).

40. Proleg. Protibia, apex with excavated internal margin. (0) absent; (1) present, inconspicuous; (2) present, conspicuous (Fig. S45).

41. Proleg. Protibia, anterior outer- margin along tibia expanded anteriorly to accommodate tarsi. (0) absent; (1) present, poorly distinct; (2) present, conspicuous (Fig. S46).

42. Prosternum. Proendosternite, development: (0) not lobed (Fig. S47); (1) lobed (Fig. S48).

43. Prosternum. Proendosternite, consistency: (0) membranous; (1) semi-membranous (Fig. S49); (2) sclerotized (Fig. S48).

Mesothorax

44. Mesoscutum. Concealed portion of mesotergum with transversal ridges: (0) absent (Fig. S51); (1) present, poorly developed (Fig. S50); (2) present, conspicuous (Fig. S52).

45. Scutellum: (0) impunctate (Fig. S51); (1) punctate (Fig. S52).

46. Scutellum. Shape: (0) triangular (Figs S3, S51); (1) diamond-shaped (Figs S2, S52).

Note: Maulik (1916) split the genus *Batanota* Hope (=*Dorynota* Monrós & Viana) into more two other new genera — *Akantaka* for species with a short postscutellar spine, and *Trikona* for species with gibbous elytra. The dichotomous state of mesoscutellum shape employed in our study, was the main morphological trait used to subdivide the genus *Batonota* Hope (=*Dorynota* Chevrolat) into three genera (*Batonota* Hope, *Akantaka* Maulik and *Trikona* Maulik). A modified version of this character was also employed by Chaboo (character 115; 2007), where it is described as presenting the anterior margin depressed or not from the pronotal posterior margin.

47. Scutellum. Surface: (0) not depressed (Fig. S54); (1) depressed (Fig. S53).

48. Scutellum. Anterior edge of scutellar shield: (0) does not overlap posterior angle of pronotum (Fig. S53); (1) overlaps posterior angle of pronotum (Fig. S54). [Character 114 in Chaboo (2007)].

49. Elytra. Insertion pocket or sulcus on anterior margin. (0) absent; (1) present, sulcus; (2) present, pocket (Fig. S55).

Note: Monrós & Viana (1949) indicated that the pronotum of Dorynotini species are placed in a pocket in the anterior margin of elytra. The insertion region might be poorly-developed shown as a sulcus, or well-developed, as a pocket.

50. Elytra. Humeral ridge. (0) absent (Fig. S3); (1) present (Fig. S2).

51. Elytra. Setae. (0) glabrous; (1) setose.

52. Elytra. Setae. (0) inconspicuous (Fig. S35); (1) conspicuous. (Fig. S2).

53. Elytra. Lateral margins: (0) concave (Fig. S3); (1) convex or straight (Fig. S3).

Note: This character was used by Monrós & Viana (1949) to distinguish *Dorynota* and *Akantaka* in the key of Dorynotini genera.

54. Elytra. Disc punctuation. (0) unorganized; (1) organized in rows.

55. Elytra. Punctuation: (0) shallowly impressed; (1) deeply impressed.

56. Elytra. Dorsum: (0) aspinose and atuberculate (Fig. S3); (1) spinose or tuberculate (Fig. S2). [Character 151 in Chaboo (2007)].

57. Elytra. Post-scutellar projection shape: (0) tubercle, conical (Fig. S34, S37); (1) triangular tubercle, extended laterally (Figs S35, S56); (2) spine (Figs S58, S59).

Note: This is a modified version of character 150 in Chaboo (2007) — "*Elytra, post-scutellar umbo or spine: Present = 0; Absent = 1*". Chevrolat (in Dejean, 1836) first proposed the genus *Dorynota* for Neotropical cassids with a postscutellar spine. Maulik (1916) erected two new genera, *Akantaka* for species with a short postscutellar spine, thus

appearing rather gibbous than spinose and with broadly explanate elytra with straight or convex lateral sides, and *Trikona* for species with triangular scutellum, with gibbous elytra, deeply punctuate. Despite being regarded as the most important character for the identification and characterization of Dorynotini, the presence of the spine at the elytral suture has never been cladistically tested.

58. Elytra. Anterior margin: (0) convex or subconvex; (1) truncate or subtruncate.

59. Elytra. Deep excavate area posterior to elytral humerus, on disc line: (0) absent (Fig. S35); (1) present (Fig. S59).

60. Elytra. Humeral angle: (0) impunctate; (1) punctate.

61. Elytra. Internal surface: (0) same color as external surfice; (1) red (Fig. S62).

62. Elytra. Basal margin: (0) smooth (Fig. S23); (1) crenulated, inconspicuous (Fig. S15); (2) crenulated, conspicuous (Fig. S17).

Note: This is a modified version of character 139 in Chaboo (2007) — "*Elytra, basal margin: smooth = 0; crenulate = 1*". Here however, we detail the crenulation as poorly or well-marked.

63. Elytra. Basal margin: (0) not visible from dorsal view (Fig. S19); (1) visible from dorsal view (Fig. S20).

64. Elytra. Locking system at elytral suture (Fig. S61): (0) absent (Fig. S63); (1) present (Fig. S60–S62).

Note: In Dorynotini, the region with spine or tubercle presents an extension that inserts over a cavity present on the left elytra suture.

65. Elytra. Epipleural ridge tooth (Figs S65, S66). (0) absent (Fig. S64); (1) inconspicuous (Fig. S65); (2) conspicuous (Fig. S66).

Note: Monrós & Viana (1949) described this character in the diagnosis of genus *Dorynota*, as internal projection departing from the epipleura ridge— "*dentículo elitral*". In our study all Dorynotini members show this character, varying from conspicuously to poorly-conspicuous.

66. Elytra. Epipleura ridge tooth apex. (0) curved (Fig. S69); (1) truncate (Fig. S68); (2) acute (Fig. S67).

67. Elytra. Epipleura ridge tooth. (0) not elevated; (1) elevated, inconspicuous; (2) elevated, conspicuous.

68. Elytra. Internal longitudinal carina (Figs S60, S62): (0) absent; (1) present, poorly conspicuous (); (2) present, conspicuous.

69. Elytra. Epipleura brace and internal carina. (0) disonnected (Fig. S60); (1) connected (Fig. S63). [Character 156 in Chaboo (2007)].

70. Elytra. Deep depression parallel to epipleura: (0) absent; (1) present.

71. Elytra. Punctuation, wide and conspicuous: (0) absent (Fig. S2); (1) present (Fig. S3).

72. Elytra. Internal longitudinal carina. (0) parallel (Fig. S63); (1) subparallel (Fig. S62).

73. Mesepisternum. (0) flat (Fig. S71); (1) depressed (Fig. S73).

74. Metasternum. Posterior margin: (0) continuous (Fig. S71); (1) elevated (Fig. S73); (2) elevated, strongly (Fig. S74).

75. Metasternum. Posterior margin elevation: (0) flat laterally (Fig. S73); (1) flat under (Fig S75)

76. Metasternum. Median suture: (0) incomplete (Fig. S75); (1) complete (Fig. S74).

77. Metepisternum. Anterior margin followed by parallel depression: (0) absent; (1) present.

78. Metaleg. Metatibia, curved. (0) absent (Fig. S76); (1) present (Fig. S77).

79. Metendosternite. Shape of anterior lamina: (0) convex (Fig. S78); (1) sinuous (Fig. S79); (2) straight. (Fig. S80).

Legs

80. Pretarsal claws. (0) appendiculate; (1) simple, pectinate; (2) simple, smooth.

Note: This character is a modified version of character 12 in Borowiec (1995) that is recognized as trichotomous, with three states, simple, appendiculate and pectinate. Simple claws are defined as not showing basal tooth, appendiculate claws showing a basal tooth and pectinate claws showing serrate internal edge. Here we recognize the character dichotomous, appendiculate or simple, with the state "simple" characterized as pectinate or smooth. Dorynotini is characterized by showing simple claws (Monrós & Viana, 1949; Borowiec, 1995; Simões, 2014).

81. Claws. Tarsal formula: (0) 1-1-1; (1) 2-2-2.

Note: Monrós & Viana (1949) included *Heteronychocassis acuticollis* in the Dorynotini tribe diagnosed as showing two not divergent and asymmetrical claws in each leg. Hincks (1952) expanded Dorynotini diagnosis, to include species presenting one of the claws occasionally missing. Simões & Sekerka, (2014) redescribed the species *H. acuticollis* and pointed out that Monrós & Viana (1949) placed the monotypic species in the tribe despite not analyzing its type-specimen. Moreover, they add that most of its diagnostic features are shared with its sister tribe, Cassidini. This character was not excluded from

the analysis as its information was considered potentially useful in future studies, possibly supporting small groupings of taxa.

82. Pretarsal claws. Angle formed at the base of claws (only applicable when two claws are present): (0) obtuse (close to 180); (1) straight (close to 90) (Fig. S81); (2) acute (Fig. 82); (3) subparallel, no angle near base (Fig. S83).

Note: Borowiec (1995) used this character in the cladistics analysis of Cassidinae (character 13), with dichotomous states, diverging or approximated. Here we employ a modified version, recognizing four states: opposite, between 90˚ and 150˚ (Shin 2013); divergent, up to 90˚; subparallel, less than 45˚; and parallel. Monrós & Viana (1949) diagnosed the tribe Dorynotini for presenting parallel or slightly divergent claws. In our study, Dorynotini is recognized as presenting a broader diversity of angle formed at the base of the claws, obtuse, straight, acute and, not forming angle, subparallel.

83. Pretarsal claws. Symmetry: (0) symmetric (Fig. S81); (1) asymmetric, slightly (Fig. S83); (2) asymmetric, distinctly (Fig. S82).

Note: Monrós and Viana (1949) diagnoses *Paranota* as "markedly distinguished by the asymmetrical tarsal claws, with the internal claw distinctly shorter than the external one".

84. Pretarsal claws. Base exposed in dorsal view: (0) absent; (1) present.

<u>Hindwings</u>

85. Hindwing, Pcu-Cu1b: (0) absent (fused) (Fig. S87); (1) vestigial (Fig. S84); (2) well-developed (Fig. S86).

Note: This is a modified version of character 157 in Chaboo (2007), that scores 1Cuc (=CuA cell 1, Chaboo, 2007) as closed or open. In our study we observed that the cross vein (=cv1, Suzuki, 1994) connecting Pcu and Cu1b, might be absent (=fused), vestigial, or well-developed. This information was not checked in some rare species of Dorynotini for which only the type specimens were available.

86. Hindwing, setae at the base of Cu1b: (0) absent (Fig. S84); (1) present (Fig. S85).

Note: This is a unique character, only observed in some species within Dorynotini.

87. Hindwing, 2Cuc closed: (0) open, conspicuous (Fig. S87); (1) closed, vestigial vein (Fig. S86); (2) closed, well-marked vein (Fig. S88).

Note: This is a modified version of character 158 in Chaboo (2007), that scores 2Cuc (=CuA cell 2, Chaboo, 2007) as closed or open. In our study, we add that the second cubital cell might be closed and vestigial, with a faint mark of vein or well-marked.

88. Hindwing, Cu1a-Cu1b: (0) absent (Fig. S86); (1) present (Fig. S87).

Note: The cross vein connecting Cu1a and Cu1b is absent in all outgroups studied here. Within Dorynotini, the Greater Antilles clade is the only one that presents it.

89. Hindwing, vestigial, M3+4-Cu1a: (0) absent (Fig. S84); (1) present (Fig. S88).

Figure captions of plates showing morphological characters.

Figures. S1–S3. Dorsal habitus. S1, *Physonota gigantea* Boheman; S2, *Dorynota* (*s. str*.) *bidens* (Fabricius); S3, *Omoteina humeralis* (Olivier); S4–S6, dorsal view of head. S4, *Dorynota* (*s. str*.) *monoceros*; S5, *Stolas modica* (Boheman); S6, *Dorynota* (*s. str*.) *aculeata* (Boheman); S7–S9, frontal view of head. S7, *Paranota spinosa* (Boheman); S8, *Mesomphalia variolaris* Boheman; S9, *Omoteina humeralis* (Olivier); S10–S12, antenna. S10, *Metriona elatior* (Klug); S11, *Paranota spinosa* (Boheman); S12, *Stolas modica* (Boheman); S13–14, antennomeres X–XI. S13, *Coptocycla* (*Podostraba*) *arcuata* (Swederus); S14, *Dorynota* (*s. str*.) *parallela* Blanchard (*Cl*, clypeus; *Frs*: frons; *Hr*: humeral ridge).

Figures. S15–S24. Pronotum. S15, *Physonota gigantea* Boheman; S16, *Dorynota* (*s. str*.) *parallela* Blanchard; S17, *Paratrikona rubescens* Blake; S18, *Eremionycha bahiana* (Boheman); S19, *Stolas modica* (Boheman); S20, *Dorynota* (*s. str*.) *bidens* (Fabricius); S21, *Mesomphalia variolaris* Boheman; S22, *Omoteina humeralis* (Olivier); S23, *Coptocycla* (*Podostraba*) *arcuata* (Swederus); S24, *Dorynota* (*Akantaka*) *collucens* (Spaeth).

Figures. S25–S33. Prosternum. S25–S27, Prosternal process. S25, *Physonota gigantea* Boheman; S26, *Dorynota* (*s. str*.) *aculeata* (Boheman), S27, *Mesomphalia variolaris* Boheman; S28, *Coptocycla* (*Podostraba*) *arcuata* (Swederus); S29, *Dorynota* (*s. str*.) *bidens* (Fabricius); S30–S31, *Dorynota* (*s. str*.) *parallela* Blanchard; S32, *Paranota spinosa* (Boheman); S33, *Omoteina humeralis* (Olivier) (*AnC*: antennal calli; *TgS*: tergosternal suture; *Tgd*: tergosternal depression).

Figures. S34–S35. Lateral habitus. S34, *Paratrikona rubescens* Blake; S35, *Dorynota* (*Akantaka*) *collucens* (Spaeth); S36–S43, prosternum. S36, *Eremionycha bahiana* (Boheman); S37, *Dorynota* (*s. str.*) *pugionata* (Boheman); S38, *Eremionycha bahiana* (Boheman); S39, *Stolas modica* (Boheman); S40, *Paranota spinosa* (Boheman);S41, *Dorynota* (*s. str*) *parallela* Blanchard; S42, *Dorynota* (*s. str.*) *bidens* (Fabricius); S43, *Coptocycla* (*Podostraba*) *arcuata* (Swederus); S44–S46, Proleg. 44, *Dorynota* (*s. str.*) *aculeata* (Boheman), arrow indicates protibial spur; S45, *Dorynota* (*s. str.*) *bidens* (Fabricius), arrow indicates excavated internal margin of protibia; S46, *Dorynota* (*s. str.*) *pugionata* (Germar) (arrow indicates protibia with projected anterior margin).

Figures. S47–S49. Proendosternite, posterior view. S47, *Stolas modica* (Boheman); S48, *Omoteina humeralis* (Olivier), S49, *Omoteina humeralis* (Olivier); S50, *Paratrikona rubescens* Blake, dotted lines delineate membranous lobes; S50–S52, mesoscutellum. S50, *Eurypepla calachroma* (Blake); S51, *O. humeralis*; S52, *Dorynota* (*s. str.*) *parallela* Blanchard; S53–S54, dorsal view, showing scutellum. S53, *Dorynota* (*s. str.*) *bidens* (Fabricius); S54, *Dorynota* (*s. str.*) *parallela*; S55, *Dorynota* (*Akantaka*) *truncata* (Fabricius), arrow indicates pocket on the anterior margin of the elytra.

Figures. S56–S58. Postscutellar projection frontal view. S56, *Dorynota* (*Akantaka*) *collucens* (Spaeth); S57, *Paratrikona rubescens* Blake; S58, *Dorynota* (*s. str.*) *bidens* (Fabricius); S59, *Dorynota* (*s. str.*) *aculeata* (Boheman), arrow indicates depression posterior to humeral angle; S60–S63, elytra. S60, *Dorynota* (*s. str.*) *parallela* Blanchard; S61a–b, locking mechanism. 61a,

right elytra, dotted lines delimiting area of insertion; 61b, left elytra, dotted line delimiting projection area; S62, *moteina humeralis* (Olivier); S63, *Mesomphalia variolaris* Boheman; S64, *Physonota gigantea* Boheman; S65, *Omoteina humeralis* (Olivier); S66, *Dorynota* (*s. str*) *parallela* Blanchard (*br*: brace; *Ept*: epipleural tooth; *lc*: longitudinal carina).

Figures. S67–S70. Metepisternum. S67, *Paranota spinosa*; S68, *Dorynota* (*Akantaka*) *funesta* (Boheman); S69, *Dorynota* (*s. str.*) *bidens* (Fabricius); S70, *Eremionycha bahiana* (Boheman); S71–S73, metepisternum (arrow indicates projection of posterior margin). S71, *Stolas modica* (Boheman); S72, *Dorynota* (*s. str.*) *aculeata* (Boheman); S73, *Dorynota* (*s. str*.) *parallela* Blanchard; S74–S75, metasternum (dotted line indicates median suture). S74, *Dorynota* (*s. str*.) *aculeata* (Boheman); S75, *Omoteina humeralis* (Olivier); S76–77, metaleg. S76, *Dorynota* (*s. str*.) *aculeata* (Boheman); S77, *Dorynota* (*s. str.*) *parallela* Blanchard.

Figures. S78–S80. Metendosternite, posterior view. S78, *Paratrikona rubescens* Blake; S79, *Dorynota* (*s. str.*) *aculeata* (Boheman); S80, *Omoteina humeralis* (Olivier); S81–S83, pretarsal claws. S81, *Omoteiona humeralis*; S82, *Dorynota* (*s. str.*) *aculeata*; S83, *Dorynota* (*s. str*.) *parallela* Blanchard; S84–S88, hindwings. S84, *Dorynota* (*s. str*.) *pugionata* (Germar); S85, *Paranota rugosa* (Wagener); S86, *Physonota gigantea* Boheman; S87, Eurypepla calachroma (Blake); S88, *Dorynota* (*s. str.*) *aculeata* (Boheman). (*1Cuc*: first Cubital cell; *2Cuc*: second Cubital cell; *anla*: anterior lamina; *Ap*: Apertum cell; *C*: Costal; *Cu1b*: second subbranch of *Cu1*; M: Media; *Pcu*: Postcubital; *Sc*: Subcosta; *R*: Radius; *r*: small crossvein; *Rc*: Radial cell; *Rs*: Radial sector).


1
2
Hr
3
4
5
6
7
Frs
Cl
8
9
10
11
12
13
14


15


16


17


18


19

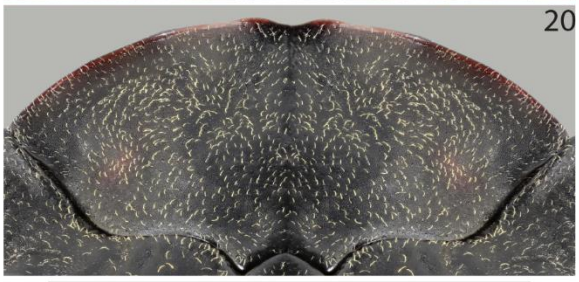
20


21


22


23


24


25
26
PrC
27
28
29
AnC
TgS
30
Tgd
31
32
33


34
35
36
37
38
39
40
41
42
43
44
45
46


47

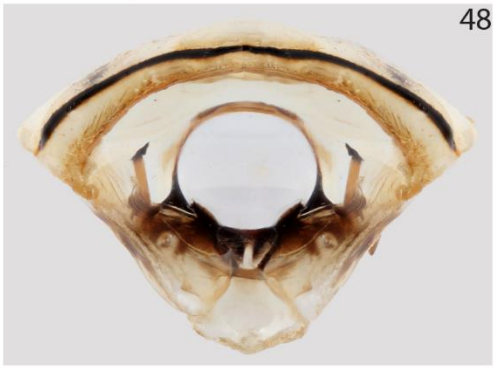
48

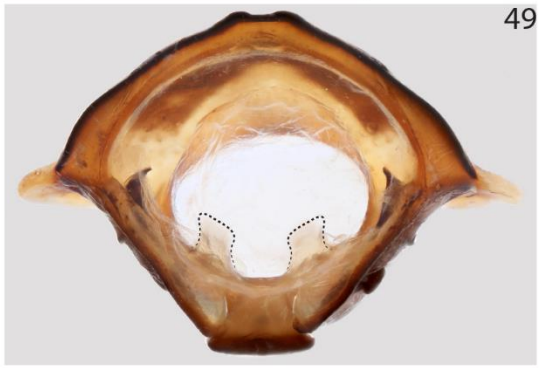
49


50

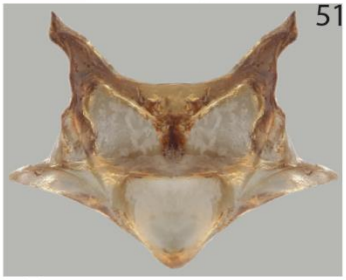
51


52


53


54


55

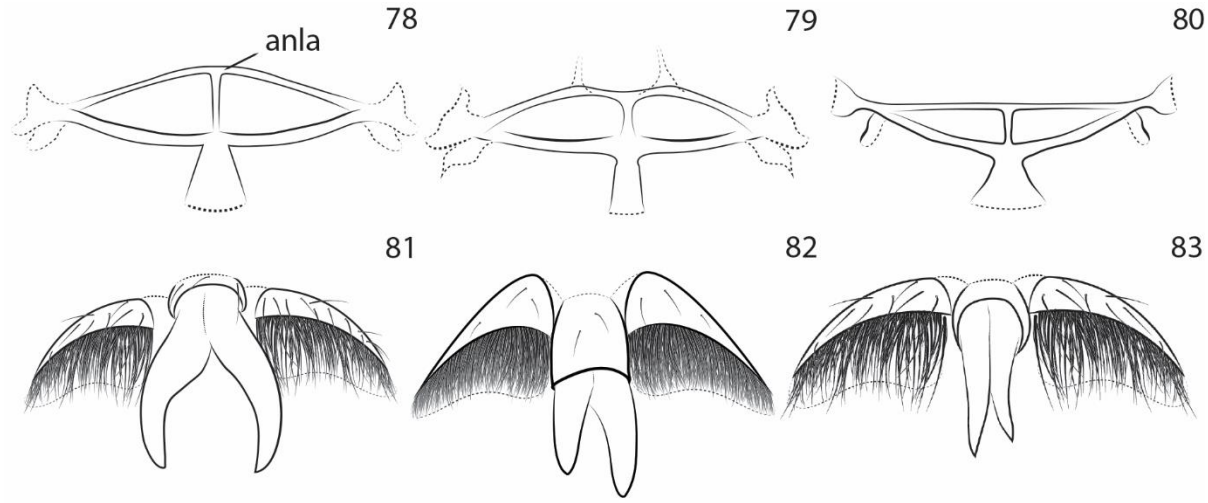
78
anla
79
80
81
82
83

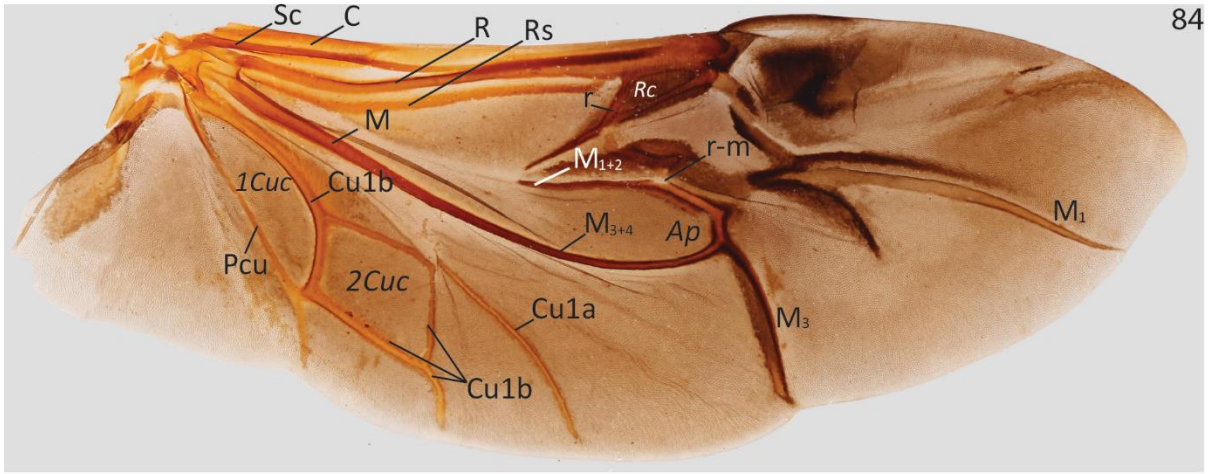
84
Sc
C
R
Rs
r
Rc
M
M1+2
r-m
1Cuc
Cu1b
M3+4
Ap
M1
Pcu
2Cuc
Cu1a
M3
Cu1b

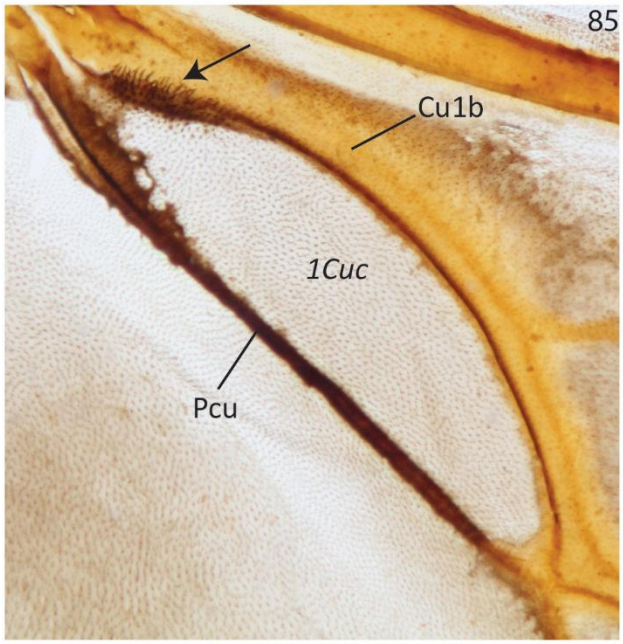
85
Cu1b
1Cuc
Pcu

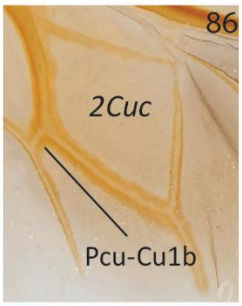
86
2Cuc
Pcu-Cu1b

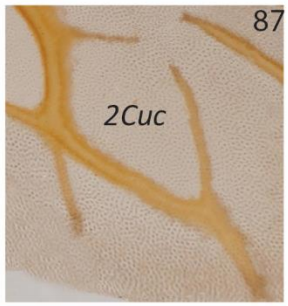
87
2Cuc

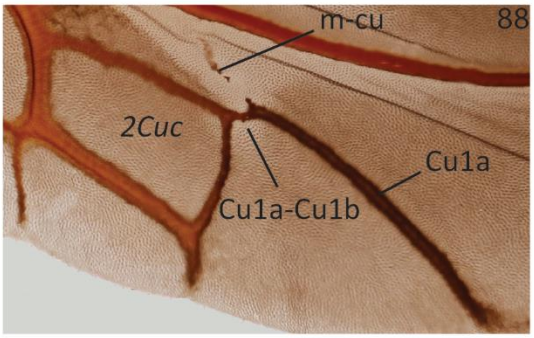
m-cu
88
2Cuc
Cu1a
Cu1a-Cu1b

Appendix V

Appendix S2. Phylogenetic results (Chapter 5).

Figure S89. Maximum likelihood tree (28S). Tribe Dorynotini with orange branches.

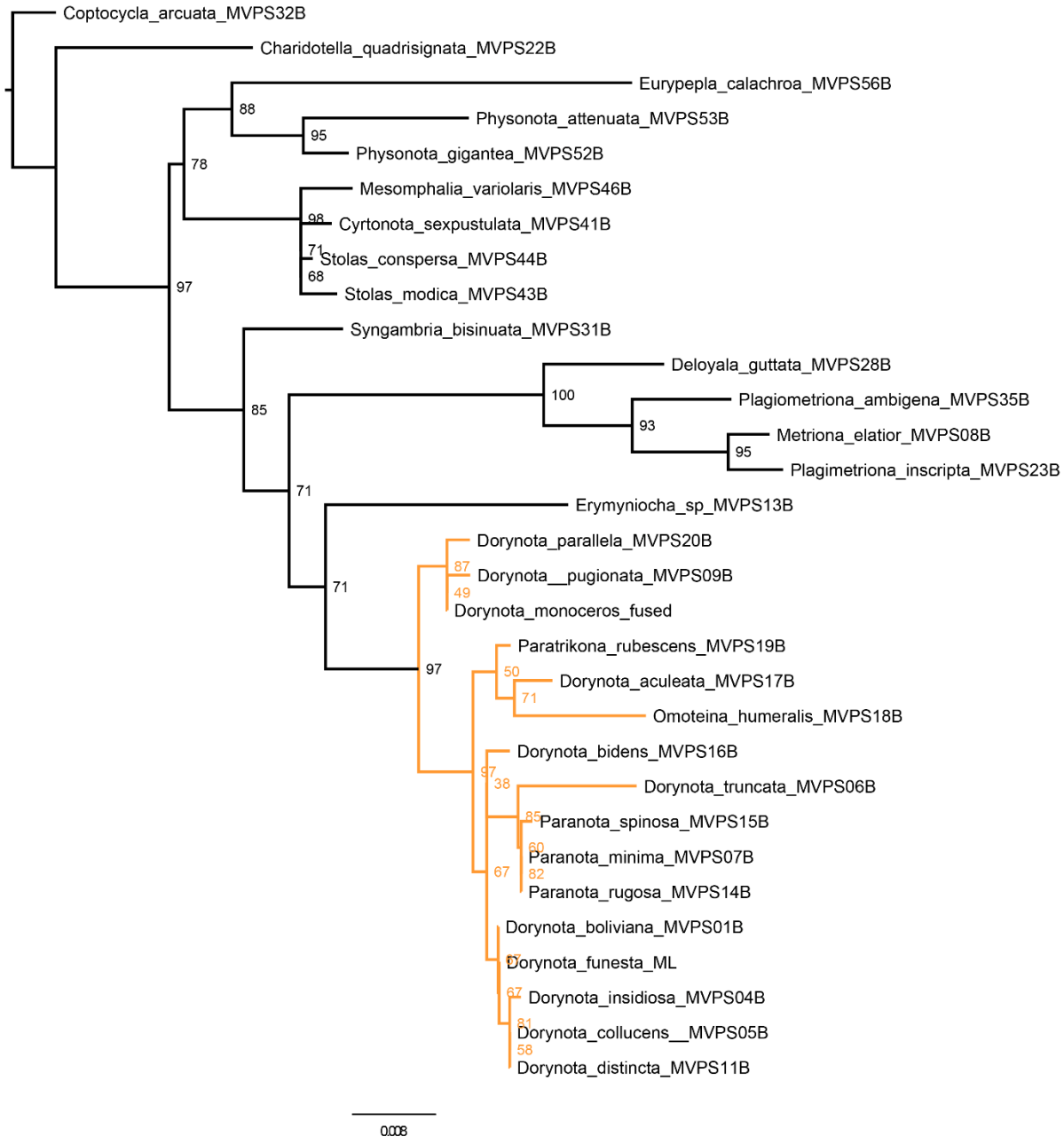

Figure S91. Maximum likelihood tree (CO1). Tribe Dorynotini with orange branches.

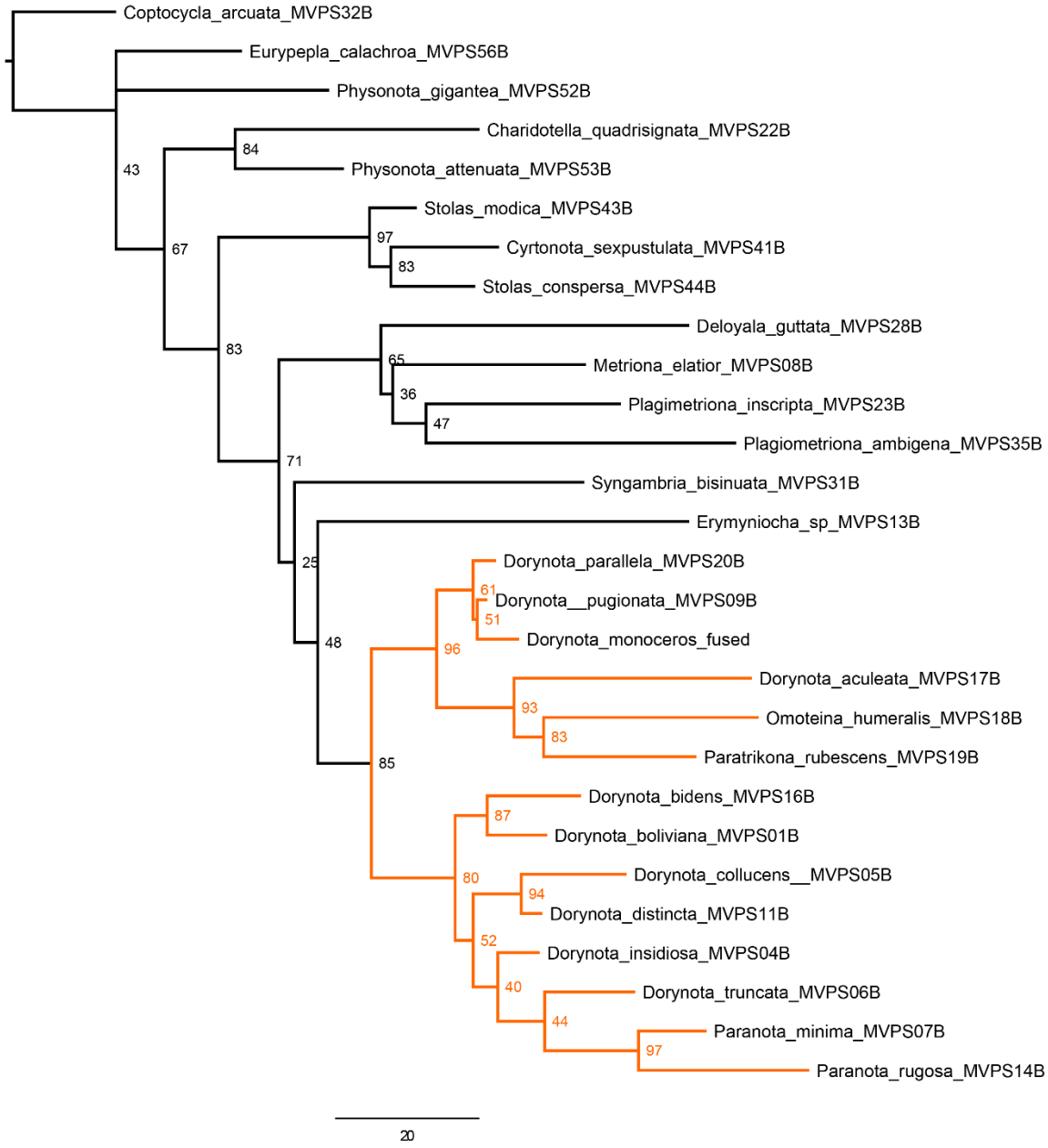

Figure S92. Bayesian analysis tree (28S). Tribe Dorynotini with orange branches.

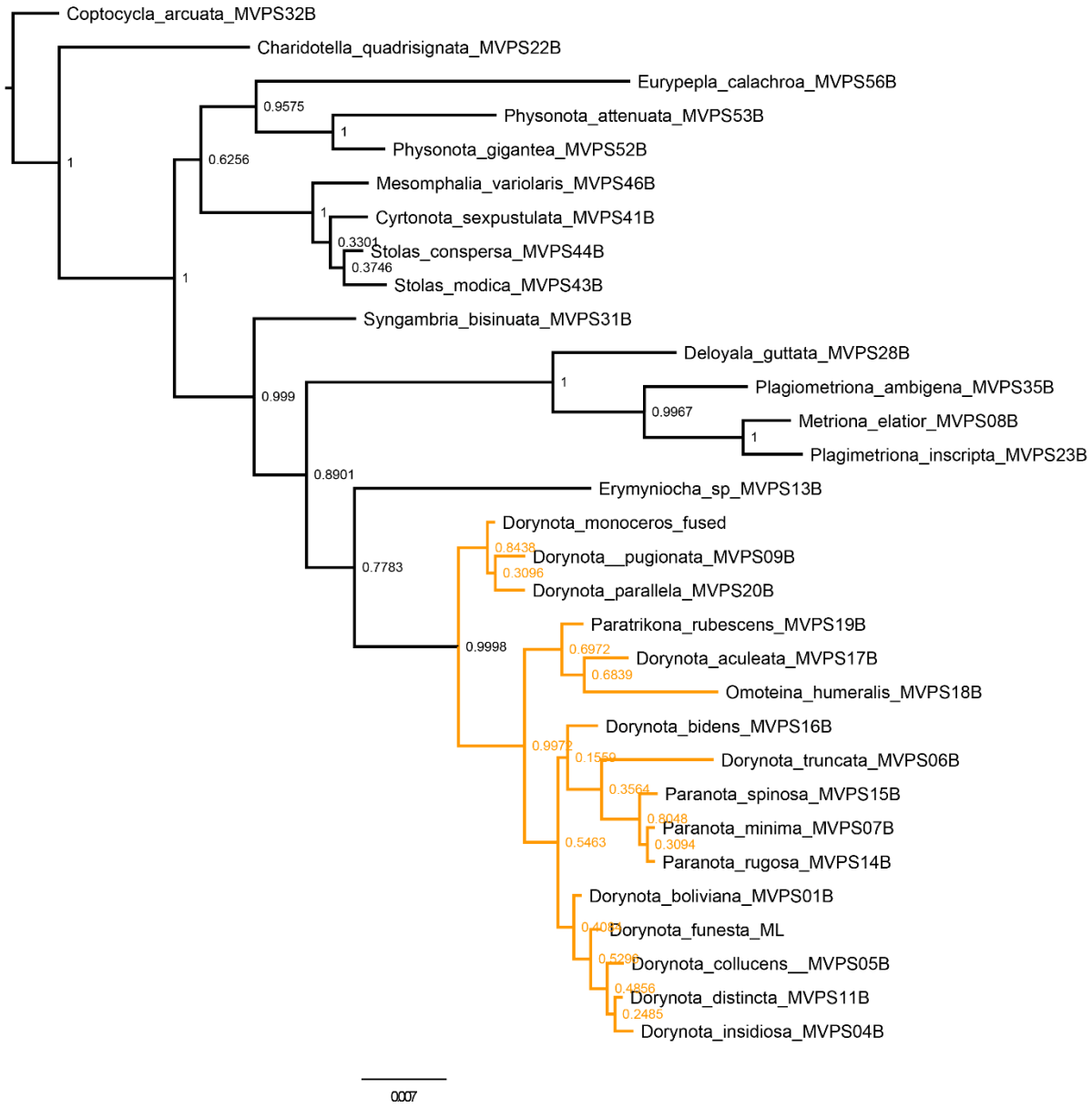

Figure S93. Bayesian analysis tree (CAD). Tribe Dorynotini with orange branches.

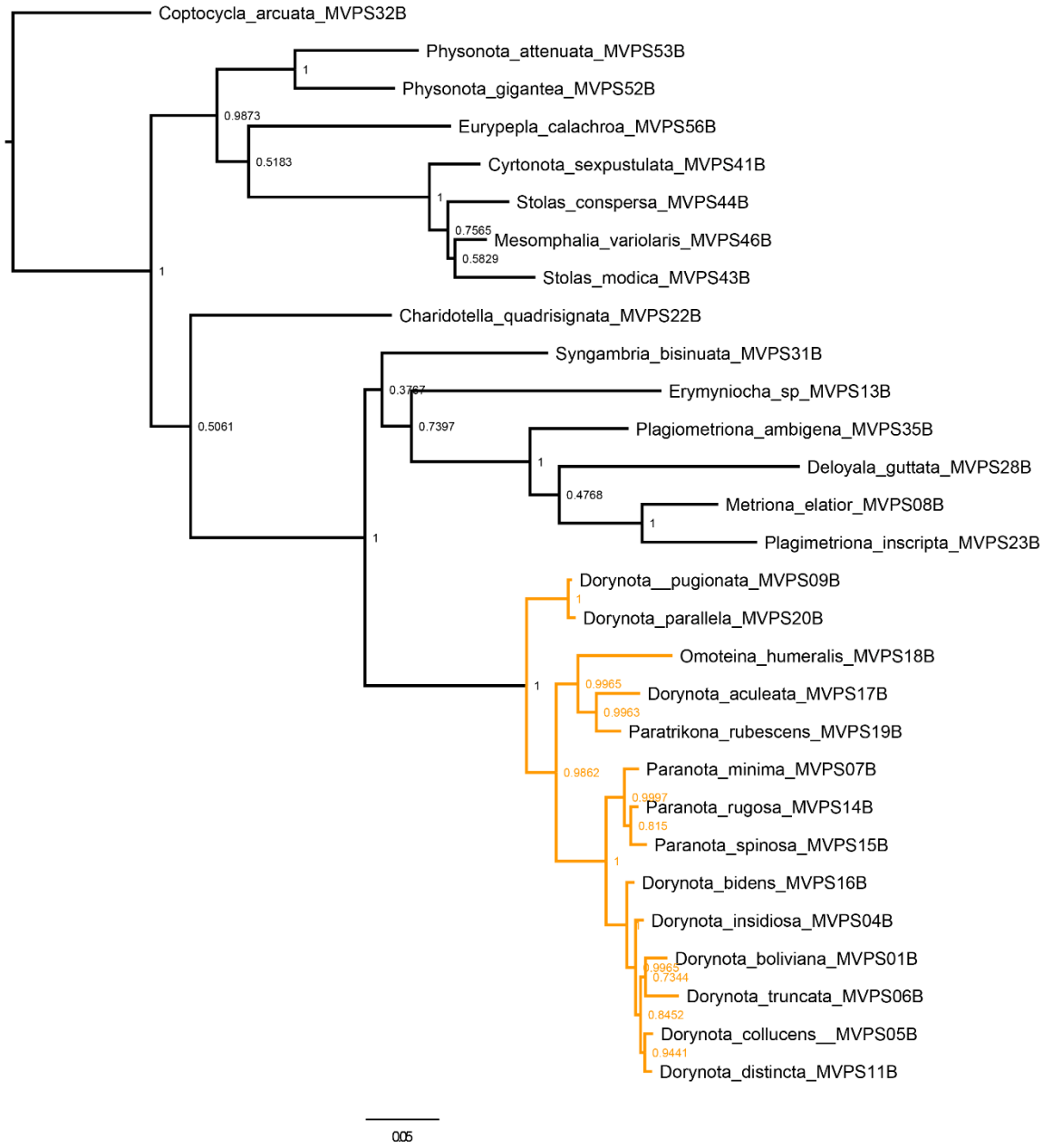

Figure S94. Bayesian analysis tree (CO1). Tribe Dorynotini with orange branches.

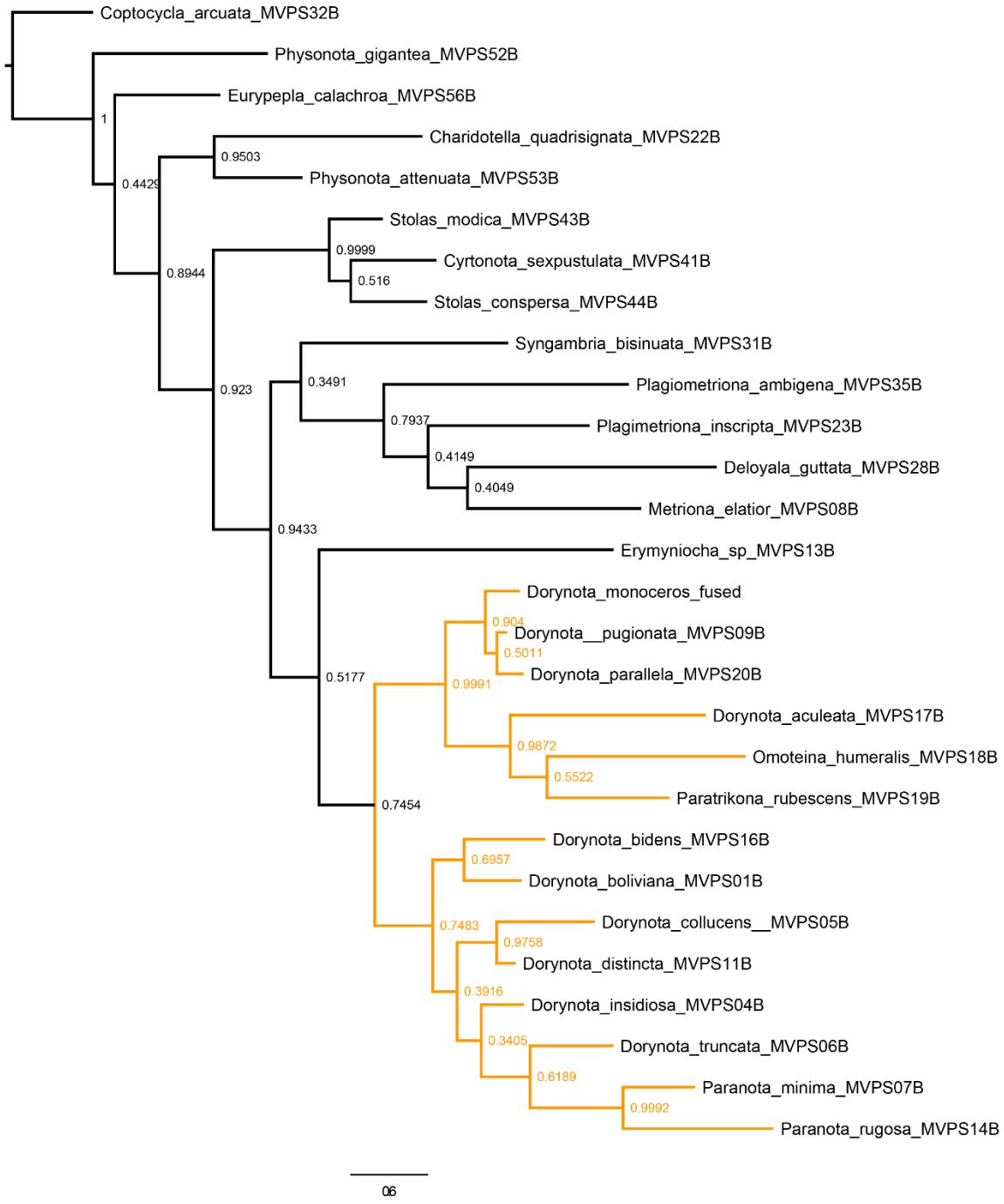

Figure S95. Maximum parsimony tree based on morphological data. Bootstrap and Bremer support on nodes.

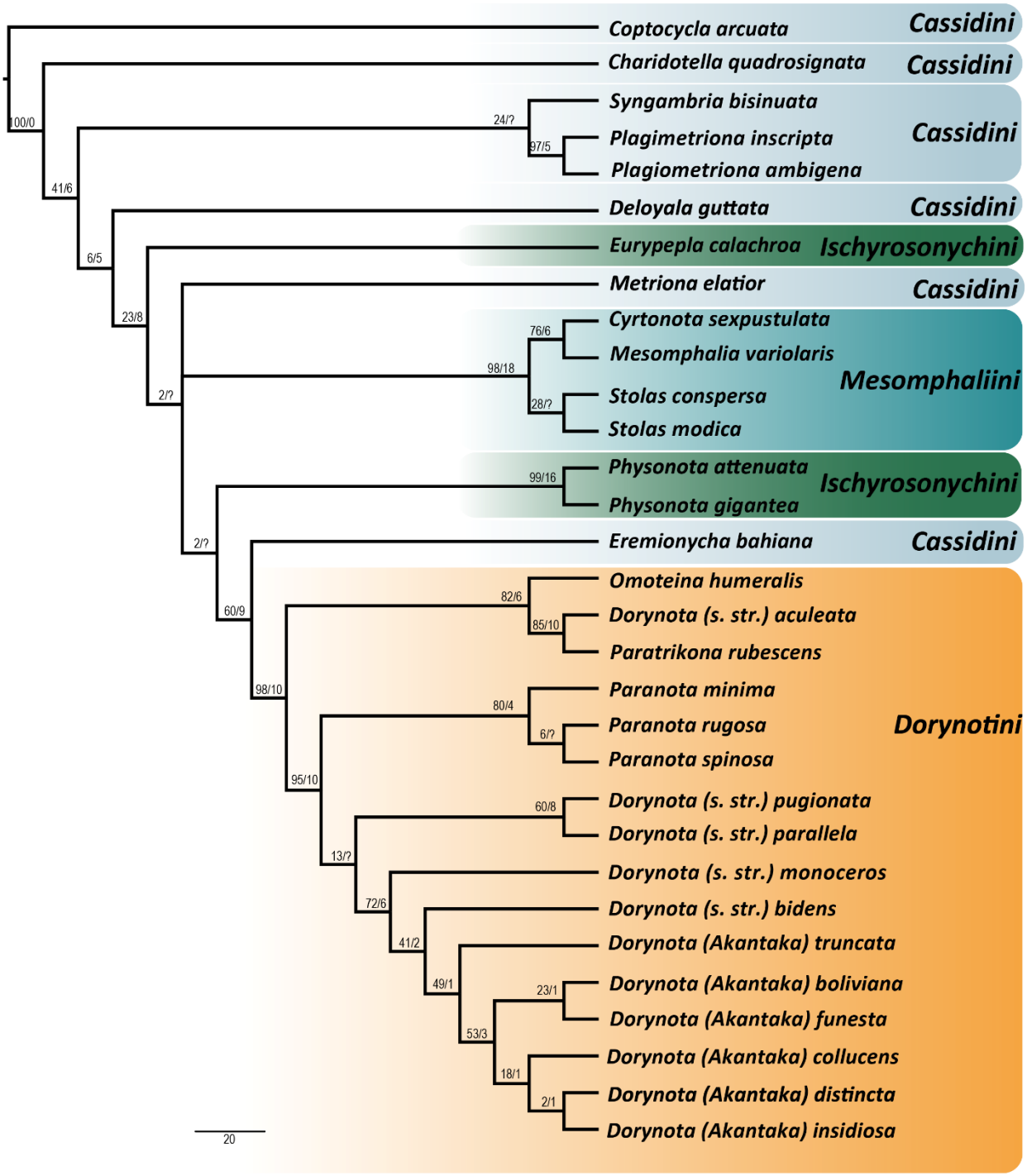

Figure S96. Total evidence tree, resulted from Bayesian analysis with morphological and molecular dataset.

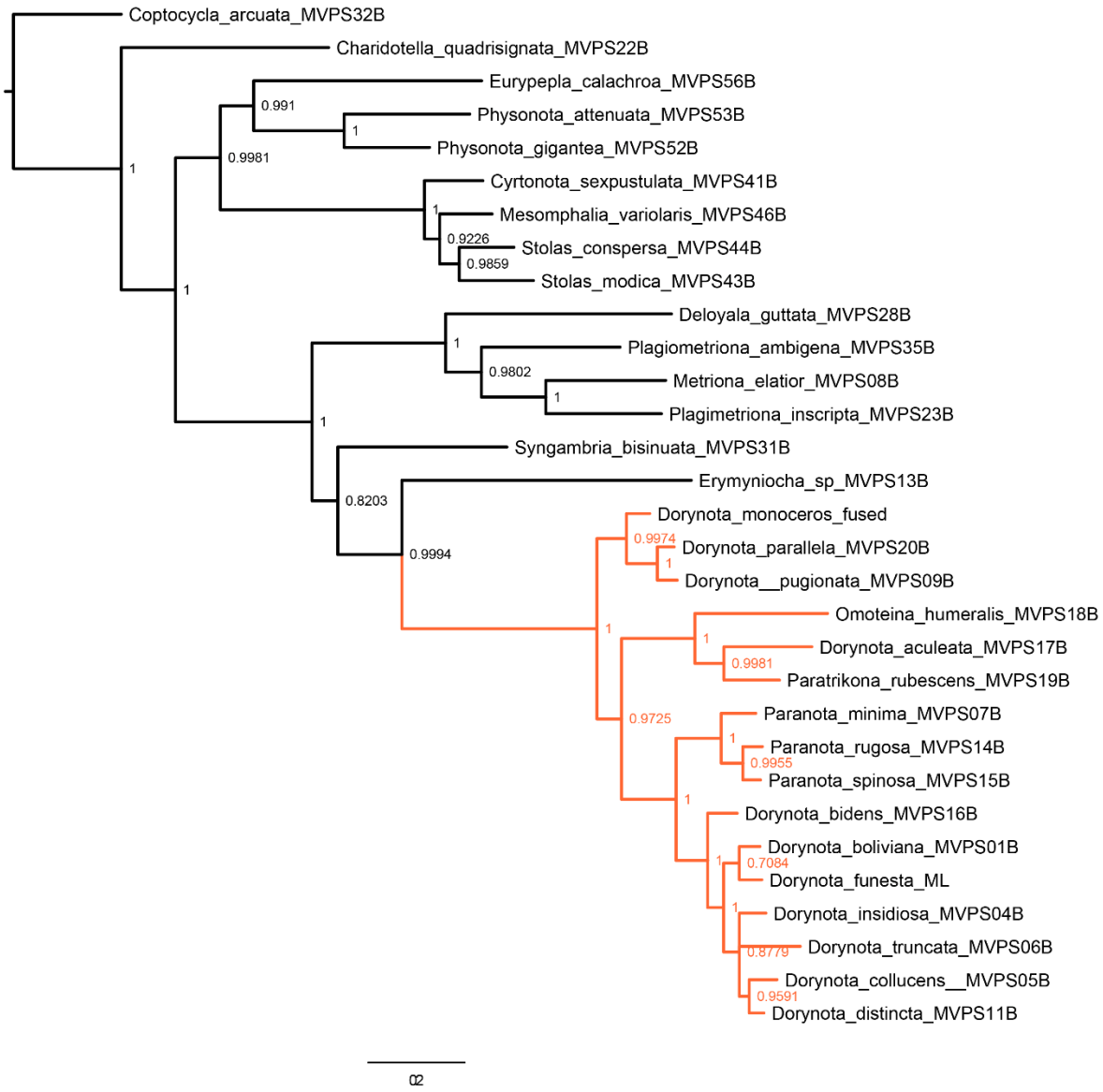

Appendix VI

Appendix S3. Ancestral character state reconstruction. Branch color indicating evolution of states along the tree based on maximum parsimony.

Figure S97. Ancestral state reconstruction of pronotum punctuation (character 18).

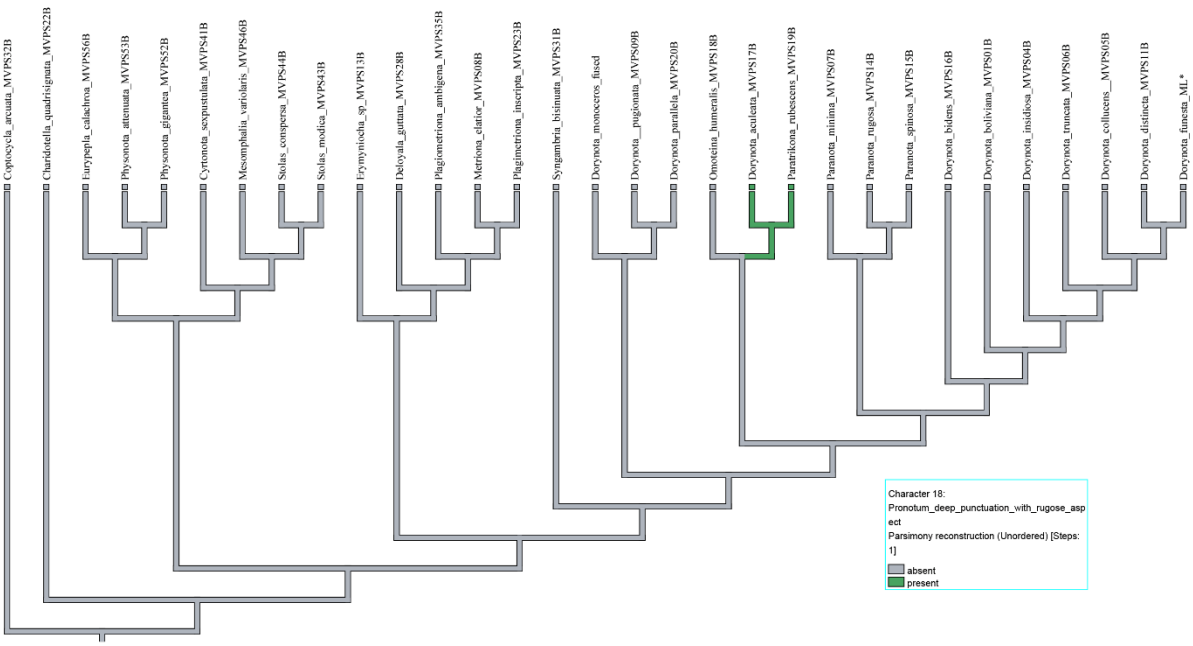

Figure S98. Ancestral state reconstruction of posterior angle of pronotum (character 25).

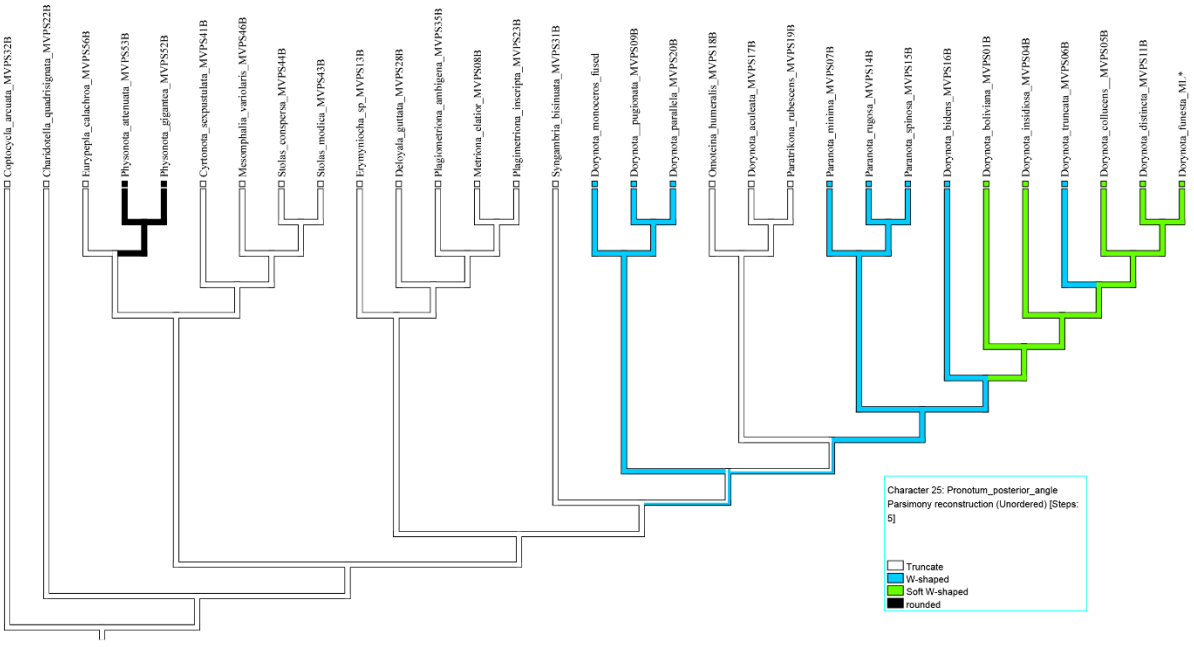

Figure S99. Ancestral state reconstruction of antenal calli (character 28).

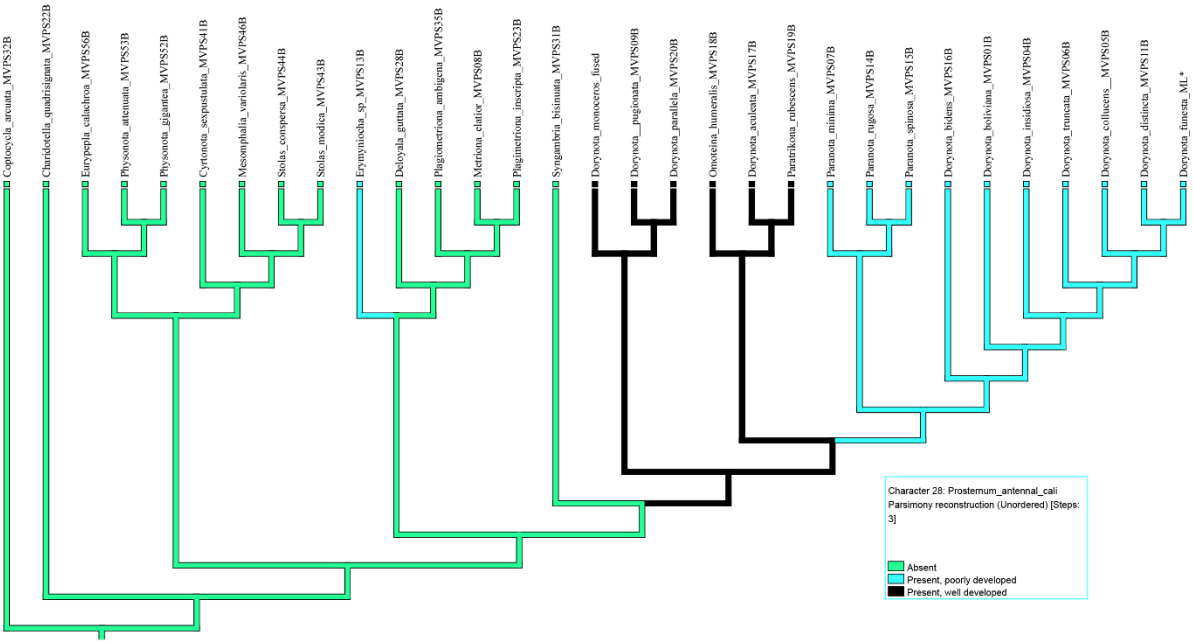

Figure S100. Ancestral state reconstruction of hypomeron depression (character 36).

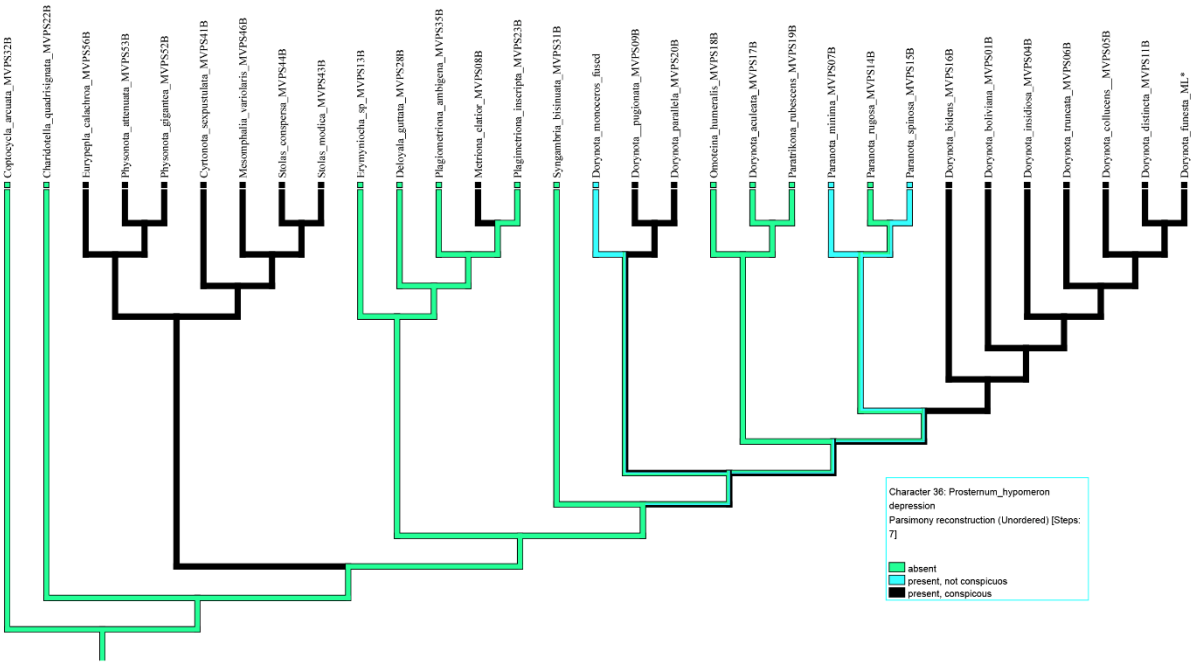

Figure S101. Ancestral state reconstruction of protibia apex depression (character 40).

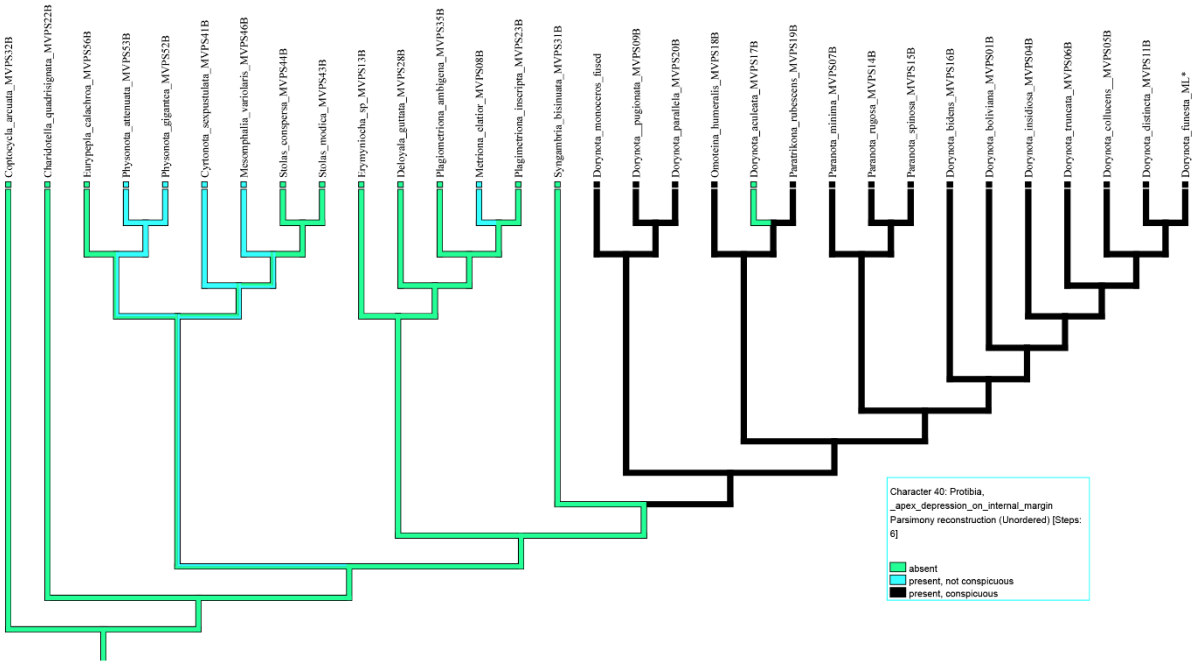

Figure S102. Ancestral state reconstruction of transversal ridges on mesoscutellum (character 44).

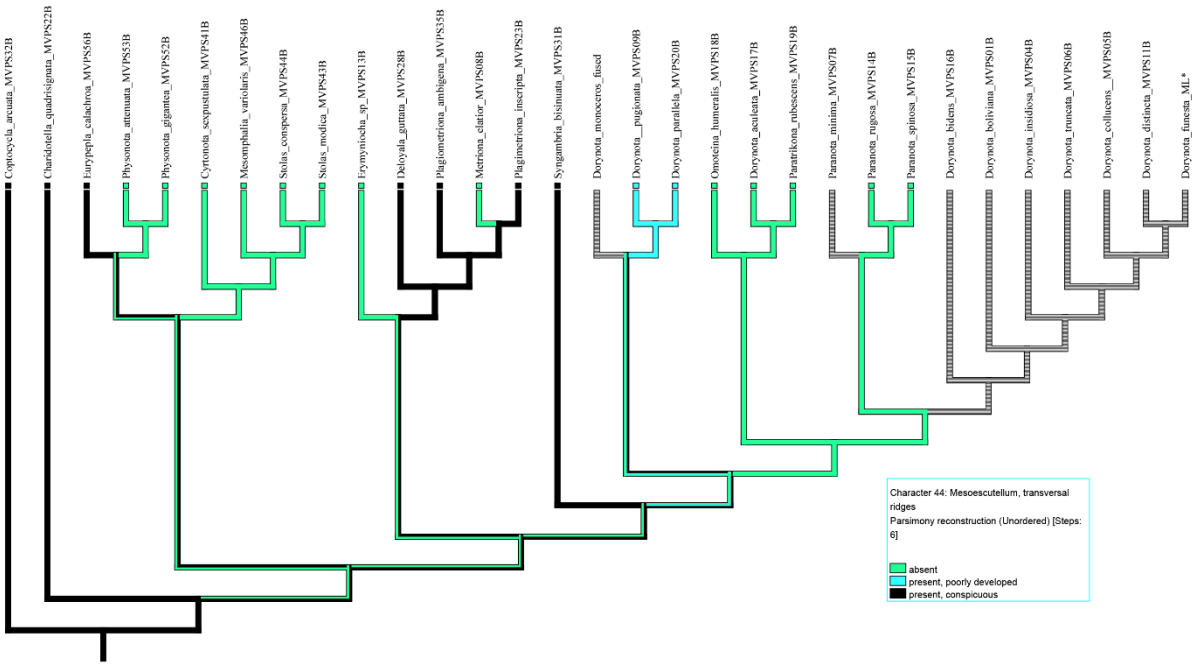

Figure S103. Ancestral state reconstruction of scutellum shape (character 46).

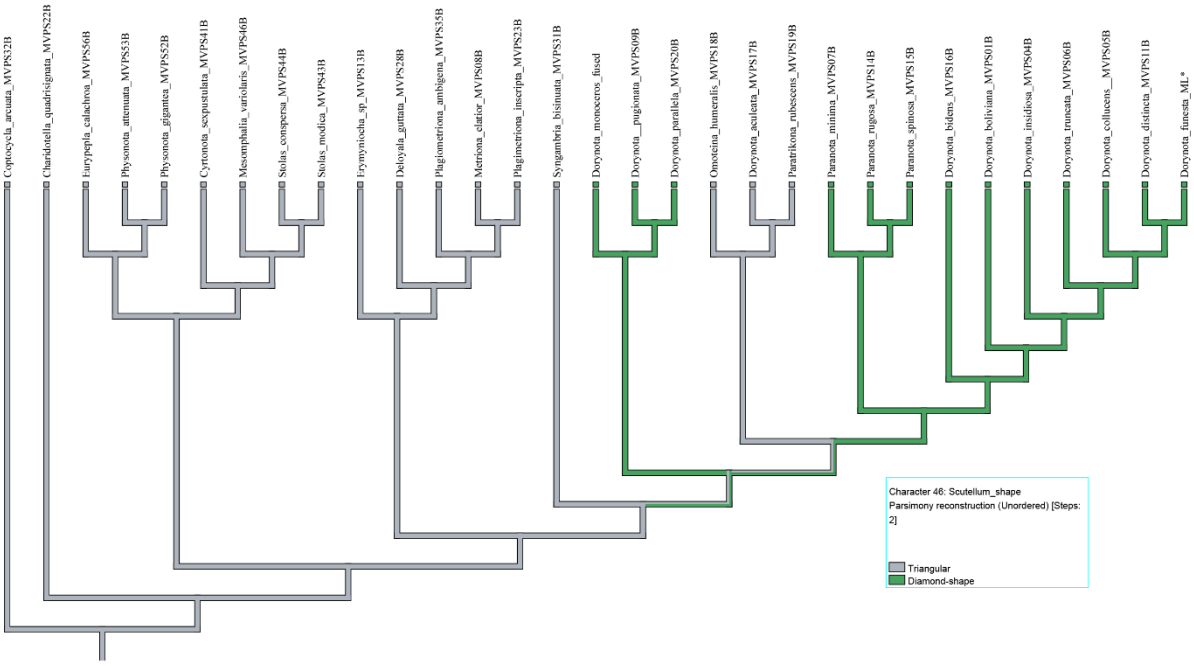

Figure S104. Ancestral state reconstruction of insertion pocket on lateral of elytral anterior margin (character 49).

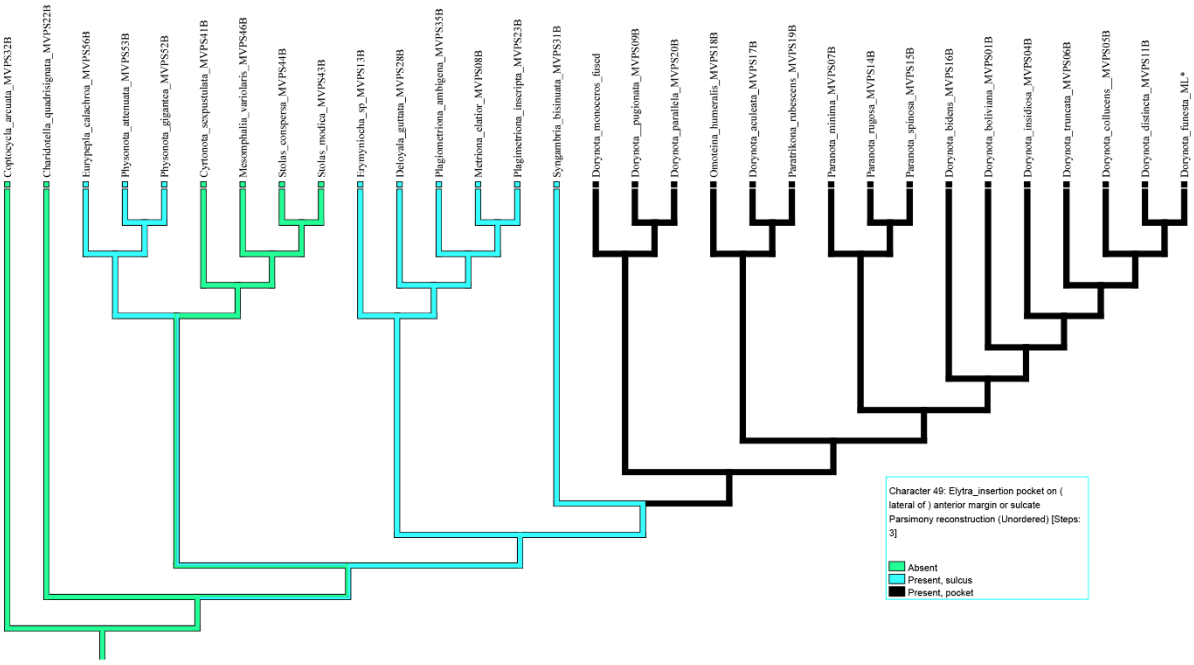

Figure S105. Ancestral state reconstruction of humeral ridge (character 50).

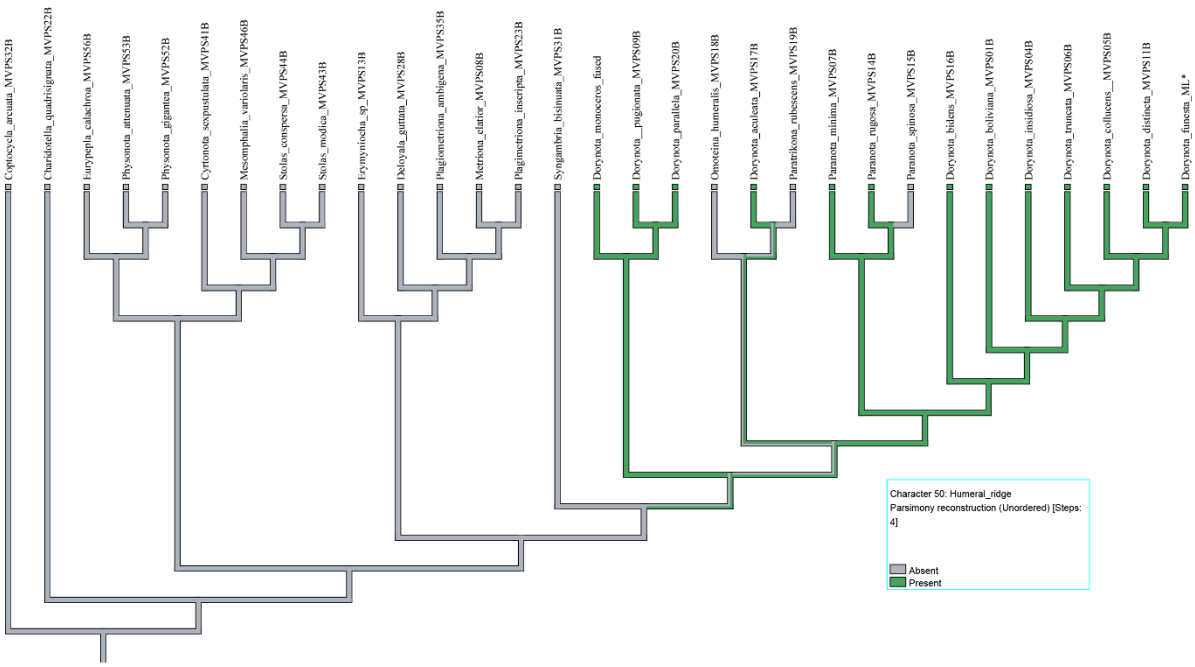

Figure S106. Ancestral state reconstruction of elytral lateral of margins shape (character 53).

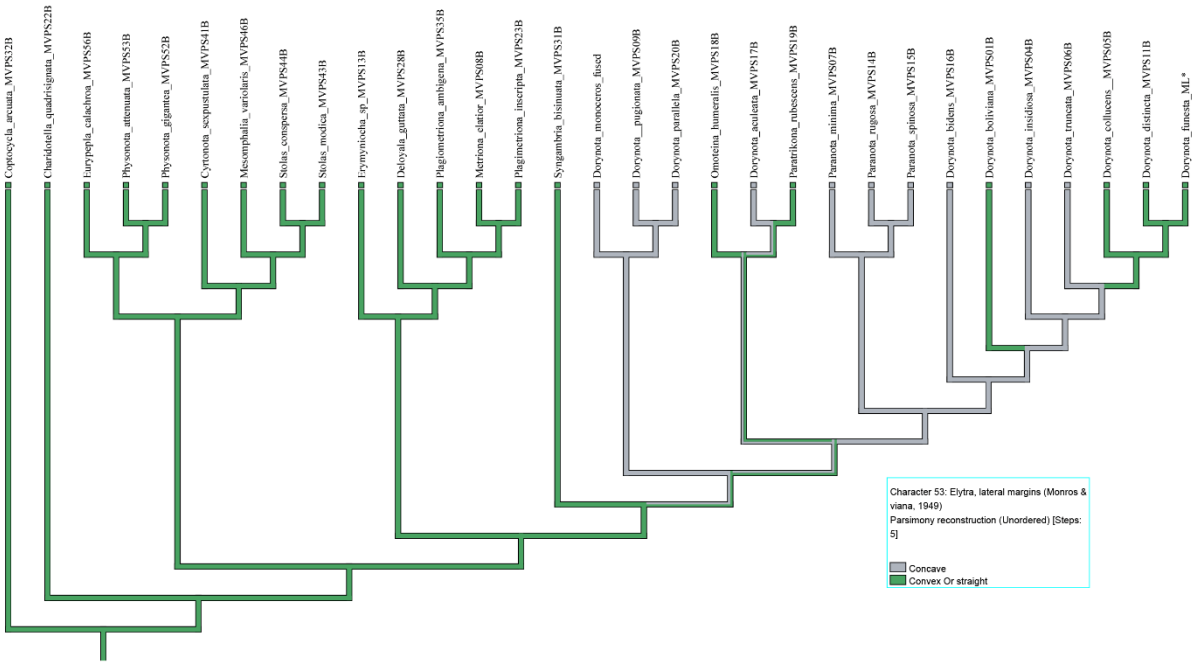

Figure S107. Ancestral state reconstruction of elytral dorsum (character 56).

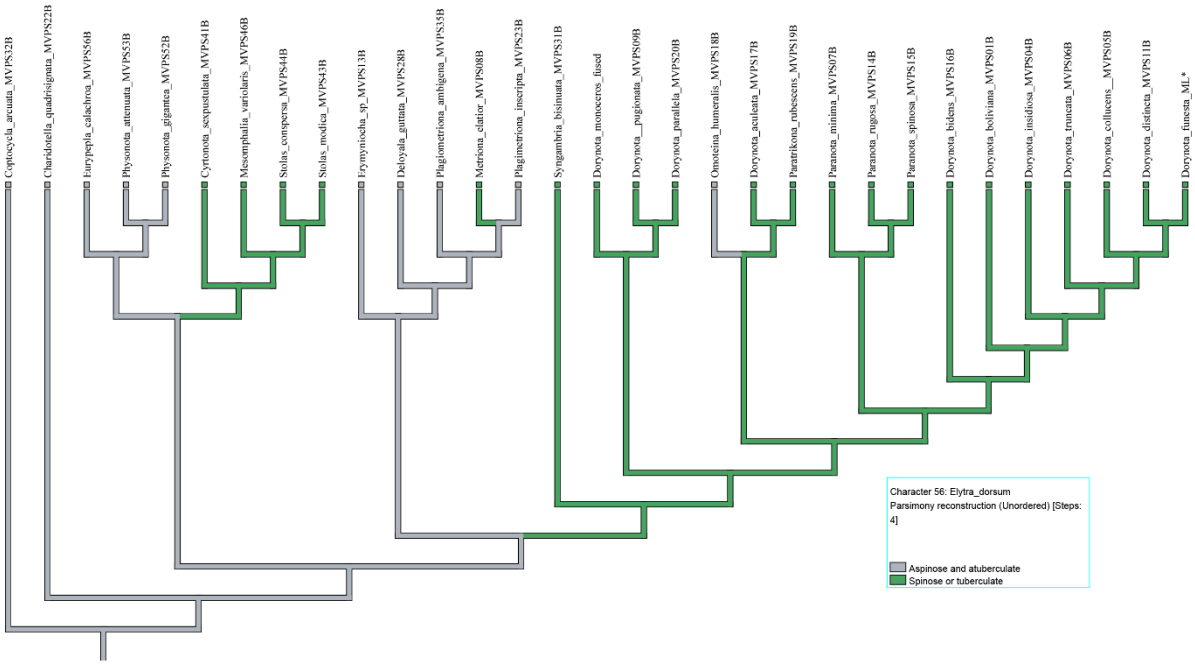

Figure S108. Ancestral state reconstruction of elytral post-scutellar projection shape (character 57).

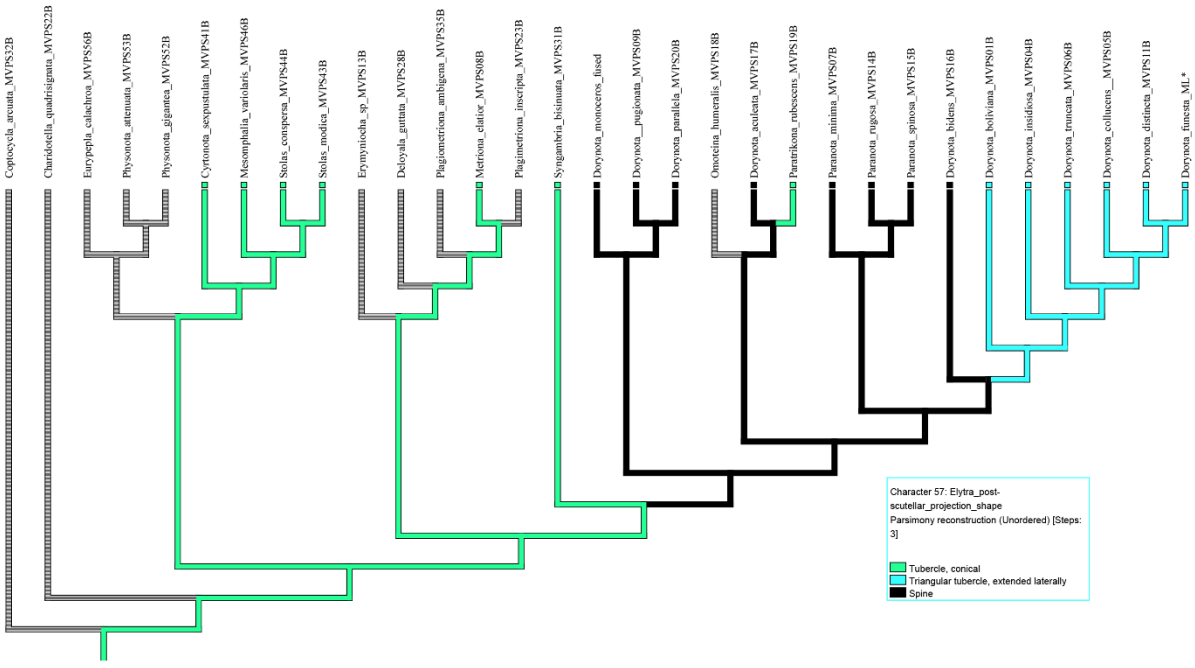

Figure S109. Ancestral state reconstruction of elytral suture locking system (character 64).

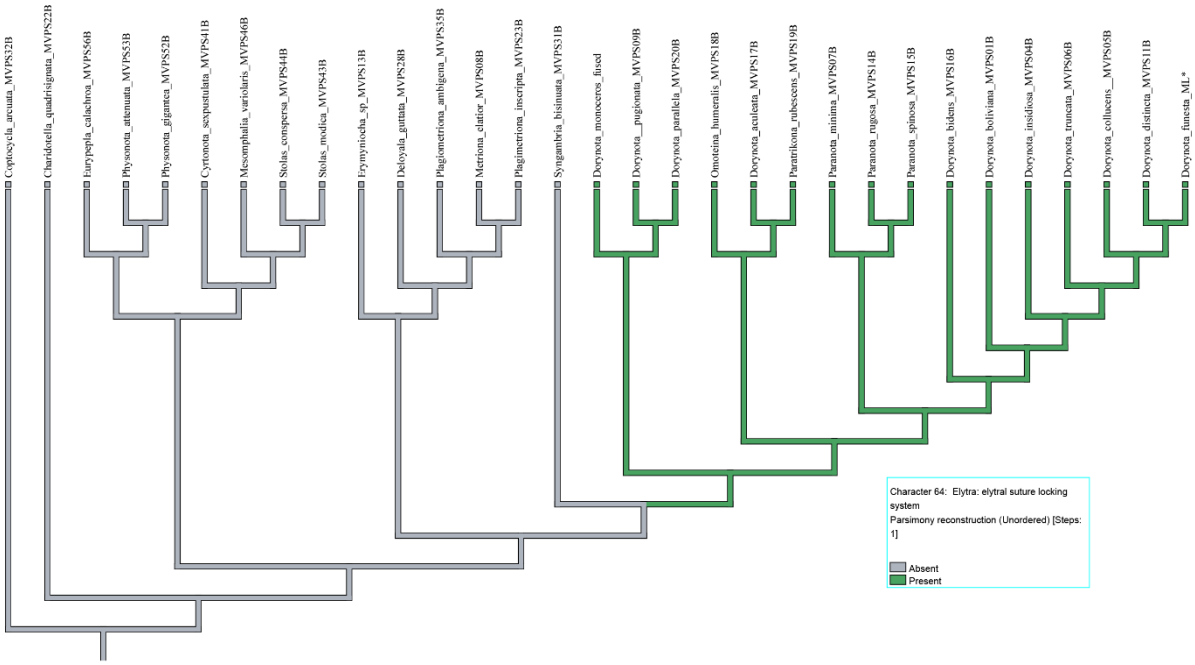

Figure S110. Ancestral state reconstruction of epipleural tooth shape (character 65).

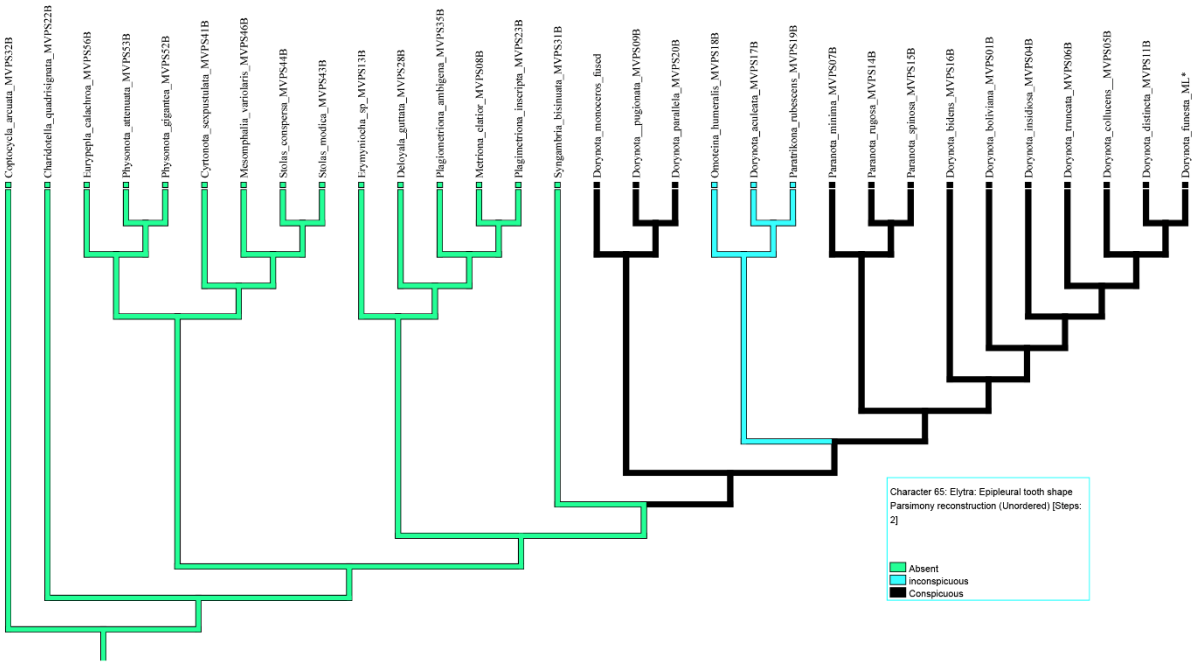

Figure S111. Ancestral state reconstruction of epipleural tooth elevation (character 67).

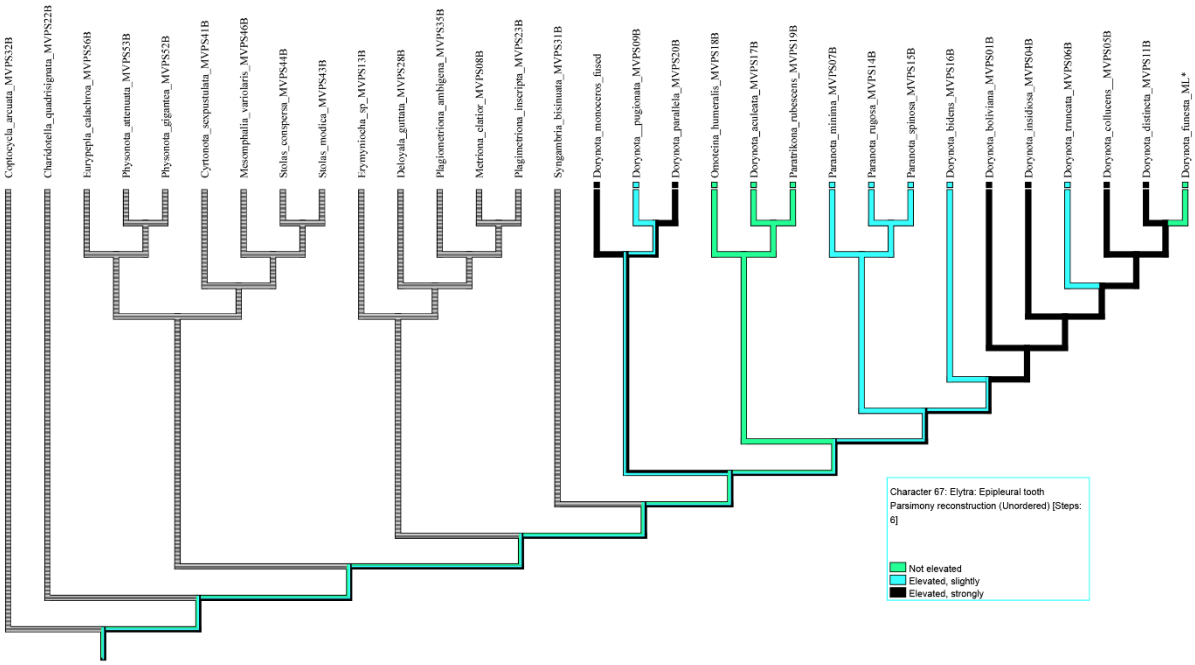

Figure S112. Ancestral state reconstruction of elytral punctuation width and depth (character 71).

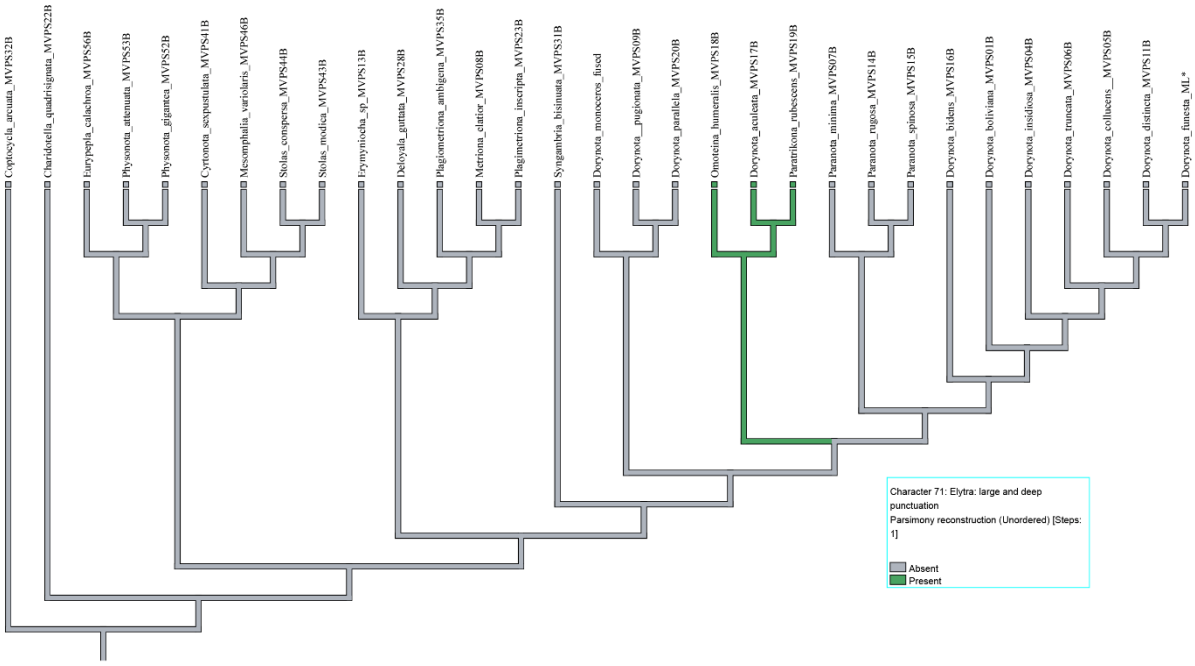

Figure S113. Ancestral state reconstruction of posterior margin of metasternum (character 74).

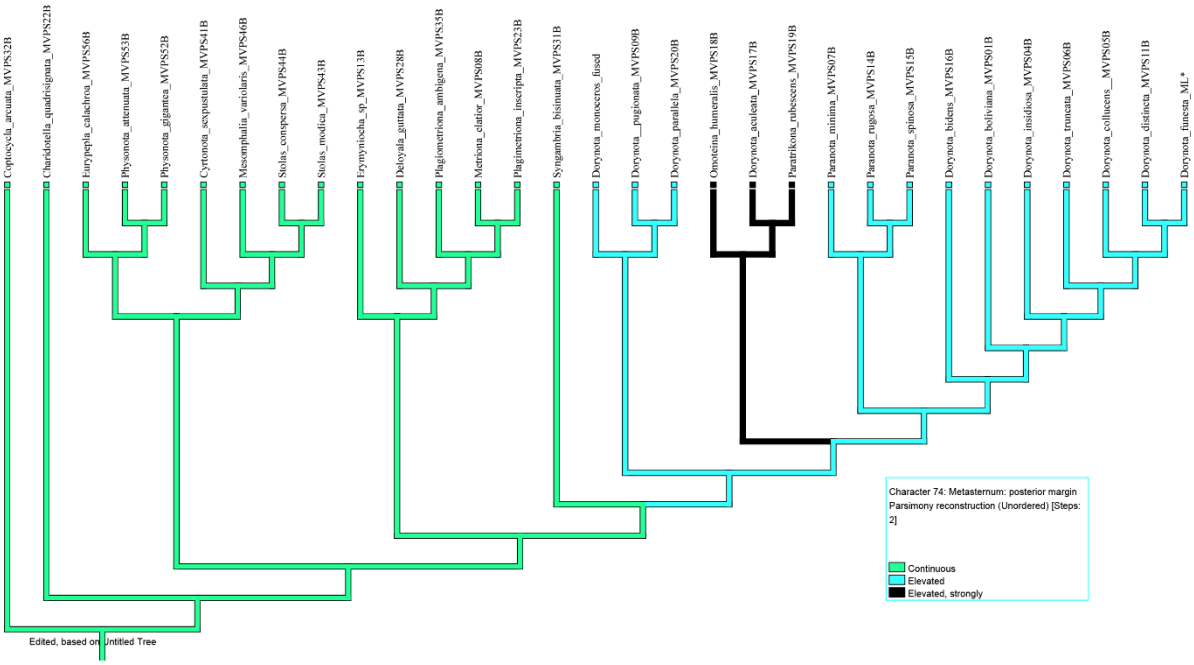

Figure S114 . Ancestral state reconstruction of angle at the base of pretarsal claws (character 82).

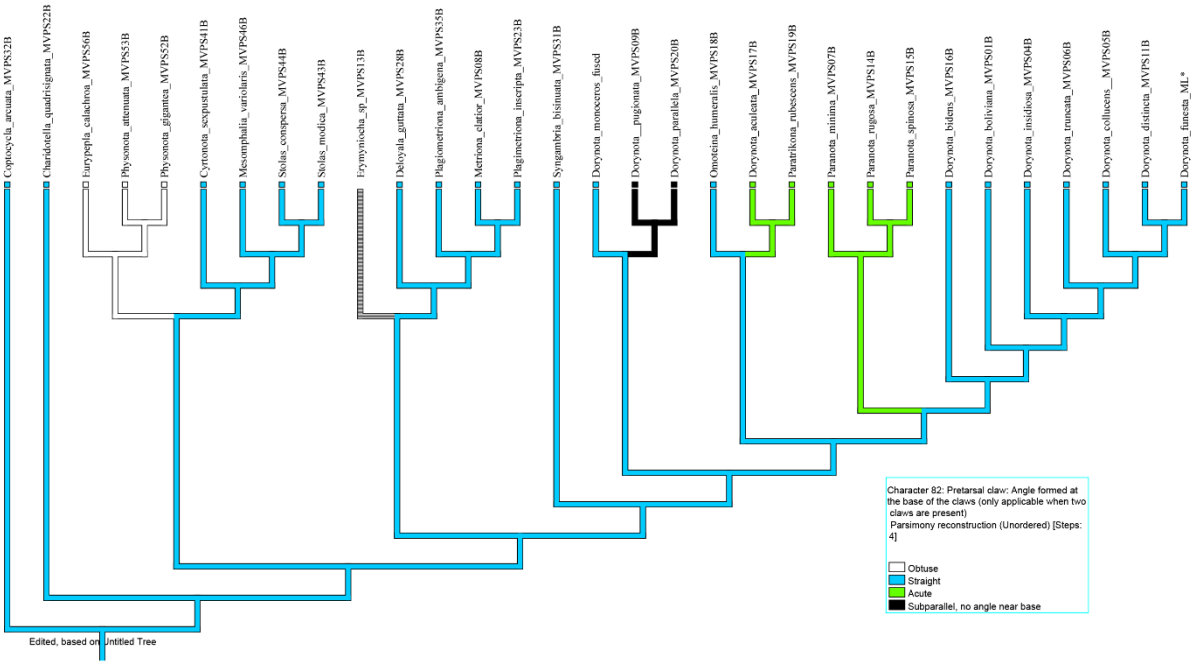

Figure S115 . Ancestral state reconstruction of symmetry between pretarsal claws (character 83).

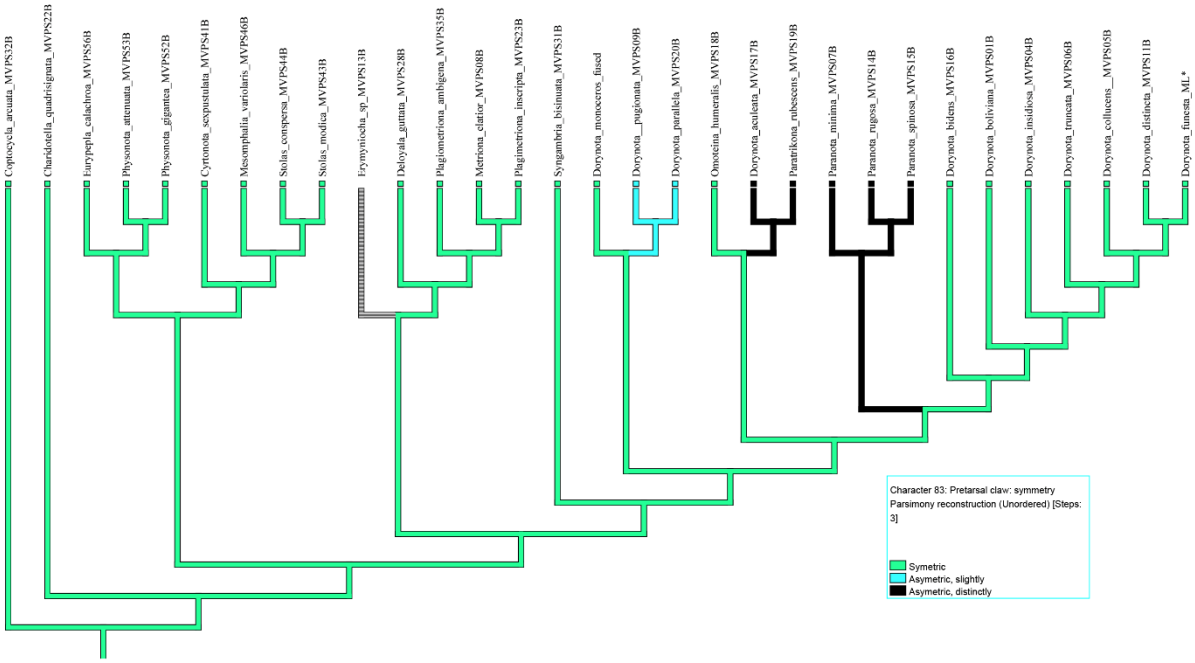

Appendix VII

Appendix S1. Measurements taken from specimens, along with histograms and scatterplots of data. (Chapter 6, Simões *et al*, 2017)

Figure S1: Hypothetical correlation matrices relating morphology and environment occupied on the vertical and horizontal axes, respectively, with degree of correlation shown using a heat map and the figure on the left representing the type of clinal hypothesis proposed by Spaeth (1923). By contrast, the figure on the right illustrates a hypothetical example in which no direct correlation exists between morphology and environment.

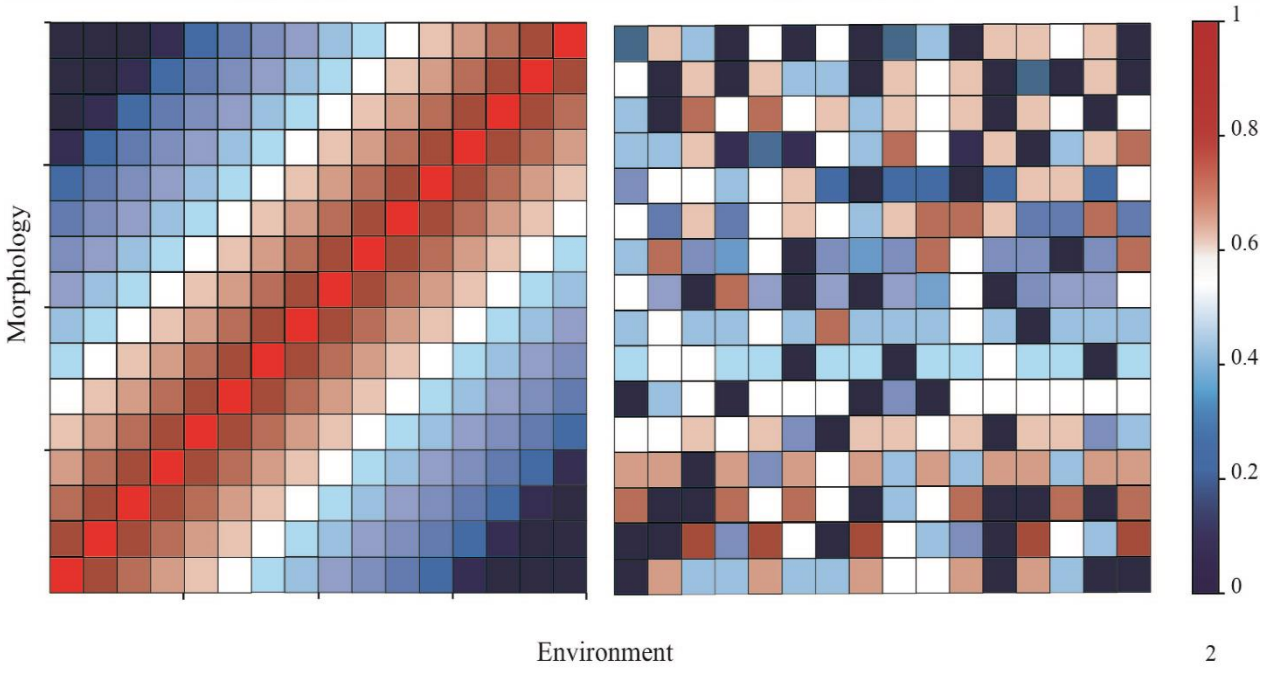

Figure S2. Measurements taken from specimens, used to quantify aspects of the tribe morphology: (1) pronotum length; (2) pronotum width; (3) elytra length; (4) elytra width at humeral angle; (5) elytra width at meadian region; and (6) body total height.

S1

Figure S3. Histogram showing that species excluded from the analysis, because of small sample size, did not influence on the distribution of spine height.

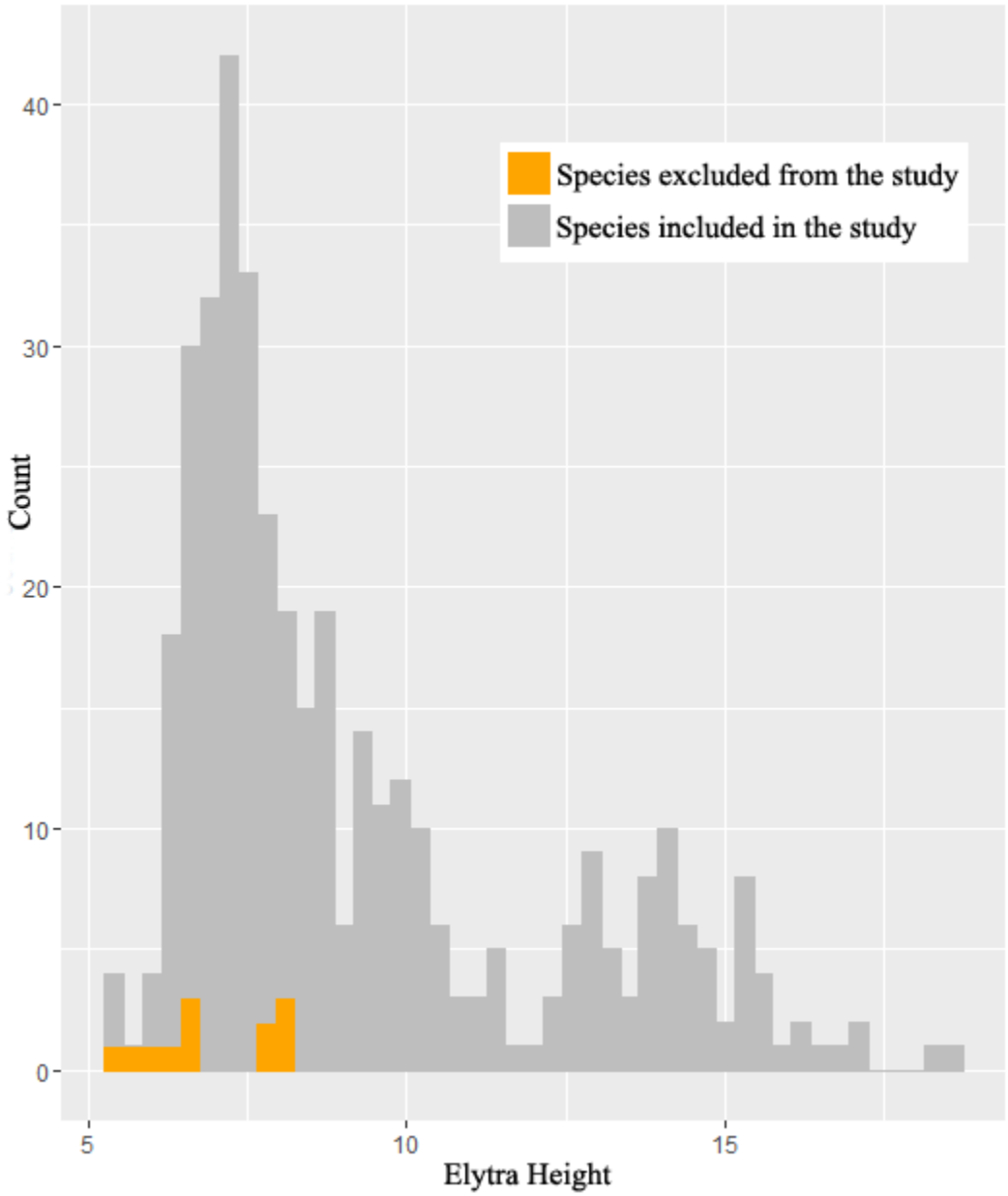

Figure S4. Correlation plot between body size and spine height.

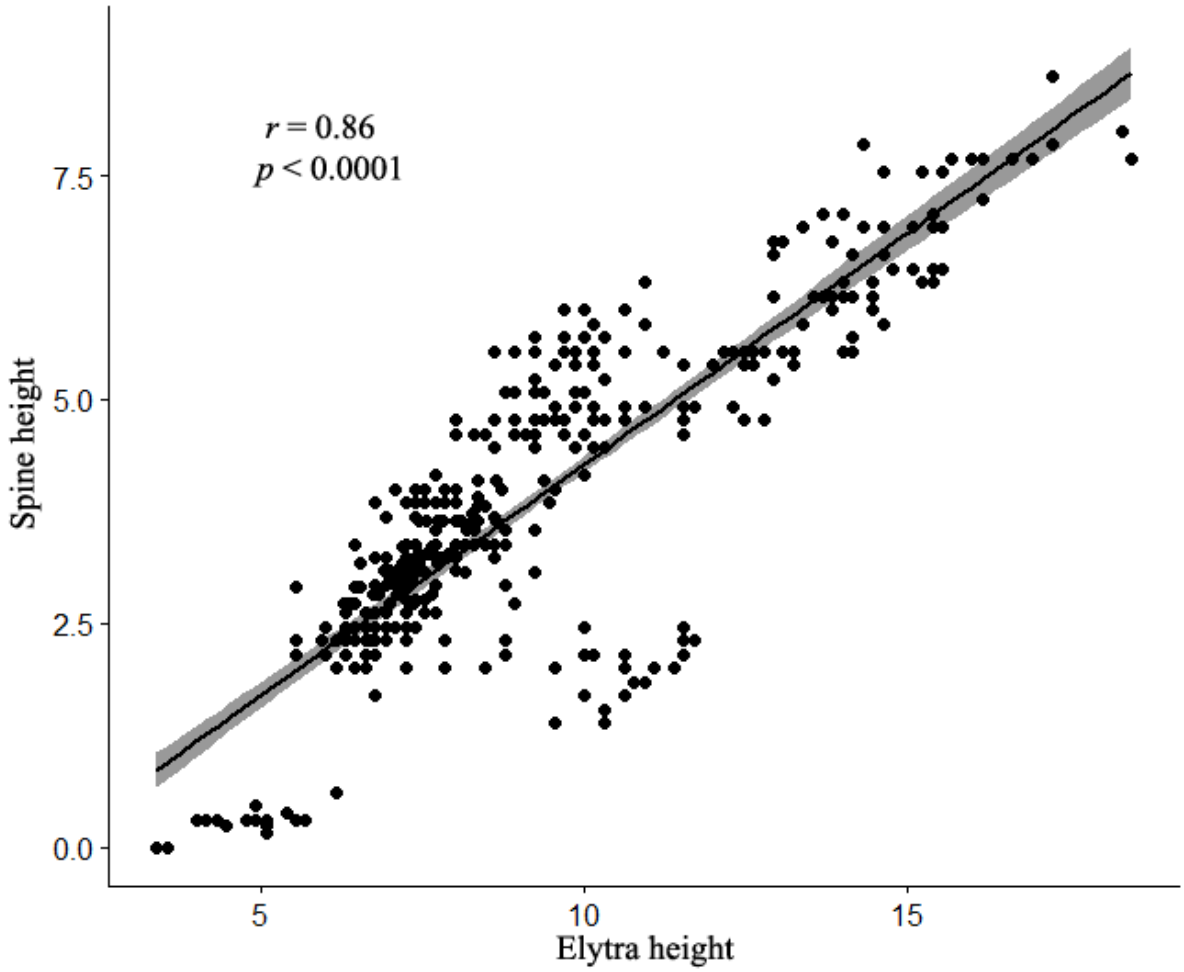

Appendix VIII

Appendix S2. List of institutions and number of specimens examined for the study and measurements taken from specimens. (Chapter 6, Simões *et al*, 2017)

Table S1: List of specimens examined and theirs institutional repositories.

Institutional repositories	**Number of examined specimens**
Coleção de Entomolgia de Pe. Jesus S. Moure, Universidade Federal do Paraná, Paraná, Brazil (**DZUP**)	107
Department of Biodiversity and Evolutionary Taxonomy, University of Wrocław, Poland (**DBET**)	34
Finnish Museum of Natural History, University of Helsinki, Finland (**MZH**)	48
Museum of Comparative Zoology, Harvard University, Cambridge, U.S.A. **(MCZ)**	51
Manchester Museum, Manchester, U.K. **(MM)**	16
Muséum National d'Histoire Naturelle, Paris, France (**MNHN**)	15
Museu Nacional, Universidade Federal do Rio de Janeiro, Rio de Janeiro, Brazil **(MNRJ**)	115
Museu de Zoologia, Universidade de São Paulo, São Paulo, Brazil (**MZUSP**)	49
Natural History Museum, London, U.K. (**NHM**)	111
Swedish Museum of Natural History, Stockholm, Sweden **(SMNH**)	4
National Museum of Natural History, Smithsonian Institution, Washington D.C., U.S.A. **(USNM**)	9
Texas A&M University, College Station, U.S.A. (**TAMU**)	113
Total of examined specimens	672

Table S2: Morphological measurements by genus.

Genera of the tribe Dorynotini	Pronotum Width	Pronotum Length	Elytra Width (Humeral Angle)	ElytraWidth (Median Region)	Elytra Length	Body Total Height
Dorynota	10.153	5.538	17.231	13.538	16.154	14.462
Dorynota	11.231	6.923	19.077	16.154	17.231	18.308
Dorynota	11.692	6.462	19.231	15.231	17.231	17.231
Dorynota	11.231	6.923	19.077	16.154	17.231	16.923
Dorynota	12.000	7.077	20.000	16.462	16.923	18.462
Dorynota	10.923	6.615	20.462	14.615	16.462	17.231
Dorynota	10.308	5.692	18.154	14.615	16.154	15.385
Dorynota	10.615	5.846	16.462	13.385	16.000	14.462
Dorynota	10.615	5.846	17.077	13.692	15.692	15.538
Dorynota	10.000	6.154	16.154	12.615	15.538	15.077
Dorynota	10.462	5.538	18.462	15.077	15.385	16.154
Dorynota	10.615	6.000	18.154	14.615	15.385	15.385
Dorynota	10.000	4.923	16.154	12.615	15.385	13.846
Dorynota	10.308	6.769	17.538	14.462	15.231	15.538
Dorynota	11.231	6.923	18.615	14.308	15.231	15.538
Dorynota	10.615	5.692	16.000	15.077	15.231	15.231
Dorynota	10.154	5.538	16.462	13.846	15.231	13.846
Dorynota	9.692	5.385	15.692	12.923	15.231	12.462
Dorynota	10.000	5.538	16.615	13.385	15.077	13.846
Dorynota	10.615	6.154	18.154	13.692	14.923	16.615
Dorynota	9.385	5.385	18.615	12.308	14.923	14.615
Dorynota	9.846	5.385	16.154	13.077	14.923	14.462
Dorynota	8.769	4.923	17.231	11.385	14.923	14.308
Dorynota	9.385	4.923	16.000	12.769	14.923	14.154
Dorynota	10.462	6.154	16.615	13.538	14.923	14.154
Dorynota	9.692	5.231	15.538	12.923	14.923	13.692
Dorynota	9.385	4.923	16.923	11.846	14.923	13.385
Dorynota	10.154	6.000	17.385	13.692	14.769	15.385
Dorynota	10.000	6.000	16.769	12.615	14.769	14.154
Dorynota	9.077	5.231	17.231	12.000	14.769	13.077
Dorynota	10.615	6.000	18.308	13.846	14.615	15.385
Dorynota	9.231	5.231	17.846	11.846	14.615	13.692
Dorynota	9.231	4.769	15.692	12.308	14.462	14.000
Dorynota	9.692	5.231	16.000	12.923	14.462	13.231
Dorynota	10.154	6.154	16.923	12.923	14.308	15.385
Dorynota	10.000	6.154	18.308	13.385	14.308	15.077
Dorynota	10.308	6.308	17.538	13.692	14.308	14.308

Dorynota	9.692	5.538	16.154	12.769	14.308	14.000
Dorynota	9.692	5.538	16.154	12.615	14.308	14.000
Dorynota	10.000	5.538	17.538	14.462	14.154	14.769
Dorynota	9.385	4.923	16.308	13.692	14.154	14.154
Dorynota	9.692	5.692	15.846	13.385	14.000	15.692
Dorynota	9.538	5.538	15.846	13.231	14.000	14.154
Dorynota	9.846	5.385	16.308	13.077	14.000	13.231
Dorynota	9.692	5.385	15.538	12.769	14.000	13.077
Dorynota	9.231	5.077	15.231	12.462	14.000	12.769
Dorynota	10.000	5.231	16.462	13.846	13.846	16.154
Dorynota	10.154	6.308	17.231	14.000	13.846	15.231
Dorynota	10.000	5.538	16.462	13.231	13.846	14.615
Dorynota	9.385	5.077	15.077	12.154	13.846	12.615
Dorynota	10.154	5.846	16.462	14.154	13.692	16.000
Dorynota	9.692	6.154	17.077	13.231	13.692	14.615
Dorynota	9.692	5.077	15.692	12.462	13.692	14.000
Dorynota	9.231	5.385	15.231	11.846	13.692	13.846
Dorynota	9.385	5.231	15.692	12.308	13.692	13.077
Dorynota	9.231	5.385	14.923	12.154	13.538	13.385
Dorynota	9.385	4.923	16.154	12.308	13.538	12.923
Dorynota	10.000	6.000	15.846	13.385	13.385	15.385
Dorynota	9.692	5.692	16.000	13.077	13.385	13.692
Dorynota	9.231	4.615	16.923	11.846	13.385	12.923
Dorynota	9.692	5.077	16.000	12.769	13.231	14.000
Dorynota	9.692	5.538	15.385	12.308	13.231	13.538
Dorynota	9.077	4.923	14.769	11.846	13.231	12.308
Dorynota	9.846	6.000	16.154	13.846	13.077	14.615
Dorynota	9.692	6.154	16.462	14.154	13.077	14.462
Dorynota	9.692	5.385	14.923	12.462	13.077	12.769
Dorynota	8.769	4.923	14.000	11.538	13.077	12.308
Dorynota	9.385	5.538	15.231	12.923	12.923	13.846
Dorynota	8.923	4.462	15.692	11.231	12.923	12.923
Dorynota	9.077	4.615	16.308	11.077	12.923	12.923
Dorynota	8.769	4.769	15.077	12.462	12.769	12.462
Dorynota	8.308	5.385	14.923	12.308	12.769	12.615
Dorynota	9.692	5.231	15.692	12.308	12.769	12.615
Dorynota	9.231	4.923	15.308	11.846	12.615	12.154
Dorynota	8.769	5.692	14.000	11.077	12.615	12.000
Dorynota	8.538	4.923	14.154	10.923	12.462	11.231
Dorynota	8.769	4.769	14.769	11.692	12.308	12.769
Dorynota	8.000	5.385	16.154	14.000	12.308	12.462
Dorynota	8.615	5.385	14.000	11.846	12.308	11.538

Dorynota	8.769	5.077	14.615	12.615	12.308	11.538
Dorynota	8.615	5.692	14.154	11.692	12.000	11.538
Dorynota	8.615	5.231	14.154	11.692	11.692	12.923
Dorynota	8.615	4.923	14.000	11.692	11.692	11.692
Dorynota	8.923	4.923	14.769	11.846	11.538	12.769
Dorynota	8.462	5.077	14.000	11.385	11.538	11.231
Dorynota	7.538	4.462	13.231	9.077	11.538	10.308
Dorynota	8.615	4.923	14.923	11.846	11.385	11.538
Dorynota	7.231	3.538	11.077	9.077	10.923	10.000
Dorynota	6.923	3.077	13.385	9.385	10.769	10.615
Dorynota	7.385	4.462	12.769	8.769	10.769	10.308
Dorynota	6.000	3.077	12.000	8.615	10.615	10.923
Dorynota	7.538	3.538	11.846	9.385	10.615	10.615
Dorynota	6.308	2.769	10.769	7.077	10.615	9.231
Dorynota	7.385	3.692	11.692	9.077	10.462	10.615
Dorynota	6.769	3.538	13.692	8.923	10.462	10.154
Dorynota	6.154	2.923	11.538	7.538	10.462	9.846
Dorynota	7.077	4.462	12.154	8.769	10.462	9.846
Dorynota	7.385	4.000	11.538	9.231	10.308	11.231
Dorynota	7.538	4.154	12.000	8.769	10.308	10.154
Dorynota	7.077	4.154	12.615	9.231	10.308	9.538
Dorynota	5.846	3.077	11.846	7.231	10.154	10.154
Dorynota	6.462	2.923	12.615	8.615	10.154	9.846
Dorynota	6.462	3.231	13.231	8.615	10.000	10.615
Dorynota	7.385	3.692	11.692	8.923	10.000	10.308
Dorynota	6.462	3.077	12.769	6.923	10.000	10.000
Dorynota	6.308	3.077	12.462	8.462	10.000	9.231
Dorynota	7.385	3.692	11.231	9.077	9.846	10.154
Dorynota	6.308	3.231	12.308	8.615	9.846	10.000
Dorynota	5.846	2.923	11.538	8.000	9.846	9.077
Dorynota	7.846	4.000	12.308	9.692	9.692	11.538
Dorynota	6.154	2.923	12.000	8.462	9.692	9.538
Dorynota	6.462	2.769	12.154	8.462	9.692	9.231
Dorynota	7.077	3.385	11.077	8.615	9.538	10.000
Dorynota	5.846	3.077	12.000	7.385	9.538	10.000
Dorynota	7.077	3.692	11.077	8.615	9.538	9.846
Dorynota	7.077	3.846	10.615	8.462	9.538	9.692
Dorynota	6.923	3.538	11.077	8.769	9.538	9.692
Dorynota	5.692	2.615	9.692	6.000	9.538	7.538
Dorynota	5.692	2.923	10.308	7.231	9.385	9.385
Dorynota	5.538	3.077	11.077	6.462	9.385	9.231
Dorynota	5.231	2.462	10.462	6.923	9.385	8.923

Dorynota	4.308	2.154	8.308	5.231	9.385	6.769
Dorynota	10.923	4.000	11.091	8.182	9.273	9.364
Dorynota	5.385	3.077	10.769	7.231	9.231	10.000
Dorynota	6.615	3.846	10.769	7.538	9.231	9.538
Dorynota	6.154	3.077	12.154	8.154	9.231	9.231
Dorynota	5.538	2.308	8.615	5.538	9.231	7.385
Dorynota	5.538	3.231	12.000	8.462	9.077	10.615
Dorynota	5.231	2.615	10.615	6.923	9.077	9.385
Dorynota	5.385	2.615	9.538	6.769	9.077	8.769
Dorynota	9.846	3.636	10.273	7.545	9.000	8.636
Dorynota	5.231	2.769	10.769	7.231	8.923	10.154
Dorynota	5.692	3.231	10.154	7.692	8.923	9.231
Dorynota	5.846	2.769	10.154	6.615	8.923	9.231
Dorynota	6.154	3.077	9.846	8.000	8.923	8.615
Dorynota	5.692	2.923	9.846	7.385	8.923	8.000
Dorynota	5.538	3.077	10.462	8.000	8.769	9.462
Dorynota	6.000	2.923	11.385	8.000	8.769	9.385
Dorynota	5.538	2.615	10.923	7.231	8.769	9.231
Dorynota	5.538	2.769	10.769	7.538	8.769	8.923
Dorynota	5.846	3.077	11.538	7.692	8.769	8.923
Dorynota	5.538	2.615	9.692	7.385	8.769	8.769
Dorynota	5.538	2.923	10.154	7.385	8.769	8.769
Dorynota	6.154	3.538	9.538	7.692	8.769	8.308
Dorynota	9.385	3.364	9.636	7.455	8.727	8.909
Dorynota	9.385	2.818	9.091	7.455	8.727	8.364
Dorynota	9.846	2.909	9.636	7.545	8.636	8.636
Dorynota	9.308	2.818	9.273	7.545	8.636	8.364
Dorynota	5.538	2.769	10.308	7.538	8.615	9.846
Dorynota	6.154	3.077	8.308	9.231	8.615	9.692
Dorynota	5.077	2.615	10.308	7.077	8.615	9.538
Dorynota	5.692	3.385	10.308	7.385	8.615	8.769
Dorynota	5.385	3.077	9.385	7.231	8.615	8.615
Dorynota	5.538	2.615	9.077	8.154	8.615	7.538
Dorynota	9.077	3.364	9.545	7.364	8.545	8.273
Dorynota	5.538	2.923	11.538	8.154	8.462	10.308
Dorynota	5.385	2.923	11.692	7.385	8.462	9.692
Dorynota	5.385	2.615	10.769	7.385	8.462	9.231
Dorynota	5.077	2.615	10.154	6.769	8.462	8.769
Dorynota	5.231	2.769	10.308	6.462	8.462	8.615
Dorynota	5.385	2.615	10.615	7.385	8.462	8.615
Dorynota	5.538	3.231	9.538	7.077	8.462	8.462
Dorynota	5.385	2.615	9.385	7.231	8.462	8.000

Dorynota	8.923	2.909	8.909	7.091	8.455	8.091
Dorynota	9.077	3.182	9.364	7.182	8.364	8.636
Dorynota	5.538	2.923	10.462	7.231	8.308	9.231
Dorynota	5.385	2.769	10.308	7.231	8.308	8.615
Dorynota	5.231	2.923	10.769	6.769	8.308	8.615
Dorynota	5.077	2.769	9.385	7.077	8.308	8.308
Dorynota	5.231	2.615	9.846	6.769	8.308	8.308
Dorynota	5.692	3.077	9.231	7.077	8.308	8.154
Dorynota	5.846	3.231	10.000	7.385	8.308	8.154
Dorynota	5.385	2.769	9.077	7.077	8.308	8.000
Dorynota	5.538	2.462	9.846	7.231	8.308	7.846
Dorynota	4.615	2.769	8.923	7.077	8.308	7.385
Dorynota	8.615	2.727	8.727	7.000	8.273	8.364
Dorynota	5.182	3.091	8.818	7.000	8.273	8.273
Dorynota	9.231	2.909	9.455	7.273	8.182	8.636
Dorynota	9.385	2.818	9.727	7.182	8.182	8.455
Dorynota	9.077	3.000	9.455	7.091	8.182	8.273
Dorynota	9.385	3.000	9.273	7.000	8.182	8.182
Dorynota	9.538	3.000	9.455	7.091	8.182	8.000
Dorynota	8.769	3.182	9.273	6.727	8.182	7.909
Dorynota	9.385	2.909	9.182	7.364	8.182	7.727
Dorynota	5.231	2.769	11.846	7.385	8.154	10.923
Dorynota	5.385	3.077	10.923	7.385	8.154	9.692
Dorynota	5.538	3.231	9.692	7.077	8.154	8.615
Dorynota	5.385	3.231	10.000	6.923	8.154	8.615
Dorynota	5.538	2.462	10.308	7.077	8.154	8.308
Dorynota	5.538	2.615	10.769	7.077	8.154	8.000
Dorynota	4.923	2.154	9.846	6.154	8.154	7.846
Dorynota	5.231	3.231	12.308	8.769	8.000	10.923
Dorynota	5.231	2.769	10.308	7.231	8.000	8.462
Dorynota	4.636	2.818	7.818	6.273	8.000	8.000
Dorynota	4.769	3.077	8.462	6.615	8.000	8.000
Dorynota	5.077	2.615	8.923	6.923	8.000	8.000
Dorynota	5.231	2.769	9.231	6.923	8.000	8.000
Dorynota	5.385	2.615	9.846	6.615	8.000	8.000
Dorynota	5.364	2.818	8.636	7.636	8.000	7.909
Dorynota	5.231	2.615	8.923	6.615	8.000	7.846
Dorynota	5.385	2.769	8.154	6.923	8.000	7.692
Dorynota	5.385	2.769	8.615	6.615	8.000	7.692
Dorynota	6.000	3.077	8.923	6.615	8.000	7.692
Dorynota	5.077	2.769	8.923	6.615	8.000	7.692
Dorynota	5.538	3.077	9.385	7.538	8.000	7.692

Dorynota	5.077	2.923	8.923	6.462	8.000	7.538
Dorynota	8.308	2.636	8.455	6.636	8.000	7.455
Dorynota	5.077	2.615	7.077	6.769	8.000	7.231
Dorynota	5.091	2.818	7.818	7.818	7.909	8.727
Dorynota	5.077	2.923	9.231	6.615	7.846	7.769
Dorynota	5.692	2.769	8.615	7.231	7.846	7.692
Dorynota	5.077	2.615	9.769	6.615	7.846	7.692
Dorynota	5.538	2.769	8.000	7.077	7.846	7.231
Dorynota	9.154	3.091	8.364	7.091	7.818	8.000
Dorynota	8.154	2.818	8.545	6.364	7.818	7.182
Dorynota	8.923	3.091	9.091	7.000	7.727	7.545
Dorynota	4.923	3.231	11.538	7.538	7.692	10.615
Dorynota	5.538	2.923	10.923	7.385	7.692	9.846
Dorynota	4.923	2.462	9.154	6.000	7.692	7.846
Dorynota	5.308	2.615	6.769	7.077	7.692	7.692
Dorynota	5.077	2.308	9.692	6.615	7.692	7.538
Dorynota	4.615	2.308	8.154	7.077	7.692	7.385
Dorynota	5.538	3.077	8.462	7.077	7.692	7.385
Dorynota	5.231	2.615	8.462	6.923	7.692	7.231
Dorynota	5.538	2.923	8.615	7.538	7.692	7.231
Dorynota	5.455	3.182	8.727	7.364	7.545	7.727
Dorynota	5.000	2.727	8.000	7.091	7.545	7.000
Dorynota	4.923	2.615	10.769	7.231	7.538	8.923
Dorynota	5.077	2.462	9.077	6.154	7.538	7.846
Dorynota	5.077	2.615	9.692	6.769	7.538	7.846
Dorynota	5.231	2.615	8.000	6.923	7.538	7.538
Dorynota	5.538	3.077	8.923	7.385	7.538	7.538
Dorynota	4.923	3.077	8.462	6.462	7.538	7.385
Dorynota	4.923	2.615	8.615	6.308	7.538	7.385
Dorynota	5.308	2.923	7.692	6.462	7.538	7.231
Dorynota	5.077	2.615	8.462	6.308	7.538	7.231
Dorynota	5.077	2.615	8.462	6.462	7.538	7.231
Dorynota	5.077	2.923	7.846	6.769	7.538	6.923
Dorynota	4.923	2.462	8.000	6.769	7.538	6.923
Dorynota	5.077	2.154	9.538	6.769	7.538	6.923
Dorynota	5.000	2.769	7.231	6.923	7.538	6.615
Dorynota	5.091	3.273	8.000	6.818	7.455	8.364
Dorynota	7.692	2.818	8.591	6.545	7.455	7.545
Dorynota	8.154	2.727	8.000	6.545	7.455	7.455
Dorynota	8.308	2.909	8.364	6.818	7.455	7.455
Dorynota	8.308	3.000	8.182	6.364	7.455	7.273
Dorynota	8.000	3.000	8.000	6.000	7.455	6.545

Dorynota	5.231	2.769	8.000	6.769	7.385	7.077
Dorynota	4.923	2.923	8.308	6.769	7.385	7.077
Dorynota	5.385	2.923	8.615	7.231	7.385	7.077
Dorynota	5.077	2.769	8.000	6.923	7.385	6.923
Dorynota	4.769	2.615	8.308	6.308	7.385	6.923
Dorynota	4.923	2.769	8.000	6.769	7.385	6.769
Dorynota	4.909	3.000	8.273	7.182	7.364	7.273
Dorynota	5.091	2.818	8.273	7.182	7.364	7.091
Dorynota	8.308	2.636	8.545	6.545	7.318	7.818
Dorynota	4.923	2.923	7.692	6.923	7.308	7.077
Dorynota	5.136	2.818	8.273	7.455	7.273	7.636
Dorynota	8.769	3.000	8.455	7.000	7.273	7.455
Dorynota	5.182	2.909	8.636	7.273	7.273	7.318
Dorynota	7.846	2.818	7.909	6.000	7.273	7.182
Dorynota	5.231	2.923	12.000	8.769	7.231	10.154
Dorynota	5.692	3.077	11.077	7.231	7.231	9.692
Dorynota	4.846	2.615	9.231	5.846	7.231	8.000
Dorynota	4.923	2.308	9.231	6.000	7.231	7.385
Dorynota	5.077	2.923	7.846	6.923	7.231	7.231
Dorynota	5.077	2.462	8.000	6.308	7.231	7.231
Dorynota	4.769	2.769	8.154	6.308	7.231	7.231
Dorynota	4.769	2.615	8.308	6.615	7.231	7.231
Dorynota	5.000	4.154	8.615	6.000	7.231	7.231
Dorynota	4.769	2.923	8.000	6.154	7.231	7.077
Dorynota	4.692	2.462	8.308	6.308	7.231	7.077
Dorynota	5.385	2.615	6.923	7.231	7.231	6.923
Dorynota	4.692	2.615	8.308	6.000	7.231	6.769
Dorynota	4.923	2.615	7.538	6.769	7.231	6.308
Dorynota	8.308	2.727	8.182	6.091	7.182	7.364
Dorynota	8.000	2.727	8.000	6.182	7.182	7.273
Dorynota	5.000	2.818	8.545	7.182	7.091	8.364
Dorynota	4.909	2.818	7.818	6.818	7.091	7.636
Dorynota	4.818	2.818	7.636	6.727	7.091	7.455
Dorynota	5.000	2.909	8.182	7.091	7.091	7.364
Dorynota	4.909	2.909	7.818	7.091	7.091	7.182
Dorynota	5.000	2.455	8.000	7.000	7.091	7.091
Dorynota	4.308	2.615	8.000	6.462	7.077	8.615
Dorynota	5.231	3.231	7.692	6.615	7.077	7.538
Dorynota	4.769	2.462	9.077	5.692	7.077	7.385
Dorynota	4.615	2.769	8.000	6.154	7.077	7.231
Dorynota	5.077	2.462	8.000	6.462	7.077	7.231
Dorynota	5.385	3.231	8.462	7.077	7.077	7.231

Dorynota	5.077	2.615	7.846	6.923	7.077	7.077
Dorynota	5.231	2.923	7.692	6.923	7.077	6.923
Dorynota	5.000	2.615	9.077	7.385	7.077	6.923
Dorynota	5.231	2.923	7.385	6.923	7.077	6.769
Dorynota	5.077	2.769	7.538	6.462	7.077	6.769
Dorynota	5.308	2.615	8.000	6.923	7.077	6.769
Dorynota	4.923	2.462	9.077	6.154	7.077	6.769
Dorynota	4.769	2.462	7.692	6.923	7.077	6.615
Dorynota	4.923	2.923	7.846	6.615	7.077	6.615
Dorynota	5.077	2.769	7.692	6.769	7.077	6.462
Dorynota	5.091	3.000	8.364	7.273	7.000	7.636
Dorynota	7.538	2.727	7.636	5.636	7.000	6.364
Dorynota	4.923	2.769	6.923	6.769	6.923	6.923
Dorynota	5.231	2.923	7.385	6.769	6.923	6.923
Dorynota	5.077	2.462	7.538	6.615	6.923	6.923
Dorynota	4.462	2.308	7.846	6.154	6.923	6.923
Dorynota	5.308	2.923	7.846	6.308	6.923	6.692
Dorynota	5.077	2.769	7.077	6.462	6.923	6.308
Dorynota	4.909	2.909	8.091	6.909	6.909	7.455
Dorynota	4.727	2.909	7.727	6.909	6.909	6.818
Dorynota	7.692	2.727	7.909	6.000	6.909	6.455
Dorynota	4.818	2.818	8.182	6.909	6.818	7.455
Dorynota	5.091	2.909	8.182	7.182	6.818	7.455
Dorynota	5.000	3.000	8.000	6.818	6.818	7.273
Dorynota	5.000	2.818	8.182	6.818	6.818	7.273
Dorynota	4.909	2.818	8.182	7.000	6.818	7.273
Dorynota	4.727	2.818	8.000	6.636	6.818	6.909
Dorynota	5.077	2.769	8.154	6.923	6.769	7.538
Dorynota	4.769	2.769	8.154	6.154	6.769	6.923
Dorynota	4.923	2.615	7.231	6.615	6.769	6.615
Dorynota	5.091	2.909	8.364	7.273	6.727	7.727
Dorynota	4.909	2.818	7.818	6.636	6.727	7.364
Dorynota	4.818	3.000	7.455	6.818	6.727	7.091
Dorynota	7.538	2.727	7.636	6.182	6.727	6.545
Dorynota	4.727	2.909	7.818	6.727	6.727	6.455
Dorynota	4.818	2.545	7.455	6.818	6.727	6.273
Dorynota	4.727	2.909	7.818	6.636	6.636	7.182
Dorynota	4.727	2.818	7.818	6.727	6.636	6.818
Dorynota	4.769	4.000	9.077	5.846	6.615	7.538
Dorynota	4.923	2.923	7.231	6.462	6.615	7.077
Dorynota	5.077	2.462	8.308	6.923	6.615	7.077
Dorynota	4.923	2.615	7.846	6.769	6.615	6.769

Dorynota	5.231	2.923	8.000	6.923	6.615	6.769
Dorynota	4.769	2.769	7.846	6.615	6.615	6.615
Dorynota	4.769	2.308	8.385	6.154	6.615	6.308
Dorynota	4.364	2.818	7.000	6.455	6.545	7.273
Dorynota	4.909	3.000	8.182	6.818	6.545	7.273
Dorynota	4.545	2.000	7.273	6.455	6.545	7.000
Dorynota	4.636	2.818	7.636	6.864	6.545	7.000
Dorynota	4.818	2.909	7.727	6.727	6.545	6.545
Dorynota	7.231	2.545	7.182	5.455	6.545	5.545
Dorynota	4.923	2.923	8.462	6.462	6.462	7.077
Dorynota	4.692	2.462	7.692	6.462	6.462	6.923
Dorynota	4.769	2.615	7.077	6.308	6.462	6.615
Dorynota	5.385	2.462	7.385	6.615	6.462	6.615
Dorynota	4.769	2.462	7.846	6.462	6.462	6.615
Dorynota	5.077	2.923	7.846	6.308	6.462	6.615
Dorynota	5.231	2.923	8.000	6.615	6.462	6.615
Dorynota	4.923	2.615	7.231	6.462	6.462	6.462
Dorynota	4.615	2.692	7.231	6.615	6.462	6.308
Dorynota	4.769	2.615	7.538	6.462	6.462	6.308
Dorynota	4.923	2.769	7.846	6.462	6.462	6.308
Dorynota	4.923	2.923	7.538	6.615	6.462	6.154
Dorynota	4.909	2.909	8.455	6.818	6.455	7.091
Dorynota	5.045	3.000	8.455	7.000	6.455	6.909
Dorynota	5.182	3.000	8.091	6.727	6.455	6.818
Dorynota	4.545	2.727	7.409	6.364	6.455	6.273
Dorynota	4.818	2.909	7.727	6.636	6.364	7.000
Dorynota	4.615	2.462	7.077	6.154	6.308	6.615
Dorynota	5.000	2.462	7.308	6.462	6.308	6.615
Dorynota	4.769	3.077	7.231	6.308	6.308	6.462
Dorynota	4.769	2.462	7.846	6.308	6.308	6.462
Dorynota	4.615	2.769	8.462	6.308	6.308	6.462
Dorynota	4.538	2.308	8.615	5.385	6.308	6.462
Dorynota	4.769	2.769	7.231	6.000	6.308	6.308
Dorynota	4.615	2.462	7.385	6.000	6.308	6.154
Dorynota	4.308	2.615	7.538	5.846	6.308	5.923
Dorynota	4.615	2.462	6.769	6.154	6.308	5.538
Dorynota	4.727	2.909	7.545	6.818	6.182	6.727
Dorynota	5.077	3.077	8.000	6.462	6.154	6.615
Dorynota	4.692	2.769	7.231	5.692	6.077	6.308
Dorynota	4.615	2.462	8.000	6.308	6.077	6.308
Dorynota	4.615	2.769	6.846	5.846	6.000	6.462
Dorynota	4.308	2.308	6.769	6.000	6.000	6.308

Dorynota	4.615	2.923	7.231	5.692	6.000	6.308
Dorynota	4.846	2.923	7.538	6.308	5.692	6.154
Dorynota	4.462	3.077	6.923	5.231	5.692	6.000
Dorynota	4.154	2.462	6.308	5.538	5.692	5.538
Dorynota	4.000	2.455	6.636	6.000	5.455	6.000
Paratrikona	8.000	5.077	11.538	12.308	11.538	8.769
Paratrikona	7.846	4.769	11.538	11.538	10.308	8.769
Paratrikona	7.538	4.462	10.923	10.769	10.308	8.462
Paratrikona	7.231	4.000	10.308	10.923	9.538	7.846
Paratrikona	7.452	4.308	11.375	10.856	9.047	7.846
Paratrikona	7.077	4.558	11.385	10.744	9.454	7.876
Paratrikona	7.345	4.140	10.442	10.745	9.077	8.247
Paratrikona	7.745	4.387	11.477	10.445	9.747	7.887
Omoteina	6.308	3.077	8.000	10.462	10.462	5.692
Omoteina	5.538	2.769	7.231	10.308	10.308	5.538
Omoteina	5.692	2.615	7.846	10.000	10.000	5.692
Omoteina	6.154	3.077	8.000	10.000	10.000	5.385
Omoteina	5.692	3.077	7.231	7.692	10.000	5.077
Omoteina	6.000	2.923	8.000	9.692	9.692	5.538
Omoteina	6.000	3.538	7.692	9.538	9.538	6.154
Omoteina	6.000	3.077	7.538	9.538	9.538	5.538
Omoteina	5.538	2.769	7.231	9.385	9.385	5.077
Omoteina	5.538	2.923	7.538	9.231	9.231	5.692
Omoteina	5.231	2.769	7.231	9.077	9.077	5.538
Omoteina	5.538	2.769	7.385	9.077	9.077	5.077
Omoteina	5.692	2.923	7.231	8.615	8.615	4.769
Omoteina	5.538	2.615	6.923	8.615	8.615	4.308
Omoteina	5.385	2.923	6.769	8.615	8.615	4.154
Omoteina	5.231	2.462	6.769	8.308	8.308	5.077
Omoteina	5.231	2.769	6.769	8.308	8.308	4.923
Omoteina	5.385	2.615	6.462	8.154	8.154	4.923
Omoteina	5.538	2.923	7.077	7.846	7.846	4.923
Omoteina	5.385	2.923	6.923	7.846	7.846	4.462
Omoteina	5.077	3.077	6.615	8.769	7.692	4.154
Omoteina	5.231	2.923	6.923	7.538	7.538	4.769
Omoteina	5.077	2.769	6.154	7.077	7.077	4.000
Akantaka	13.077	6.769	23.538	18.923	19.385	11.692
Akantaka	13.538	6.923	24.462	23.385	19.231	11.538
Akantaka	12.923	6.615	23.692	21.846	19.231	10.000
Akantaka	12.923	6.615	22.615	22.923	19.077	10.615
Akantaka	11.538	6.154	20.000	19.538	19.077	10.308
Akantaka	13.385	6.923	24.923	23.385	18.923	11.385

Akantaka	11.692	5.846	21.538	20.615	18.462	10.308
Akantaka	10.769	5.538	20.462	18.462	17.385	11.077
Akantaka	11.538	6.000	19.846	19.231	17.231	11.538
Akantaka	11.846	5.846	21.846	18.462	17.231	11.538
Akantaka	10.923	5.538	20.154	20.000	17.077	9.538
Akantaka	11.231	5.846	21.385	18.462	16.923	10.615
Akantaka	12.769	6.308	23.077	21.231	16.769	10.769
Akantaka	11.538	6.000	20.615	18.769	16.308	10.615
Akantaka	11.538	6.000	22.154	18.462	16.308	10.615
Akantaka	10.462	5.385	18.769	18.154	16.000	10.000
Akantaka	11.538	6.308	20.154	18.462	15.846	10.923
Akantaka	11.077	5.692	19.692	18.462	15.846	9.538
Akantaka	11.077	5.692	19.846	17.231	15.385	10.154
Akantaka	11.231	5.385	20.000	17.846	15.385	10.000

Table S2: Morphological measurements by species.

Species with spine on the elytra suture	Pronotum Width	Pronotum Length	Elytra Width (Humeral Angle)	ElytraWidth (Median Region)	Elytra Length	Body Total Height
D. aculeata	10.000	5.538	16.615	13.385	15.077	13.846
D. aculeata	8.538	4.923	14.154	10.923	12.462	11.231
D. aculeata	9.231	4.923	15.308	11.846	12.615	12.154
D. aculeata	8.769	4.769	15.077	12.462	12.769	12.462
D. aculeata	8.615	4.923	14.000	11.692	11.692	11.692
D. aculeata	9.692	5.538	16.154	12.769	14.308	14.000
D. aculeata	9.077	4.923	14.769	11.846	13.231	12.308
D. aculeata	9.846	5.385	16.308	13.077	14.000	13.231
D. aculeata	9.692	5.077	16.000	12.769	13.231	14.000
D. aculeata	10.462	6.154	16.615	13.538	14.923	14.154
D. aculeata	8.000	5.385	16.154	14.000	12.308	12.462
D. aculeata	10.154	5.538	16.462	13.846	15.231	13.846
D. aculeata	9.692	5.231	16.000	12.923	14.462	13.231
D. aculeata	8.769	5.077	14.615	12.615	12.308	11.538
D. aculeata	8.769	5.692	14.000	11.077	12.615	12.000
D. aculeata	8.308	5.385	14.923	12.308	12.769	12.615
D. aculeata	9.692	5.538	16.154	12.615	14.308	14.000
D. aculeata	8.615	5.692	14.154	11.692	12.000	11.538
D. aculeata	9.385	4.923	16.000	12.769	14.923	14.154
D. aculeata	9.385	4.923	16.154	12.308	13.538	12.923
D. aculeata	8.615	4.923	14.923	11.846	11.385	11.538
D. aculeata	8.923	4.923	14.769	11.846	11.538	12.769
D. aculeata	9.692	5.385	14.923	12.462	13.077	12.769
D. aculeata	10.154	5.538	17.231	13.538	16.538	14.462
D. aculeata	8.615	5.385	14.000	11.846	12.308	11.538
D. aculeata	10.000	5.538	16.462	13.231	13.846	14.615
D. aculeata	9.692	5.385	15.692	12.923	15.231	12.462
D. aculeata	8.462	5.077	14.000	11.385	11.538	11.231
D. aculeata	9.231	5.077	15.231	12.462	14.000	12.769
D. aculeata	8.769	4.769	14.769	11.692	12.308	12.769
D. aurita	10.615	5.846	16.462	13.385	16.000	14.462
D. aurita	9.231	5.385	14.923	12.154	13.538	13.385
D. aurita	9.385	5.077	15.077	12.154	13.846	12.615
D. aurita	9.692	5.385	15.538	12.769	14.000	13.077
D. aurita	10.615	5.846	17.077	13.692	15.692	15.538
D. aurita	9.692	5.077	15.692	12.462	13.692	14.000

D. aurita	9.692	5.231	15.538	12.923	14.923	13.692
D. aurita	9.692	5.231	15.692	12.308	12.769	12.615
D. aurita	9.692	5.538	15.385	12.308	13.231	13.538
D. aurita	9.846	5.385	16.154	13.077	14.923	14.462
D. aurita	9.385	5.231	15.692	12.308	13.692	13.077
D. aurita	10.000	6.154	16.154	12.615	15.538	15.077
D. aurita	8.769	4.923	14.000	11.538	13.077	12.308
D. aurita	9.231	5.385	15.231	11.846	13.692	13.846
D. aurita	10.000	4.923	16.154	12.615	15.385	13.846
D. aurita	9.231	4.769	15.692	12.308	14.462	14.000
D. aurita	10.000	6.000	16.769	12.615	14.769	14.154
D. bidens	6.308	3.077	12.462	8.462	10.000	9.231
D. bidens	6.462	3.077	12.769	6.923	10.000	10.000
D. bidens	6.923	3.077	13.385	9.385	10.769	10.615
D. bidens	6.154	2.923	12.000	8.462	9.692	9.538
D. bidens	6.462	3.231	13.231	8.615	10.000	10.615
D. bidens	5.385	2.769	10.308	7.231	8.308	8.615
D. bidens	5.538	2.615	10.769	7.077	8.154	8.000
D. bidens	6.154	3.077	12.154	8.154	9.231	9.231
D. bidens	6.769	3.538	13.692	8.923	10.462	10.154
D. bidens	5.538	2.769	10.769	7.538	8.769	8.923
D. bidens	5.385	2.615	10.769	7.385	8.462	9.231
D. bidens	5.846	3.077	11.538	7.692	8.769	8.923
D. bidens	6.154	3.077	8.308	9.231	8.615	9.692
D. bidens	6.308	3.231	12.308	8.615	9.846	10.000
D. bidens	5.846	2.923	11.538	8.000	9.846	9.077
D. cornigera	7.077	4.154	12.615	9.231	10.308	9.538
D. cornigera	9.385	5.385	18.615	12.308	14.923	14.615
D. cornigera	7.385	4.462	12.769	8.769	10.769	10.308
D. cornigera	9.231	5.231	17.846	11.846	14.615	13.692
D. cornigera	7.538	4.462	13.231	9.077	11.538	10.308
D. cornigera	9.077	5.231	17.231	12.000	14.769	13.077
D. cornigera	8.769	4.923	17.231	11.385	14.923	14.308
D. cornigera	7.077	4.462	12.154	8.769	10.462	9.846
D. moneorum	9.692	5.692	15.846	13.385	14.000	15.692
D. moneorum	8.615	5.231	14.154	11.692	11.692	12.923
D. moneorum	10.000	5.231	16.462	13.846	13.846	16.154
D. moneorum	9.385	5.538	15.231	12.923	12.923	13.846
D. moneorum	10.220	5.354	15.846	13.385	13.385	13.085
D. moneorum	9.004	5.224	15.711	13.385	12.392	15.485
D. moneorum	10.000	5.457	14.874	13.385	13. 925	12.385
D. parallela	5.077	2.769	9.385	7.077	8.308	8.308

D. parallela	5.385	2.769	8.615	6.615	8.000	7.692
D. parallela	5.538	3.231	9.538	7.077	8.462	8.462
D. parallela	5.538	3.077	9.385	7.538	8.000	7.692
D. parallela	5.385	2.769	9.077	7.077	8.308	8.000
D. parallela	4.692	2.615	8.308	6.000	7.231	6.769
D. parallela	4.769	2.615	8.308	6.615	7.231	7.231
D. parallela	4.923	3.077	8.462	6.462	7.538	7.385
D. parallela	4.923	2.615	8.615	6.308	7.538	7.385
D. parallela	5.385	3.231	10.000	6.923	8.154	8.615
D. parallela	5.538	2.615	9.692	7.385	8.769	8.769
D. parallela	5.692	2.923	9.846	7.385	8.923	8.000
D. parallela	5.538	2.923	10.154	7.385	8.769	8.769
D. parallela	5.385	3.077	9.385	7.231	8.615	8.615
D. parallela	4.615	2.769	8.000	6.154	7.077	7.231
D. parallela	4.923	2.923	8.308	6.769	7.385	7.077
D. parallela	4.692	2.462	8.308	6.308	7.231	7.077
D. parallela	5.692	3.231	10.154	7.692	8.923	9.231
D. parallela	5.231	2.769	9.231	6.923	8.000	8.000
D. parallela	5.077	2.769	8.923	6.615	8.000	7.692
D. parallela	5.077	2.615	8.462	6.462	7.538	7.231
D. parallela	5.077	2.923	9.231	6.615	7.846	7.769
D. parallela	5.538	3.231	9.692	7.077	8.154	8.615
D. parallela	4.769	2.615	8.308	6.308	7.385	6.923
D. parallela	5.692	3.385	10.308	7.385	8.615	8.769
D. parallela	4.769	2.923	8.000	6.154	7.231	7.077
D. parallela	5.077	2.923	8.923	6.462	8.000	7.538
D. parallela	5.692	3.077	9.231	7.077	8.308	8.154
D. parallela	5.846	3.231	10.000	7.385	8.308	8.154
D. parallela	5.385	2.615	9.385	7.231	8.462	8.000
D. parallela	4.769	2.769	8.154	6.154	6.769	6.923
D. parallela	4.769	2.769	8.154	6.308	7.231	7.231
D. parallela	4.462	2.308	7.846	6.154	6.923	6.923
D. parallela	5.182	3.091	8.818	7.000	8.273	8.273
D. parallela	9.231	2.909	9.455	7.273	8.182	8.636
D. parallela	9.154	3.091	8.364	7.091	7.818	8.000
D. parallela	8.308	2.909	8.364	6.818	7.455	7.455
D. parallela	7.692	2.818	8.591	6.545	7.455	7.545
D. parallela	8.923	2.909	8.909	7.091	8.455	8.091
D. parallela	9.385	3.364	9.636	7.455	8.727	8.909
D. parallela	8.308	2.636	8.455	6.636	8.000	7.455
D. parallela	9.308	2.818	9.273	7.545	8.636	8.364
D. parallela	8.308	2.636	8.545	6.545	7.318	7.818

D. parallela	9.385	2.818	9.727	7.182	8.182	8.455
D. parallela	9.385	2.909	9.182	7.364	8.182	7.727
D. parallela	8.154	2.727	8.000	6.545	7.455	7.455
D. parallela	8.615	2.727	8.727	7.000	8.273	8.364
D. parallela	9.077	3.182	9.364	7.182	8.364	8.636
D. parallela	8.923	3.091	9.091	7.000	7.727	7.545
D. parallela	9.077	3.364	9.545	7.364	8.545	8.273
D. parallela	8.000	3.000	8.000	6.000	7.455	6.545
D. parallela	9.385	2.818	9.091	7.455	8.727	8.364
D. parallela	8.769	3.000	8.455	7.000	7.273	7.455
D. parallela	7.231	2.545	7.182	5.455	6.545	5.545
D. parallela	7.692	2.727	7.909	6.000	6.909	6.455
D. parallela	8.154	2.818	8.545	6.364	7.818	7.182
D. parallela	7.538	2.727	7.636	6.182	6.727	6.545
D. parallela	10.923	4.000	11.091	8.182	9.273	9.364
D. parallela	9.385	3.000	9.273	7.000	8.182	8.182
D. parallela	9.538	3.000	9.455	7.091	8.182	8.000
D. parallela	7.538	2.727	7.636	5.636	7.000	6.364
D. parallela	8.769	3.182	9.273	6.727	8.182	7.909
D. parallela	9.846	2.909	9.636	7.545	8.636	8.636
D. parallela	9.846	3.636	10.273	7.545	9.000	8.636
D. parallela	9.077	3.000	9.455	7.091	8.182	8.273
D. parallela	8.308	3.000	8.182	6.364	7.455	7.273
D. parallela	7.846	2.818	7.909	6.000	7.273	7.182
D. parallela	8.308	2.727	8.182	6.091	7.182	7.364
D. parallela	8.000	2.727	8.000	6.182	7.182	7.273
D. pugionata	4.846	2.615	9.231	5.846	7.231	8.000
D. pugionata	5.846	3.077	12.000	7.385	9.538	10.000
D. pugionata	5.077	2.615	10.154	6.769	8.462	8.769
D. pugionata	5.231	2.615	9.846	6.769	8.308	8.308
D. pugionata	5.231	2.615	10.615	6.923	9.077	9.385
D. pugionata	5.231	2.923	10.769	6.769	8.308	8.615
D. pugionata	6.000	3.077	12.000	8.615	10.615	10.923
D. pugionata	4.923	2.462	9.154	6.000	7.692	7.846
D. pugionata	5.077	2.615	10.308	7.077	8.615	9.538
D. pugionata	5.385	3.077	10.923	7.385	8.154	9.692
D. pugionata	5.692	3.077	11.077	7.231	7.231	9.692
D. pugionata	4.769	4.000	9.077	5.846	6.615	7.538
D. pugionata	4.308	2.154	8.308	5.231	9.385	6.769
D. pugionata	5.538	2.923	11.538	8.154	8.462	10.308
D. pugionata	5.385	3.077	10.769	7.231	9.231	10.000
D. pugionata	5.538	2.923	10.923	7.385	7.692	9.846

D. pugionata	5.231	2.769	10.308	6.462	8.462	8.615
D. pugionata	5.538	2.923	10.462	7.231	8.308	9.231
D. pugionata	6.308	2.769	10.769	7.077	10.615	9.231
D. pugionata	5.231	3.231	12.308	8.769	8.000	10.923
D. pugionata	5.385	2.615	9.846	6.615	8.000	8.000
D. pugionata	4.923	2.615	10.769	7.231	7.538	8.923
D. pugionata	5.385	2.615	9.538	6.769	9.077	8.769
D. pugionata	5.538	2.769	10.308	7.538	8.615	9.846
D. pugionata	5.538	3.077	11.077	6.462	9.385	9.231
D. pugionata	5.231	2.769	11.846	7.385	8.154	10.923
D. pugionata	5.846	2.769	10.154	6.615	8.923	9.231
D. pugionata	5.846	3.077	11.846	7.231	10.154	10.154
D. pugionata	5.231	2.923	12.000	8.769	7.231	10.154
D. pugionata	5.692	2.615	9.692	6.000	9.538	7.538
D. pugionata	4.923	3.231	11.538	7.538	7.692	10.615
D. pugionata	4.308	2.615	8.000	6.462	7.077	8.615
D. pugionata	5.538	2.308	8.615	5.538	9.231	7.385
D. pugionata	5.231	2.769	10.769	7.231	8.923	10.154
D. pugionata	5.692	2.923	10.308	7.231	9.385	9.385
D. pugionata	6.154	2.923	11.538	7.538	10.462	9.846
D. pugionata	5.538	3.231	12.000	8.462	9.077	10.615
D. pugionata	5.385	2.923	11.692	7.385	8.462	9.692
D. pugionata	5.231	2.462	10.462	6.923	9.385	8.923
D. rileyi	11.231	6.425	18.615	14.308	15.231	15.538
D. rileyi	11.123	6.615	20.462	14.615	16.462	17.231
D. rileyi	10.154	6.000	17.385	13.692	14.769	15.385
D. rileyi	11.652	6.462	19.231	14.450	17.231	17.231
D. rileyi	11.72	6.512	19.500	15.231	14.852	16.031
D. rileyi	11.505	6.574	19.845	15.548	17.231	17.100
D. rileyi	11.458	6.100	19.794	15.222	16.940	16.924
D. yucatana	7.538	3.538	11.846	9.385	10.615	10.615
D. yucatana	7.385	3.692	11.231	9.077	9.846	10.154
D. yucatana	7.077	3.846	10.615	8.462	9.538	9.692
D. yucatana	7.385	3.692	11.692	9.077	10.462	10.615
D. yucatana	7.385	3.692	11.692	8.923	10.000	10.308
D. yucatana	7.077	3.692	11.077	8.615	9.538	9.846
D. yucatana	7.077	3.385	11.077	8.615	9.538	10.000
D. yucatana	7.846	4.000	12.308	9.692	9.692	11.538
D. yucatana	7.231	3.538	11.077	9.077	10.923	10.000
D. yucatana	7.385	4.000	11.538	9.231	10.308	11.231
D. yucatana	6.923	3.538	11.077	8.769	9.538	9.692
D. monoceros	5.077	2.615	9.692	6.769	7.538	7.846

D. monoceros	5.538	2.462	9.846	7.231	8.308	7.846
D. monoceros	4.923	2.308	9.231	6.000	7.231	7.385
D. monoceros	4.923	2.154	9.846	6.154	8.154	7.846
D. monoceros	4.769	2.308	8.385	6.154	6.615	6.308
D. monoceros	6.462	2.769	12.154	8.462	9.692	9.231
D. monoceros	4.923	2.462	9.077	6.154	7.077	6.769
D. monoceros	5.077	2.615	9.769	6.615	7.846	7.692
D. monoceros	4.538	2.308	8.615	5.385	6.308	6.462
D. monoceros	5.385	2.615	10.615	7.385	8.462	8.615
D. monoceros	5.077	2.154	9.538	6.769	7.538	6.923
D. monoceros	5.077	2.308	9.692	6.615	7.692	7.538
D. monoceros	6.462	2.923	12.615	8.615	10.154	9.846
D. monoceros	6.000	2.923	11.385	8.000	8.769	9.385
D. monoceros	5.077	2.462	9.077	6.154	7.538	7.846
D. monoceros	4.769	2.462	9.077	5.692	7.077	7.385
D. monoceros	5.231	2.769	10.308	7.231	8.000	8.462
D. monoceros	5.538	2.615	10.923	7.231	8.769	9.231
D. monoceros	5.538	2.462	10.308	7.077	8.154	8.308
D. ensifera	4.909	3.000	8.273	7.182	7.364	7.273
D. ensifera	4.727	2.818	8.000	6.636	6.818	6.909
D. ensifera	4.636	2.818	7.818	6.273	8.000	8.000
D. ensifera	5.091	2.909	8.364	7.273	6.727	7.727
D. ensifera	4.727	2.909	7.727	6.909	6.909	6.818
D. ensifera	5.364	2.818	8.636	7.636	8.000	7.909
D. ensifera	5.000	3.000	8.000	6.818	6.818	7.273
D. ensifera	5.091	3.273	8.000	6.818	7.455	8.364
D. ensifera	4.909	2.818	7.818	6.818	7.091	7.636
D. ensifera	4.909	2.909	8.455	6.818	6.455	7.091
D. ensifera	5.000	2.727	8.000	7.091	7.545	7.000
D. ensifera	4.727	2.909	7.545	6.818	6.182	6.727
D. ensifera	4.727	2.818	7.818	6.727	6.636	6.818
D. ensifera	5.182	3.000	8.091	6.727	6.455	6.818
D. ensifera	5.000	2.818	8.182	6.818	6.818	7.273
D. ensifera	4.636	2.818	7.636	6.864	6.545	7.000
D. ensifera	4.909	2.818	8.182	7.000	6.818	7.273
D. ensifera	4.818	2.818	8.182	6.909	6.818	7.455
D. ensifera	4.727	2.909	7.818	6.636	6.636	7.182
D. ensifera	4.545	2.000	7.273	6.455	6.545	7.000
D. ensifera	4.818	2.545	7.455	6.818	6.727	6.273
D. ensifera	4.818	3.000	7.455	6.818	6.727	7.091
D. ensifera	5.045	3.000	8.455	7.000	6.455	6.909
D. ensifera	4.364	2.818	7.000	6.455	6.545	7.273

D. ensifera	4.727	2.909	7.818	6.727	6.727	6.455
D. ensifera	4.909	3.000	8.182	6.818	6.545	7.273
D. ensifera	5.091	3.000	8.364	7.273	7.000	7.636
D. ensifera	4.818	2.909	7.727	6.636	6.364	7.000
D. ensifera	5.182	2.909	8.636	7.273	7.273	7.318
D. ensifera	4.909	2.909	7.818	7.091	7.091	7.182
D. ensifera	4.818	2.909	7.727	6.727	6.545	6.545
D. ensifera	5.091	2.818	8.273	7.182	7.364	7.091
D. ensifera	4.909	2.818	7.818	6.636	6.727	7.364
D. ensifera	5.091	2.818	7.818	7.818	7.909	8.727
D. ensifera	4.909	2.909	8.091	6.909	6.909	7.455
D. ensifera	5.455	3.182	8.727	7.364	7.545	7.727
D. ensifera	4.818	2.818	7.636	6.727	7.091	7.455
D. ensifera	5.136	2.818	8.273	7.455	7.273	7.636
D. ensifera	4.000	2.455	6.636	6.000	5.455	6.000
D. ensifera	5.091	2.909	8.182	7.182	6.818	7.455
D. ensifera	5.000	2.818	8.545	7.182	7.091	8.364
D. ensifera	4.545	2.727	7.409	6.364	6.455	6.273
D. ensifera	5.000	2.455	8.000	7.000	7.091	7.091
D. ensifera	5.000	2.909	8.182	7.091	7.091	7.364
D. apiculata	5.231	2.923	8.000	6.923	6.615	6.769
D. apiculata	5.531	2.923	8.000	6.923	6.615	6.400
D. apiculata	5.245	2.923	8.000	6.923	6.615	6.842
D. apiculata	5.231	2.923	8.000	6.923	6.615	6.769
D. apiculata	5.385	2.462	7.385	6.615	6.462	6.615
D. apiculata	4.308	2.308	6.769	6.000	6.000	6.308
D. apiculata	5.538	2.615	9.077	8.154	8.615	7.538
D. minima	6.154	3.538	9.538	7.692	8.769	8.308
D. minima	6.615	3.846	10.769	7.538	9.231	9.538
D. minima	7.538	4.154	10.551	8.769	10.308	9.541
D. minima	7.102	4.783	10.201	8.357	10.308	10.586
D. minima	7.512	4.102	10.400	8.769	10.308	9.254
D. minima	7.538	4.552	10.000	8.845	10.308	9.516
D. minima	7.200	4.154	11.000	8.121	10.308	10.154
D. rugosa	10.615	6.000	18.308	13.846	14.615	15.385
D. rugosa	10.462	5.538	18.462	15.077	15.385	16.154
D. rugosa	9.692	5.692	16.000	13.077	13.385	13.692
D. rugosa	10.308	5.692	18.154	14.615	16.154	15.385
D. rugosa	10.615	6.000	18.154	14.615	15.385	15.385
D. rugosa	10.308	6.769	17.538	14.462	15.231	15.538
D. rugosa	9.538	5.538	15.846	13.231	14.000	14.154
D. rugosa	10.154	6.308	17.231	14.000	13.846	15.231

D. rugosa	11.231	6.923	19.077	16.154	17.231	16.923
D. rugosa	11.231	6.923	19.077	16.154	17.231	18.308
D. rugosa	10.615	6.154	18.154	13.692	14.923	16.615
D. rugosa	9.692	6.154	17.077	13.231	13.692	14.615
D. rugosa	10.154	5.846	16.462	14.154	13.692	16.000
D. rugosa	12.000	7.077	20.000	16.462	16.923	18.462
D. rugosa	10.000	5.538	17.538	14.462	14.154	14.769
D. rugosa	10.308	6.308	17.538	13.692	14.308	14.308
D. rugosa	9.846	6.000	16.154	13.846	13.077	14.615
D. rugosa	10.000	6.154	18.308	13.385	14.308	15.077
D. rugosa	10.615	5.692	16.000	15.077	15.231	15.231
D. rugosa	9.385	4.923	16.308	13.692	14.154	14.154
D. rugosa	9.692	6.154	16.462	14.154	13.077	14.462
D. rugosa	10.154	6.154	16.923	12.923	14.308	15.385
D. spinosa	4.154	2.462	6.308	5.538	5.692	5.538
D. spinosa	4.692	2.769	7.231	5.692	6.077	6.308
D. spinosa	4.615	2.462	6.769	6.154	6.308	5.538
D. spinosa	5.308	2.615	8.000	6.923	7.077	6.769
D. spinosa	5.077	2.462	8.000	6.462	7.077	7.231
D. spinosa	4.615	2.462	8.000	6.308	6.077	6.308
D. spinosa	4.615	2.462	7.385	6.000	6.308	6.154
D. spinosa	4.615	2.769	6.846	5.846	6.000	6.462
D. spinosa	4.769	2.615	7.077	6.308	6.462	6.615
D. spinosa	4.615	2.923	7.231	5.692	6.000	6.308
D. spinosa	5.385	2.615	6.923	7.231	7.231	6.923
D. spinosa	5.077	2.462	8.308	6.923	6.615	7.077
D. spinosa	4.692	2.462	7.692	6.462	6.462	6.923
D. spinosa	5.077	2.769	7.538	6.462	7.077	6.769
D. spinosa	4.615	2.692	7.231	6.615	6.462	6.308
D. spinosa	5.000	2.769	7.231	6.923	7.538	6.615
D. spinosa	4.769	2.462	7.846	6.308	6.308	6.462
D. spinosa	4.769	3.077	7.231	6.308	6.308	6.462
D. spinosa	5.000	2.462	7.308	6.462	6.308	6.615
D. spinosa	4.769	2.615	7.538	6.462	6.462	6.308
D. spinosa	5.077	2.615	7.077	6.769	8.000	7.231
D. spinosa	4.769	2.462	7.846	6.462	6.462	6.615
D. spinosa	4.308	2.615	7.538	5.846	6.308	5.923
D. spinosa	4.462	3.077	6.923	5.231	5.692	6.000
D. spinosa	5.308	2.615	6.769	7.077	7.692	7.692
D. spinosa	4.615	2.769	8.462	6.308	6.308	6.462
D. spinosa	4.923	2.769	6.923	6.769	6.923	6.923
D. spinosa	4.923	2.923	7.692	6.923	7.308	7.077

D. spinosa	5.077	2.462	8.000	6.308	7.231	7.231
D. spinosa	4.769	2.769	7.846	6.615	6.615	6.615
D. spinosa	4.923	2.923	7.231	6.462	6.615	7.077
D. spinosa	4.923	2.923	7.538	6.615	6.462	6.154
D. spinosa	5.231	2.923	7.385	6.923	7.077	6.769
D. spinosa	5.231	2.615	8.000	6.923	7.538	7.538
D. spinosa	4.923	2.923	8.462	6.462	6.462	7.077
D. spinosa	5.077	2.769	7.077	6.462	6.923	6.308
D. spinosa	4.923	2.923	7.846	6.615	7.077	6.615
D. spinosa	5.231	2.923	8.000	6.615	6.462	6.615
D. spinosa	5.308	2.923	7.692	6.462	7.538	7.231
D. spinosa	5.231	2.615	8.462	6.923	7.692	7.231
D. spinosa	5.538	2.769	8.000	7.077	7.846	7.231
D. spinosa	5.231	2.923	7.385	6.769	6.923	6.923
D. spinosa	5.077	3.077	8.000	6.462	6.154	6.615
D. spinosa	4.923	2.769	8.000	6.769	7.385	6.769
D. spinosa	4.923	2.462	8.000	6.769	7.538	6.923
D. spinosa	5.231	2.923	7.692	6.923	7.077	6.923
D. spinosa	5.077	2.769	7.692	6.769	7.077	6.462
D. spinosa	5.385	3.231	8.462	7.077	7.077	7.231
D. spinosa	5.538	2.923	8.615	7.538	7.692	7.231
D. spinosa	4.923	2.769	7.846	6.462	6.462	6.308
D. spinosa	4.846	2.923	7.538	6.308	5.692	6.154
D. spinosa	4.923	2.615	7.538	6.769	7.231	6.308
D. spinosa	5.077	2.462	7.538	6.615	6.923	6.923
D. spinosa	5.385	2.769	8.154	6.923	8.000	7.692
D. spinosa	4.923	2.615	7.846	6.769	6.615	6.769
D. spinosa	5.231	2.769	8.000	6.769	7.385	7.077
D. spinosa	5.538	3.077	8.923	7.385	7.538	7.538
D. spinosa	5.077	2.923	7.846	6.923	7.231	7.231
D. spinosa	5.077	2.769	8.000	6.923	7.385	6.923
D. spinosa	4.923	2.615	7.231	6.462	6.462	6.462
D. spinosa	4.615	2.462	7.077	6.154	6.308	6.615
D. spinosa	5.308	2.923	7.846	6.308	6.923	6.692
D. spinosa	5.077	2.923	7.846	6.769	7.538	6.923
D. spinosa	5.077	2.923	7.846	6.308	6.462	6.615
D. spinosa	5.538	3.077	8.462	7.077	7.692	7.385
D. spinosa	4.769	2.462	7.692	6.923	7.077	6.615
D. spinosa	4.769	2.769	7.231	6.000	6.308	6.308
D. spinosa	5.231	3.231	7.692	6.615	7.077	7.538
D. spinosa	5.077	2.769	8.154	6.923	6.769	7.538
D. spinosa	4.923	2.615	7.231	6.615	6.769	6.615

D. spinosa	5.692	2.769	8.615	7.231	7.846	7.692
D. spinosa	4.615	2.308	8.154	7.077	7.692	7.385
D. spinosa	5.077	2.615	7.846	6.923	7.077	7.077
D. spinosa	5.385	2.923	8.615	7.231	7.385	7.077

Table S3: Environmental values extracted from principal components analysis, and used to calculate the environmental hypervolume of each genus.

Genera of the tribe Dorynotini	PC1	PC2	PC3
Dorynota	2.160717487	-0.683842063	0.146651223
Dorynota	3.222491503	1.188108683	-1.173117042
Dorynota	-4.347625732	2.502254725	3.551447392
Dorynota	1.110706568	-0.260135055	-0.632510424
Dorynota	2.77591753	0.466528952	-0.389748842
Dorynota	-4.499828339	1.482945204	-0.440833271
Dorynota	-3.06240344	-0.526823282	-1.676807046
Dorynota	2.080801487	-0.563340783	0.013816207
Dorynota	2.743959904	-0.090146042	0.520831466
Dorynota	-2.454711437	-1.076149821	-1.635972857
Dorynota	-2.57847023	0.899682879	-2.276895761
Dorynota	0.207375854	-0.174450487	1.157434106
Dorynota	2.885266304	0.801439703	1.33025682
Dorynota	0.661309183	-1.731092095	1.960820556
Dorynota	-0.446071655	-1.61284554	-0.844477177
Dorynota	0.490307778	-0.433484823	1.011810303
Dorynota	2.655630589	0.005264436	0.061372962
Dorynota	-3.152178288	-0.528999269	0.418224633
Dorynota	0.635997593	-1.101252556	-0.053010035
Dorynota	-0.454788774	2.049920797	-1.707583427
Dorynota	-1.221531391	3.687760353	2.273490667
Dorynota	1.17942059	1.094367146	0.577387691
Dorynota	-2.145944595	-0.703303039	1.171702385
Dorynota	-2.924150229	-0.642740846	-1.296611786
Dorynota	0.435538679	-0.79487896	-0.678055525
Dorynota	0.709317625	-0.577649236	1.113395929
Dorynota	-3.51823473	1.364067912	3.720723629
Dorynota	0.206510633	0.114455163	1.120776534
Dorynota	-2.083191395	-0.892129064	0.878891706
Dorynota	2.136711597	-0.008042546	0.098646186
Dorynota	-3.559484959	1.897653341	3.147813559
Dorynota	0.129325598	0.025514135	-0.268658668
Dorynota	2.839903355	1.148198485	0.281542659
Dorynota	-2.084222078	-1.581454873	0.842587948
Dorynota	0.417442411	-0.772439837	0.083327591
Dorynota	-1.500791669	3.476173162	3.207568407

Dorynota	0.17756933	-1.611426353	-0.703207195
Dorynota	-0.289845735	-0.250428855	1.265561938
Dorynota	-2.410963058	0.432559043	-2.441517353
Dorynota	-4.573923111	1.414452314	-0.727983594
Dorynota	-0.453257173	2.099392653	-2.08885622
Dorynota	0.027767988	-1.288893104	0.223128572
Dorynota	2.790606499	-0.192260459	0.458168089
Dorynota	1.576054573	-0.13620612	0.296220452
Dorynota	1.766161799	-0.759443164	0.778575659
Dorynota	-0.185676247	0.524401903	0.523239315
Dorynota	-1.561261058	1.161873102	-2.845009089
Dorynota	4.8435359	3.229712009	-1.58782208
Dorynota	1.520039201	1.130316377	1.125313878
Dorynota	3.688591719	0.042063594	0.706497848
Dorynota	-0.697748661	-1.336423755	0.99516809
Dorynota	1.890577674	-0.28611955	0.305650055
Dorynota	2.854225159	0.26854378	0.329788089
Dorynota	3.241285324	0.675483704	-0.268573791
Dorynota	-0.000940727	-1.442802668	-0.778175294
Dorynota	4.73585844	2.942363977	-1.652336717
Dorynota	1.403260827	-0.302218556	-0.545358956
Dorynota	0.854910433	-0.86859858	-0.514618099
Dorynota	-2.138366938	2.717291117	2.59426856
Dorynota	1.120169759	-1.22486937	0.641160309
Dorynota	1.114967465	-1.207242489	0.891988218
Dorynota	-0.226773128	3.460544825	-1.979548335
Dorynota	4.475766659	2.364629984	-1.353074431
Dorynota	0.884629667	-2.226742029	1.34663868
Dorynota	-0.770832062	-3.044690609	0.029277524
Dorynota	0.029092871	1.989206672	-2.800082684
Dorynota	2.922473192	0.626787901	-0.012470286
Dorynota	-2.670099974	0.077284001	-1.966097355
Dorynota	0.656736374	-0.614903867	0.112367727
Dorynota	1.695559144	-2.497190714	1.526550174
Dorynota	2.485901356	-0.16583702	0.877161503
Dorynota	0.717699528	-0.796004355	0.477499276
Dorynota	0.256100714	0.063518241	-0.555239737
Dorynota	0.733687937	-1.232678413	-0.332352132
Dorynota	-0.40814811	-0.616911173	-0.050529972
Dorynota	0.184225261	-1.01404047	1.240271449
Dorynota	-2.799288988	-2.51677084	-2.923262835
Dorynota	2.179011106	-0.125022441	-0.095559321

Dorynota	1.714983344	0.244425789	-0.511007547
Dorynota	0.563532829	-1.550171137	-0.219420463
Paratrikona	2.940686226	-0.61813283	-0.024214316
Paratrikona	-2.606433868	0.725618005	2.51607275
Paratrikona	3.342772007	-0.80607152	1.318124056
Paratrikona	-4.497088432	4.465332985	1.152300596
Paratrikona	-1.5433532	1.245481372	-2.900403023
Paratrikona	-4.5009408	1.499901056	2.532402515
Paratrikona	2.104436874	-0.579261184	1.131050229
Paratrikona	-1.514738917	1.475622773	1.989844441
Paratrikona	3.680289984	0.549762845	-0.035600498
Paratrikona	2.896120787	-0.073250078	0.703457475
Paratrikona	3.185506582	-0.54681617	1.155384064
Paratrikona	3.043774605	0.629833937	0.166836694
Paratrikona	4.377363682	3.522583485	-1.733361363
Paratrikona	3.010461092	0.424109489	0.255303979
Paratrikona	1.070874095	-1.4995085	0.253539532
Paratrikona	2.455085754	-0.771577656	1.113457799
Paratrikona	3.907623053	1.64085269	-0.670499802
Paratrikona	2.308876753	-0.533096433	-0.845386088
Paratrikona	-0.870043755	2.598694563	-2.009639502
Paratrikona	-2.440175056	-0.134579852	-1.640927434
Paratrikona	3.053599358	0.321000218	0.252289146
Paratrikona	1.680313945	-0.73796761	-0.110272624
Paratrikona	4.865039349	1.764383674	-0.840987742
Paratrikona	-0.506331623	1.632983923	-2.433238506
Paratrikona	1.233408928	-1.816822052	1.672736287
Paratrikona	0.970592082	-0.687621295	0.192681387
Paratrikona	2.792175293	-0.650675595	0.340358347
Paratrikona	-3.903101921	-0.128607422	-1.99172318
Paratrikona	0.326779187	-0.76849997	0.858145535
Paratrikona	1.058576107	-1.847586751	0.545448065
Paratrikona	-3.531318665	6.173923016	1.337443829
Paratrikona	1.483341932	-0.660309136	0.441183865
Paratrikona	3.369625092	0.019243199	0.158218592
Paratrikona	2.070703745	-0.640141547	1.328453541
Paratrikona	2.547025204	-1.43564868	0.827509403
Paratrikona	0.534637034	-0.115895912	-0.387412101
Paratrikona	0.967788339	1.824384093	1.974962234
Paratrikona	-4.402787209	-0.063138247	-1.967909932
Paratrikona	2.979066133	-0.064749248	0.500792921
Paratrikona	2.728738546	-1.501237512	0.576543927

Omoteina	0.907087088	8.717647552	-1.198122263
Omoteina	2.891217232	-0.727595866	0.377108842
Omoteina	3.433434248	1.334811091	-1.18579638
Omoteina	3.606654644	0.091598213	0.574865043
Omoteina	4.154444695	1.751636624	-0.774962068
Omoteina	4.596979618	3.512328386	-1.651243567
Omoteina	3.767888784	0.401762217	-0.137906849
Omoteina	4.121812344	2.67536211	-1.395738602
Omoteina	2.656768322	-1.417225957	1.005758524
Omoteina	2.132788181	-1.012810588	0.256781638
Omoteina	2.630461931	-0.37301296	0.286656529
Omoteina	3.742253304	1.963464499	-1.122656584
Omoteina	3.193135977	-0.598039627	1.152557373
Omoteina	3.15474391	-0.264733344	-0.185993686
Omoteina	1.730899572	0.916237593	-0.02131159
Omoteina	2.336292982	-1.309853911	1.12625885
Omoteina	1.772059321	1.576207876	-0.086323515
Omoteina	3.530268669	0.503456712	-0.036998004
Omoteina	3.163468599	1.317017555	1.01751709
Omoteina	2.717949867	-0.711594462	0.690328777
Omoteina	3.483008623	0.233811378	0.356589228
Omoteina	3.6216259	0.639050305	-0.225046247
Omoteina	4.249320984	3.089475393	-1.770909786
Omoteina	2.105811357	-0.799929023	0.620207548
Omoteina	3.349636078	0.530605972	-0.360183179
Omoteina	3.19172287	0.234412	-0.419435143
Omoteina	2.63081193	0.998826921	-0.610842407
Omoteina	3.204815626	1.051810145	-0.39780274
Omoteina	1.685715318	-2.468907118	1.498587132
Omoteina	1.457729816	-1.886445642	0.708660364
Omoteina	4.144622803	0.57999742	-0.618237436
Omoteina	2.935331821	-0.16581361	-0.083758518
Omoteina	2.393479586	-0.078843571	0.865160167
Omoteina	3.191621542	0.06724494	0.222296298
Omoteina	2.382138491	-0.507208347	0.618977249
Omoteina	1.965942979	-0.701084316	0.544935942
Omoteina	3.438491583	1.313124061	-0.969982982
Omoteina	2.945651293	0.334990472	0.484739602
Omoteina	3.590889215	-0.652157366	1.273104429
Omoteina	3.694276094	0.584692955	0.605253935
Akantaka	0.689405262	-0.941909015	0.862703145
Akantaka	-0.88219285	1.866538405	-0.89554733

Akantaka	0.66572988	-1.071849585	-0.569906175
Akantaka	-3.570836782	-2.267297506	-1.444820285
Akantaka	-2.785732746	4.776368141	0.906375766
Akantaka	0.585700393	-0.954380035	0.947127342
Akantaka	0.472875983	-1.209874153	0.778904021
Akantaka	-4.457966805	-2.553295374	-1.755360842
Akantaka	3.046734333	-0.597068906	-0.169439986
Akantaka	-2.841833115	-1.688669562	-1.531768918
Akantaka	2.256473303	0.963739216	-0.051857721
Akantaka	-2.604594707	-2.212085009	-1.745011687
Akantaka	3.56955266	0.486536562	-0.117263637
Akantaka	-0.27905947	0.67739749	-2.218659639
Akantaka	-5.942140579	3.303767681	2.157890081
Akantaka	-4.729735851	-1.565668464	-1.513498783
Akantaka	-1.386447906	4.056928158	0.483731568
Akantaka	4.496689796	2.327572823	-0.684491873
Akantaka	0.016241657	-0.899065554	0.763034761
Akantaka	-4.742344856	2.063722134	0.781752825
Akantaka	4.383394241	3.192693949	-1.582076788
Akantaka	-1.783825278	-1.744715571	-1.483559489
Akantaka	-0.448320031	3.192540646	-1.714174271
Akantaka	2.778079748	-0.197254777	0.084342748
Akantaka	-6.418259144	3.800798416	2.181259155
Akantaka	1.508824229	1.187882066	0.501608133
Akantaka	-6.785242081	1.186565399	3.823048353
Akantaka	2.943216324	0.288220108	0.492109895
Akantaka	0.691087723	0.511730611	0.082929745
Akantaka	-3.422060966	5.999722958	0.511854827
Akantaka	-4.5169034	-0.73741591	-2.111563921
Akantaka	-0.817619443	0.877942502	2.029953003
Akantaka	3.307427883	-0.01445526	0.068404451
Akantaka	-0.265158892	-1.051840425	0.862872183
Akantaka	-2.047694206	-1.818733335	-1.930006385
Akantaka	-0.910681725	4.802848816	2.367709637
Akantaka	-4.593752861	2.580102921	1.59941411
Akantaka	-0.748511434	-0.58090508	1.299360991
Akantaka	4.573727608	2.862555981	-1.859164476
Akantaka	3.864194632	2.347947836	-1.256936073

Table S4: Environmental values extracted from principal components analysis, and used to calculate the environmental hypervolume of each species.

Species of the tribe Dorynotini	PC 1	PC 2	PC 3
D. aculeata	-1.712426901	3.038529158	2.66493082
D. aculeata	4.89874506	0.364204466	0.838284075
D. aculeata	0.386327416	-1.656338215	-0.406795681
D. aculeata	3.077800751	2.103940487	1.02514565
D. aculeata	-4.921949387	2.668030739	0.15731512
D. aculeata	-4.068965912	-2.335612774	-1.890761256
D. aculeata	-0.329525948	1.321674228	-2.584608555
D. aculeata	-3.562934875	-0.436869383	-0.904733181
D. aculeata	3.7351408	-0.704627752	1.222819448
D. aculeata	3.183760166	1.322918773	-0.660581291
D. aculeata	3.060708046	0.346587569	0.199865967
D. aculeata	3.673196077	0.607950866	-0.041682158
D. aculeata	0.6885342	0.494217664	0.516033888
D. aculeata	2.666903734	-1.223541617	1.283714294
D. aculeata	2.683289766	-1.156803608	1.070363045
D. aculeata	-2.372172832	-0.075713977	-1.645170808
D. aculeata	5.174158096	3.575513124	-1.795558333
D. aculeata	-1.208811641	2.083225727	-2.133384943
D. aculeata	-0.275108993	-1.602240324	0.949239492
D. aculeata	-1.86363709	-3.263952017	-1.144080997
D. aculeata	2.820014954	0.771932721	-0.408765852
D. aculeata	3.267798185	0.329155654	0.345570028
D. aculeata	-4.963735104	-2.853136539	-2.468687534
D. aculeata	-4.546530724	-0.200204834	-2.027932405
D. aculeata	-3.359581947	0.763728976	-1.98975575
D. aculeata	-0.740495384	-0.343242735	0.962579668
D. aculeata	-5.030652523	1.133152366	-1.446613431
D. aculeata	3.666077852	-0.88078016	1.321601272
D. aculeata	2.986537218	0.23986423	0.41393432
D. aculeata	2.37941885	-0.803130805	1.252995014
D. aculeata	3.980564833	1.348163962	-0.411673039
D. aculeata	-0.907147348	1.747437954	-2.871883869
D. aculeata	0.943737268	-1.840245008	0.971501231
D. aculeata	-0.254318565	0.630362988	1.151614904
D. aculeata	0.79167074	-1.433579206	1.191634178
D. aculeata	3.176245689	0.961177528	-0.725519478
D. aculeata	0.892772615	0.03365878	2.14022398

D. aculeata	4.519609928	2.823056221	-1.27705586
D. aculeata	3.549815178	-0.396764636	0.445295691
D. aculeata	-4.321032047	4.206900597	1.127524018
D. aurita	-3.223269701	-2.25508976	1.946850419
D. aurita	1.395585895	-1.524022222	0.814360559
D. aurita	-1.601058125	-1.799745321	0.638719678
D. aurita	0.939900339	-1.920456171	0.811239302
D. aurita	-2.204907417	-2.111791134	-1.459587455
D. aurita	1.117848873	-1.827696085	1.132778049
D. aurita	2.412932396	-0.61495775	0.159896791
D. aurita	-1.910101771	-0.550377309	-2.097733736
D. aurita	0.427667409	-1.680033922	0.342965901
D. aurita	-3.27876997	-0.285301387	1.467702985
D. aurita	1.468975186	-1.473884702	0.776557446
D. aurita	-4.137392998	-2.273527384	-1.506233931
D. aurita	-1.597010016	1.536383986	-3.053117514
D. aurita	0.829754353	-1.742725253	0.872739017
D. aurita	-2.37604785	-1.589242339	-1.886155128
D. aurita	-3.06777668	-0.623622537	-1.201611757
D. aurita	-0.827118814	2.787963152	2.172111273
D. aurita	-3.168780088	-1.045304775	2.607977152
D. aurita	1.01278007	-1.468247175	0.52841574
D. aurita	-0.683360636	-1.340738058	0.981678963
D. aurita	-0.104285844	-0.49668777	0.335940719
D. aurita	1.612553358	-1.911663294	0.755144238
D. aurita	1.554195285	-1.719227791	0.830518901
D. aurita	-0.273295909	-1.580717921	1.075582743
D. aurita	1.480983138	-1.418518782	1.0002985
D. aurita	0.83812958	-1.632688403	1.034468532
D. aurita	1.610170722	-1.209207058	0.55108875
D. aurita	-2.434971809	0.788688302	-2.358433008
D. aurita	-3.711954594	-0.547571182	-2.213610888
D. aurita	-5.803647518	-0.070182085	2.208688259
D. aurita	-6.291242599	0.160665855	3.042360067
D. aurita	0.509401798	-0.545755088	1.025100231
D. aurita	-2.873545647	1.323899388	-1.936459899
D. aurita	-0.303186327	-1.445009232	1.075515032
D. aurita	1.110013008	-0.665311873	1.203379512
D. aurita	-4.599050999	-0.852467716	-2.041690111
D. aurita	1.250977993	-1.517521381	0.19848381
D. aurita	-4.193220615	-0.670719206	-2.162191868
D. aurita	0.90216887	-1.381888151	0.575998485

D. aurita	-1.13248837	2.936702728	2.875478268
D. bidens	0.753869712	-0.37214452	-0.435896784
D. bidens	-3.116764545	6.099059582	0.351669937
D. bidens	3.020220995	-0.056790274	0.30813092
D. bidens	0.028748214	-0.497738391	1.081978321
D. bidens	2.68231535	-0.485744655	0.619557083
D. bidens	-5.042443752	3.893243551	0.710934341
D. bidens	2.694615602	-0.368557304	0.422022104
D. bidens	3.190850973	0.37838307	-0.166942045
D. bidens	-4.092299938	4.792078495	0.548486173
D. bidens	-1.645516515	1.758997321	-2.566665411
D. bidens	3.714302778	0.947181225	-0.501079142
D. bidens	1.633895516	1.206759572	-1.301541448
D. bidens	1.77053678	-1.715870619	0.366731256
D. bidens	-0.591384649	5.018242359	1.974752307
D. bidens	1.782316327	-0.447979122	0.354084879
D. bidens	1.881001234	0.801270664	-0.127018362
D. bidens	-0.260131747	-0.684385121	-0.342977166
D. bidens	3.663216352	1.17776227	-0.282302707
D. bidens	-0.093852118	0.418464929	0.675029516
D. bidens	-4.00662899	5.572159767	1.395736337
D. bidens	-0.070288166	-0.080880299	-1.342778683
D. bidens	-0.487991452	1.372007132	0.306369424
D. bidens	3.13625741	0.559099734	0.21698159
D. bidens	1.937655449	-0.850291431	0.524684608
D. bidens	2.036514521	2.726294518	1.029958844
D. bidens	-0.42971018	2.690036297	-2.168826342
D. bidens	3.806729317	1.851417661	-0.792702556
D. bidens	-5.077837944	4.491211414	0.907202542
D. bidens	-3.076301336	0.235165313	1.501797438
D. bidens	3.25248909	0.674603105	-0.219755203
D. bidens	2.934571266	0.240272075	-0.214014202
D. bidens	0.823834479	2.927840471	1.516636372
D. bidens	2.34550333	0.694845617	1.147936463
D. bidens	-0.127118289	1.793789506	-1.721055865
D. bidens	4.096514702	0.591882467	-0.426948816
D. bidens	2.518585443	-0.976374865	0.869046152
D. bidens	3.616782427	0.074778058	1.019350767
D. bidens	-0.506634593	0.180542663	0.567768514
D. bidens	-1.223153591	3.812111616	2.602607489
D. bidens	-2.586660385	4.650015831	-0.282344162
D. cornigera	-5.704860687	0.121516459	2.578589916

D. cornigera	1.444477201	-1.55523932	0.710567415
D. cornigera	1.985092282	-1.031596899	0.71669066
D. cornigera	0.731247783	-1.090624571	2.061140299
D. cornigera	3.842588663	0.894117653	-0.103285693
D. cornigera	-1.484368682	-0.113936	1.808356285
D. cornigera	3.828937054	1.265832424	-0.687566817
D. cornigera	1.740489244	-1.106466055	0.470376223
D. cornigera	0.723139107	-0.579497218	1.201541662
D. cornigera	0.590285361	-1.392542958	0.073434964
D. cornigera	3.62661624	0.772916734	-0.125531077
D. cornigera	1.545945406	-2.022297144	0.759682596
D. cornigera	0.440464854	0.39427492	1.180547476
D. cornigera	0.135082901	-0.634689152	0.837786376
D. cornigera	3.912763834	0.156255871	0.031799439
D. cornigera	0.138358399	-0.44873336	1.162253857
D. cornigera	-5.76132822	0.64730078	3.679658413
D. cornigera	-0.335975707	2.430623055	-2.774692297
D. cornigera	1.685763836	-0.245531321	0.207960278
D. cornigera	-2.036936522	-1.6831671	-2.518415928
D. cornigera	3.685111284	0.869960964	-0.298022598
D. cornigera	3.361448765	0.009512149	0.242111698
D. cornigera	3.07752943	0.028749662	0.276853293
D. cornigera	2.770445347	-0.608084977	0.576112568
D. cornigera	1.795263886	-0.311441839	0.33275789
D. cornigera	-5.62006712	-0.236103639	1.952889204
D. cornigera	1.635787845	-1.44729054	0.706541181
D. cornigera	3.469761133	1.418682814	-1.192473292
D. cornigera	2.112345219	-0.84785831	0.17814216
D. cornigera	-0.363698959	6.485514164	-0.40974018
D. cornigera	2.724751234	0.1281555	0.623548806
D. cornigera	4.323094845	2.325524092	-1.242584944
D. cornigera	3.966976404	0.091333762	0.617894292
D. cornigera	-0.353594601	-0.211266786	0.597319782
D. cornigera	3.389992714	-0.976940095	1.427477598
D. cornigera	3.21014595	0.324772209	0.16523768
D. cornigera	-1.763029337	1.228562474	-2.458537579
D. cornigera	2.861102343	-0.259356022	0.265039921
D. cornigera	-2.67421174	0.883928716	-0.382731974
D. cornigera	-0.129394084	-0.478955388	1.296875119
D. moneorum	0.715120196	-1.079673886	-0.541078866
D. moneorum	-0.237273201	-2.202604771	0.502665162
D. moneorum	1.245552421	-1.493077159	0.691492498

D. moneorum	1.578385472	-0.827248871	-0.092114411
D. moneorum	-0.537742198	-0.205079585	-0.495682895
D. moneorum	-4.89319849	-0.508169532	-0.260685951
D. moneorum	0.012158725	-1.336535454	-0.482811749
D. moneorum	-5.066021442	2.656597853	-0.018754277
D. moneorum	-0.595250189	0.34588778	-0.730837286
D. moneorum	0.551586926	-0.944303393	-0.273721069
D. moneorum	3.659355879	0.618729353	0.011866901
D. moneorum	5.050326347	2.369782686	-1.314041853
D. moneorum	0.16139023	-1.617874026	1.180094957
D. moneorum	-1.381193399	-1.903413653	-1.169743657
D. moneorum	-2.442377806	-0.400235415	0.48315841
D. moneorum	-5.824107647	3.086420536	2.961401224
D. moneorum	-5.403342247	2.967634916	4.153562546
D. moneorum	-0.323901385	-0.512214661	0.538248122
D. moneorum	-1.056206346	2.534054518	2.001389027
D. moneorum	1.123185992	-1.135996103	-0.043996401
D. moneorum	5.075049877	0.957435012	0.820338249
D. moneorum	1.299908876	-1.033697009	-0.139571026
D. moneorum	1.694161654	-0.57434684	0.451432496
D. moneorum	-3.493005991	-2.273782015	-2.178673029
D. moneorum	-0.049917296	-0.98572278	-1.687432408
D. moneorum	-5.013402462	2.622616768	0.057620637
D. moneorum	1.467404485	-0.352452517	-0.660404325
D. moneorum	-5.343673229	1.237671018	-1.14210546
D. moneorum	1.428159595	-0.741765738	-0.345172197
D. moneorum	2.553020477	0.757314563	1.866193891
D. moneorum	1.659054518	-0.962771416	0.537697852
D. moneorum	-1.039924622	-2.105372667	-1.57112968
D. moneorum	1.892178297	-1.915430069	0.812901199
D. moneorum	-3.020804167	-0.768719792	0.463267297
D. moneorum	-5.8831563	2.994220018	4.043285847
D. moneorum	1.073190093	-1.834490299	0.804003537
D. moneorum	1.43726325	-0.632432878	0.513254464
D. moneorum	1.719951153	0.09912876	1.481934309
D. moneorum	0.672955334	-1.33824718	-0.480115771
D. moneorum	-3.623786926	2.081105471	3.437127352
D. parallela	-1.802979589	-1.652154446	0.691694856
D. parallela	-1.20476532	-0.561814189	-1.932533741
D. parallela	2.184324265	-0.804173827	0.10291937
D. parallela	-4.233384132	1.159372449	-0.903718591
D. parallela	1.411799312	-2.393663406	1.543362856

D. parallela	-1.290927052	2.22393012	-1.852617145
D. parallela	-0.910089254	0.940160573	-1.247984648
D. parallela	3.207748413	0.720233619	0.058532074
D. parallela	3.919845343	0.753997684	-0.195497528
D. parallela	-4.985341549	0.345866799	-1.906178355
D. parallela	3.48893857	0.466857255	-0.244067803
D. parallela	0.6407215	-0.174681976	0.071478285
D. parallela	2.172340393	-0.772157848	0.091716051
D. parallela	0.178535029	-1.267077804	1.03948772
D. parallela	3.72119832	0.163220644	0.564648509
D. parallela	2.340847254	-0.742519557	-0.092608497
D. parallela	-1.289166689	-2.106160164	1.503667831
D. parallela	-1.81880796	-1.578863621	1.019072533
D. parallela	3.50733161	0.608567715	0.024835553
D. parallela	-2.94045496	-0.610402763	-1.40198946
D. parallela	0.204967722	-0.291171402	0.229912341
D. parallela	-4.011235237	4.952739716	1.23463285
D. parallela	4.220780849	0.918498516	-0.199081838
D. parallela	1.614001155	-0.493683428	-0.179146841
D. parallela	3.471892357	-0.106392376	0.801056087
D. parallela	2.709004402	-0.278457552	0.648573875
D. parallela	2.604670286	-0.366904527	0.425648123
D. parallela	4.861830711	2.605904818	-1.564028859
D. parallela	-0.347681314	0.666010976	-1.818171501
D. parallela	1.376728535	-1.254915595	0.946246684
D. parallela	-2.319262266	-2.987159491	-0.899937868
D. parallela	-0.465468913	-0.400125682	0.86622566
D. parallela	-2.766324043	-1.79842937	-1.412571788
D. parallela	0.882591009	-1.673502445	2.175987482
D. parallela	1.387722015	-1.890369534	0.636493385
D. parallela	1.545941114	0.379966438	-0.082902879
D. parallela	-0.128385976	-0.199300364	2.016491652
D. parallela	0.921086431	-0.671133339	0.133729845
D. parallela	-2.276373148	0.042008061	-0.142977774
D. parallela	1.816356063	-0.577127934	0.127108023
D. pugionata	-0.003546383	-0.66140002	0.964984655
D. pugionata	2.819382906	-0.146961689	0.197684884
D. pugionata	2.923972845	0.576492488	-0.169325233
D. pugionata	2.878895998	0.089627363	0.38989532
D. pugionata	2.151789188	-0.021544477	-0.586670756
D. pugionata	-3.081554413	-1.295894146	-1.190862775
D. pugionata	2.434484005	-0.636103451	0.423541665

D. pugionata	3.374368429	0.559340358	-0.197190613
D. pugionata	-0.949545264	1.120333672	0.811753631
D. pugionata	3.697885752	1.163539171	-0.54750061
D. pugionata	0.701235592	0.167748064	-0.795084059
D. pugionata	-5.663070679	0.346463025	3.354137421
D. pugionata	-4.408370018	-0.123451009	-2.037857771
D. pugionata	-2.768455029	-1.171675801	-0.528657377
D. pugionata	-0.107472502	-0.112661667	0.86034739
D. pugionata	2.578079462	-0.515203536	0.427507252
D. pugionata	0.620518744	-0.874915123	-0.395754933
D. pugionata	2.803275108	0.025149209	0.636798859
D. pugionata	-0.943500161	-1.812990308	-0.824935853
D. pugionata	0.580296755	-0.252683491	-0.603059053
D. pugionata	2.347578049	-0.529776335	0.114183709
D. pugionata	3.175335407	0.002354872	0.242573678
D. pugionata	-0.396758109	-0.210157737	1.19927001
D. pugionata	0.77041769	-0.705718279	-0.214432999
D. pugionata	3.649665833	0.734981358	-0.170842037
D. pugionata	3.013098001	0.909183681	-0.753575683
D. pugionata	-0.332894176	-1.575717211	-0.918777287
D. pugionata	-0.423604071	-0.65925914	1.136993527
D. pugionata	2.062822104	-0.149110183	0.563481927
D. pugionata	-0.261527836	-1.334057689	-1.463426828
D. pugionata	2.272753954	-0.081914611	1.017500281
D. pugionata	0.347545147	0.20748058	-0.323125571
D. pugionata	-3.133000851	-0.083778247	1.643269658
D. pugionata	3.108604908	1.022339225	-0.432911813
D. pugionata	-3.090556622	-0.842486799	0.385724783
D. pugionata	-4.103758812	0.541040719	-1.869367838
D. pugionata	2.326383114	0.210438207	-0.090456776
D. pugionata	0.304862887	-1.211510301	-0.535088658
D. pugionata	-4.472745895	-0.896032751	-1.66148901
D. pugionata	-4.048094749	0.235086665	-1.918019414
D. rileyi	3.365027428	0.145668134	0.749087811
D. rileyi	-2.254102468	5.944205284	0.09780544
D. rileyi	3.45739913	0.809223235	0.909016371
D. rileyi	1.734630585	-1.780143976	0.459142983
D. rileyi	-0.440518767	2.616439342	-2.201820374
D. rileyi	3.488502264	0.424003512	-0.200789079
D. rileyi	2.652154446	-1.164670348	0.478182346
D. rileyi	-3.426678419	2.154229403	1.069496155
D. rileyi	1.334303737	-0.122454613	-0.57136327

D. rileyi	3.040574789	-0.670430839	-0.452023447
D. rileyi	2.561170101	1.587659717	1.131213784
D. rileyi	2.560326338	-0.875452042	0.402951092
D. rileyi	2.629674196	-0.789765656	0.751465738
D. rileyi	-3.497675657	3.676136017	1.115808964
D. rileyi	1.764959335	-0.698699117	-0.70658958
D. rileyi	1.624609113	-0.746281028	-0.135893002
D. rileyi	3.530693054	1.03809464	-0.295130104
D. rileyi	-0.208971769	-0.149400666	-1.898440719
D. rileyi	2.986734867	0.733683765	-0.017248586
D. rileyi	3.963568687	0.862878621	-0.264102399
D. rileyi	3.488194942	0.872163057	-0.642119825
D. rileyi	0.38016215	-1.203322649	-0.948797464
D. rileyi	0.163042963	1.459780097	-1.60872817
D. rileyi	3.334758759	-0.265209496	0.194770291
D. rileyi	-0.604655325	2.323535681	-2.321131229
D. rileyi	-0.424337029	0.863253713	0.419574797
D. rileyi	4.369076729	-0.078451678	1.088114858
D. rileyi	3.647943258	0.725441456	-0.306940168
D. rileyi	-0.661281288	6.572976589	-0.614944935
D. rileyi	0.561882794	-0.766693652	0.076599471
D. rileyi	3.217776299	0.283786893	-0.079929344
D. rileyi	-4.504585743	4.102663517	0.991687
D. rileyi	2.432660818	-1.769919872	0.704649568
D. rileyi	2.603933096	-1.005614758	1.189670086
D. rileyi	-3.091164351	4.86920023	-0.15287976
D. rileyi	3.038702726	-0.411567241	0.341203064
D. rileyi	5.207406044	2.229052544	0.901397347
D. rileyi	-2.020047188	0.08929906	-1.007601976
D. rileyi	0.606673837	2.205569744	2.633021116
D. rileyi	0.380879313	-1.779847383	-0.278178602
D. yucatana	3.399015903	0.528425813	0.064402044
D. yucatana	1.899611354	-1.921083093	0.804320931
D. yucatana	-4.905813217	0.629212618	-1.682274818
D. yucatana	3.466868639	-0.868549705	1.351037621
D. yucatana	-2.051433086	-1.722182512	-0.624157488
D. yucatana	0.664136648	-0.819761515	0.090194546
D. yucatana	2.264621973	1.388450503	-0.966102302
D. yucatana	3.696202993	0.21573706	0.560155571
D. yucatana	-3.884236574	1.838841796	2.959642887
D. yucatana	-2.927882433	-0.657770038	-1.193442345
D. yucatana	-1.90139997	-1.467640162	-0.285376251

D. yucatana	3.451903343	0.801944137	-0.173164234
D. yucatana	-0.214237869	0.405978441	-2.189277411
D. yucatana	1.596663952	-1.787538767	0.793341339
D. yucatana	3.888985634	0.795063674	-0.233368695
D. yucatana	3.546499491	1.265071273	-0.273232281
D. yucatana	4.314805031	2.477794647	-1.24149406
D. yucatana	-1.312054038	3.810257435	0.011327239
D. yucatana	2.95075345	-0.407581568	0.454966992
D. yucatana	5.042959213	3.371458054	-1.790258646
D. yucatana	3.970841885	0.34566471	-0.065953068
D. yucatana	0.407400489	-1.331632495	0.615161359
D. yucatana	4.405728817	2.630912066	-1.663360596
D. yucatana	6.247490406	3.886011362	-1.293359756
D. yucatana	-1.77548027	-0.323335439	-2.185975552
D. yucatana	-0.61738342	0.156443909	-0.202781171
D. yucatana	1.21952498	-1.515319824	0.797930241
D. yucatana	3.386509418	0.287157863	0.195388451
D. yucatana	-0.615011394	0.010458744	-2.66937685
D. yucatana	-0.419426441	0.734064996	-1.451235533
D. yucatana	1.894235492	-0.293062299	0.723682702
D. yucatana	1.283523798	-1.549353838	0.69513309
D. yucatana	2.230735779	-1.037147522	0.494123757
D. yucatana	3.691802979	0.603453517	0.000570545
D. yucatana	-1.261991739	1.523012996	-1.324169755
D. yucatana	-3.502690077	0.197011188	-1.882180452
D. yucatana	4.161304474	2.95801425	-1.977455139
D. yucatana	-1.323275566	-3.141470671	-0.533112109
D. yucatana	-3.055147171	0.967431664	1.724180222
D. yucatana	-0.879958987	-3.184425116	1.749220729
D. monoceros	2.976541996	0.549679279	0.034309898
D. monoceros	3.301778078	1.499832988	-0.862444818
D. monoceros	-2.76089859	3.097848892	3.15795064
D. monoceros	0.144089967	-1.25494945	0.677035391
D. monoceros	1.588104606	0.129514918	-1.299758315
D. monoceros	-0.490579009	1.145224094	3.025582552
D. monoceros	0.782603025	-1.298564911	-0.369224429
D. monoceros	-4.311241627	-0.167941272	1.02971971
D. monoceros	1.438148975	-0.630356073	-0.281625122
D. monoceros	-2.721757889	-0.348050356	-1.719698787
D. monoceros	2.249140024	0.044569891	-0.217288136
D. monoceros	2.047623873	-0.792844772	0.480655402
D. monoceros	1.359769225	-0.418353111	-0.422978699

D. monoceros	-1.912536025	-0.567436099	-2.075406075
D. monoceros	-0.309216797	1.081425309	-2.372395992
D. monoceros	-0.132967308	-1.146981239	-1.572137356
D. monoceros	-0.271365047	0.043907501	0.08085493
D. monoceros	0.389965981	-1.225463748	1.336427808
D. monoceros	0.100559376	-1.160280704	0.583513439
D. monoceros	-3.170912504	0.01047203	1.35668242
D. monoceros	-3.429423809	5.324690342	0.637591481
D. monoceros	3.092650414	1.114652514	-0.518061101
D. monoceros	0.595936596	-0.455555111	0.808770061
D. monoceros	-1.122159839	2.80656147	1.725049257
D. monoceros	0.781524658	-0.04169495	-0.547152758
D. monoceros	1.156009674	-0.35717997	-0.725255311
D. monoceros	-3.883150339	1.241345286	-0.53471756
D. monoceros	-1.646255612	-1.634331703	-1.468019843
D. monoceros	2.944181442	-0.033955395	0.803003311
D. monoceros	-0.114785723	-0.479569167	0.697209418
D. monoceros	-3.452941179	0.775156677	3.159131289
D. monoceros	0.881557345	1.029756546	-0.268159896
D. monoceros	-2.441694021	6.05146265	0.678336203
D. monoceros	1.751548648	2.750278234	1.14521718
D. monoceros	1.091166019	-0.303886026	0.94054687
D. monoceros	-5.577650547	2.884577751	3.913733482
D. monoceros	-1.576114893	-0.410162956	-2.065324545
D. monoceros	0.383605719	-0.977454603	0.516263723
D. monoceros	2.22094202	-0.355685085	-0.024457606
D. monoceros	4.082550049	1.462750793	-0.573888063
D. ensifera	-3.522612572	0.60718739	-1.704552412
D. ensifera	-2.775925636	-2.508175373	-2.960489273
D. ensifera	-1.430830359	2.233408928	-1.813066363
D. ensifera	0.683361471	-1.042686105	-0.431392521
D. ensifera	1.471925855	-1.26365602	1.003344178
D. ensifera	-1.890057325	2.304499626	-2.093695879
D. ensifera	-0.338683397	-0.226244748	0.68381691
D. ensifera	2.933598042	-0.568380058	1.248601198
D. ensifera	-5.850311756	2.703196287	2.157356977
D. ensifera	0.627509296	-1.771493316	-0.067249976
D. ensifera	-4.839889526	2.003630161	-0.532826006
D. ensifera	2.163403988	-1.169262171	0.687844276
D. ensifera	-5.805427551	2.506262541	0.516782641
D. ensifera	2.246669769	-0.689374983	0.571399093
D. ensifera	3.357093334	0.244382605	0.089495644

D. ensifera	-6.282464981	0.417137206	2.271901608
D. ensifera	2.084219694	-1.842324853	1.066656113
D. ensifera	0.414527267	0.348681539	1.854946852
D. ensifera	-4.885773182	0.675888062	-1.621911526
D. ensifera	-1.136942267	4.496357918	0.155066192
D. ensifera	2.659065247	-0.287472457	0.842713952
D. ensifera	1.273195505	-1.841064095	0.534594774
D. ensifera	2.682262897	-0.145174593	0.908238113
D. ensifera	-0.381873578	-0.861178041	1.091393471
D. ensifera	3.760490179	0.404649496	-0.090343371
D. ensifera	-0.534573078	-0.734603047	0.683913589
D. ensifera	0.02466994	-1.3163234	0.637582779
D. ensifera	3.841668844	0.456521571	-0.065827079
D. ensifera	-2.009270906	-1.927319646	-1.600835919
D. ensifera	1.797057748	-1.525119543	0.89266175
D. ensifera	0.473404557	-1.146057844	-0.585598409
D. ensifera	-0.437895328	0.416222364	-2.45041275
D. ensifera	-3.343561411	0.315100044	1.793380499
D. ensifera	-5.174077511	0.45659861	2.780941486
D. ensifera	2.359122038	-0.908123672	1.364761472
D. ensifera	1.976707339	-1.24473381	0.281230301
D. ensifera	-5.327617168	2.001369476	0.876902103
D. ensifera	-0.521748781	-0.117447414	0.529315352
D. ensifera	-0.458034813	-2.183468819	0.713962018
D. ensifera	-0.614371002	0.834554911	0.722590804
D. apiculata	-1.285785675	-0.107857212	-2.258304834
D. apiculata	2.26058054	-0.204898953	1.069226623
D. apiculata	3.916347742	1.357767701	-0.568680763
D. apiculata	-1.784618974	1.981675267	-2.252316713
D. apiculata	3.289459467	1.537173033	-0.854782462
D. apiculata	-2.012987375	-0.373826742	0.531852067
D. apiculata	1.968739152	-0.85894978	0.566287041
D. apiculata	-2.577850103	1.467435837	2.282667637
D. apiculata	-1.470029354	-1.164647222	-1.87364471
D. apiculata	-0.990043819	-1.119760394	-1.937374115
D. apiculata	-3.827400923	4.991635323	1.213000655
D. apiculata	-3.055211306	-0.591901004	0.589125574
D. apiculata	-0.199455172	0.23957324	0.476827502
D. apiculata	2.750545025	0.678193212	-0.307453275
D. apiculata	-3.354334354	-0.912430346	0.081104852
D. apiculata	-3.028759956	-0.943605423	-1.097315311
D. apiculata	2.178122282	-0.770337522	0.487452954

D. apiculata	-1.402636766	-0.861370385	-1.851754069
D. apiculata	2.692507744	0.025421837	0.447359711
D. apiculata	-5.222430706	3.28071475	0.389440656
D. apiculata	2.639236212	0.537805676	0.74804318
D. apiculata	2.275761604	-0.441929013	0.123404093
D. apiculata	-1.610613108	1.274357557	-2.933562756
D. apiculata	-5.629462719	-0.040875658	1.927745819
D. apiculata	1.859256744	-0.49344182	0.385702014
D. apiculata	2.755827188	-0.490338862	0.477517992
D. apiculata	-2.955476284	-0.586865962	-1.449917436
D. apiculata	2.691904068	0.618279696	-0.440391421
D. apiculata	-1.674230337	-1.344843864	-2.288284779
D. apiculata	1.950085878	-0.959345877	0.288485944
D. apiculata	-2.960026979	0.657976568	-1.976142168
D. apiculata	3.240742683	0.642166913	-0.086108945
D. apiculata	2.814657688	-0.853535831	0.369352549
D. apiculata	1.468063951	-1.304163694	0.994201422
D. apiculata	-2.954427481	2.791606188	3.080189228
D. apiculata	-0.49116075	-0.246336862	-0.33931908
D. apiculata	-3.927762985	6.883266449	0.971280456
D. apiculata	0.917505205	-0.902473629	1.162039638
D. apiculata	-0.592520356	4.879990578	0.474788398
D. apiculata	-3.062609196	1.251338124	2.521998405
D. minima	-3.413470268	0.679403245	-1.712381005
D. minima	1.360066414	-0.859476626	0.210212305
D. minima	2.073651791	-0.788099468	0.525266111
D. minima	1.062577844	-2.105506897	0.625645638
D. minima	-4.218405724	-2.977527618	-2.651711941
D. minima	-2.993154287	-0.597127557	-1.277976274
D. minima	10.6115551	7.623424053	-4.074031353
D. minima	2.1268332	-0.689525664	0.475359946
D. minima	-2.767484665	0.324581057	-2.128599644
D. minima	4.122885227	0.456225961	-0.110976137
D. minima	5.154314518	3.726817846	-2.039506912
D. minima	0.668306947	-1.118576527	-0.539116085
D. minima	-5.087824821	1.141698599	-1.331477404
D. minima	1.896737814	-0.197495908	-0.008575536
D. minima	2.770005703	-0.482562512	0.492858976
D. minima	1.860862374	0.908994198	0.366886467
D. minima	-2.495183945	-2.275254965	-1.44946146
D. minima	-5.294082642	2.738992691	-0.158345863
D. minima	-1.426059008	0.113149136	-2.268635511

D. minima	-0.15032576	-2.258138657	0.693384469
D. minima	0.661963046	-1.076596975	0.218481824
D. minima	2.68999052	0.461029053	-0.74696672
D. minima	3.469384193	-0.372436941	0.106116779
D. minima	4.229215145	2.049554825	-1.07882762
D. minima	1.856317878	0.854361773	1.058666706
D. minima	2.769355536	0.865997136	-0.441002697
D. minima	0.645794153	-1.340499282	0.878127456
D. minima	1.34466064	-0.567593634	0.362699717
D. minima	4.046407223	1.503848076	-0.557347178
D. minima	-1.253350258	1.042425513	-2.95462966
D. minima	4.070641518	2.273304701	-1.461405277
D. minima	0.568154752	-1.066167951	0.811881661
D. minima	0.510965347	-1.266219258	-0.535112321
D. minima	-5.115084648	0.337388515	2.609283924
D. minima	3.313955307	0.396090448	0.122779146
D. minima	-2.348567486	-3.612421513	-1.411676645
D. minima	0.642918408	-1.613892913	0.680018246
D. minima	0.600223839	-2.049513578	0.572677195
D. minima	3.351237059	0.144305691	0.112181589
D. minima	4.483979702	3.256629705	-1.700822115
D. rugosa	-5.020782471	1.58685565	2.437778234
D. rugosa	-4.128796577	1.577983856	2.856608391
D. rugosa	4.82959795	1.661463141	0.065110721
D. rugosa	4.068727016	2.155040741	-1.199909687
D. rugosa	2.082445383	-0.562993824	0.787526965
D. rugosa	-2.798833609	0.563345671	-2.151346445
D. rugosa	2.060447931	-1.039672256	0.257993847
D. rugosa	0.04261275	-1.531059504	0.964527786
D. rugosa	3.898683786	0.133194983	0.006967841
D. rugosa	0.095964275	-1.000170469	1.165039063
D. rugosa	-3.196964741	0.290821701	-2.016277075
D. rugosa	-3.441362858	0.196754619	1.285365224
D. rugosa	-1.805056214	2.332343102	-1.691901088
D. rugosa	2.836849213	1.489813447	-0.005145443
D. rugosa	3.68333149	1.560463548	-0.673612475
D. rugosa	-2.123007536	-3.715573072	-1.559693575
D. rugosa	3.180412054	-0.51434505	0.220041156
D. rugosa	-2.975414038	-0.716508925	-1.502367973
D. rugosa	4.187573433	2.357042313	-1.225017428
D. rugosa	0.963136196	0.892767608	-0.736282468
D. rugosa	-0.388264835	-0.617059708	0.736438036

D. rugosa	2.822688341	0.528477728	-0.057984188
D. rugosa	1.979442835	-0.747923553	0.34552601
D. rugosa	0.354896903	-0.589743972	0.921387672
D. rugosa	-0.297090411	0.438057721	-2.516535282
D. rugosa	-1.592762351	1.101033092	-2.829599619
D. rugosa	3.866202116	0.718400419	0.291270286
D. rugosa	-1.081897616	2.990077019	-1.446716666
D. rugosa	0.735651731	-0.925378203	-0.410077929
D. rugosa	-3.644694328	0.55527091	2.064631701
D. rugosa	0.648937941	-0.719729781	0.684854209
D. rugosa	2.609362841	-0.459297687	0.973226607
D. rugosa	-2.619932652	-0.649203241	0.835216701
D. rugosa	0.708377004	-0.015531017	-0.23286362
D. rugosa	0.663710833	-0.605231166	0.541342437
D. rugosa	1.540028095	-0.286985129	0.19806923
D. rugosa	3.833209515	1.283198237	-0.326864094
D. rugosa	3.285163879	0.502473474	-0.311972558
D. rugosa	-0.39449504	-0.42078802	0.707368195
D. rugosa	0.417508364	0.321927518	-0.971364498
D. spinosa	-0.746993721	-0.106317967	-2.234945297
D. spinosa	1.071998477	-0.473487586	-0.093214683
D. spinosa	-1.43321979	0.292758971	-2.473396301
D. spinosa	0.625251174	-0.389978617	1.396081448
D. spinosa	-0.014199363	-0.95498091	-1.691853642
D. spinosa	0.608742595	-1.523816705	-0.302889436
D. spinosa	2.70729661	0.723378897	-0.284829825
D. spinosa	5.821313858	3.45016408	-0.987502813
D. spinosa	-0.032077774	-0.548228383	1.270870566
D. spinosa	2.520559072	-0.519231379	1.2383039
D. spinosa	0.327673346	-1.321187735	0.275171608
D. spinosa	1.117383599	-1.47825253	-0.431262821
D. spinosa	0.785848618	-0.569321275	-0.116084926
D. spinosa	0.017940382	-0.932418585	0.584676862
D. spinosa	-0.213745341	-0.2699866	0.781973541
D. spinosa	1.971813202	0.769132197	2.516767502
D. spinosa	-0.282609701	-0.940522015	-0.131074741
D. spinosa	3.493897915	0.588105619	0.029796211
D. spinosa	-2.724605083	0.452098966	-2.230666637
D. spinosa	0.490092576	-0.270014077	-0.146057203
D. spinosa	0.152146474	-1.539126396	-0.695987284
D. spinosa	1.172141552	-1.181955934	-0.708007991
D. spinosa	-0.1139559	-0.558103681	0.786296666

D. spinosa	1.243592143	-1.371686816	0.70958066
D. spinosa	3.148165703	0.71120131	0.04804327
D. spinosa	-4.546345711	2.833249331	0.310920566
D. spinosa	3.401122093	0.247805893	-0.118887693
D. spinosa	0.919012368	-1.711469412	0.677730262
D. spinosa	2.294533968	-0.565726161	0.547031701
D. spinosa	1.566440821	0.827303827	0.706535161
D. spinosa	1.436713457	-0.709820807	0.57866025
D. spinosa	0.381958187	-0.534197688	1.203396678
D. spinosa	-3.574136257	0.439847738	1.970817208
D. spinosa	2.989369631	-0.102158412	0.263886154
D. spinosa	-2.70069766	-2.214376211	-1.895662069
D. spinosa	1.859267473	-0.504567862	0.390487909
D. spinosa	3.155590296	0.426599681	0.152509838
D. spinosa	-5.329902649	2.758565187	-0.232636809
D. spinosa	-2.342128038	-2.130831718	-1.655002713
D. spinosa	0.791644633	-1.514407158	-0.536253572

Appendix IX

Appendix S1. Hypervolume calculations showing results from various environmental and morphological comparisons (Chapter 6, Simões *et al*, 2017).

Table S6: Overlap matrix of environmental hypervolumes at genus level.

	Dorynota	***Paratrikona***	***Omoteina***	***Akantaka***
Dorynota	1	0.723	0.317	0.606
Paratrikona	0.723	1	0.280	0.701
Omoteina	0.318	0.280	1	0.177
Akantaka	0.606	0.701	0.177	1

Table S7: Overlap matrix of environmental hypervolumes at species level.

	D_aculeat	*D_aurit*	*D_biden*	*D_cornige*	*D_moneoru*	*D_paralle*	*D_pugiona*	*D_riley*	*D_yucatan*	*D_monocer*	*P_ensifer*	*P_apicula*	*P_minim*	*P_rugos*	*P_spinos*
D_aculeata	0.000	0.566	0.671	0.587	0.769	0.648	0.368	0.643	0.778	0.700	0.719	0.740	0.809	0.652	0.539
D_aurita	0.566	0.000	0.492	0.663	0.590	0.621	0.545	0.466	0.613	0.644	0.642	0.653	0.558	0.646	0.568
D_bidens	0.671	0.492	0.000	0.643	0.609	0.615	0.420	0.815	0.648	0.765	0.683	0.771	0.545	0.660	0.576
D_cornigera	0.587	0.663	0.643	0.000	0.628	0.702	0.512	0.659	0.692	0.725	0.730	0.722	0.627	0.752	0.623
D_moneorum	0.769	0.590	0.609	0.628	0.000	0.660	0.436	0.598	0.755	0.761	0.753	0.741	0.702	0.667	0.591
D_parallela	0.648	0.621	0.615	0.702	0.660	0.000	0.563	0.647	0.716	0.656	0.688	0.641	0.595	0.752	0.673
D_pugionata	0.368	0.545	0.420	0.512	0.436	0.563	0.000	0.428	0.467	0.460	0.480	0.430	0.377	0.575	0.626
D_riley	0.643	0.466	0.815	0.659	0.598	0.647	0.428	0.000	0.637	0.706	0.666	0.710	0.554	0.646	0.589
D_yucatana	0.778	0.613	0.648	0.692	0.755	0.716	0.467	0.637	0.000	0.718	0.761	0.724	0.750	0.751	0.595
D_monoceros	0.700	0.644	0.765	0.725	0.761	0.656	0.460	0.706	0.718	0.000	0.738	0.825	0.620	0.711	0.602
P_ensifera	0.719	0.642	0.683	0.730	0.753	0.688	0.480	0.666	0.761	0.738	0.000	0.804	0.711	0.719	0.615
P_apiculata	0.740	0.653	0.771	0.722	0.741	0.641	0.430	0.710	0.724	0.825	0.804	0.000	0.681	0.702	0.568
P_minima	0.809	0.558	0.545	0.627	0.702	0.595	0.377	0.554	0.750	0.620	0.711	0.681	0.000	0.660	0.514
P_rugosa	0.652	0.646	0.660	0.752	0.667	0.752	0.575	0.646	0.751	0.711	0.719	0.702	0.660	0.000	0.669
P_spinosa	0.539	0.568	0.576	0.623	0.591	0.673	0.626	0.589	0.595	0.602	0.615	0.568	0.514	0.669	0.000

Table S8: Overlap matrix of morphological hypervolume at genus level, including all principal components except PC 1, using log-transformed data.

	Dorynota	***Paratrikona***	***Omotein a***	***Akantak a***
Dorynota	1	0.002	0	0
Paratrikona	0.002	1		0
Omoteina	0	0	1	0
Akantaka	0	0	0	1

Table S9: Overlap matrix of morphological hypervolumes at genus level, including all principal components.

	Dorynota	***Paratrikona***	***Omoteina***	***Akantaka***
Dorynota	1	0	0	0
Paratrikona	0	1	4.83E-05	0
Omoteina	0	4.83E-05	1	0
Akantaka	0	0	0	1

Table S10: Overlap matrix of morphological hypervolumes at genus level: including all principal components, except PC1.

	Dorynota	***Paratrikona***	***Omoteina***	***Akantaka***
Dorynota	1	0.001	0	0
Paratrikona	0.001	1	0.007	0
Omoteina	0	0.007	1	0.002
Akantaka	0	0	0.002	1

Table S11: Overlap matrix of morphological hypervolumes at genus level, including all principal components, excluding body height from dataset.

	Dorynota	***Paratrikona***	***Omoteina***	***Akantaka***
Dorynota	1	0.002	0.012	0.002
Paratrikona	0.002	1	0	0
Omoteina	0.012	0	1	0
Akantaka	0.002	0	0	1

Table S12: Overlap matrix of morphological hypervolume at genus level, including all but PC1, excluding body height from dataset.

	Dorynota	***Paratrikona***	***Omoteina***	***Akantaka***
Dorynota	1	0.019	0.033	0.089
Paratrikona	0.019	1	0.112	0.008
Omoteina	0.033	0.112	1	0.033
Akantaka	0.089	0.008	0.033	1

Table S13: Overlap matrix of morphological hypervolume at genus level, including only principal components 2, 3 & 4, using log-transformed data.

	Dorynota	***Paratrikona***	***Omoteina***	***Akantaka***
Dorynota	1	0.003	0	0
Paratrikona	0.003	1	0.001	0
Omoteina	0	0.001	1	0.293
Akantaka	0	0	0.293	1

Table S14: Overlap matrix of morphological hypervolume at genus level, including principal components 2, 3 & 4 using non-log-transformed data.

	Dorynota	***Paratrikona***	***Omoteina***	***Akantaka***
Dorynota	1	0.002	0	0
Paratrikona	0.002	1	0.056	0
Omoteina	0	0.056	1	0.176
Akantaka	0	0	0.176	1

Table S15: Overlap matrix of morphological hypervolume at genus level, inclding principal components 2, 3 & 4 using log-transformed data.

	Dorynota	***Paratrikona***	***Omoteina***	***Akantaka***
Dorynota	1	0.029	0.079	0.179
Paratrikona	0.029	1	0.256	0.010
Omoteina	0.079	0.256	1	0.286
Akantaka	0.179	0.010	0.286	1

Table S16: Overlap matrix of morphological hypervolume at genus level, including principal components 2, 3 & 4 using non-log-transformed data.

	Dorynota	***Paratrikona***	***Omoteina***	***Akantaka***
Dorynota	1	0.032	0.075	0.173
Paratrikona	0.032	1	0.240	0.015
Omoteina	0.075	0.240	1	0.292
Akantaka	0.173	0.015	0.292	1

Morphological Overlap: Including body height in the dataset

Table S17: Overlap matrix of morphological hypervolume at species level, including all principal components using log-transformed data.

	D_aculeat	D_aurit	D. biden	D_cornige	D_moneoru	D_paralle	D_pugiona	D_rile	D_yucatan	D_monocer	P_ensifer	P_apicula	P_minim	P_rugos	P_spinos
D_aculeata	0.000	0.268	0.000	0.041	0.091	0.000	0.000	0.037	0.000	0.000	0.000	0.000	0.003	0.133	0.000
D_aurita	0.268	0.000	0.000	0.004	0.059	0.000	0.000	0.061	0.000	0.000	0.000	0.000	0.001	0.099	0.000
D. bidens	0.000	0.000	0.000	0.002	0.000	0.039	0.133	0.000	0.000	0.237	0.000	0.020	0.000	0.000	0.000
D_cornigera	0.041	0.004	0.002	0.000	0.000	0.006	0.000	0.011	0.000	0.000	0.000	0.000	0.037	0.003	0.000
D_moneorum	0.091	0.059	0.000	0.000	0.000	0.000	0.000	0.047	0.000	0.000	0.000	0.000	0.000	0.218	0.000
D_parallela	0.000	0.000	0.000	0.000	0.000	0.000	0.061	0.000	0.002	0.020	0.022	0.053	0.010	0.000	0.068
D_pugionata	0.000	0.000	0.133	0.000	0.000	0.061	0.000	0.000	0.000	0.067	0.000	0.004	0.000	0.000	0.001
D_riley	0.037	0.061	0.000	0.011	0.047	0.000	0.000	0.000	0.000	0.000	0.000	0.000	0.000	0.167	0.000
D_yucatana	0.000	0.000	0.000	0.000	0.000	0.002	0.000	0.000	0.000	0.000	0.000	0.000	0.055	0.000	0.000
D_monoceros	0.000	0.000	0.237	0.000	0.000	0.020	0.067	0.000	0.000	0.000	0.000	0.018	0.000	0.000	0.006
P_ensifera	0.000	0.000	0.000	0.000	0.000	0.022	0.000	0.000	0.000	0.000	0.000	0.073	0.000	0.000	0.257
P_apiculata	0.000	0.000	0.020	0.000	0.000	0.053	0.004	0.000	0.000	0.018	0.073	0.000	0.000	0.000	0.139
P_minima	0.003	0.001	0.000	0.037	0.000	0.010	0.000	0.000	0.055	0.000	0.000	0.000	0.000	0.000	0.013
P_rugosa	0.133	0.099	0.000	0.003	0.218	0.000	0.000	0.167	0.000	0.000	0.000	0.000	0.000	0.000	0.000
P_spinosa	0.000	0.000	0.000	0.000	0.000	0.068	0.001	0.000	0.000	0.006	0.257	0.139	0.013	0.000	0.000

Table S18: Overlap matrix of morphological hypervolume at species level, including all principal components but PC1 using log-transformed data.

	D_aculeat	D_aurita	D. biden	D_cornige	D_moneoru	D_paralle	D_pugiona	D_riley	D_yucatan	D_monocer	P_ensifer	P_apicula	P_minim	P_rugos	P_spinos
D_aculeata	0.000	0.319	0.005	0.072	0.087	0.121	0.006	0.124	0.129	0.017	0.257	0.157	0.057	0.293	0.442
D_aurita	0.319	0.000	0.001	0.027	0.070	0.079	0.002	0.231	0.339	0.002	0.063	0.048	0.172	0.197	0.209
D. bidens	0.005	0.001	0.000	0.070	0.000	0.061	0.145	0.006	0.000	0.352	0.002	0.050	0.000	0.006	0.007
D_cornigera	0.072	0.027	0.070	0.000	0.000	0.080	0.036	0.021	0.000	0.093	0.011	0.005	0.045	0.020	0.060
D_moneorum	0.087	0.070	0.000	0.000	0.000	0.009	0.001	0.120	0.102	0.000	0.189	0.067	0.000	0.363	0.105
D_parallela	0.121	0.079	0.061	0.080	0.009	0.000	0.074	0.048	0.033	0.027	0.037	0.090	0.021	0.052	0.117
D_pugionata	0.006	0.002	0.145	0.036	0.001	0.074	0.000	0.004	0.001	0.063	0.002	0.015	0.000	0.004	0.005
D_riley	0.124	0.231	0.006	0.021	0.120	0.048	0.004	0.000	0.188	0.011	0.091	0.057	0.005	0.233	0.107
D_yucatana	0.129	0.339	0.000	0.000	0.102	0.033	0.001	0.188	0.000	0.000	0.008	0.040	0.074	0.098	0.092
D_monoceros	0.017	0.002	0.352	0.093	0.000	0.027	0.063	0.011	0.000	0.000	0.000	0.024	0.000	0.005	0.007
P_ensifera	0.257	0.063	0.002	0.011	0.189	0.037	0.002	0.091	0.008	0.000	0.000	0.202	0.001	0.417	0.324
P_apiculata	0.157	0.048	0.050	0.005	0.067	0.090	0.015	0.057	0.040	0.024	0.202	0.000	0.001	0.161	0.297
P_minima	0.057	0.172	0.000	0.045	0.000	0.021	0.000	0.005	0.074	0.000	0.001	0.001	0.000	0.013	0.037
P_rugosa	0.293	0.197	0.006	0.020	0.363	0.052	0.004	0.233	0.098	0.005	0.417	0.161	0.013	0.000	0.318
P_spinosa	0.442	0.209	0.007	0.060	0.105	0.117	0.005	0.107	0.092	0.007	0.324	0.297	0.037	0.318	0.000

Morphological Overlap: Excluding body height in the dataset

Table S19: Overlap matrix of morphological hypervolume at species level, including all principal components using non-log-transformed data

	D_aculeat	D_aurita	D. biden	D_corniger	D_moneorur	D_parallel	D_pugionat	D_riley	D_yucatan	D_monocer	P_ensifer	P_apiculat	P_minim	P_rugosa	P_spinosa
D_aculeata	0.000	0.341	0.000	0.070	0.243	0.000	0.000	0.097	0.000	0.000	0.000	0.000	0.003	0.220	0.000
D_aurita	0.341	0.000	0.000	0.011	0.188	0.000	0.000	0.092	0.000	0.000	0.000	0.000	0.000	0.123	0.000
D. bidens	0.000	0.000	0.000	0.029	0.000	0.037	0.227	0.000	0.000	0.229	0.001	0.054	0.000	0.000	0.002
D_cornigera	0.070	0.011	0.029	0.000	0.016	0.019	0.033	0.060	0.002	0.009	0.000	0.006	0.041	0.013	0.000
D_moneorum	0.243	0.188	0.000	0.016	0.000	0.000	0.000	0.099	0.000	0.000	0.000	0.000	0.000	0.211	0.000
D_parallela	0.000	0.000	0.037	0.019	0.000	0.000	0.107	0.000	0.002	0.028	0.013	0.069	0.025	0.000	0.053
D_pugionata	0.000	0.000	0.227	0.033	0.000	0.107	0.000	0.000	0.000	0.088	0.006	0.034	0.001	0.000	0.010
D_riley	0.097	0.092	0.000	0.060	0.099	0.000	0.000	0.000	0.000	0.000	0.000	0.000	0.000	0.286	0.000
D_yucatana	0.000	0.000	0.000	0.002	0.000	0.002	0.000	0.000	0.000	0.000	0.000	0.001	0.104	0.000	0.000
D_monoceros	0.000	0.000	0.229	0.009	0.000	0.028	0.088	0.000	0.000	0.000	0.001	0.043	0.000	0.000	0.022
P_ensifera	0.000	0.000	0.001	0.000	0.000	0.013	0.006	0.000	0.000	0.001	0.000	0.078	0.005	0.000	0.258
P_apiculata	0.000	0.000	0.054	0.006	0.000	0.069	0.034	0.000	0.001	0.043	0.078	0.000	0.000	0.000	0.186
P_minima	0.003	0.000	0.000	0.041	0.000	0.025	0.001	0.000	0.104	0.000	0.005	0.000	0.000	0.000	0.043
P_rugosa	0.220	0.123	0.000	0.013	0.211	0.000	0.000	0.286	0.000	0.000	0.000	0.000	0.000	0.000	0.000
P_spinosa	0.000	0.000	0.002	0.000	0.000	0.053	0.010	0.000	0.000	0.022	0.258	0.186	0.043	0.000	0.000

Table S20: Overlap matrix of morphological hypervolume at species level, including all principal components using log-transformed data

	D_aculeat	D_aurit	D. biden	D_cornige	D_moneoru	D_paralle	D_pugiona	D_riley	D_yucatan	D_monocer	P_ensifer	P_apicula	P_minim	P_rugos	P_spinos
D_aculeata	0.000	0.299	0.000	0.053	0.092	0.000	0.000	0.074	0.000	0.000	0.000	0.000	0.003	0.155	0.000
D_aurita	0.299	0.000	0.000	0.003	0.058	0.000	0.000	0.061	0.000	0.000	0.000	0.000	0.000	0.097	0.000
D. bidens	0.000	0.000	0.000	0.011	0.000	0.027	0.129	0.000	0.000	0.172	0.000	0.008	0.000	0.000	0.000
D_cornigera	0.053	0.003	0.011	0.000	0.001	0.004	0.006	0.023	0.000	0.001	0.000	0.003	0.034	0.004	0.000
D_moneorum	0.092	0.058	0.000	0.001	0.000	0.000	0.000	0.063	0.000	0.000	0.000	0.000	0.001	0.184	0.000
D_parallela	0.000	0.000	0.027	0.004	0.000	0.000	0.047	0.000	0.001	0.018	0.013	0.062	0.038	0.000	0.045
D_pugionata	0.000	0.000	0.129	0.006	0.000	0.047	0.000	0.000	0.000	0.046	0.000	0.005	0.000	0.000	0.002
D_riley	0.074	0.061	0.000	0.023	0.063	0.000	0.000	0.000	0.000	0.000	0.000	0.000	0.000	0.282	0.000
D_yucatana	0.000	0.000	0.000	0.000	0.000	0.001	0.000	0.000	0.000	0.000	0.000	0.000	0.050	0.000	0.000
D_monoceros	0.000	0.000	0.172	0.001	0.000	0.018	0.046	0.000	0.000	0.000	0.001	0.015	0.000	0.000	0.011
P_ensifera	0.000	0.000	0.000	0.000	0.000	0.013	0.000	0.000	0.000	0.001	0.000	0.046	0.013	0.000	0.254
P_apiculata	0.000	0.000	0.008	0.003	0.000	0.062	0.005	0.000	0.000	0.015	0.046	0.000	0.012	0.000	0.104
P_minima	0.003	0.000	0.000	0.034	0.001	0.038	0.000	0.000	0.050	0.000	0.013	0.012	0.000	0.000	0.058
P_rugosa	0.000	0.155	0.097	0.000	0.004	0.184	0.000	0.000	0.282	0.000	0.000	0.000	0.000	0.000	0.000
P_spinosa	0.000	0.000	0.000	0.000	0.000	0.045	0.002	0.000	0.000	0.011	0.254	0.104	0.058	0.000	0.000

Table S21: Overlap matrix of morphological hypervolume at species level, including all principal components but PC1 using log-transformed data.

	D_aculeat	D_aurit	D. biden	D_cornige	D_moneoru	D_paralle	D_pugiona	D_riley	D_yucatan	D_monocer	P_ensifer	P_apicula	P_minim	P_rugos	P_spinos
D_aculeata	0.000	0.357	0.017	0.086	0.219	0.139	0.056	0.015	0.329	0.307	0.388	0.289	0.353	0.575	0.538
D_aurita	0.357	0.000	0.001	0.054	0.198	0.081	0.020	0.002	0.378	0.165	0.078	0.035	0.105	0.238	0.207
D. bidens	0.017	0.001	0.000	0.103	0.000	0.052	0.182	0.276	0.012	0.487	0.156	0.025	0.008	0.034	0.049
D_cornigera	0.086	0.054	0.103	0.000	0.025	0.114	0.065	0.077	0.155	0.125	0.122	0.069	0.016	0.176	0.085
D_moneorum	0.219	0.198	0.000	0.025	0.000	0.019	0.004	0.000	0.205	0.071	0.141	0.151	0.238	0.230	0.145
D_parallela	0.139	0.081	0.052	0.114	0.019	0.000	0.150	0.135	0.125	0.162	0.071	0.030	0.057	0.132	0.139
D_pugionata	0.056	0.020	0.182	0.065	0.004	0.150	0.000	0.484	0.034	0.248	0.071	0.016	0.022	0.042	0.051
D_riley	0.015	0.002	0.276	0.077	0.000	0.135	0.484	0.000	0.012	0.297	0.067	0.005	0.008	0.004	0.008
D_yucatana	0.329	0.378	0.012	0.155	0.205	0.125	0.034	0.012	0.000	0.208	0.108	0.117	0.165	0.279	0.231
D_monoceros	0.307	0.165	0.487	0.125	0.071	0.162	0.248	0.297	0.208	0.000	0.198	0.064	0.145	0.215	0.237
P_ensifera	0.388	0.078	0.156	0.122	0.141	0.071	0.071	0.067	0.108	0.198	0.000	0.336	0.309	0.467	0.430
P_apiculata	0.289	0.035	0.025	0.069	0.151	0.030	0.016	0.005	0.117	0.064	0.336	0.000	0.290	0.345	0.226
P_minima	0.353	0.105	0.008	0.016	0.238	0.057	0.022	0.008	0.165	0.145	0.309	0.290	0.000	0.312	0.325
P_rugosa	0.575	0.238	0.034	0.176	0.230	0.132	0.042	0.004	0.279	0.215	0.467	0.345	0.312	0.000	0.537
P_spinosa	0.538	0.207	0.049	0.085	0.145	0.139	0.051	0.008	0.231	0.237	0.430	0.226	0.325	0.537	0.000

Table S22: Overlap matrix of morphological hypervolume at species level, including all principal components using log-transformed data

	D_aculeat	D_aurit	D. biden	D_cornige	D_moneoru	D_paralle	D_pugiona	D_riley	D_yucatan	D_monocer	P_ensifer	P_apicula	P_minim	P_rugos	P_spinos
D_aculeata	0.000	0.298	0.000	0.053	0.207	0.000	0.022	0.000	0.226	0.027	0.000	0.000	0.000	0.288	0.044
D_aurita	0.298	0.000	0.000	0.006	0.181	0.000	0.008	0.000	0.122	0.001	0.000	0.000	0.000	0.068	0.020
D. bidens	0.000	0.000	0.000	0.010	0.000	0.034	0.124	0.268	0.000	0.329	0.067	0.008	0.001	0.006	0.010
D_cornigera	0.053	0.006	0.010	0.000	0.006	0.014	0.044	0.003	0.085	0.025	0.000	0.000	0.000	0.118	0.006
D_moneorum	0.207	0.181	0.000	0.006	0.000	0.000	0.002	0.000	0.083	0.004	0.000	0.000	0.000	0.093	0.024
D_parallela	0.000	0.000	0.034	0.014	0.000	0.000	0.097	0.084	0.074	0.093	0.048	0.023	0.029	0.035	0.126
D_pugionata	0.022	0.008	0.124	0.044	0.002	0.097	0.000	0.295	0.027	0.219	0.025	0.009	0.009	0.026	0.031
D_riley	0.000	0.000	0.268	0.003	0.000	0.084	0.295	0.000	0.005	0.218	0.030	0.001	0.000	0.000	0.001
D_yucatana	0.226	0.122	0.000	0.085	0.083	0.074	0.027	0.005	0.000	0.151	0.007	0.002	0.021	0.294	0.103
D_monoceros	0.027	0.001	0.329	0.025	0.004	0.093	0.219	0.218	0.151	0.000	0.052	0.015	0.017	0.066	0.089
P_ensifera	0.000	0.000	0.067	0.000	0.000	0.048	0.025	0.030	0.007	0.052	0.000	0.324	0.222	0.021	0.229
P_apiculata	0.000	0.000	0.008	0.000	0.000	0.023	0.009	0.001	0.002	0.015	0.324	0.000	0.167	0.011	0.109
P_minima	0.000	0.000	0.001	0.000	0.000	0.029	0.009	0.000	0.021	0.017	0.222	0.167	0.000	0.001	0.279
P_rugosa	0.288	0.068	0.006	0.118	0.093	0.035	0.026	0.000	0.294	0.066	0.021	0.011	0.001	0.000	0.163
P_spinosa	0.044	0.020	0.010	0.006	0.024	0.126	0.031	0.001	0.103	0.089	0.229	0.109	0.279	0.163	0.000

Table S23: Overlap matrix of morphological hypervolume at species level, including all principal components but PC1 using non-log-transformed data**.**

	D_aculeata	D_aurita	D. bidens	D_corniger	D_moneorum	D_parallela	D_pugionat	D_riley	D_yucatana	D_monocero	P_ensifer	P_apiculat	P_minima	P_rugosa	P_spinosa
D_aculeata	0.000	0.400	0.065	0.120	0.267	0.173	0.176	0.333	0.131	0.062	0.079	0.243	0.038	0.524	0.228
D_aurita	0.400	0.000	0.010	0.096	0.219	0.172	0.068	0.314	0.329	0.036	0.039	0.208	0.127	0.193	0.294
D. bidens	0.065	0.010	0.000	0.167	0.011	0.047	0.221	0.108	0.000	0.317	0.002	0.091	0.000	0.163	0.022
D_cornigera	0.120	0.096	0.167	0.000	0.045	0.073	0.222	0.222	0.003	0.106	0.027	0.053	0.066	0.140	0.102
D_moneorum	0.267	0.219	0.011	0.045	0.000	0.046	0.009	0.199	0.087	0.011	0.192	0.323	0.041	0.278	0.487
D_parallela	0.173	0.172	0.047	0.073	0.046	0.000	0.112	0.234	0.103	0.029	0.022	0.073	0.046	0.120	0.095
D_pugionata	0.176	0.068	0.221	0.222	0.009	0.112	0.000	0.160	0.011	0.084	0.013	0.043	0.001	0.158	0.024
D_riley	0.333	0.314	0.108	0.222	0.199	0.234	0.160	0.000	0.136	0.090	0.081	0.187	0.056	0.355	0.265
D_yucatana	0.131	0.329	0.000	0.003	0.087	0.103	0.011	0.136	0.000	0.000	0.001	0.160	0.142	0.061	0.159
D_monoceros	0.062	0.036	0.317	0.106	0.011	0.029	0.084	0.090	0.000	0.000	0.003	0.055	0.000	0.076	0.026
P_ensifera	0.079	0.039	0.002	0.027	0.192	0.022	0.013	0.081	0.001	0.003	0.000	0.202	0.011	0.085	0.327
P_apiculata	0.243	0.208	0.091	0.053	0.323	0.073	0.043	0.187	0.160	0.055	0.202	0.000	0.000	0.259	0.335
P_minima	0.038	0.127	0.000	0.066	0.041	0.046	0.001	0.056	0.142	0.000	0.011	0.000	0.000	0.049	0.112
P_rugosa	0.524	0.193	0.163	0.140	0.278	0.120	0.158	0.355	0.061	0.076	0.085	0.259	0.049	0.000	0.235
P_spinosa	0.228	0.294	0.022	0.102	0.487	0.095	0.024	0.265	0.159	0.026	0.327	0.335	0.112	0.235	0.000

Morphological Overlap: Overlap calculation using only 3 axes of principal components (2, 3, 4)

Table S24: Overlap matrix of morphological hypervolume at species level, including principal components 2, 3 & 4 using log-transformed data.

	D_aculeat	D_aurita	D. biden	D_cornige	D_moneoru	D_paralle	D_pugiona	D_riley	D_yucatan	D_monocer	P_ensifer	P_apicula	P_minim	P_rugos	P_spinos
D_aculeata	0.000	0.550	0.030	0.199	0.476	0.165	0.020	0.560	0.318	0.090	0.477	0.315	0.241	0.565	0.583
D_aurita	0.550	0.000	0.023	0.204	0.489	0.112	0.015	0.472	0.582	0.096	0.180	0.158	0.394	0.435	0.334
D. bidens	0.030	0.023	0.000	0.232	0.011	0.141	0.380	0.056	0.002	0.596	0.065	0.153	0.000	0.052	0.098
D_cornigera	0.199	0.204	0.232	0.000	0.272	0.193	0.153	0.560	0.168	0.396	0.229	0.205	0.288	0.394	0.282
D_moneorum	0.476	0.489	0.011	0.272	0.000	0.081	0.015	0.450	0.209	0.096	0.394	0.130	0.260	0.594	0.301
D_parallela	0.165	0.112	0.141	0.193	0.081	0.000	0.263	0.237	0.069	0.144	0.108	0.306	0.075	0.124	0.187
D_pugionata	0.020	0.015	0.380	0.153	0.015	0.263	0.000	0.058	0.003	0.347	0.015	0.046	0.000	0.008	0.020
D_riley	0.560	0.472	0.056	0.560	0.450	0.237	0.058	0.000	0.302	0.159	0.361	0.315	0.329	0.552	0.514
D_yucatana	0.318	0.582	0.002	0.168	0.209	0.069	0.003	0.302	0.000	0.045	0.028	0.095	0.346	0.174	0.178
D_monoceros	0.090	0.096	0.596	0.396	0.096	0.144	0.347	0.159	0.045	0.000	0.049	0.094	0.003	0.079	0.069
P_ensifera	0.477	0.180	0.065	0.229	0.394	0.108	0.015	0.361	0.028	0.049	0.000	0.300	0.094	0.552	0.410
P_apiculata	0.315	0.158	0.153	0.205	0.130	0.306	0.046	0.315	0.095	0.094	0.300	0.000	0.088	0.251	0.498
P_minima	0.241	0.394	0.000	0.288	0.260	0.075	0.000	0.329	0.346	0.003	0.094	0.088	0.000	0.305	0.168
P_rugosa	0.565	0.435	0.052	0.394	0.594	0.124	0.008	0.552	0.174	0.079	0.552	0.251	0.305	0.000	0.505
P_spinosa	0.583	0.334	0.098	0.282	0.301	0.187	0.020	0.514	0.178	0.069	0.410	0.498	0.168	0.505	0.000

Table S25: Overlap matrix of morphological hypervolume at species level, including principal components 2, 3 & 4 using non-log-transformed data

	D_aculeat	D_aurit	D. biden	D_cornige	D_moneoru	D_paralle	D_pugiona	D_rile	D_yucatan	D_monocer	P_ensifer	P_apicula	P_minim	P_rugos	P_spinos
D_aculeata	0.000	0.481	0.098	0.431	0.221	0.248	0.157	0.527	0.198	0.108	0.148	0.610	0.149	0.537	0.266
D_aurita	0.481	0.000	0.134	0.432	0.109	0.221	0.102	0.367	0.369	0.144	0.152	0.555	0.337	0.399	0.430
D. bidens	0.098	0.134	0.000	0.421	0.063	0.118	0.191	0.221	0.046	0.606	0.162	0.131	0.120	0.205	0.170
D_cornigera	0.431	0.432	0.421	0.000	0.099	0.303	0.329	0.443	0.189	0.321	0.217	0.521	0.175	0.504	0.357
D_moneorum	0.221	0.109	0.063	0.099	0.000	0.042	0.079	0.320	0.126	0.076	0.224	0.251	0.197	0.427	0.273
D_parallela	0.248	0.221	0.118	0.303	0.042	0.000	0.146	0.310	0.113	0.100	0.091	0.320	0.096	0.218	0.135
D_pugionata	0.157	0.102	0.191	0.329	0.079	0.146	0.000	0.294	0.026	0.144	0.024	0.113	0.003	0.204	0.030
D_riley	0.527	0.367	0.221	0.443	0.320	0.310	0.294	0.000	0.171	0.194	0.175	0.523	0.153	0.598	0.252
D_yucatana	0.198	0.369	0.046	0.189	0.126	0.113	0.026	0.171	0.000	0.034	0.012	0.244	0.453	0.207	0.220
D_monoceros	0.108	0.144	0.606	0.321	0.076	0.100	0.144	0.194	0.034	0.000	0.100	0.104	0.044	0.220	0.104
P_ensifera	0.148	0.152	0.162	0.217	0.224	0.091	0.024	0.175	0.012	0.100	0.000	0.271	0.164	0.257	0.500
P_apiculata	0.610	0.555	0.131	0.521	0.251	0.320	0.113	0.523	0.244	0.104	0.271	0.000	0.243	0.604	0.420
P_minima	0.149	0.337	0.120	0.175	0.197	0.096	0.003	0.153	0.453	0.044	0.164	0.243	0.000	0.206	0.429
P_rugosa	0.537	0.399	0.205	0.504	0.427	0.218	0.204	0.598	0.207	0.220	0.257	0.604	0.206	0.000	0.403
P_spinosa	0.266	0.430	0.170	0.357	0.273	0.135	0.030	0.252	0.220	0.104	0.500	0.420	0.429	0.403	0.000

Morphological Overlap: Overlap calculation using only 3 axes of principal components (2, 3, 4) & excluding body height

Table S26: Overlap matrix of morphological hypervolume at species level, including principal components 2, 3 & 4 using log-transformed data

	D_aculeata	D_aurita	D. bidens	D_corniger	D_moneorum	D_parallela	D_pugionat	D_riley	D_yucatana	D_monocero	P_ensifera	P_apiculat	P_minima	P_rugosa	P_spinosa
D_aculeata	0.000	0.449	0.039	0.116	0.387	0.159	0.114	0.021	0.558	0.319	0.454	0.430	0.462	0.612	0.589
D_aurita	0.449	0.000	0.008	0.081	0.479	0.091	0.056	0.010	0.473	0.212	0.144	0.153	0.201	0.335	0.282
D. bidens	0.039	0.008	0.000	0.208	0.000	0.113	0.406	0.463	0.026	0.537	0.232	0.039	0.020	0.044	0.088
D_cornigera	0.116	0.081	0.208	0.000	0.036	0.123	0.190	0.177	0.249	0.274	0.272	0.101	0.035	0.304	0.187
D_moneorum	0.387	0.479	0.000	0.036	0.000	0.042	0.012	0.000	0.276	0.127	0.234	0.169	0.276	0.341	0.264
D_parallela	0.159	0.091	0.113	0.123	0.042	0.000	0.342	0.221	0.224	0.281	0.139	0.065	0.137	0.164	0.176
D_pugionata	0.114	0.056	0.406	0.190	0.012	0.342	0.000	0.587	0.133	0.469	0.167	0.054	0.050	0.100	0.089
D_riley	0.021	0.010	0.463	0.177	0.000	0.221	0.587	0.000	0.032	0.492	0.177	0.010	0.014	0.005	0.012
D_yucatana	0.558	0.473	0.026	0.249	0.276	0.224	0.133	0.032	0.000	0.409	0.235	0.206	0.332	0.457	0.467
D_monoceros	0.319	0.212	0.537	0.274	0.127	0.281	0.469	0.492	0.409	0.000	0.321	0.110	0.225	0.251	0.274
P_ensifera	0.454	0.144	0.232	0.272	0.234	0.139	0.167	0.177	0.235	0.321	0.000	0.472	0.387	0.499	0.474
P_apiculata	0.430	0.153	0.039	0.101	0.169	0.065	0.054	0.010	0.206	0.110	0.472	0.000	0.343	0.465	0.392
P_minima	0.462	0.201	0.020	0.035	0.276	0.137	0.050	0.014	0.332	0.225	0.387	0.343	0.000	0.415	0.520
P_rugosa	0.612	0.335	0.044	0.304	0.341	0.164	0.100	0.005	0.457	0.251	0.499	0.465	0.415	0.000	0.605
P_spinosa	0.589	0.282	0.088	0.187	0.264	0.176	0.089	0.012	0.467	0.274	0.474	0.392	0.520	0.605	0.000

Table S27: Overlap matrix of morphological hypervolume at species level, including principal components 2, 3 & 4 using non-log-transformed data

	D_aculeat	D_aurita	D. biden	D_corniger	D_moneoru	D_parallel	D_pugionat	D_riley	D_yucatana	D_monocero	P_ensifer	P_apiculat	P_minima	P_rugosa	P_spinosa
D_aculeata	0.000	0.501	0.127	0.182	0.415	0.272	0.219	0.556	0.207	0.123	0.180	0.658	0.144	0.614	0.423
D_aurita	0.501	0.000	0.052	0.115	0.496	0.196	0.115	0.323	0.437	0.112	0.141	0.438	0.345	0.331	0.432
D. bidens	0.127	0.052	0.000	0.382	0.020	0.093	0.480	0.213	0.000	0.359	0.011	0.132	0.000	0.231	0.067
D_cornigera	0.182	0.115	0.382	0.000	0.090	0.092	0.393	0.335	0.003	0.224	0.045	0.120	0.127	0.297	0.155
D_moneorum	0.415	0.496	0.020	0.090	0.000	0.089	0.028	0.243	0.245	0.021	0.240	0.387	0.266	0.353	0.631
D_parallela	0.272	0.196	0.093	0.092	0.089	0.000	0.239	0.264	0.112	0.077	0.052	0.233	0.081	0.179	0.122
D_pugionata	0.219	0.115	0.480	0.393	0.028	0.239	0.000	0.389	0.023	0.241	0.039	0.134	0.016	0.243	0.070
D_riley	0.556	0.323	0.213	0.335	0.243	0.264	0.389	0.000	0.116	0.123	0.101	0.497	0.113	0.550	0.262
D_yucatana	0.207	0.437	0.000	0.003	0.245	0.112	0.023	0.116	0.000	0.000	0.000	0.174	0.277	0.079	0.173
D_monoceros	0.123	0.112	0.359	0.224	0.021	0.077	0.241	0.123	0.000	0.000	0.006	0.063	0.004	0.139	0.042
P_ensifera	0.180	0.141	0.011	0.045	0.240	0.052	0.039	0.101	0.000	0.006	0.000	0.182	0.128	0.164	0.392
P_apiculata	0.658	0.438	0.132	0.120	0.387	0.233	0.134	0.497	0.174	0.063	0.182	0.000	0.144	0.627	0.426
P_minima	0.144	0.345	0.000	0.127	0.266	0.081	0.016	0.113	0.277	0.004	0.128	0.144	0.000	0.154	0.243
P_rugosa	0.614	0.331	0.231	0.297	0.353	0.179	0.243	0.550	0.079	0.139	0.164	0.627	0.154	0.000	0.408
P_spinosa	0.423	0.432	0.067	0.155	0.631	0.122	0.070	0.262	0.173	0.042	0.392	0.426	0.243	0.408	0.000

Morphological Overlap: Overlap calculation using only 3 axes of principal components (1, 2, 3) & including body height

Table S28: Overlap matrix of morphological hypervolume at species level, including principal components 4, 5 & 6 using log-transformed data

	D_aculeat	D_aurit	D. biden	D_cornige	D_moneoru	D_paralle	D_pugiona	D_rile	D_yucatan	D_monocer	P_ensifer	P_apicula	P_minim	P_rugos	P_spinos
D_aculeata	0.000	0.510	0.000	0.332	0.501	0.000	0.000	0.226	0.000	0.000	0.000	0.000	0.036	0.341	0.000
D_aurita	0.510	0.000	0.000	0.158	0.478	0.000	0.000	0.232	0.000	0.000	0.000	0.000	0.010	0.400	0.000
D. bidens	0.000	0.000	0.000	0.094	0.000	0.128	0.339	0.000	0.017	0.553	0.032	0.192	0.122	0.000	0.028
D_cornigera	0.332	0.158	0.094	0.000	0.181	0.035	0.014	0.177	0.109	0.001	0.000	0.057	0.188	0.151	0.000
D_moneorum	0.501	0.478	0.000	0.181	0.000	0.000	0.000	0.306	0.000	0.000	0.000	0.000	0.006	0.602	0.000
D_parallela	0.000	0.000	0.128	0.035	0.000	0.000	0.305	0.000	0.003	0.150	0.100	0.371	0.033	0.000	0.142
D_pugionata	0.000	0.000	0.339	0.014	0.000	0.305	0.000	0.000	0.000	0.418	0.062	0.218	0.001	0.000	0.049
D_riley	0.226	0.232	0.000	0.177	0.306	0.000	0.000	0.000	0.000	0.000	0.000	0.000	0.000	0.561	0.000
D_yucatana	0.000	0.000	0.017	0.109	0.000	0.000	0.003	0.000	0.000	0.000	0.000	0.011	0.415	0.000	0.000
D_monoceros	0.000	0.000	0.553	0.001	0.000	0.150	0.418	0.000	0.000	0.000	0.085	0.232	0.000	0.000	0.139
P_ensifera	0.000	0.000	0.032	0.000	0.000	0.100	0.062	0.000	0.000	0.085	0.000	0.237	0.036	0.000	0.453
P_apiculata	0.000	0.000	0.192	0.057	0.000	0.371	0.218	0.000	0.011	0.232	0.237	0.000	0.057	0.000	0.371
P_minima	0.036	0.010	0.122	0.188	0.006	0.033	0.001	0.415	0.000	0.036	0.057	0.000	0.000	0.000	0.078
P_rugosa	0.341	0.400	0.000	0.151	0.602	0.000	0.000	0.561	0.000	0.000	0.000	0.000	0.000	0.000	0.000
P_spinosa	0.000	0.000	0.028	0.000	0.000	0.142	0.049	0.000	0.000	0.139	0.453	0.371	0.078	0.000	0.000

Table S29: Overlap matrix of morphological hypervolume at species level, including principal components 4, 5 & 6 using non-log-transformed data

	D_aculeat	D_aurit	D. biden	D_cornige	D_moneoru	D_paralle	D_pugiona	D_rile	D_yucatan	D_monocer	P_ensifer	P_apicula	P_minim	P_rugos	P_spinos
D_aculeata	0.000	0.530	0.000	0.344	0.481	0.000	0.000	0.216	0.000	0.000	0.000	0.000	0.015	0.383	0.000
D_aurita	0.530	0.000	0.000	0.181	0.468	0.000	0.000	0.205	0.000	0.000	0.000	0.000	0.002	0.373	0.000
D. bidens	0.000	0.000	0.000	0.095	0.000	0.108	0.371	0.000	0.017	0.561	0.022	0.175	0.149	0.000	0.027
D_cornigera	0.344	0.181	0.095	0.000	0.223	0.072	0.055	0.188	0.060	0.042	0.019	0.122	0.115	0.204	0.013
D_moneorum	0.481	0.468	0.000	0.223	0.000	0.000	0.000	0.241	0.000	0.000	0.000	0.000	0.004	0.518	0.000
D_parallela	0.000	0.000	0.108	0.072	0.000	0.000	0.240	0.000	0.008	0.129	0.062	0.302	0.053	0.000	0.089
D_pugionata	0.000	0.000	0.371	0.055	0.000	0.240	0.000	0.000	0.000	0.424	0.037	0.180	0.002	0.000	0.041
D_riley	0.216	0.205	0.000	0.188	0.241	0.000	0.000	0.000	0.000	0.000	0.000	0.000	0.000	0.518	0.000
D_yucatana	0.000	0.000	0.017	0.060	0.000	0.008	0.000	0.000	0.000	0.000	0.000	0.008	0.345	0.000	0.000
D_monoceros	0.000	0.000	0.561	0.042	0.000	0.129	0.424	0.000	0.000	0.000	0.092	0.262	0.003	0.000	0.135
P_ensifera	0.000	0.000	0.022	0.019	0.000	0.062	0.037	0.000	0.000	0.092	0.000	0.227	0.067	0.000	0.449
P_apiculata	0.000	0.000	0.175	0.122	0.000	0.302	0.180	0.000	0.008	0.262	0.227	0.000	0.128	0.000	0.344
P_minima	0.015	0.002	0.149	0.115	0.004	0.053	0.002	0.000	0.345	0.003	0.067	0.128	0.000	0.000	0.137
P_rugosa	0.383	0.373	0.000	0.204	0.518	0.000	0.000	0.518	0.000	0.000	0.000	0.000	0.000	0.000	0.000
P_spinosa	0.000	0.000	0.027	0.013	0.000	0.089	0.041	0.000	0.000	0.135	0.449	0.344	0.137	0.000	0.000

Morphological Overlap: Overlap calculation using only 3 axes of principal components (1, 2, 3) & including body height

Table S30: Overlap matrix of morphological hypervolume at species level, including all principal components but PC1, 2, 3 using log-transformed data.

	D_aculeat	D_aurit	D. biden	D_cornige	D_moneoru	D_paralle	D_pugiona	D_rile	D_yucatan	D_monocer	P_ensife	P_apicula	P_minim	P_rugos	P_spinos
D_aculeata	0.000	0.544	0.000	0.350	0.495	0.000	0.000	0.217	0.000	0.000	0.000	0.000	0.019	0.372	0.000
D_aurita	0.544	0.000	0.000	0.156	0.471	0.000	0.000	0.211	0.000	0.000	0.000	0.000	0.004	0.387	0.000
D. bidens	0.000	0.000	0.000	0.093	0.000	0.117	0.380	0.000	0.014	0.560	0.024	0.189	0.140	0.000	0.027
D_cornigera	0.350	0.156	0.093	0.000	0.210	0.073	0.058	0.181	0.060	0.041	0.011	0.114	0.111	0.203	0.011
D_moneorum	0.495	0.471	0.000	0.210	0.000	0.000	0.000	0.233	0.000	0.000	0.000	0.000	0.003	0.528	0.000
D_parallela	0.000	0.000	0.117	0.073	0.000	0.000	0.257	0.000	0.004	0.134	0.057	0.284	0.048	0.000	0.087
D_pugionata	0.000	0.000	0.380	0.058	0.000	0.257	0.000	0.000	0.000	0.417	0.038	0.194	0.002	0.000	0.042
D_riley	0.217	0.211	0.000	0.181	0.233	0.000	0.000	0.000	0.000	0.000	0.000	0.000	0.000	0.517	0.000
D_yucatana	0.000	0.000	0.014	0.060	0.000	0.004	0.000	0.000	0.000	0.000	0.000	0.005	0.343	0.000	0.000
D_monoceros	0.000	0.000	0.560	0.041	0.000	0.134	0.417	0.000	0.000	0.000	0.086	0.264	0.004	0.000	0.141
P_ensifera	0.000	0.000	0.041	0.000	0.134	0.417	0.000	0.000	0.000	0.000	0.000	0.229	0.072	0.000	0.454
P_apiculata	0.000	0.000	0.189	0.114	0.000	0.284	0.194	0.000	0.005	0.264	0.229	0.000	0.124	0.000	0.340
P_minima	0.019	0.004	0.140	0.111	0.003	0.048	0.002	0.000	0.343	0.004	0.072	0.124	0.000	0.000	0.143
P_rugosa	0.372	0.387	0.000	0.203	0.528	0.000	0.000	0.517	0.000	0.000	0.000	0.000	0.000	0.000	0.000
P_spinosa	0.000	0.000	0.027	0.011	0.000	0.087	0.042	0.000	0.000	0.141	0.454	0.340	0.143	0.000	0.000

Table S31: Overlap matrix of morphological hypervolume at species level, including all principal components but PC1, 2, 3 using non-log-transformed data

	D_aculeat	D_aurita	D. biden	D_cornige	D_moneoru	D_parallel	D_pugiona	D_riley	D_yucatan	D_monocer	P_ensifer	P_apicula	P_minim	P_rugos	P_spinos
D_aculeata	0.000	0.454	0.000	0.318	0.371	0.000	0.000	0.252	0.000	0.000	0.000	0.000	0.011	0.433	0.000
D_aurita	0.454	0.000	0.000	0.105	0.503	0.000	0.000	0.205	0.000	0.000	0.000	0.000	0.001	0.324	0.000
D. bidens	0.000	0.000	0.000	0.158	0.000	0.106	0.416	0.000	0.016	0.483	0.022	0.269	0.129	0.000	0.060
D_cornigera	0.318	0.105	0.158	0.000	0.100	0.065	0.078	0.130	0.046	0.052	0.004	0.126	0.099	0.171	0.006
D_moneorum	0.371	0.503	0.000	0.100	0.000	0.000	0.000	0.189	0.000	0.000	0.000	0.000	0.002	0.353	0.000
D_parallela	0.000	0.000	0.106	0.065	0.000	0.000	0.276	0.000	0.006	0.104	0.043	0.328	0.037	0.000	0.089
D_pugionata	0.000	0.000	0.416	0.078	0.000	0.276	0.000	0.000	0.000	0.387	0.062	0.323	0.016	0.000	0.090
D_riley	0.252	0.205	0.000	0.130	0.189	0.000	0.000	0.000	0.000	0.000	0.000	0.000	0.000	0.583	0.000
D_yucatana	0.000	0.000	0.016	0.046	0.000	0.006	0.000	0.000	0.000	0.000	0.000	0.004	0.390	0.000	0.000
D_monoceros	0.000	0.000	0.483	0.052	0.000	0.104	0.387	0.000	0.000	0.000	0.067	0.256	0.000	0.000	0.124
P_ensifera	0.000	0.000	0.022	0.004	0.000	0.043	0.062	0.000	0.000	0.067	0.000	0.144	0.053	0.000	0.444
P_apiculata	0.000	0.000	0.269	0.126	0.000	0.328	0.323	0.000	0.004	0.256	0.144	0.000	0.091	0.000	0.291
P_minima	0.011	0.001	0.129	0.099	0.002	0.037	0.016	0.000	0.390	0.000	0.053	0.091	0.000	0.000	0.131
P_rugosa	0.433	0.324	0.000	0.171	0.353	0.000	0.000	0.583	0.000	0.000	0.000	0.000	0.000	0.000	0.000
P_spinosa	0.000	0.000	0.060	0.006	0.000	0.089	0.090	0.000	0.000	0.124	0.444	0.291	0.131	0.000	0.000

Table S32: Results of Mantel test between pairwise comparison of morphological and environmental hypervolumes, including log-transformed data.

Mantel Test Species Morphological Overlap		PC's (All)	PC's (except 1)	PC's 2, 3, & 4
With Spine	Natural Log	-0.051 (0.718)	0.043 (0.388)	0.103 (0.261)
	No Log	-0.002 (0.527)	-0.052 (0.611)	0.127 (0.266)
No Spine	Natural Log	0.090 (0.160)	0.227 (0.059)	0.216 (0.040)
	No Log	-0.082 (0.797)	-0.046 (0.046)	-0.052 (0.611)
Mantel Test Genus Morphological Overlap		PC's (All)	PC's (except 1)	PC's 2, 3, & 4
With Spine	Natural Log	NA (NA)	0.003 (0.527)	-0.597 (1)
	No Log	-0.387 (0.833)	-0.497 (0.833)	-0.730 (1)
No Spine	Natural Log	-0.210 (0.583)	-0.275 (0.958)	-0.778 (1)
	No Log	-0.183 (0.542)	-0.333 (0.958)	-0.776 (1)

Table S33: Overlap matrix of EDHC in the environmental space at genus level.

	Dorynota	***Paratrikona***	***Omoteina***	***Akantaka***
Dorynota	1	0.727	3.303	1.286
Paratrikona	0.727	1	2.963	1.255
Omoteina	3.303	2.963	1	4.209
Akantaka	1.286	1.255	4.209	1

Table S34: Overlap matrix of EDHC in the environmental space at species level.

	D. aculeata	*D. aurita*	*D. bidens*	*D. cornigera*	*D. moneorum*	*D. parallela*	*D. pugionata*	*D. rileyi*	*D. yucatana*	*D. monoceros*	*D. ensifera*	*D. apiculata*	*D. minima*	*D. rugosa*	*D. spinosa*
D. aculeata	1	2.034	1.533	0.444	1.18	0.546	0.972	1.284	0.646	1.229	1.325	1.339	0.904	0.3	0.532
D. aurita	2.034	1	2.954	2.074	1.269	1.86	1.28	3.119	2.511	1.906	0.91	1.816	2.848	1.917	2.126
D. bidens	1.533	2.954	1	1.436	1.767	1.979	2.312	0.814	1.748	1.125	2.097	1.28	1.871	1.797	1.875
D. cornigera	0.444	2.074	1.436	1	1.044	0.576	1.019	1.164	0.62	1.059	1.418	1.365	1.157	0.491	0.492
D. moneorum	1.18	1.269	1.767	1.044	1	1.185	0.988	1.944	1.635	0.7	0.692	0.92	2.082	1.175	1.343
D. parallela	0.546	1.86	1.979	0.576	1.185	1	0.613	1.665	0.677	1.475	1.377	1.673	1.156	0.255	0.279
D. pugionata	0.972	1.28	2.312	1.019	0.988	0.613	1	2.168	1.289	1.53	1.013	1.644	1.692	0.741	0.888
D. rileyi	1.284	3.119	0.814	1.164	1.944	1.665	2.168	1	1.194	1.496	2.316	1.761	1.32	1.508	1.465
D. yucatana	0.646	2.511	1.748	0.62	1.635	0.677	1.289	1.194	1	1.656	1.91	1.906	0.716	0.622	0.409
D. monoceros	1.229	1.906	1.125	1.059	0.7	1.475	1.53	1.496	1.656	1	1.152	0.597	2.028	1.373	1.52
D. ensifera	1.325	0.91	2.097	1.418	0.692	1.377	1.013	2.316	1.91	1.152	1	0.96	2.172	1.324	1.599
D.apiculata	1.339	1.816	1.28	1.365	0.92	1.673	1.644	1.761	1.906	0.597	0.96	1	2.1	1.519	1.763
D. minima	0.904	2.848	1.871	1.157	2.082	1.156	1.692	1.32	0.716	2.028	2.172	2.1	1	0.997	0.986
D.rugosa	0.3	1.917	1.797	0.491	1.175	0.255	0.741	1.508	0.622	1.373	1.324	1.519	0.997	1	0.334
D.spinosa	0.532	2.126	1.875	0.492	1.343	0.279	0.888	1.465	0.409	1.52	1.599	1.763	0.986	0.334	1

Morphological Overlap: Including body height in the dataset

Table S35: Overlap matrix of EDHC in the morphological space at genus level, including all principal components except PC 1, using log-transformed data

	Dorynota	***Paratrikona***	***Omoteina***	***Akantaka***
Dorynota	1	1.054	1.384	2.048
Paratrikona	1.054	1	0.748	1.451
Omoteina	1.384	0.748	1	1.071
Akantaka	2.048	1.451	1.071	1

Table S36: Overlap matrix of EDHC in the morphological space at genus level, including all principal components

	Dorynota	***Paratrikona***	***Omoteina***	***Akantaka***
Dorynota	1	1.061	2.421	5.164
Paratrikona	1.061	1	2.286	4.798
Omoteina	2.421	2.286	1	6.818
Akantaka	5.164	4.798	6.818	1

Table S37: Overlap matrix of EDHC in the morphological space at genus level, including all principal components, except PC1

	Dorynota	***Paratrikona***	***Omoteina***	***Akantaka***
Dorynota	1	1.054	1.384	2.048
Paratrikona	1.054	1	0.748	1.451
Omoteina	1.384	0.748	1	1.071
Akantaka	2.048	1.451	1.071	1

Morphological Overlap: Excluding body height in the dataset

Table S38: Overlap matrix of EDHC in the morphological space at genus level, including all principal components, excluding body height from dataset.

	Dorynota	***Paratrikona***	***Omoteina***	***Akantaka***
Dorynota	1	0.774	1.711	5.065
Paratrikona	0.774	1	1.980	4.734
Omoteina	1.711	1.980	1	6.530
Akantaka	5.065	4.734	6.530	1

Table S39: Overlap matrix of EDHC in the morphological space at genus level, including all but PC1, excluding body height from dataset.

	Dorynota	***Paratrikona***	***Omoteina***	***Akantaka***
Dorynota	1	0.698	0.837	0.907
Paratrikona	0.698	1	0.691	1.010
Omoteina	0.837	0.691	1	0.815
Akantaka	0.907	1.010	0.815	1

Morphological Overlap: Including body height in the dataset

Table S40: Overlap matrix of EDHC in the morphological space at genus level, including all but principal components 1, 5 & 6, using log-transformed data.

	Dorynota	***Paratrikona***	***Omoteina***	***Akantaka***
Dorynota	1	1.097	1.840	1.469
Paratrikona	1.097	1	1.007	0.907
Omoteina	1.840	1.007	1	0.482
Akantaka	1.469	0.907	0.482	1

Table S41: Overlap matrix of EDHC in the morphological space at genus level, including all but principal components 1, 5 & 6 using non-log-transformed data.

	Dorynota	***Paratrikona***	***Omoteina***	***Akantaka***
Dorynota	1	1.047	1.330	2.024
Paratrikona	1.047	1	0.598	1.420
Omoteina	1.330	0.598	1	0.827
Akantaka	2.024	1.420	0.827	1

Table S42: Overlap matrix of EDHC in the morphological space at genus level, including all but principal components 1, 5 using log-transformed data

	Dorynota	***Paratrikona***	***Omoteina***	***Akantaka***
Dorynota	1	0.697	0.784	0.883
Paratrikona	0.697	1	0.538	0.984
Omoteina	0.784	0.538	1	0.506
Akantaka	0.883	0.984	0.506	1

Table S43: Overlap matrix of EDHC in the morphological space at genus level, including all but principal components 1, 5 using non-log-transformed data.

	Dorynota	***Paratrikona***	***Omoteina***	***Akantaka***
Dorynota	1	0.696	0.783	0.881
Paratrikona	0.696	1	0.536	0.983
Omoteina	0.783	0.536	1	0.508
Akantaka	0.881	0.983	0.508	1

Morphological Overlap: Including body height in the dataset

Table S44: Overlap matrix of EDHC in the morphological space at species level, including all principal components using log-transformed data.

	D. aculeata	*D. aurita*	*D. bidens*	*D. cornigera*	*D. moneorum*	*D. parallela*	*D. pugionata*	*D. rileyi*	*D. yucatana*	*D. monoceros*	*D. ensifera*	*D. apiculata*	*D. minima*	*D. rugosa*	*D. spinosa*
D. aculeata	1	0.454	3.35	0.887	0.597	4.383	4.151	1.692	2.395	4.761	5.231	5.406	2.941	1.199	5.466
D. aurita	0.454	1	3.714	1.22	0.428	4.751	4.512	1.308	2.763	5.134	5.625	5.799	3.318	0.844	5.858
D. bidens	3.35	3.714	1	2.578	3.777	1.484	0.864	4.985	1.096	1.437	2.145	2.28	0.944	4.501	2.373
D. cornigera	0.887	1.22	2.578	1	1.366	3.661	3.358	2.463	1.689	3.985	4.507	4.69	2.189	2.009	4.738
D. moneorum	0.597	0.428	3.777	1.366	1	4.815	4.559	1.291	2.812	5.194	5.65	5.838	3.376	0.783	5.896
D. parallela	4.383	4.751	1.484	3.661	4.815	1	1.208	6.037	2.037	1.09	1.311	1.321	1.557	5.555	1.38
D. pugionata	4.151	4.512	0.864	3.358	4.559	1.208	1	5.776	1.839	0.76	1.489	1.658	1.443	5.295	1.716
D. rileyi	1.692	1.308	4.985	2.463	1.291	6.037	5.776	1	4.049	6.411	6.903	7.086	4.595	0.531	7.143
D. yucatana	2.395	2.763	1.096	1.689	2.812	2.037	1.839	4.049	1	2.422	2.898	3.06	0.697	3.558	3.125
D. monoceros	4.761	5.134	1.437	3.985	5.194	1.09	0.76	6.411	2.422	1	1.066	1.086	1.994	5.925	1.199
D. ensifera	5.231	5.625	2.145	4.507	5.65	1.311	1.489	6.903	2.898	1.066	1	0.41	2.368	6.402	0.334
D.apiculata	5.406	5.799	2.28	4.69	5.838	1.321	1.658	7.086	3.06	1.086	0.41	1	2.562	6.584	0.288
D. minima	2.941	3.318	0.944	2.189	3.376	1.557	1.443	4.595	0.697	1.994	2.368	2.562	1	4.114	2.583
D.rugosa	1.199	0.844	4.501	2.009	0.783	5.555	5.295	0.531	3.558	5.925	6.402	6.584	4.114	1	6.644
D.spinosa	5.466	5.858	2.373	4.738	5.896	1.38	1.716	7.143	3.125	1.199	0.334	0.288	2.583	6.644	1

Table S45: Overlap matrix of EDHC in the morphological space at species level, including all principal components but PC1 using log-transformed data.

	D. aculeata	*D. aurita*	*D. bidens*	*D. cornigera*	*D. moneorum*	*D. parallela*	*D. pugionata*	*D. rileyi*	*D. yucatana*	*D. monoceros*	*D. ensifera*	*D. apiculata*	*D. minima*	*D. rugosa*	*D. spinosa*
D. aculeata	1	0.246	0.79	0.467	0.427	0.765	0.917	0.248	0.396	0.826	0.307	0.276	0.407	0.229	0.137
D. aurita	0.246	1	0.703	0.42	0.427	0.648	0.814	0.238	0.231	0.752	0.401	0.348	0.33	0.3	0.252
D. bidens	0.79	0.703	1	0.63	0.839	1.032	0.354	0.733	0.625	0.129	0.841	0.77	0.872	0.768	0.855
D. cornigera	0.467	0.42	0.63	1	0.692	0.857	0.659	0.394	0.519	0.632	0.62	0.67	0.381	0.544	0.547
D. moneorum	0.427	0.427	0.839	0.692	1	0.849	0.877	0.319	0.373	0.91	0.258	0.431	0.524	0.208	0.344
D. parallela	0.765	0.648	1.032	0.857	0.849	1	1.189	0.735	0.583	1.029	0.961	0.771	0.683	0.81	0.783
D. pugionata	0.917	0.814	0.354	0.659	0.877	1.189	1	0.781	0.738	0.409	0.895	0.96	0.883	0.846	0.956
D. rileyi	0.248	0.238	0.733	0.394	0.319	0.735	0.781	1	0.293	0.775	0.314	0.425	0.261	0.19	0.249
D. yucatana	0.396	0.231	0.625	0.519	0.373	0.583	0.738	0.293	1	0.679	0.47	0.394	0.425	0.334	0.391
D. monoceros	0.826	0.752	0.129	0.632	0.91	1.029	0.409	0.775	0.679	1	0.91	0.822	0.897	0.824	0.906
D. ensifera	0.307	0.401	0.841	0.62	0.258	0.961	0.895	0.314	0.47	0.91	1	0.37	0.529	0.168	0.231
D.apiculata	0.276	0.348	0.77	0.67	0.431	0.771	0.96	0.425	0.394	0.822	0.37	1	0.622	0.307	0.28
D. minima	0.407	0.33	0.872	0.381	0.524	0.683	0.883	0.261	0.425	0.897	0.529	0.622	1	0.433	0.409
D.rugosa	0.229	0.3	0.768	0.544	0.208	0.81	0.846	0.19	0.334	0.824	0.168	0.307	0.433	1	0.182
D.spinosa	0.137	0.252	0.855	0.547	0.344	0.783	0.956	0.249	0.391	0.906	0.231	0.28	0.409	0.182	1

Morphological Overlap: Excluding body height in the dataset

Table S46: Overlap matrix of EDHC in the morphological space at species level, including all principal components using non-log-transformed data.

	D. aculeata	*D. aurita*	*D. bidens*	*D. cornigera*	*D. moneorum*	*D. parallela*	*D. pugionata*	*D. rileyi*	*D. yucatana*	*D. monoceros*	*D. ensifera*	*D. apiculata*	*D. minima*	*D. rugosa*	*D. spinosa*
D. aculeata	1	0.48	3.354	0.994	0.368	4.003	4.021	2.068	2.612	4.338	4.721	4.758	3.009	1.354	4.818
D. aurita	0.48	1	3.739	1.319	0.475	4.372	4.41	1.694	2.999	4.727	5.129	5.16	3.399	1.037	5.221
D. bidens	3.354	3.739	1	2.518	3.67	1.16	0.721	5.387	0.896	1.005	1.594	1.589	0.807	4.693	1.675
D. cornigera	0.994	1.319	2.518	1	1.342	3.251	3.171	2.905	1.864	3.505	3.952	3.993	2.221	2.263	4.044
D. moneorum	0.368	0.475	3.67	1.342	1	4.285	4.334	1.808	2.91	4.646	5.006	5.045	3.304	1.073	5.104
D. parallela	4.003	4.372	1.16	3.251	4.285	1	1.001	6.03	1.434	0.992	1.176	1.109	1.154	5.341	1.166
D. pugionata	4.021	4.41	0.721	3.171	4.334	1.001	1	6.057	1.493	0.384	0.985	1	1.175	5.366	1.053
D. rileyi	2.068	1.694	5.387	2.905	1.808	6.03	6.057	1	4.663	6.379	6.78	6.82	5.046	0.769	6.876
D. yucatana	2.612	2.999	0.896	1.864	2.91	1.434	1.493	4.663	1	1.777	2.161	2.175	0.539	3.962	2.241
D. monoceros	4.338	4.727	1.005	3.505	4.646	0.992	0.384	6.379	1.777	1	0.802	0.749	1.484	5.682	0.839
D. ensifera	4.721	5.129	1.594	3.952	5.006	1.176	0.985	6.78	2.161	0.802	1	0.24	1.783	6.067	0.157
D.apiculata	4.758	5.16	1.589	3.993	5.045	1.109	1	6.82	2.175	0.749	0.24	1	1.834	6.105	0.212
D. minima	3.009	3.399	0.807	2.221	3.304	1.154	1.175	5.046	0.539	1.484	1.783	1.834	1	4.357	1.86
D.rugosa	1.354	1.037	4.693	2.263	1.073	5.341	5.366	0.769	3.962	5.682	6.067	6.105	4.357	1	6.166
D.spinosa	4.818	5.221	1.675	4.044	5.104	1.166	1.053	6.876	2.241	0.839	0.157	0.212	1.86	6.166	1

Table S47: Overlap matrix of EDHC in the morphological space at species level, including all principal components using log-transformed data.

	D. aculeata	*D. aurita*	*D. bidens*	*D. cornigera*	*D. moneorum*	*D. parallela*	*D. pugionata*	*D. rileyi*	*D. yucatana*	*D. monoceros*	*D. ensifera*	*D. apiculata*	*D. minima*	*D. rugosa*	*D. spinosa*
D. aculeata	1	0.475	3.36	1.011	0.36	4.009	4.025	2.063	2.617	4.344	4.725	4.781	3.017	1.351	4.821
D. aurita	0.475	1	3.741	1.336	0.478	4.374	4.409	1.694	3	4.729	5.128	5.178	3.402	1.039	5.219
D. bidens	3.36	3.741	1	2.501	3.665	1.159	0.718	5.389	0.897	1.004	1.591	1.604	0.807	4.697	1.671
D. cornigera	1.011	1.336	2.501	1	1.349	3.233	3.151	2.924	1.845	3.487	3.931	3.991	2.203	2.283	4.022
D. moneorum	0.36	0.478	3.665	1.349	1	4.279	4.326	1.815	2.903	4.64	4.997	5.055	3.299	1.083	5.094
D. parallela	4.009	4.374	1.159	3.233	4.279	1	1.001	6.032	1.435	0.992	1.174	1.12	1.154	5.344	1.164
D. pugionata	4.025	4.409	0.718	3.151	4.326	1.001	1	6.056	1.491	0.385	0.985	1.016	1.173	5.368	1.052
D. rileyi	2.063	1.694	5.389	2.924	1.815	6.032	6.056	1	4.664	6.38	6.779	6.838	5.048	0.766	6.873
D. yucatana	2.617	3	0.897	1.845	2.903	1.435	1.491	4.664	1	1.778	2.159	2.191	0.539	3.965	2.238
D. monoceros	4.344	4.729	1.004	3.487	4.64	0.992	0.385	6.38	1.778	1	0.799	0.76	1.482	5.686	0.836
D. ensifera	4.725	5.128	1.591	3.931	4.997	1.174	0.985	6.779	2.159	0.799	1	0.244	1.779	6.067	0.157
D.apiculata	4.781	5.178	1.604	3.991	5.055	1.12	1.016	6.838	2.191	0.76	0.244	1	1.849	6.124	0.207
D. minima	3.017	3.402	0.807	2.203	3.299	1.154	1.173	5.048	0.539	1.482	1.779	1.849	1	4.361	1.856
D.rugosa	1.351	1.039	4.697	2.283	1.083	5.344	5.368	0.766	3.965	5.686	6.067	6.124	4.361	1	6.165
D.spinosa	4.821	5.219	1.671	4.022	5.094	1.164	1.052	6.873	2.238	0.836	0.157	0.207	1.856	6.165	1

Table S48: Overlap matrix of EDHC in the morphological space at species level, including all principal components but PC1 using log-transformed data

	D. aculeata	*D. aurita*	*D. bidens*	*D. cornigera*	*D. moneorum*	*D. parallela*	*D. pugionata*	*D. rileyi*	*D. yucatana*	*D. monoceros*	*D. ensifera*	*D. apiculata*	*D. minima*	*D. rugosa*	*D. spinosa*
D. aculeata	1	0.234	0.686	0.458	0.152	0.779	0.662	0.869	0.219	0.601	0.106	0.156	0.253	0.041	0.124
D. aurita	0.234	1	0.617	0.403	0.336	0.64	0.612	0.81	0.143	0.524	0.298	0.344	0.371	0.225	0.263
D. bidens	0.686	0.617	1	0.554	0.802	0.945	0.294	0.278	0.608	0.14	0.655	0.687	0.81	0.668	0.793
D. cornigera	0.458	0.403	0.554	1	0.591	0.849	0.36	0.625	0.39	0.487	0.467	0.56	0.68	0.434	0.544
D. moneorum	0.152	0.336	0.802	0.591	1	0.771	0.798	1.002	0.297	0.709	0.218	0.204	0.144	0.164	0.114
D. parallela	0.779	0.64	0.945	0.849	0.771	1	1.009	1.175	0.589	0.816	0.87	0.886	0.711	0.754	0.76
D. pugionata	0.662	0.612	0.294	0.36	0.798	1.009	1	0.274	0.599	0.31	0.631	0.698	0.855	0.641	0.776
D. rileyi	0.869	0.81	0.278	0.625	1.002	1.175	0.274	1	0.813	0.391	0.824	0.871	1.038	0.854	0.983
D. yucatana	0.219	0.143	0.608	0.39	0.297	0.589	0.599	0.813	1	0.496	0.297	0.345	0.329	0.188	0.266
D. monoceros	0.601	0.524	0.14	0.487	0.709	0.816	0.31	0.391	0.496	1	0.588	0.623	0.713	0.578	0.704
D. ensifera	0.106	0.298	0.655	0.467	0.218	0.87	0.631	0.824	0.297	0.588	1	0.099	0.314	0.129	0.207
D.apiculata	0.156	0.344	0.687	0.56	0.204	0.886	0.698	0.871	0.345	0.623	0.099	1	0.268	0.185	0.219
D. minima	0.253	0.371	0.81	0.68	0.144	0.711	0.855	1.038	0.329	0.713	0.314	0.268	1	0.261	0.213
D.rugosa	0.041	0.225	0.668	0.434	0.164	0.754	0.641	0.854	0.188	0.578	0.129	0.185	0.261	1	0.146
D.spinosa	0.124	0.263	0.793	0.544	0.114	0.76	0.776	0.983	0.266	0.704	0.207	0.219	0.213	0.146	1

Table S49: Overlap matrix of EDHC in the morphological space at species level, including all principal components but PC1 using non-log-transformed data

	D. aculeata	*D. aurita*	*D. bidens*	*D. cornigera*	*D. moneorum*	*D. parallela*	*D. pugionata*	*D. rileyi*	*D. yucatana*	*D. monoceros*	*D. ensifera*	*D. apiculata*	*D. minima*	*D. rugosa*	*D. spinosa*
D. aculeata	1	0.307	0.606	0.568	0.217	0.799	0.548	0.252	0.294	0.572	0.13	0.187	0.36	0.117	0.092
D. aurita	0.307	1	0.564	0.506	0.462	0.653	0.531	0.346	0.188	0.54	0.407	0.338	0.326	0.417	0.308
D. bidens	0.606	0.564	1	0.454	0.779	0.972	0.246	0.609	0.542	0.066	0.707	0.615	0.732	0.66	0.687
D. cornigera	0.568	0.506	0.454	1	0.759	0.971	0.244	0.418	0.566	0.417	0.655	0.693	0.484	0.645	0.624
D. moneorum	0.217	0.462	0.779	0.759	1	0.783	0.744	0.376	0.394	0.742	0.202	0.24	0.456	0.149	0.192
D. parallela	0.799	0.653	0.972	0.971	0.783	1	1.021	0.762	0.55	0.936	0.895	0.76	0.691	0.84	0.783
D. pugionata	0.548	0.531	0.246	0.244	0.744	1.021	1	0.49	0.557	0.22	0.636	0.629	0.613	0.61	0.625
D. rileyi	0.252	0.346	0.609	0.418	0.376	0.762	0.49	1	0.34	0.558	0.336	0.412	0.197	0.306	0.285
D. yucatana	0.294	0.188	0.542	0.566	0.394	0.55	0.557	0.34	1	0.508	0.413	0.276	0.37	0.368	0.313
D. monoceros	0.572	0.54	0.066	0.417	0.742	0.936	0.22	0.558	0.508	1	0.677	0.593	0.686	0.623	0.654
D. ensifera	0.13	0.407	0.707	0.655	0.202	0.895	0.636	0.336	0.413	0.677	1	0.24	0.43	0.125	0.12
D.apiculata	0.187	0.338	0.615	0.693	0.24	0.76	0.629	0.412	0.276	0.593	0.24	1	0.498	0.206	0.204
D. minima	0.36	0.326	0.732	0.484	0.456	0.691	0.613	0.197	0.37	0.686	0.43	0.498	1	0.434	0.345
D.rugosa	0.117	0.417	0.66	0.645	0.149	0.84	0.61	0.306	0.368	0.623	0.125	0.206	0.434	1	0.156
D.spinosa	0.092	0.308	0.687	0.624	0.192	0.783	0.625	0.285	0.313	0.654	0.12	0.204	0.345	0.156	1

Morphological Overlap: Overlap calculation using only 3 axes of principal components (2, 3, 4)

Table S50: Overlap matrix of EDHC in the morphological space at species level, including principal components 2, 3 & 4 using log-transformed data

	D. aculeata	*D. aurita*	*D. bidens*	*D. cornigera*	*D. moneorum*	*D. parallela*	*D. pugionata*	*D. rileyi*	*D. yucatana*	*D. monoceros*	*D. ensifera*	*D. apiculata*	*D. minima*	*D. rugosa*	*D. spinosa*
D. aculeata	1	0.232	0.775	0.426	0.075	0.741	0.869	0.21	0.336	0.838	0.161	0.242	0.343	0.06	0.048
D. aurita	0.232	1	0.61	0.358	0.227	0.58	0.762	0.243	0.115	0.667	0.335	0.228	0.347	0.217	0.257
D. bidens	0.775	0.61	1	0.523	0.739	0.93	0.336	0.705	0.565	0.1	0.765	0.741	0.793	0.729	0.817
D. cornigera	0.426	0.358	0.523	1	0.358	0.75	0.505	0.253	0.337	0.546	0.461	0.557	0.311	0.369	0.47
D. moneorum	0.075	0.227	0.739	0.358	1	0.739	0.812	0.143	0.318	0.797	0.176	0.296	0.29	0.031	0.116
D. parallela	0.741	0.58	0.93	0.75	0.739	1	1.098	0.682	0.503	0.937	0.889	0.701	0.615	0.745	0.739
D. pugionata	0.869	0.762	0.336	0.505	0.812	1.098	1	0.746	0.721	0.303	0.842	0.924	0.812	0.812	0.917
D. rileyi	0.21	0.243	0.705	0.253	0.143	0.682	0.746	1	0.284	0.747	0.305	0.399	0.166	0.167	0.242
D. yucatana	0.336	0.115	0.565	0.337	0.318	0.503	0.721	0.284	1	0.608	0.441	0.328	0.346	0.314	0.361
D. monoceros	0.838	0.667	0.1	0.546	0.797	0.937	0.303	0.747	0.608	1	0.838	0.816	0.818	0.79	0.881
D. ensifera	0.161	0.335	0.765	0.461	0.176	0.889	0.842	0.305	0.441	0.838	1	0.302	0.46	0.156	0.185
D.apiculata	0.242	0.228	0.741	0.557	0.296	0.701	0.924	0.399	0.328	0.816	0.302	1	0.52	0.271	0.24
D. minima	0.343	0.347	0.793	0.311	0.29	0.615	0.812	0.166	0.346	0.818	0.46	0.52	1	0.317	0.36
D.rugosa	0.06	0.217	0.729	0.369	0.031	0.745	0.812	0.167	0.314	0.79	0.156	0.271	0.317	1	0.108
D.spinosa	0.048	0.257	0.817	0.47	0.116	0.739	0.917	0.242	0.361	0.881	0.185	0.24	0.36	0.108	1

Table S51: Overlap matrix of EDHC in the morphological space at species level, including principal components 2, 3 & 4 using non-log-transformed data.

	D. aculeata	*D. aurita*	*D. bidens*	*D. cornigera*	*D. moneorum*	*D. parallela*	*D. pugionata*	*D. rileyi*	*D. yucatana*	*D. monoceros*	*D. ensifera*	*D. apiculata*	*D. minima*	*D. rugosa*	*D. spinosa*
D. aculeata	1	0.261	0.679	0.428	0.421	0.784	0.694	0.276	0.337	0.622	0.194	0.069	0.175	0.23	0.074
D. aurita	0.261	1	0.56	0.339	0.549	0.635	0.636	0.358	0.227	0.5	0.411	0.216	0.264	0.403	0.312
D. bidens	0.679	0.56	1	0.269	0.718	1	0.173	0.579	0.511	0.064	0.672	0.636	0.667	0.654	0.695
D. cornigera	0.428	0.339	0.269	1	0.583	0.901	0.324	0.409	0.362	0.222	0.45	0.395	0.457	0.456	0.455
D. moneorum	0.421	0.549	0.718	0.583	1	0.846	0.665	0.197	0.401	0.666	0.299	0.392	0.317	0.202	0.354
D. parallela	0.784	0.635	1	0.901	0.846	1	1.096	0.755	0.584	0.944	0.905	0.734	0.659	0.836	0.796
D. pugionata	0.694	0.636	0.173	0.324	0.665	1.096	1	0.562	0.563	0.193	0.638	0.656	0.684	0.622	0.694
D. rileyi	0.276	0.358	0.579	0.409	0.197	0.755	0.562	1	0.23	0.521	0.22	0.229	0.173	0.125	0.232
D. yucatana	0.337	0.227	0.511	0.362	0.401	0.584	0.563	0.23	1	0.448	0.399	0.268	0.221	0.335	0.34
D. monoceros	0.622	0.5	0.064	0.222	0.666	0.944	0.193	0.521	0.448	1	0.62	0.576	0.605	0.599	0.637
D. ensifera	0.194	0.411	0.672	0.45	0.299	0.905	0.638	0.22	0.399	0.62	1	0.21	0.246	0.109	0.14
D.apiculata	0.069	0.216	0.636	0.395	0.392	0.734	0.656	0.229	0.268	0.576	0.21	1	0.124	0.214	0.096
D. minima	0.175	0.264	0.667	0.457	0.317	0.659	0.684	0.173	0.221	0.605	0.246	0.124	1	0.194	0.151
D.rugosa	0.23	0.403	0.654	0.456	0.202	0.836	0.622	0.125	0.335	0.599	0.109	0.214	0.194	1	0.166
D.spinosa	0.074	0.312	0.695	0.455	0.354	0.796	0.694	0.232	0.34	0.637	0.14	0.096	0.151	0.166	1

Morphological Overlap: Overlap calculation using only 3 axes of principal components (2, 3, 4) & excluding body height

Table S52: Overlap matrix of EDHC in the morphological space at species level, including principal components 2, 3 & 4 using log-transformed data.

	D. aculeata	*D. aurita*	*D. bidens*	*D. cornigera*	*D. moneorum*	*D. parallela*	*D. pugionata*	*D. rileyi*	*D. yucatana*	*D. monoceros*	*D. ensifera*	*D. apiculata*	*D. minima*	*D. rugosa*	*D. spinosa*
D. aculeata	1	0.224	0.666	0.436	0.135	0.77	0.661	0.882	0.231	0.627	0.145	0.142	0.237	0.07	0.124
D. aurita	0.224	1	0.522	0.402	0.275	0.593	0.582	0.783	0.098	0.466	0.215	0.27	0.273	0.164	0.268
D. bidens	0.666	0.522	1	0.506	0.771	0.861	0.316	0.309	0.566	0.107	0.544	0.645	0.776	0.621	0.762
D. cornigera	0.436	0.402	0.506	1	0.544	0.802	0.325	0.621	0.356	0.44	0.399	0.519	0.622	0.391	0.529
D. moneorum	0.135	0.275	0.771	0.544	1	0.735	0.784	1.005	0.275	0.726	0.268	0.213	0.137	0.165	0.015
D. parallela	0.77	0.593	0.861	0.802	0.735	1	0.96	1.133	0.567	0.771	0.808	0.839	0.661	0.713	0.733
D. pugionata	0.661	0.582	0.316	0.325	0.784	0.96	1	0.303	0.582	0.297	0.559	0.684	0.839	0.619	0.772
D. rileyi	0.882	0.783	0.309	0.621	1.005	1.133	0.303	1	0.812	0.37	0.754	0.865	1.038	0.846	0.995
D. yucatana	0.231	0.098	0.566	0.356	0.275	0.567	0.582	0.812	1	0.498	0.26	0.322	0.295	0.163	0.264
D. monoceros	0.627	0.466	0.107	0.44	0.726	0.771	0.297	0.37	0.498	1	0.52	0.627	0.731	0.574	0.717
D. ensifera	0.145	0.215	0.544	0.399	0.268	0.808	0.559	0.754	0.26	0.52	1	0.128	0.331	0.146	0.259
D.apiculata	0.142	0.27	0.645	0.519	0.213	0.839	0.684	0.865	0.322	0.627	0.128	1	0.266	0.184	0.211
D. minima	0.237	0.273	0.776	0.622	0.137	0.661	0.839	1.038	0.295	0.731	0.331	0.266	1	0.244	0.147
D.rugosa	0.07	0.164	0.621	0.391	0.165	0.713	0.619	0.846	0.163	0.574	0.146	0.184	0.244	1	0.153
D.spinosa	0.124	0.268	0.762	0.529	0.015	0.733	0.772	0.995	0.264	0.717	0.259	0.211	0.147	0.153	1

Table S53: Overlap matrix of EDHC in the morphological space at species level, including principal components 2, 3 & 4 using non-log-transformed data.

	D. aculeata	*D. aurita*	*D. bidens*	*D. cornigera*	*D. moneorum*	*D. parallela*	*D. pugionata*	*D. rileyi*	*D. yucatana*	*D. monoceros*	*D. ensifera*	*D. apiculata*	*D. minima*	*D. rugosa*	*D. spinosa*
D. aculeata	1	0.283	0.583	0.538	0.192	0.829	0.529	0.261	0.323	0.57	0.096	0.185	0.295	0.056	0.082
D. aurita	0.283	1	0.438	0.51	0.375	0.638	0.489	0.352	0.09	0.436	0.361	0.208	0.348	0.319	0.293
D. bidens	0.583	0.438	1	0.341	0.752	0.934	0.231	0.569	0.494	0.064	0.659	0.581	0.636	0.637	0.643
D. cornigera	0.538	0.51	0.341	1	0.694	0.957	0.154	0.395	0.54	0.281	0.62	0.633	0.487	0.582	0.607
D. moneorum	0.192	0.375	0.752	0.694	1	0.774	0.707	0.337	0.375	0.738	0.178	0.246	0.306	0.143	0.119
D. parallela	0.829	0.638	0.934	0.957	0.774	1	1.007	0.769	0.552	0.92	0.892	0.753	0.67	0.83	0.793
D. pugionata	0.529	0.489	0.231	0.154	0.707	1.007	1	0.461	0.541	0.185	0.603	0.601	0.557	0.58	0.604
D. rileyi	0.261	0.352	0.569	0.395	0.337	0.769	0.461	1	0.35	0.53	0.338	0.396	0.12	0.273	0.297
D. yucatana	0.323	0.09	0.494	0.54	0.375	0.552	0.541	0.35	1	0.486	0.402	0.254	0.317	0.348	0.318
D. monoceros	0.57	0.436	0.064	0.281	0.738	0.92	0.185	0.53	0.486	1	0.65	0.585	0.599	0.623	0.632
D. ensifera	0.096	0.361	0.659	0.62	0.178	0.892	0.603	0.338	0.402	0.65	1	0.211	0.367	0.076	0.1
D.apiculata	0.185	0.208	0.581	0.633	0.246	0.753	0.601	0.396	0.254	0.585	0.211	1	0.394	0.202	0.162
D. minima	0.295	0.348	0.636	0.487	0.306	0.67	0.557	0.12	0.317	0.599	0.367	0.394	1	0.293	0.299
D.rugosa	0.056	0.319	0.637	0.582	0.143	0.83	0.58	0.273	0.348	0.623	0.076	0.202	0.293	1	0.053
D.spinosa	0.082	0.293	0.643	0.607	0.119	0.793	0.604	0.297	0.318	0.632	0.1	0.162	0.299	0.053	1

Morphological Overlap: Overlap calculation using only 3 axes of principal components (1, 2, 3) & excluding body height

Table S54: Overlap matrix of EDHC in the morphological space at species level, including principal components 4, 5 & 6 using log-transformed data.

	D. aculeata	*D. aurita*	*D. bidens*	*D. cornigera*	*D. moneorum*	*D. parallela*	*D. pugionata*	*D. rileyi*	*D. yucatana*	*D. monoceros*	*D. ensifera*	*D. apiculata*	*D. minima*	*D. rugosa*	*D. spinosa*
D. aculeata	1	0.398	3.426	0.798	0.358	4.416	4.301	1.615	2.429	4.711	5.345	5.444	2.962	1.185	5.564
D. aurita	0.398	1	3.735	1.098	0.225	4.733	4.619	1.28	2.754	5.025	5.694	5.785	3.302	0.87	5.91
D. bidens	3.426	3.735	1	2.645	3.775	1.41	0.893	5.003	1.095	1.298	2.145	2.213	0.836	4.585	2.364
D. cornigera	0.798	1.098	2.645	1	1.135	3.702	3.526	2.36	1.694	3.938	4.622	4.717	2.248	1.94	4.843
D. moneorum	0.358	0.225	3.775	1.135	1	4.773	4.652	1.259	2.786	5.063	5.701	5.801	3.32	0.828	5.92
D. parallela	4.416	4.733	1.41	3.702	4.773	1	1.134	6.009	2.016	1.039	1.347	1.272	1.521	5.592	1.426
D. pugionata	4.301	4.619	0.893	3.526	4.652	1.134	1	5.885	1.938	0.458	1.381	1.447	1.513	5.464	1.6
D. rileyi	1.615	1.28	5.003	2.36	1.259	6.009	5.885	1	4.031	6.297	6.959	7.056	4.573	0.435	7.177
D. yucatana	2.429	2.754	1.095	1.694	2.786	2.016	1.938	4.031	1	2.315	2.964	3.039	0.586	3.608	3.171
D. monoceros	4.711	5.025	1.298	3.938	5.063	1.039	0.458	6.297	2.315	1	1.114	1.114	1.865	5.877	1.283
D. ensifera	5.345	5.694	2.145	4.622	5.701	1.347	1.381	6.959	2.964	1.114	1	0.28	2.404	6.528	0.284
D.apiculata	5.444	5.785	2.213	4.717	5.801	1.272	1.447	7.056	3.039	1.114	0.28	1	2.485	6.628	0.188
D. minima	2.962	3.302	0.836	2.248	3.32	1.521	1.513	4.573	0.586	1.865	2.404	2.485	1	4.146	2.609
D.rugosa	1.185	0.87	4.585	1.94	0.828	5.592	5.464	0.435	3.608	5.877	6.528	6.628	4.146	1	6.748
D.spinosa	5.564	5.91	2.364	4.843	5.92	1.426	1.6	7.177	3.171	1.283	0.284	0.188	2.609	6.748	1

Table S55: Overlap matrix of EDHC in the morphological space at species level, including principal components 4, 5 & 6 using non-log-transformed data.

	D. aculeata	*D. aurita*	*D. bidens*	*D. cornigera*	*D. moneorum*	*D. parallela*	*D. pugionata*	*D. rileyi*	*D. yucatana*	*D. monoceros*	*D. ensifera*	*D. apiculata*	*D. Minima*	*D. rugosa*	*D. spinosa*
D. aculeata	1	0.513	3.628	0.906	0.466	4.375	4.31	2.278	2.779	4.614	5.179	5.235	3.265	1.702	5.321
D. aurita	0.513	1	4.04	1.278	0.291	4.786	4.733	1.844	3.205	5.033	5.63	5.679	3.708	1.296	5.769
D. bidens	3.628	4.04	1	2.779	4.086	1.248	0.705	5.87	0.949	1.004	1.744	1.777	0.723	5.307	1.885
D. cornigera	0.906	1.278	2.779	1	1.335	3.622	3.471	3.091	1.994	3.779	4.402	4.455	2.505	2.532	4.547
D. moneorum	0.466	0.291	4.086	1.335	1	4.838	4.77	1.815	3.245	5.075	5.643	5.7	3.731	1.237	5.786
D. parallela	4.375	4.786	1.248	3.622	4.838	1	1.102	6.625	1.651	1	1.257	1.18	1.231	6.065	1.286
D. pugionata	4.31	4.733	0.705	3.471	4.77	1.102	1	6.56	1.598	0.35	1.12	1.157	1.206	5.994	1.264
D. rileyi	2.278	1.844	5.87	3.091	1.815	6.625	6.56	1	5.044	6.867	7.455	7.511	5.54	0.586	7.598
D. yucatana	2.779	3.205	0.949	1.994	3.245	1.651	1.598	5.044	1	1.866	2.446	2.481	0.542	4.477	2.578
D. monoceros	4.614	5.033	1.004	3.779	5.075	1	0.35	6.867	1.866	1	0.889	0.884	1.448	6.302	1.002
D. ensifera	5.179	5.63	1.744	4.402	5.643	1.257	1.12	7.455	2.446	0.889	1	0.194	1.931	6.878	0.189
D.apiculata	5.235	5.679	1.777	4.455	5.7	1.18	1.157	7.511	2.481	0.884	0.194	1	1.973	6.937	0.132
D. minima	3.265	3.708	0.723	2.505	3.731	1.231	1.206	5.54	0.542	1.448	1.931	1.973	1	4.967	2.063
D.rugosa	1.702	1.296	5.307	2.532	1.237	6.065	5.994	0.586	4.477	6.302	6.878	6.937	4.967	1	7.022
D.spinosa	5.321	5.769	1.885	4.547	5.786	1.286	1.264	7.598	2.578	1.002	0.189	0.132	2.063	7.022	1

Morphological Overlap: Overlap calculation using only 3 axes of principal components (1, 2, 3) & including body height

Table S56: Overlap matrix of EDHC in the morphological space at species level, including principal components PC 1, 2, 3 using log-transformed data.

	D. aculeata	*D. aurita*	*D. bidens*	*D. cornigera*	*D. moneorum*	*D. parallela*	*D. pugionata*	*D. rileyi*	*D. yucatana*	*D. monoceros*	*D. Ensifera*	*D. apiculata*	*D. minima*	*D. rugosa*	*D. spinosa*
D. aculeata	1	0.519	3.622	0.899	0.479	4.365	4.3	2.285	2.772	4.609	5.172	5.224	3.27	1.702	5.318
D. aurita	0.519	1	4.04	1.277	0.29	4.782	4.73	1.844	3.204	5.035	5.629	5.674	3.719	1.288	5.773
D. bidens	3.622	4.04	1	2.781	4.094	1.249	0.701	5.871	0.951	1.005	1.744	1.773	0.72	5.301	1.889
D. cornigera	0.899	1.277	2.781	1	1.34	3.62	3.468	3.091	1.994	3.782	4.403	4.451	2.516	2.524	4.552
D. moneorum	0.479	0.29	4.094	1.34	1	4.841	4.773	1.808	3.25	5.084	5.649	5.703	3.749	1.223	5.797
D. parallela	4.365	4.782	1.249	3.62	4.841	1	1.107	6.621	1.65	1.007	1.264	1.182	1.221	6.054	1.297
D. pugionata	4.3	4.73	0.701	3.468	4.773	1.107	1	6.557	1.595	0.355	1.123	1.157	1.194	5.983	1.271
D. rileyi	2.285	1.844	5.871	3.091	1.808	6.621	6.557	1	5.043	6.869	7.455	7.507	5.552	0.595	7.602
D. yucatana	2.772	3.204	0.951	1.994	3.25	1.65	1.595	5.043	1	1.869	2.447	2.478	0.553	4.469	2.583
D. monoceros	4.609	5.035	1.005	3.782	5.084	1.007	0.355	6.869	1.869	1	0.887	0.88	1.44	6.296	1.005
D. ensifera	5.172	5.629	1.744	4.403	5.649	1.264	1.123	7.455	2.447	0.887	1	0.195	1.919	6.871	0.192
D.apiculata	5.224	5.674	1.773	4.451	5.703	1.182	1.157	7.507	2.478	0.88	0.195	1	1.958	6.925	0.14
D. minima	3.27	3.719	0.72	2.516	3.749	1.221	1.194	5.552	0.553	1.44	1.919	1.958	1	4.971	2.056
D.rugosa	1.702	1.288	5.301	2.524	1.223	6.054	5.983	0.595	4.469	6.296	6.871	6.925	4.971	1	7.019
D.spinosa	5.318	5.773	1.889	4.552	5.797	1.297	1.271	7.602	2.583	1.005	0.192	0.14	2.056	7.019	1

Table S57: Overlap matrix of EDHC in the morphological space at species level, including principal components PC 1, 2, 3 using non-log-transformed data.

	D. aculeata	*D. aurita*	*D. bidens*	*D. cornigera*	*D. moneorum*	*D. parallela*	*D. pugionata*	*D. rileyi*	*D. yucatana*	*D. monoceros*	*D. ensifera*	*D. apiculata*	*D. minima*	*D. rugosa*	*D. spinosa*
D. aculeata	1	0.407	3.427	0.968	0.297	4.028	4.123	1.967	2.674	4.295	4.821	4.813	3.048	1.398	4.894
D. aurita	0.407	1	3.723	1.244	0.394	4.308	4.431	1.66	2.976	4.595	5.15	5.132	3.365	1.125	5.218
D. bidens	3.427	3.723	1	2.505	3.671	1.114	0.723	5.373	0.885	0.876	1.585	1.534	0.698	4.819	1.642
D. cornigera	0.968	1.244	2.505	1	1.249	3.202	3.213	2.872	1.825	3.381	3.97	3.952	2.214	2.326	4.041
D. moneorum	0.297	0.394	3.671	1.249	1	4.228	4.361	1.77	2.893	4.533	5.034	5.027	3.259	1.194	5.106
D. parallela	4.028	4.308	1.114	3.202	4.228	1	1.026	5.959	1.401	1.004	1.251	1.133	1.115	5.406	1.237
D. pugionata	4.123	4.431	0.723	3.213	4.361	1.026	1	6.077	1.525	0.219	0.933	0.879	1.199	5.518	0.988
D. rileyi	1.967	1.66	5.373	2.872	1.77	5.959	6.077	1	4.63	6.246	6.788	6.778	5.01	0.584	6.86
D. yucatana	2.674	2.976	0.885	1.825	2.893	1.401	1.525	4.63	1	1.679	2.198	2.164	0.426	4.068	2.256
D. monoceros	4.295	4.595	0.876	3.381	4.533	1.004	0.219	6.246	1.679	1	0.877	0.787	1.361	5.689	0.907
D. ensifera	4.821	5.15	1.585	3.97	5.034	1.251	0.933	6.788	2.198	0.877	1	0.191	1.793	6.216	0.124
D.apiculata	4.813	5.132	1.534	3.952	5.027	1.133	0.879	6.778	2.164	0.787	0.191	1	1.771	6.209	0.135
D. minima	3.048	3.365	0.698	2.214	3.259	1.115	1.199	5.01	0.426	1.361	1.793	1.771	1	4.443	1.856
D.rugosa	1.398	1.125	4.819	2.326	1.194	5.406	5.518	0.584	4.068	5.689	6.216	6.209	4.443	1	6.289
D.spinosa	4.894	5.218	1.642	4.041	5.106	1.237	0.988	6.86	2.256	0.907	0.124	0.135	1.856	6.289	1

Table S58: Results of Mantel test between pairwise comparisons of morphological and environmental hypervolumes, including log-transformed data.

Species Level - r (*p*-value)		PC's (All)	PC's (except 1)	PC's 2, 3, & 4
With Spine	Natural Log	-0.057 (0.709)	-0.069 (0.624)	-0.032 (0.561)
	No Log	-0.048 (0.618)	-0.124 (0.797)	-0.118 (0.741)
No Spine	Natural Log	-0.042 (0.612)	0.086 (0.257)	0.062 (0.315)
	No Log	-0.042 (0.596)	-0.079 (0.683)	-0.106 (0.751)

Genus Level - r (*p*-value)		PC's (All)	PC's (except 1)	PC's 2, 3, & 4
With Spine	Natural Log	0.423 (0.333)	0.003 (0.417)	-0.202 (0.583)
	No Log	0.347 (0.292)	-0.400 (0.70833)	-0.515 (0.792)
No Spine	Natural Log	-0.201 (0.500)	-0.660 (0.875)	-0.660 (0.875)
	No Log	-0.277 (0.333)	-0.042 (0.596)	-0.658 (0.875)

Table S59: Contribution of each morphological variable represented in different principal components (PC).

	PC 1	PC 2	PC 3	PC 4	PC 5	PC 6
Pronotum width	0.400	0.200	0.882	-0.132	-0.049	0.053
Pronotum length	0.417	-0.034	-0.042	0.830	-0.106	-0.351
Elytra width at humeral angle	0.420	0.005	-0.275	-0.458	-0.641	-0.356
Elytra width at median region	0.408	0.487	-0.326	0.087	-0.036	0.693
Spine height	0.422	0.125	-0.197	-0.271	0.753	-0.356
Body height	0.380	-0.840	-0.009	-0.058	0.080	0.374